Dopaminergic control of the primary motor cortex microcircuits during motor skill learning

Jérémy Cousineau

université de BORDEAUX

Thèse présentée

Pour obtenir le grade de

Docteur de l'université de Bordeaux

Ecole doctorale des sciences de la vie et de la santé
Spécialité : Neurosciences

Contrôle dopaminergique des microcircuits du cortex moteur primaire pendant l'apprentissage moteur

Par **COUSINEAU Jérémy**

Sous la direction du Dr. Jérôme BAUFRETON
Au sein de l'institut des Maladies Neurodégénératives (IMN, Bordeaux)
Date de soutenance : 03/02/2022

Membres du jury :

Dr. Pascal Branchereau	Président
Dr. Marianne Benoit-Marand	Rapporteur
Dr. Alberto Bacci	Rapporteur
Dr. Luc Estebanez	Examinateur
Dr. Morgane Le Bon-Jégo	Invitée
Dr. Jérôme Baufreton	Directeur de thèse

Ce travail de thèse a été réalisé au sein de l'Institut des Maladies Neurodégénératives de Bordeaux, CNRS UMR 5293, situé au 146 Rue Léo Saignat, Centre Broca Nouvelle-Aquitaine, 3ème étage, Université de Bordeaux, 33000 Bordeaux.

Ce travail de thèse a été financé par la Fondation pour la Recherche Médicale (FRM) et la fondation Yolande CALVET (# ECO201806006853).

Une partie de ce travail a également été financé par le Neurocampus grâce au Seed Project DAMOCO (financement Bordeaux Neurocampus).

TABLE OF CONTENT

LIST OF ABREVIATIONS

6-OHDA : 6-Hydroxydopamine
AAV : **A**deno-**A**ssociated **V**irus
aCSF : **a**rtificial **C**erebro**S**pinal **F**luid
AMPA : α-amino-3-hydroxy-5-methyl-4-isoxazolepropionic acid
ANOVA : **An**alysis **o**f **Va**riance
CCor : **C**ortico-**Cor**tical
ChR2 : **Ch**annel**R**hodopsin **2**
CFA : **C**audal **F**orelimb **A**rea
ChABC: **Ch**ondroitinase **ABC**
CSPG : **C**hondroitin **S**ulfate **P**roteo**G**lycan
CStr : **C**ortico-**Str**iatal
CT : **C**ortico**T**halamic
D2R : Dopamine D2-like receptors
DBS : **D**eep **B**rain **S**timulation
DD : **D**opamine-**d**epleted
DDT: **D**opamine-**d**epleted **t**rained
GABA : **γ**-**a**mino**b**utyric **a**cid
GPe : ***G****lobus* ***P****allidus*, **e**xternal segment
GPi : ***G****lobus* ***P****allidus*, **i**nternal segment
HA : **H**y**a**luronan
HAPLN : **h**y**a**luronan/**p**roteoglycans **l**ink **p**rotein
HAS : **H**y**a**luronan **S**ynthetase
hSyn : **h**uman **Syn**apsin
i.p. : **i**ntra**p**eritoneal
IPSC : **I**nhibitory **P**ost-**S**ynaptic **C**urrent
IT : **I**ntra**T**elencephalic
L-DOPA : 3,4-Dihydroxy-L-phenylalanine methyl ester

LICI : **L**ong **I**ntra**C**ortical **I**nhibition
M1 : Primary **m**otor cortex
mTOR : **m**echanistic **T**arget **O**f **R**apamycin
MPTP : 1-**M**ethyl-4-**p**henyl-1,2,3,6 **t**etrahydro**p**yridine
mRNA : **m**essenger **R**ibo**n**ucleic **A**cid
NMDA : **N**-**m**ethyl-**D**-**a**spartate
NT : **N**on-**t**rained
PC : **P**yramidal **C**ells
PD : **P**arkinson's **D**isease
PET : **P**ositron **E**mission **T**omography
PFC : **P**re**f**rontal **C**ortex
PirB : **P**aired **i**mmunoglobulin **r**eceptor **B**
PKA : **p**rotein **k**inase **A**
PLC : **P**hopho**l**ipase-**C**
PT : **P**yramidal **T**ract
PV : **P**ar**v**albumin
ShamT: Sham-trained
SICI : **S**hort **I**ntra**c**ortical **I**nhibition
SNc : **S**ubstantia **n**igra pars **c**ompacta
SNr : **S**ubstantia **n**igra pars **r**eticulata
SPRT : **S**ingle **P**ellet **R**eaching **T**ask
SST : **S**omato**s**ta**t**in
STN : **S**ub**t**halamic **n**ucleus
Tn : **T**e**n**ascin
TH : **T**yrosine **H**ydroxylase
TTX : **T**etrodo**t**o**x**in
VIP : **V**asoactive **I**ntestinal **P**olypeptide
VTA : **V**entral **T**egmental **A**rea
WFA : **W**isteria **F**loribund**a** Lectin

ABSTRACT

TITLE: Dopaminergic control of primary motor cortex microcircuits during motor skill learning

Parkinson's disease, which affects more than 7 million people worldwide, is caused by the progressive loss of dopamine neurons in the midbrain. In addition to the characteristic motor symptoms of the disease, Parkinson's patients also have difficulty performing complex movements requiring motor learning. The primary motor cortex (M1) is crucial for this learning, and its activity is altered in parkinsonian patients. The objective of this project was to study the targets and the mechanism of action of dopamine in M1 during motor learning. We first demonstrated that parvalbumin (PV) neurons are the major neuronal population expressing D2-like dopamine receptors in layer 5 of M1 in mice. Activation of these receptors was able to increase the excitability and synaptic transmission of PV neurons on its target cells. We then showed that learning a new fine motor task induced a decrease in excitability and synaptic transmission of PV neurons. Moreover, specific dopaminergic depletion in M1 prevented fine motor learning and also altered the excitability of PV neurons. These dopamine-depleted mice also showed impaired short-term plasticity of their synaptic transmission to pyramidal cells. These data show that PV neurons in M1 layer 5 undergo dopamine-dependent plasticity when learning a new fine motor task. We next focused on a feature of cortical PV neurons, the perineuronal nets (PNN). These PNN are part of the extracellular matrix and form a mesh-like structure that wraps the soma and proximal dendrites of neurons, mainly PV neurons in M1. These PNN are known to

act as an inhibitor of cortical plasticity and that their depletion creates a new plasticity window. Our results showed that PNN are reduced in M1 during motor learning, opening a new plasticity window. We also showed that the decrease in excitability of PV neurons in M1 was sufficient to induce a decrease in PNN. Finally, using *in* vivo calcium imaging we observed the impact of the dopaminergic lesion at a larger scale, showing that the activity of M1 pyramidal cells during motor learning is decreased. This project allowed us to better understand the role of dopamine modulation of M1 circuitry, highlighting PV as a target for cortical dopamine and thus a potential source of dysfunction in M1 pathophysiology

Keywords*: Primary motor cortex, Neuronal excitability, Synaptic transmission, GABA, Parvalbumin, Parkinson's disease, Dopamine, Motor skill learning, Electrophysiology, Perineuronal nets, Mice.*

RÉSUMÉ

TITRE : Contrôle dopaminergique des microcircuits du cortex moteur primaire pendant l'apprentissage moteur

La maladie de Parkinson, qui affecte plus de 7 millions de personnes dans le monde, est due à la perte progressive des neurones dopaminergiques du mésencéphale. En plus des symptômes moteurs caractéristiques de la maladie, les patients parkinsoniens rencontrent des difficultés à exécuter des mouvements complexes nécessitant un apprentissage moteur. Le cortex moteur primaire (M1) est crucial pour cet apprentissage, et son activité est altérée chez les patients parkinsoniens. L'objectif de ce projet était d'étudier les cibles et le mécanisme d'action de la dopamine dans M1 pendant l'apprentissage moteur. Nous avons mis en évidence que les neurones à parvalbumine (PV) sont les neurones majoritaires exprimant les récepteurs D2 à la dopamine dans la couche 5 du M1 chez la souris. L'activation de ces récepteurs augmente l'excitabilité et la transmission synaptique des neurones PV sur ses cellules cibles. Nous avons ensuite montré que l'apprentissage d'une nouvelle tâche motrice fine induit une diminution de l'excitabilité et de la transmission synaptique des neurones PV. De plus, la déplétion dopaminergique spécifiquement au niveau de M1 chez des souris empêche l'apprentissage moteur fin et altère également l'excitabilité des neurones PV. Ces souris déplétées en dopamine présentent également une altération de la plasticité à court terme de leur transmission synaptique vers les cellules pyramidales. Ces effets tendent à montrer que les neurones PV de la couche 5 du M1 subissent des plasticités dopamine-dépendantes lors de l'apprentissage d'une nouvelle tâche motrice fine.

Nous nous sommes ensuite intéressés à une caractéristique des neurones PV corticaux, les réseaux périneuronaux (PNN, pour perineuronal nets en anglais). Ces PNN font partie de la matrice extracellulaire et forme une structure en filet qui enveloppe le soma et les dendrites proximales des neurones, principalement les neurones PV dans M1. Ces PNN sont connus pour agir comme inhibiteur de la plasticité corticale et leur diminution ouvre une fenêtre de plasticité. Nos résultats ont montré en effet que les PNN sont réduits dans M1 au cours de l'apprentissage moteur. Nous avons également mis en évidence que la diminution de l'excitabilité des neurones PV du M1 était suffisante pour induire une diminution des PNN. Enfin, l'utilisation de l'imagerie calcique *in vivo* nous a permis d'enregistrer de façon longitudinale l'activité des cellules pyramidales dans M1 chez des animaux réalisant la tâche motrice. En suivant l'activité du réseau chez des souris contrôles et chez des souris déplétées en dopamine au niveau de M1, nous avons pu étudier aussi l'impact de la lésion dopaminergique à plus grande échelle. Ainsi, les analyses préliminaires montrent que l'activité des cellules pyramidales du M1 pendant l'apprentissage moteur est diminuée. Ce projet a permis de mieux comprendre le rôle de la modulation dopaminergique du M1, mettant en évidence les neurones PV comme cible de la dopamine corticale et donc comme source potentielle de dysfonctionnement dans la pathologie de M1.

Mots clés : *Cortex moteur primaire, Excitabilité neuronale, Transmission synaptique, GABA, Paralbumine, Maladie de Parkinson, Dopamine, Apprentissage moteur, Electrophysiologie, Réseaux périneuronaux, Souris.*

RÉSUMÉ SUBSTANTIEL EN FRANÇAIS

En plus des symptômes moteurs caractéristiques, les patients atteints de la maladie de Parkinson ont aussi des difficultés à exécuter des mouvements complexes nécessitant un apprentissage moteur. Le cortex moteur primaire (M1) permet l'acquisition et le maintien des performances motrices. L'activité du M1 et l'apprentissage moteur étant altérés chez les patients parkinsoniens, l'objectif de ce projet est d'identifier les cibles et les mécanismes d'action de la dopamine au niveau du (M1) lors de l'apprentissage moteur. Tout d'abord, nous avons identifié et cartographié les populations neuronales exprimant le récepteur D2 à la dopamine (D2R), avec pour hypothèse que les neurones PV sont la cible majeure de la dopamine au sein de M1 (Objectif 1), et quantifié l'impact de l'activation des D2R sur les propriétés électrophysiologiques des neurones PV. Dans un deuxième temps, des souris ont été entraînées à une tâche motrice fine et les différents processus de plasticité (cellulaires et synaptiques) au sein du réseau cortical de M1 permettant cet apprentissage ont été étudiés (Objectif 2). Nous avons étudié l'impact d'une lésion dopaminergique au niveau de M1 sur tous les paramètres précédemment mesurés lors de l'apprentissage de ces animaux déplétés en dopamine.

Le premier objectif du projet était de caractériser anatomo-fonctionnellement les neurones du cortex moteur primaire (M1) exprimant les récepteurs dopaminergiques D2 (D2R). Cette étape du projet a fait l'objet d'une publication dans le journal eNeuro (Cousineau et al., 2020). Grâce aux souris transgéniques D2Cre::RiboTag, exprimant un tag HA exclusivement dans les cellules exprimant le D2R, nous avons montré que les neurones PV sont les neurones exprimant le plus ces récepteurs au sein de la couche 5 de M1. Ensuite, à l'aide de souris transgéniques PVCre::Ai9t, permettant de cibler aisément les neurones PV,

nous avons mis en évidence que l'activation des D2R augmente l' excitabilité des neurones PV ainsi que leur transmission synaptique GABAergique vers les cellules pyramidales.

Le deuxième objectif était de caractériser les propriétés électrophysiologiques et synaptiques des neurones PV lors de l'apprentissage d'une tâche motrice fine chez la souris. Des souris PVCre::AI9t ont été entrainées à attraper une récompense alimentaire en passant leur patte à travers une fente verticale étroite. Après 8 jours d'entrainement, les souris acquièrent un mouvement stéréotypé requis pour une meilleure performance dans la réalisation de cette tâche. Des enregistrements électrophysiologiques sur préparations *ex vivo* ont alors été réalisés et ont permis de montrer qu'à la suite de l'apprentissage moteur, l'excitabilité et la transmission synaptique des neurones PV sont diminués dans la couche 5 du M1 (dans la zone correspondant au membre antérieur, utilisé pendant l'apprentissage). Grâce à l'utilisation de microscope miniature couplé à l'imagerie calcique, nous avons pu mesurer *in vivo* avec une résolution cellulaire l'activité des cellules pyramidales de M1 pendant que les souris réalisaient les sessions d'entrainement. Cette méthode a permis de montrer que l'activité des cellules pyramidales augmente avec les sessions d'entrainement ce qui semble en accord avec la réduction d'excitabilité des neurones PV.

L'objectif suivant était de déterminer le rôle et l'importance des neurones PV lors de l'apprentissage. Pour cela nous avons manipulé l'excitabilité des neurones PV pendant les sessions d'entrainement grâce à une méthode chémogénétique. Des souris PVCre ont reçu une injection d'un virus permettant l'expression du récepteur excitateur hM3Dq spécifiquement dans les neurones PV, via une expression Cre-dépendante. Cette technique permet donc d'augmenter l'excitabilité des neurones PV alors que l'apprentissage induit normalement une diminution de cette dernière.

Les résultats obtenus tendent effectivement à montrer que cette manipulation des PV altère l'apprentissage moteur.

Pour finir, le dernier objectif avait pour but d'étudier l'impact d'une lésion dopaminergique spécifique au niveau de M1 sur les neurones PV lors de l'apprentissage moteur. Pour cela, les fibres dopaminergiques de M1 ont été détruites par l'injection bilatérale de 6-hydroxydopamine (6-OHDA) dans la zone correspondant aux membres antérieurs du M1. Nous avons montré que les souris déplétées en dopamine au niveau du M1 ne sont plus capables d'acquérir le mouvement requis pour la tâche de préhension de nourriture. Nous avons également montré que les neurones PV de ces souris montrent une augmentation de leur excitabilité à la suite de l'entrainement moteur, effet opposé à celui observé chez les souris contrôles. De manière intéressante, la destruction des fibres dopaminergiques du M1 induit aussi une altération de la plasticité à court terme sur la synapse neurones PV vers cellules pyramidales. En revanche, l'entraiment moteur est capable de rétablir cette altération.

Nous nous sommes ensuite intéressés à une autre caractéristique des neurones PV corticaux : les réseaux périneuronaux (PNN, pour PeriNeuronal Nets en anglais). Les PNN forment des structures denses en forme de filet enveloppant le soma et les dendrites proximales des neurones, principalement des neurones PV dans M1. Les PNN s'établissent au cours du développement et leur mise en place totale marque la fin de la période de plasticité juvénile. En effet, les PNN agissent tel des inhibiteurs de plasticité, et ce *via* différentes manières : (1) ils forment une barrière physique autour du neurone, empêchant la formation de nouvelle synapse, (2) ils sont capables de fixer des molécules inhibitrices de la synaptogenèse, (3) et enfin limitent la mobilité des récepteurs au niveau de la membrane cellulaire. Il a été montré qu'une diminution des PNN dans le cortex permet de réinstaurer une nouvelle fenêtre de plasticité, et cette diminution est observée lors de

l'apprentissage de peur. Nos résultats ont montré qu'une diminution de l'intensité des PNN dans M1 est aussi mesurée avec l'apprentissage moteur. La diminution des PNN et l'excitabilité des neurones PV sont deux caractéristiques capables de s'influencer l'une sur l'autre. En effet, la destruction des PNN dans diverses structures corticales induit une diminution de l'excitabilité des neurones PV. A l'inverse, la diminution de l'excitabilité des neurones PV est capable de diminuer l'intensité des PNN dans le cortex visuel. Etant donné que nous avons observé la diminution de ces deux paramètres lors de l'apprentissage moteur dans M1, nous avons voulu déterminer s'il existait une interaction entre eux dans M1. Nos données ont montré que la diminution de l'excitabilité des neurones PV, en utilisant une approche chémogénétique, est capable de diminuer l'intensité des PNN dans M1. En revanche, la destruction des PNN dans M1 n'a pas eu d'effet sur les propriétés électriques des neurones PV.

Enfin, l'enregistrement de l'activité des neurones pyramidaux en utilisant les microscopes miniatures et l'imagerie calcique tend à montrer que l'activité du M1 est diminuée pendant les sessions d'entrainement chez les souris déplétées en dopamine comparé à des souris contrôles.

Ce projet a mis en évidence l'importance de la dopamine dans le fonctionnement du cortex moteur primaire (M1). De plus, il met en avant les neurones PV comme une cible de la dopamine corticale ainsi qu'une source potentielle des dysfonctionnements du M1 en condition pathologique. Pour aller plus loin dans la compréhension de leur participation dans l'exécution motrice et l'apprentissage, il serait intéressant d'utiliser une tâche motrice plus complexe. Cela permettrait de décomposer chaque étape clé lors de l'entrainement afin de manipuler les neurones PV spécifiquement pendant certaines phases (initiation du mouvement, ou pendant que la souris attrape la récompense). Cela permettrait de disséquer précisément le rôle des neurones PV dans l'exécution motrice et les

processus d'apprentissage moteur. Afin de déceler plus en détail les processus dopamine-dépendants mis en jeu lors de l'apprentissage moteur au sein de M1, il serait aussi crucial d'étudier les neurones dopaminergiques du mésencéphale, source majeure de dopamine de M1. Comprendre et étudier l'activité de ces neurones pendant l'apprentissage moteur, nous permettraient de mieux comprendre le rôle de la dopamine dans ces processus d'apprentissage. L'utilisation de senseurs dopaminergiques pourrait notamment permettre de comprendre la dynamique de la libération dopaminergique dans le M1 lors de l'apprentissage moteur.

INTRODUCTION

I-Parkinson's Disease

Parkinson's disease (PD) is the second most common neurodegenerative disorder, affecting over 200 000 people in France, and 7 to 10 million people are estimated to have the disease worldwide. PD is characterized by the slow and progressive death of dopaminergic cells in the midbrain and by the presence of Lewy bodies, which are aggregates of the intracellular protein alpha-synuclein. Clinical diagnosis of PD can sometimes be difficult as motor and non-motor symptoms of the disease are highly variable between patients. PD has a strong impact on the patients' quality of life. Currently, no cure exists but treatments are available to relieve and alleviate the patients' quality of life.

1.1. Parkinson's disease risk factors

Age is one of the first risk factors for PD. The incidence (rate of newly diagnosed cases) increases with age, with a stabilization in the population older than 80. This incidence shows the importance of PD in our society, >3% of people older than 80 are affected by PD (Poewe et al., 2017). Men are 1.5 times more likely to have PD than women, likely thanks to the protective effect of female sex hormones (de Lau and Breteler, 2006). PD prevalence seems also to depend on ethnicity, genetic and environmental risk factors (Baldereschi et al., 2000; Poewe et al., 2017). Genetic research confirms that PD is a complex disease and is not explained by single pathogenesis or natural cause (Kim and Alcalay, 2017). Mutations on a wide variety of proteins are associated with PD (alpha-synuclein, LRRK-2, SNCA, VPS-35, Parkin, PINK-1, DJ-1, GBA). However, only a small proportion of PD forms are caused by

those genetic alterations. Indeed, the genetic forms of PD represent around 5 to 15% of all cases. Environmental risk factors for PD are diverse (traumatic brain injuries, exposure to chemicals are toxins…). The diversity and interaction of risk factors in PD may underlie the diversity of the disease itself.

1.2. Therapies for Parkinson's disease

1.2.1. Dopamine replacement therapies

No treatment is currently available to cure PD. However, several therapies are available to try to alleviate PD patients' symptoms and increase their quality of life. Levodopa (L-DOPA) treatment, described by Cotzias and colleagues in 1969, is the first treatment used for PD patients (Cotzias et al., 1969). L-DOPA is the precursor of the dopamine and can cross the blood-brain barrier. Once in the brain, it can then be transformed into DA (Fahn, 2008). With this DA replacement therapy, PD patients have a fast improvement in their symptoms. However, chronic L-DOPA treatment can also induce motor complications known as dyskinesia. These complications occur in 50% of PD patients who had received L-DOPA for more than 5 years, and the ratio increased in patients with the young-onset disease (Golbe, 1991; Aquino and Fox, 2015).

1.2.2. Surgical procedures

Surgical procedures can be an alternative treatment for PD, especially when DA replacement therapies are not able to improve the symptoms or when L-DOPA induced dyskinesia. Surgical procedures are including ablation, lesion, and stimulation of the subthalamic nucleus (STN) or the internal globus pallidus (GPi), but today, neurostimulation is preferred, thanks to its reversibility (Nilsson et al., 2005). STN deep brain stimulation (DBS) is often preferred and can have very effective in improving motor symptoms (Krack et al., 1997; Krause, 2001). However, it can be less effective for other symptoms, such as gait disturbances, freezing, speech, or cognition (Collomb-Clerc and Welter, 2015). DBS has other limitations as the fragility of the system and its cost (Doshi, 2011; Falowski et al., 2015).

1.3. Symptoms of Parkinson's disease

PD is highly variable, symptoms slowly appear with time, and from one to another person, they are different in combination and severity (Figure1.1).

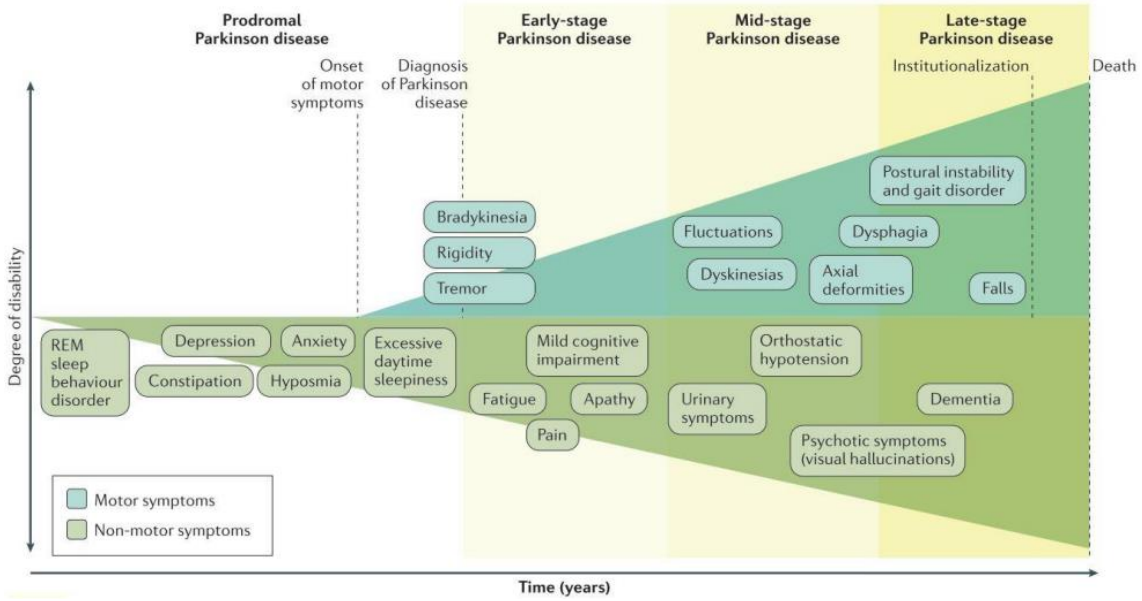

Figure1.1: Symptomatology across the development of PD. Schematic depicting the different motor and non-motor symptoms from the beginning of the illness (prodromal PD) to the late stage of the disease. Both motor and non-motor symptoms become increasingly relevant over the course of the disease. Schematics from Poewe et al., 2017.

1.3.1. Motor symptoms

The characteristic symptoms of PD are bradykinesia (slowness of movements), tremor (trembling in hands, arms, legs, jaw, or head, especially at rest), and rigidity (stiffness of the limbs and trunk). The combination of bradykinesia plus either tremor or rigidity must be displayed to diagnose PD. Other motor symptoms can be present in PD. Resulting from bradykinesia, patients can display micrographia: smaller and smaller, untidy, and continuous handwriting.

Akinesia is usually a symptom of advanced PD. It is the loss of the ability to start a voluntary movement and can take different forms in PD. Freezing is one of them: the patient will temporarily, and at any time, be unable to move, increasing risks of falling and injuries. Another symptom increasing the risk for falls is festination, which is an unwanted and uncontrollable acceleration in gait (those unwanted accelerations can also affect speech, also called tachyphemia).

1.3.2. non-motor symptoms

Even if the motor symptoms are the hallmark of PD, the disease is also associated with a wide spectrum of non-motor symptoms which can be as disabling as motor ones (Sullivan et al., 2007). As for motor symptoms, they are diverse and variable across patients. They involve various functions, such as sleep-wake cycle regulation, cognitive functions, regulation of the mood, autonomic nervous system function, sensory functions, or pain perception (Poewe et al., 2017), table1.1).

Neuropsychiatric dysfunction
Mood disorders
Apathy and anhedonia
Frontal executive dysfunction
Dementia and psychosis
Sleep disorders
Sleep fragmentation and insomnia
RBD
PLMS/RLS
Excessive daytime somnolence
Autonomic dysfunction
Orthostatic hypotension
Urogenital dysfunction
Constipation
Sensory symptoms and pain
Olfactory dysfunction
Abnormal sensations
Pain

RBD, rapid eye movement sleep behaviour disorder; PLMS, periodic limb movements in sleep; RLS, restless legs syndrome.

Table 1.1: Non-motor symptoms in PD patients. Table from Powe et al., 2017 depicting the different non-motor symptoms that PD patients can present.

1.3.3. Focus on motor learning impairments in PD

1.3.3.1 Motor learning definition

Before talking about the impairment of motor learning in PD, we first need to define it. Explicit (or declarative) processes are the capacity to have conscious learning and memory. It consists for example in learning facts or events that can be recollected, and can be general (the earth is spherical) or autobiographic (I am born on that day) (Tulving, 1985; Squire and Zola-Morgan, 1991). On the other hand, implicit (or non-declarative/procedural/anoetic) learning refers to an unconscious memory ability which includes skill learning and habit formation. Motor learning is the ability to acquire and refine skills, and it requires both explicit and implicit learning. Indeed, motor learning is a multistep mechanism, involving those 2 types of memory at different stages (Moisello et al., 2009; Marinelli et al., 2017).

The classical view of motor learning postulate that it occurs in 3 main phases: cognitive, associative, and autonomous phases (Fitts, 1964; Anderson, 1982; Logan, 1988) (Figure 1.2). First, the subject is introduced to a new motor task and needs to understand what to do. This cognitive step is mainly declarative as the learner must understand verbal or textual instructions (Anderson, 1982). At this stage, movements need great attention. They are highly variable, slow, and inaccurate, but a large gain in performances is noted (the most obvious gain in the total learning process). These improvements are mediated by declarative strategies (the subject learns *what to do*). This stage length depends on the clarity of the instruction, the quality of the training, the complexity of the task (motor or non-motor complexity), and on the subject's abilities. The second phase is the motor stage, also called the slow learning stage (Adams, 1971). This step begins with adjustments in the movement which are not perceived by the subject (increase in movement

consistency). This step takes more time, days to months, to years maybe, and performances slowly become more accurate and automatic. Finally, after this long period of practice, the learner enters the autonomous stage. Now, the skill is largely automatic and requires few attentional resources to be performed. The subject is then performing an automatized stereotyped movement, which is fast, smooth, and accurate that can be triggered by its associated cue.

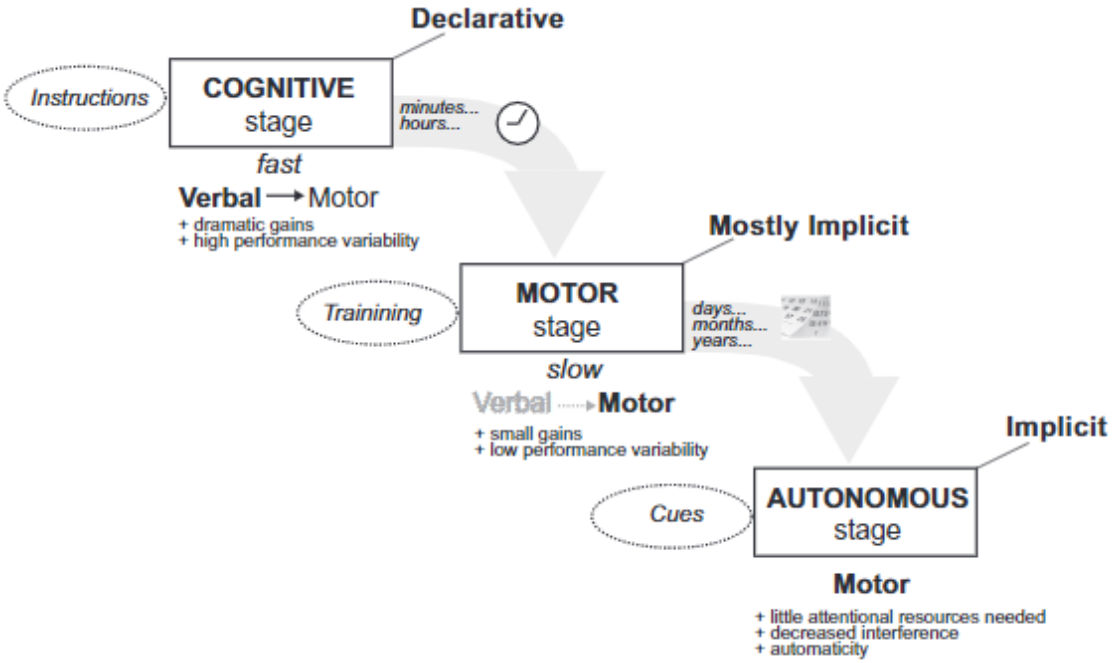

Figure 1.2: The different stages of motor learning. The cognitive step consists in understanding the instructions to perform the required motor task. At this stage, performances are highly variable. This stage is relatively low, and its duration depends on the task difficulty and the subject's abilities. Then comes the motor step which is mostly implicit and consists of training to the motor task. Small performances improvements are acquired over time here, and this step is much longer. It might take from days to years depending on the intensity, frequency, and quality of the training. Finally comes the autonomous step in which the task is now automatic. The task can be performed with little attentional resources, and the realization of it can be triggered by its associated cue. At this stage, performance is faster, effortless, and accurate. Figure from Marinelli et al., 2017.

1.3.3.2. Motor learning impairments in PD patients

Frith and colleagues were the first to look at procedural and implicit learning in PD. They tested several paradigms in which subjects needed to adapt their performances with cognitive strategies (Frith et al., 1986). In this task, patients had to follow a target on a screen by moving a joystick. In the first task, the position of the target was semi-predictable, while in the second they had to use a new joystick with movement mirrored compared to the computer screen target. In both tasks, non-demented PD patients' performances were lower than controls but were still displayed some motor learning. Other studies seemed to show also that implicit learning was still present in non-demented PD (Taylor et al., 1990; Bondi and Kaszniak, 1991). However, when performing reaching movements that require ample rotation, PD patients are presenting impairment in motor learning (Canavan et al., 1990; Contreras-Vidal and Buch, 2003). Movements needing such rotation are using cognitive and explicit strategies (Marinelli et al., 2009). Interestingly, PD patients also show impairments in mental rotation tasks, which involve the same strategies (Yamadori et al., 1996; Amick et al., 2006). For a movement with little or no rotation, the learning became more implicit, demanding less attention (Marinelli et al., 2009), and this may be the reason why PD patients are able to adapt similarly to controls (Moisello et al., 2009; Bédard and Sanes, 2011; Marinelli et al., 2017). Marinelli and colleagues have well-reviewed how motor learning is affected in PD and why the literature can be contradictory on the subject (Marinelli et al., 2017). They conclude that motor learning that does not need awareness or cognitive strategies is not affected in PD patients. However, skill learning requiring attentional resources and cognitive strategies is impaired in PD patients. In addition, even for a task where patients were able to show initial learning, retention of skills is impaired

in PD, from the early stage of the disease and does not improve with treatments (Marinelli et al., 2009; Bédard and Sanes, 2011).

1.4. Impact of PD dopaminergic loss on the motor circuits

1.4.1 The basal ganglia

In PD, the death of dopaminergic neurons from the substantia nigra pars compacta (SNc) results in the loss of dopamine in the basal ganglia. The basal ganglia are a group of organized subcortical nuclei (Figure 1.3) directly or indirectly connected to the primary motor cortex (M1). The basal ganglia are involved in movement planning and execution, but also associative learning and habit formation (Middleton and Strick, 2000). The loss of dopamine in the basal ganglia results in a reduction of the activity of the striatal spiny neurons from the direct pathway while enhancing the activity of those from the indirect pathway (Albin et al., 1989; Galvan and Wichmann, 2008; Wichmann and Dostrovsky, 2011, Figure 1.3). These activity impairments lead to a hypoactivity of the thalamo-cortical pathway, causing bradykinesia in PD.

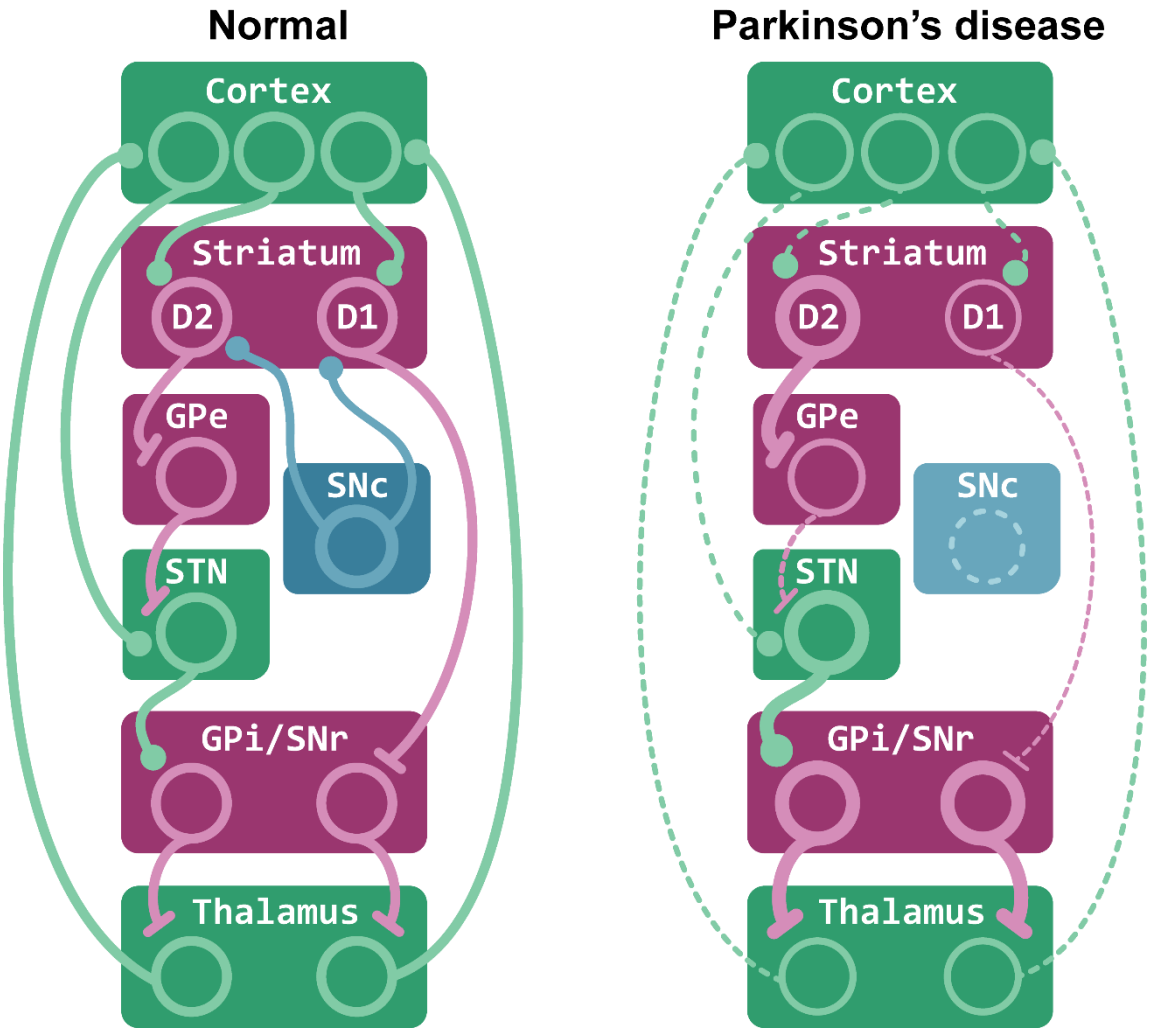

Figure 1.3: Schematic representation of the basal ganglia circuits in normal condition and PD patients. Glutamatergic, GABAergic, and dopaminergic projections are represented in green, red and blue, respectively. Dashed represent projections that have reduced activity, while increased lines represent projections that are overactivated. GPe: *Globus pallidus* external segment, GPi : *Globus pallidus* internal segment, SNr : *Substancia nigra pars reticulata*, SNc : *Substancia nigra pars compacta*, STN: Subthalamic nucleus, D1 : D1-expressing medium spiny neurons, D2 : D2-expressing medium spiny neurons.

1.4.2. M1 impairments in PD

Besides the major impact on the basal ganglia, M1 is also affected in PD. Numerous studies have highlighted the involvement of M1 in this disease (Lindenbach and Bishop, 2013; Burciu and Vaillancourt, 2018). The neuromodulation of M1 is altered in PD, as neuronal death occurs both for noradrenergic neurons from the locus coeruleus and dopaminergic neurons from the SNc (Zarow et al., 2003) and the VTA (Bogerts et al., 1983; Uhl et al., 1985; Waters et al., 1988). Linked to this neuronal death, monoamine deficits are observed in PD patients (Zarow et al., 2003; Moore et al., 2008; Pavese and Brooks, 2009; Sommerauer et al., 2018). Labeling of the tyrosine hydroxylase (TH), confirmed the loss of DA and noradrenergic fibers in M1 in PD patients (Gaspar et al., 1991). This neuronal death is visible and Lewy bodies, which are alpha-synuclein aggregation characteristic of synucleinopathies such as PD, are also present in M1 of PD patients (Braak et al., 2003; Caviness et al., 2011). Structural imaging revealed also reduced grey matter in M1 that is correlated with bradykinesia (Lyoo et al., 2011).

Regarding functional changes in M1 of PD patients, no modification stands out at rest (Berding et al., 2001; Hilker et al., 2004). However, when patients are executing movement, M1 activity is increased compared to healthy controls (Table 1.2). This M1 movement-related hyperactivity seems to be linked with the characteristic tremors displayed by PD patients. Indeed, the M1 level of activity was positively correlated with tremor (Thobois et al., 2000; Fukuda et al., 2004). In addition to rest tremors, M1 seems to be involved in the re-emergent tremors, which occur with variable delays when the arm is kept outstretched (Leodori et al., 2020).

Compilation of studies using PD patients to examine changes in regional blood flow or metabolism within subregions of the motor cortex.

Primary PD		PD OFF relative to healthy controls		
		M1 activity	SMA activity	PMC activity
(A)				
Rest		No change Berding et al. (2001)	No change Berding et al. (2001) Hilker et al. (2004) Playford et al. (1992) Rascol et al. (1992)	No change Berding et al. (2001) Samuel et al. (1997)
Movement		Increased Yu et al. (2007) Haslinger et al. (2001) Sabatini et al. (2000)	Decreased overall Playford et al. (1992) Rascol et al. (1992) Decreased in pre-SMA Haslinger et al. (2001) Sabatini et al. (2000) Yu et al. (2007) Increased in SMA proper Sabatini et al. (2000)	Increased Catalan et al. (1999) Sabatini et al. (2000) Samuel et al. (1997) Mixed Haslinger et al. (2001)
Use of dopamine therapy		PD ON relative to PD OFF		
		M1 activity	SMA activity	PMC activity
(B)				
L-DOPA	Rest	Decreased Asanuma et al. (2006)	No change Berding et al. (2001)	No change Berding et al. (2001)
	Movement	Decreased Haslinger et al. (2001)	Increased Haslinger et al. (2001) Martinu et al. (2012)	Increased Martinu et al. (2012) Mixed Haslinger et al. (2001)
Apomorphine	Rest	No change (sensorimotor) Rascol et al. (1992)	No change Jenkins et al. (1992) Rascol et al. (1992)	No change Jenkins et al. (1992)
	Movement	Increased (sensorimotor)	Increased	No change
Use of stimulators		PD ON relative to PD OFF		
		M1 activity	SMA activity	PMC activity
(C)				
STN DBS	Rest	Decreased Asanuma et al. (2006) Haslinger et al. (2005) Limousin et al. (1997)	Decreased Hershey et al. (2003) Haslinger et al. (2005)	Decreased Haslinger et al. (2005) Limousin et al. (1997)
	Movement	Decreased Ceballos-Baumann et al. (1999)	Increased overall Limousin et al. (1997) Increased in pre-SMA and Decreased in SMA proper Ceballos-Baumann et al. (1999)	Increased Ceballos-Baumann et al. (1999)
GPi DBS	Rest	No change Limousin et al. (1997)	Increased Davis et al. (1997)	No data available
	Movement	No change Limousin et al. (1997)	Increased Valalik et al. (2009)	Increased Valalik et al. (2009)

Table 1.2: Compilation of studies in PD patients looking at the motor cortices activity. Overview of studies with PD patients showing the modification of M1, supplementary motor areas (SMA), and premotor cortex (PMC) activity at rest and during movement execution compared to healthy patients (A). Same representation for PD patients under dopamine replacement therapies, the activities are compared to PD patients OFF medication (B). Same representation for PD patients under neurostimulation therapies, the activities are compared to PD patients OFF therapy (C). Table from Lindenbach and Bishop, 2013.

One important feature of M1 is its representation map of the different body parts as known as the homunculus. This somatotopic map is altered in PD patients, even in the early stages of PD. Indeed, the hand representation area is bigger in PD patients, and the larger the motor deficiency, the larger the area (Filippi et al., 2001; Thickbroom et al., 2006).

Proper motor learning requires plasticity phenomena within M1. Since this ability is altered in PD patients, it is then not surprising to find out plasticity impairment in M1. M1 plasticity can be assessed using a paired associative stimulation protocol. Cortical excitability is measured, using transcranial magnetic stimulation, before and after a paired stimulation of a sensory nerve and M1, usually done in the upper limb region (Stefan, 2000). It has been shown that M1 plasticity is suppressed in PD patients (Ueki et al., 2006; Kojovic et al., 2012). Interestingly, L-dopa treatment can restore this plasticity only in non-dyskinetic patients (Morgante et al., 2006). Theta burst stimulation is also used to measure cortical plasticity, and only requires cortical stimulation (Huang et al., 2005). Once again, this approach showed that M1 plasticity is suppressed (Eggers et al., 2010; Suppa et al., 2011). However, L-dopa treatment in this paradigm was not able to re-establish proper plasticity. These pieces of evidence show how important cortical dopamine is for proper plasticity in M1.

In the healthy brain, M1 switches between two cortical states of oscillations. At rest, M1 synchronized oscillation corresponds to alpha and beta frequency ranges (8-12 Hz and 13-30 Hz, respectively) (Schnitzler and Gross, 2005; Jenkinson and Brown, 2011). During motor execution, desynchronization occurs, and alpha/beta oscillations are decreased and move towards gamma ranges (30 to 80 Hz) (Pfurtscheller and Lopes da Silva, 1999). However, in PD patients, this switch in the state is altered, the power of beta frequencies increases during movement (Eusebio

and Brown, 2009; Jenkinson and Brown, 2011; George et al., 2013). This prominence of beta oscillations has been shown to be correlated with PD motor impairments (Devos, 2004; Kuhn et al., 2008; Whitmer et al., 2012). Current treatments can partially correct this beta band increase. Indeed, STN stimulation decreases the cortical beta power (Kuhn et al., 2008). Lesion of the pallidum, another treatment for PD patients, has been shown to increase the gamma oscillation in M1 (Hemptinne et al., 2019). L-dopa treatment is able to increase the oscillatory power in M1 which is correlated with the diminution in motor impairments (Cao et al., 2020). The enhancement of gamma oscillations in M1 of PD patients could be a potential treatment to relieve symptoms. It can be performed through transcranial alternating current stimulation, and it has been shown to restore proper plasticity in M1 (Guerra et al., 2020). In addition, it also improves the GABAergic neurotransmission in those patients, which is impaired in PD. However, those beneficial effects seem to decrease with the severity of the disease. Dyskinetic state induced by L-dopa medication is also associated with disturbed M1 oscillations. Dyskinetic PD patients show an increased narrowband gamma oscillation (60 to 90Hz), both at rest and during movement, and this increase is positively correlated with the severity of the dyskinesia (Swann et al., 2016). Altogether, those studies on M1 oscillations point out the disturbed activity on this brain structure and that the severity of those disturbances is often correlated with the severity of the symptoms. This provides new insight to target this oscillatory activity as a putative therapeutic target to relieve PD patients from the disease's symptoms.

Cortical inhibitory signaling is also impaired in PD. It has been shown that the GABAergic tone in M1 is reduced (Ridding et al., 1995) in PD patients and that both DBS and dopaminergic medication are able to restore this M1 inhibition (Strafella et al., 2000; Pierantozzi et al., 2001, 2001; Cunic et al., 2002). Intracortical inhibition

can be measured through short and long intracortical inhibition (SICI and LICI respectively, (Chu et al., 2009)). SICI and LICI are thought to be mediated by $GABA_A$ and $GABA_B$ receptors, respectively. It has been shown that SICI (Guerra et al., 2020) and LICI (Chu et al., 2009) are altered in PD patients. GABAergic signaling is crucial for cortical oscillatory activity (Yamawaki et al., 2008), restoring M1 inhibition may thus have beneficial effects on PD oscillation disturbances. A sub-sedative dose of the hypnotic drug, and $GABA_A$ receptor agonist, zolpidem can restore a proper oscillatory activity within M1 in early-stage PD patients (Hall et al., 2014). These patients also showed improvement in motor abilities following zolpidem administration. It would thus be of great interest to identify which GABAergic neuronal population in M1 could be deficient in PD, in order to identify more specific targets for future treatment.

To conclude, M1 abnormalities in PD occur both at rest and during movement execution, across all stages of the disease. These alterations seem to be partially restored by current PD treatments. As PD is strongly affecting the basal ganglia, it is then difficult to point out which M1 disturbances are due to the basal ganglia output or to the dopamine depletion within M1. However, these studies in human PD patients pointed out that M1 dysfunction in PD may not exclusively come from altered basal ganglia, but also from changes specific to M1. It is then crucial, in order to better understand the pathophysiology of PD, to find out what is the importance of M1 dopamine in its physiology.

II. The primary motor cortex (M1)

2.1. M1 neuronal populations

2.1.1. Pyramidal cells

As in other cortices, M1 is composed of two main neuronal populations; 80% are glutamatergic excitatory neurons, and the remaining 20% are GABAergic and inhibitory (GABA, γ-aminobutyric acid) (Shepherd, 2013). Cortical glutamatergic neurons are called pyramidal cells (PC), or pyramids, due to the pyramidal shape of their soma. They are the major projection neurons of the structure. In M1, they can be divided into different subtypes depending on their position in cortical layers and their projection target (Figure 1.4): Intratelencephalic (IT) neurons, pyramidal tract neurons (PT), and corticothalamic (CT) neurons (Shepherd, 2013). IT neurons can be found in layers 2 to 6. Those in layer 2/3 make projections to other cortices (ipsi- or contralaterally) and can be called IT-CCor. In addition to projecting onto other cortices as IT-CCor, those in deeper layers make projections on the striatum and are thereby called IT-CStr. PT neurons are found in layer 5 and project to the brainstem and the spinal cord but they can also project to the thalamus and the striatum for instance. Finally, CT neurons project mainly to the thalamus.

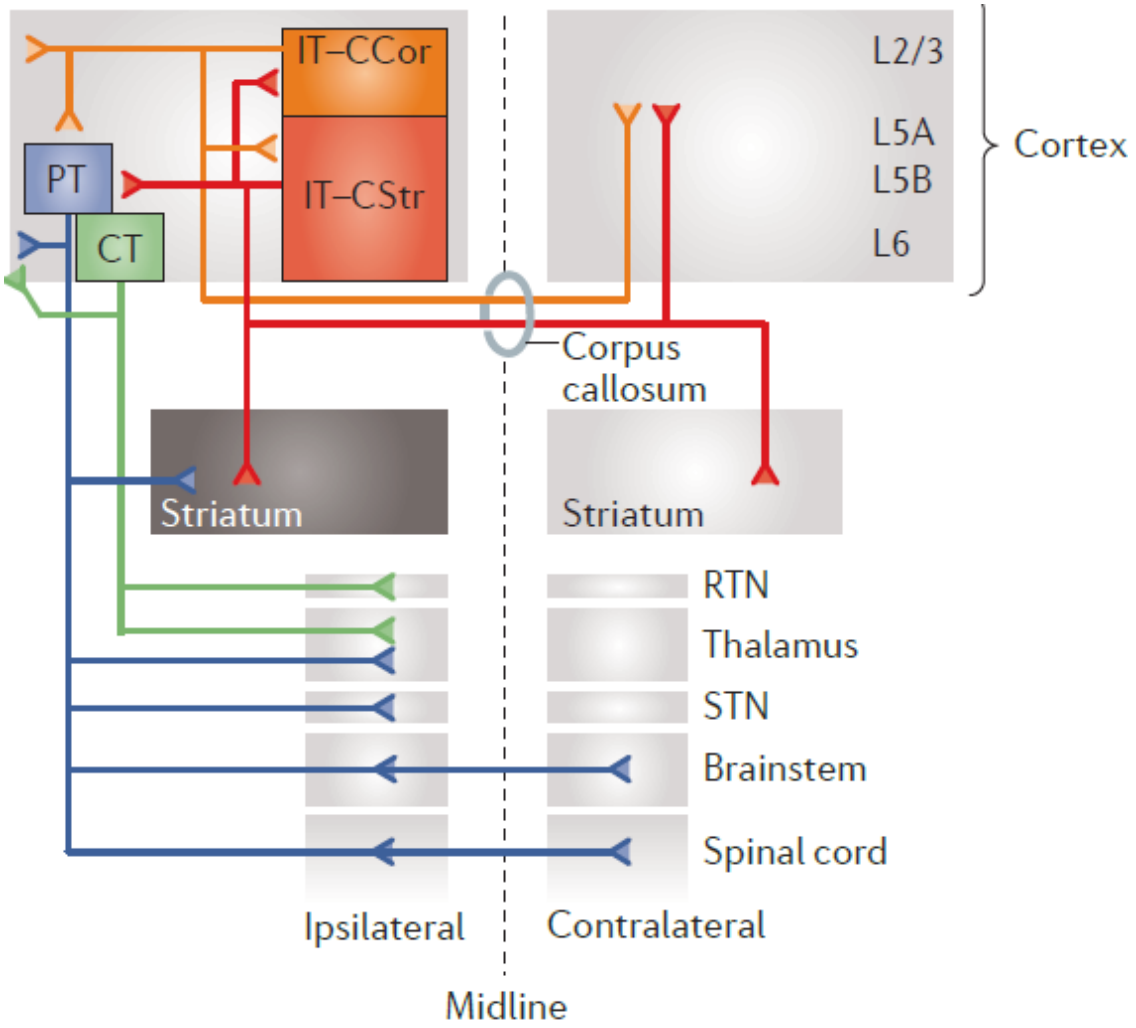

Figure 1.4: The different types of PC based on their projection sites. Schematic of the long-range projection and target of M1 PC, summarizing the part 2.1.1. PT: pyramidal tract neurons, CT: Corticothalamic neurons, IT: Intratelencephalic neurons, CCort: cortico-cortical, CStr: Cortico-striatal, STN: subthalamic nucleus, RTN: reticular nucleus. Image taken from Shepherd, 2013.

2.1.2. GABAergic neurons

Many types of GABAergic cortical neurons have been described in the cortex. All of them come from a telencephalon region, the subpallium, which also produces neurons from the basal ganglia, and then migrate to the cortex (Anderson, 1997). There are several classifications to categorize these different types of neurons. One of them classify them regarding the expression of specific molecular markers, others are based on the morphology or the intrinsic properties. Three major classes stand out regarding molecular markers (Figure 1.5), accounting for nearly 100% of cortical GABAergic neurons: the Parvalbumin-expressing (PV) neurons, the Somatostatin-expressing (SST) neurons, and the $5HT_{3A}$ receptor-expressing ($5HT_{3A}R$) neurons (Rudy et al., 2011).

PV neurons are the major group of cortical GABAergic neurons, representing 40% of them. They have clearly distinct electrical properties. They present a short action potential duration and a high spiking frequency; therefore, they are identified as fast-spiking neurons. In the neocortex, PV neurons massively project onto the soma and proximal dendrites of PC, allowing control of the output of these PC (Hu et al., 2014). An entire section is devoted to PV neurons later (part III of the introduction).

SST neurons, also classified as low-threshold spiking or regular spiking non-pyramidal neurons, are the neocortex's second main GABAergic population (Urban-Ciecko and Barth, 2016). As PV neurons, SST neurons' synaptic targets are mainly neighboring pyramidal cells. Contrary to PV neurons, SST neurons are making synapses mainly to the apical dendrite of PC, allowing control of the received excitatory inputs.

PV and SST neurons are often presented as interneurons. However, a non-negligible proportion of them is long-range neurons, especially PV neurons. Indeed, it has been reported that PV neurons from different cortices, including M1, are projecting to their contralateral homotypic area, and up to 40% of them exhibit this inter-hemispheric projection (Rock et al., 2018; Zurita et al., 2018). Furthermore, long-range M1 PV and SST neurons are projecting to the striatum (Rock et al., 2016; Melzer et al., 2017). Even if they represent a small population, up to a third of the direct pathways' spiny projection neurons respond to optogenetic stimulation of these cortical GABAergic neurons (Melzer et al., 2017). These long-range connections are functional, as PV neurons stimulation leads to a decreased locomotion, while stimulation of SST neurons increased it.

$5HT_{3A}R$ neurons represent the third largest class of GABAergic cortical neurons but are a very heterogeneous group. They can be divided into two main sub-classes; the one expressing the neuropeptide VIP and the non-VIP, also called neurogliaform. VIP-positive neurons preferentially target other GABAergic neurons in the motor cortex (Donato et al., 2013; Bohannon and Hablitz, 2018).

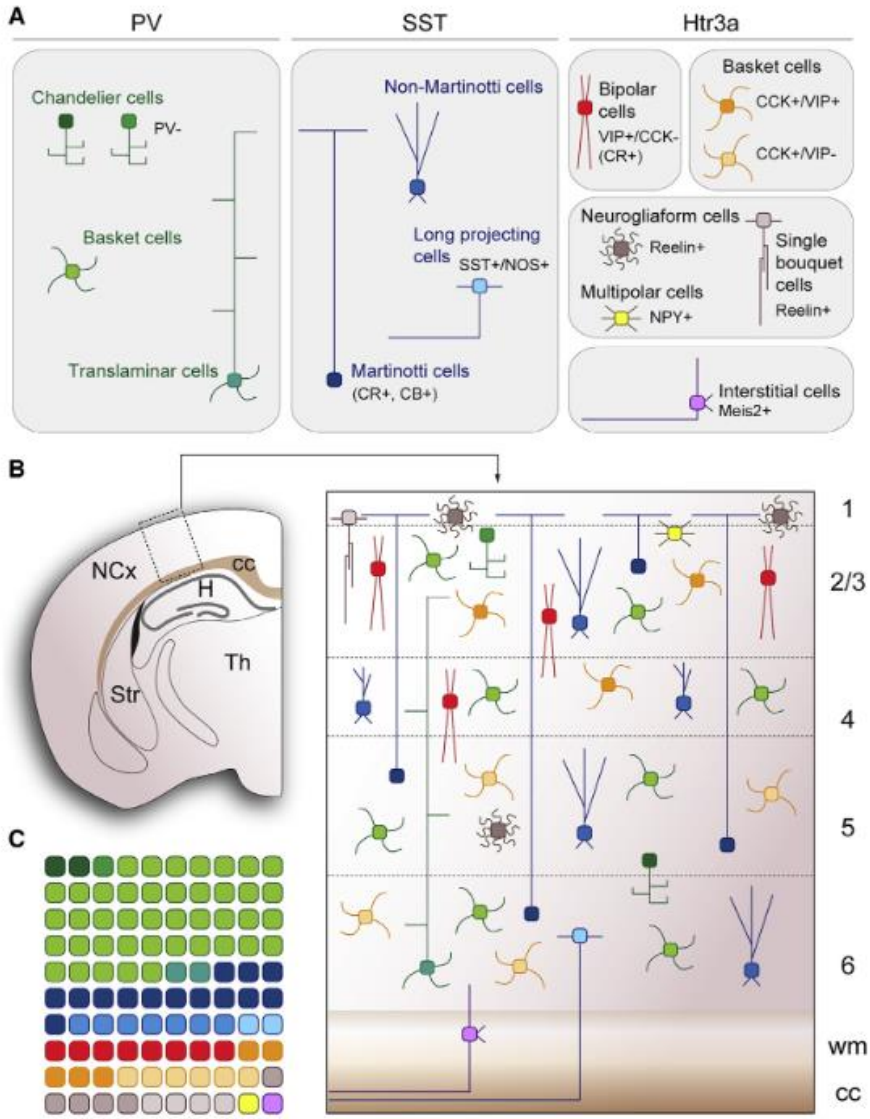

Figure 1.5: Diversity of GABAergic neurons in the neocortex. A, Schematic representation of the 3 major classes of cortical GABAergic neurons in the neocortex. **B**, Schematics representing the localization of GABAergic neuronal population across neocortical layers. C, Schematic illustrating the approximate relative proportion of cortical GABAergic neurons. The different cell-types are color-coded as in the panel A. Figure from Lim et al., 2018.

2.2. M1, a key structure in motor function and learning

2.2.1. M1 involvement in motor execution

Using short electrical stimulations and lesions of M1 it has been demonstrated a long time ago that M1 is involved in motor function. In 1870, Fritsch and Hitzig showed that electrical stimulation of specific regions of the cerebral cortex of a non-anesthetized dog induced discrete movements (Gross, 2007). Later on, in humans, Penfield and Boldrey described for the first time the motor homunculus (Penfield and Boldrey, 1937) using electrical stimulation of various cortical regions. This functional somatotopy is organized in a way that each part of the body corresponds to a specific area in M1. The size of the body part representation depends on the complexity of its achievable movements; the more complex the movements, the larger the region (Woolsey et al., 1952; Brown and Teskey, 2014). This M1 mapping has also been described across many other animal species, like non-human primates or rodents (Luppino et al., 1991; Remple et al., 2006; Tennant et al., 2011). However, defining M1 boundaries can be difficult depending on the species as it may overlap with the somatosensory cortex. Thus, in humans and other primates, these 2 cortices are well segregated (Kaas, 2004), while in rodents, a significant overlap is observed (Hall and Lindholm, 1974). Interestingly, a complete overlap between those two cortices has been reported in a marsupial opossum considered as a 'primitive' species (Frost et al., 2000), suggesting that the segregation between M1 and the sensory cortex might be linked to the appearance of more dexterous movements and may underlie a specification of pure motor M1 areas involved in dexterous abilities. In addition, unilateral lesions of the M1 forelimb area (Brown and Teskey, 2014) in rodents induce deficits in the contralateral forelimb movements with, the larger the lesion, the larger the impairments (Touvykine et al., 2016). In non-human primates,

it has also been shown that M1 lesions especially affect dexterous movements, like grasping (Savidan et al., 2017). Finally, in humans, lesions of M1 or the pyramidal tract led to paralysis that may be partially recovered if the lesion is superficial. This lesion approach shows differences among species, mainly on M1 rehabilitation. Indeed, lesions in humans induce deficits in movements and, to a more considerable extent, dexterous movements. If the lesion is too important, it can lead to total paralysis with no recovery possible (Kwakkel et al., 2003; Darling et al., 2011). Meanwhile, in other primates, M1 lesions can be recovered entirely, maybe through compensation by subcortical areas (Leyton and Sherrington, 1917; Lashley, 1924; Darling et al., 2011). Non-primate mammals, including rodents, can still perform most of their behavioral repertoire, which is already learned and mainly non-dexterous, after M1 lesions (Kawai et al., 2015). They are also capable of recovering rapidly after those lesions. Altogether, the lesion approaches strengthen the hypothesis that M1 plays an essential role in dexterous movements, which take a prominent place in the human behavioral repertoire. More recently, using an optogenetic approach in rodents, Galiñanes *et al.* showed that silencing M1 blocks movement initiation and stops the already-initiated movements in a forelimb reaching and grasping task (Galiñanes et al., 2018). This work emphasizes once again the prominent role of M1 in dexterous motor sequences.

In addition to the motor somatotopy, a behavioral repertoire mapping has been described in M1. Indeed, while a short electrical stimulation is able to elicit muscle contraction, an electrical stimulation lasting for a relevant behavioral duration (0.5 seconds) is sufficient to create complex movements (Graziano et al., 2002, 2005; Graziano and Aflalo, 2007). Those complex movements are in the behavioral repertoire of the studied species. They are arranged across the cortex depending on the target location in space to which the movement is directed. Such

arrangement of movement can be found at the cellular level in rodents: L2/3 PC are activated for specific movement directions and target positions for reaching movements (Galiñanes et al., 2018).

2.2.1. Role of M1 in motor learning

2.2.1.1. Highlighting M1 in skill learning

Besides its prominent role in motor execution, M1 is also crucial for more cognitive functions. Indeed, M1 is a key structure for learning new motor skills (Smyth et al., 2010; Kida et al., 2016; Bachtiar et al., 2018; Dupont-Hadwen et al., 2019). Complex motor skills and habits are not innate; they must be learned through trials and errors. Motor skill learning consists in improving the speed, accuracy, and consistency of a specific movement throughout training that lasts over time. Once learned, the stereotyped movement is executed automatically in response to its specific cue. M1 is instrumental both for the acquisition (Hosp et al., 2011) and the maintenance (Ohbayashi, 2020) of motor sequences. During motor training and learning, the M1 corticomotor map is reorganized with, for instance, an increase of the area corresponding to the body part involved in the trained task (Monfils et al., 2005). However, the role of M1 in the maintenance of motor sequences is still blurry when looking across species. Indeed, rodents that learn a task where they learn to pull a lever are still able to do the movement after M1 lesions (Kawai et al., 2015). The blockade of protein synthesis is also insufficient to alter a learned motor sequence in rodents, while it is sufficient to alter this same task's learning (Hosp et al., 2011). However, in primates, the protein synthesis blockade in M1 is sufficient to alter learned dexterous motor sequences without altering motor execution (Ohbayashi, 2020). Those concordant data may underlie, once again, the fact that M1

may play a more critical role for dexterous skill learning, and those subcortical areas may not be able to compensate in species with a more dexterous behavioral repertoire.

Suppressing the activity of the contralateral motor cortex *via* optogenetic stimulation of GABAergic neurons prevents the correct execution of the reaching and grasping movement in rodents (Guo et al., 2015a). Indeed, the suppression of the neuronal activity before the initiation of the movement prevents its initiation, while the suppression during the reaching or the grasping phases disturbs the movement. Once the optogenetic stimulation is over, mice were able to perform the learned prehension movement. These data suggest that a specific motor engram, corresponding to a learned behavioral action, is evoked at the inhibition termination.

M1 projection to the cerebellum seems to be important during skill execution. Disrupting this connection during a reaching/grasping movement impairs the movement precision, accuracy, and time of execution (Guo et al., 2021). The cortico-cerebellar pathway seems then to contribute to small adjustments during the movement to perfect the movement in real-time.

2.2.1.2. M1 plasticity with motor learning

Different motor learning paradigm has been used to study motor learning, especially in rodents. One quick test to assess motor coordination and learning in rodents is the rotarod test. Rodents are placed on a rotating cylinder and must learn how to stand on it (Deacon, 2013). The test can be performed for 3 days or more, and rodents improve quite rapidly their performances (Kida et al., 2016). With this rotarod learning paradigm, Kida and colleagues showed that the AMPA/NMDA ratio and mEPSCs were transiently increased while mIPSCs were decreased in layer 2/3 of the forelimb representation of M1 already after one day of training (Kida et al., 2016). Interestingly, they showed that the excitability of the pyramidal cells in this M1 area was decreased the first day of training but increased the second day compared to control non trained mice. These data indicate that dynamic and complex changes occur in M1 during motor learning, both in excitatory and inhibitory neurons. However, this rotarod task is mainly involving the hindlimb and then may not be optimal to study M1 knowing that M1 may play a more important role for dexterous movement. To that aim, the single pellet reaching task (SPRT) might be optimal. This forelimb grasping task has been used by many and some automatized versions of this paradigm have been developed (Fenrich et al., 2015; Bova et al., 2019; Salameh et al., 2020). The movement performed in this task by mice and rats is composed of different phases which are very similar to the one performed by humans in a similar ball prehension task (Klein et al., 2012). This makes the results obtained with SPRT easily transposable from rodents to humans.

Recordings of neurons in all layers of M1 during SPRT have revealed that L5 PC and PV neurons are primarily recruited during movement execution (Isomura et al., 2009; Huber et al., 2012; Li et al., 2017; Levy et al., 2020), while L2/3 neuronal activity is outcome-related in the M1 forelimb area (Levy et al., 2020). This suggests

there is a cell type- and layer-specific separation of monitoring and control of motor function during motor skill learning. Furthermore, reporting of motor outcomes by L2/3 neurons seems to emerge from the learning process, as the number of indicative neurons increases during learning (Levy et al., 2020).

In layer 2/3 of M1, mEPSCs are increased after 5 days of training at the SPRT while mIPSCs are not changed (Padmashri and Dunaevsky, 2019). Biane and colleagues showed that following SPRT learning, mEPSCs are increased specifically on L5 cortico-spinal neurons projecting to the C8 spinal region (corresponding to the distal forelimb muscles), and those also exhibit increased excitability (Biane et al., 2019). In addition, the local recurrent connectivity between these pyramidal cells is increased with learning (Biane et al., 2019), and the same is found for thalamo-cortical projections (Biane et al., 2016).

GABAergic neurons may play an important role in shaping the network during skill acquisition. In humans, the amount of GABA in M1 during motor skill learning while no change is observed on glutamate concentration (Kolasinski et al., 2019). Furthermore, a higher concentration of GABA in M1 was associated with lower learning performances.

During the learning process, a substantial proportion of L5b neurons progressively change, from being non-informative about forelimb velocity and trajectory to possessing similar information about motor behavioral outputs to neurons that exhibit clear movement-encoding firing at the beginning of training (Li et al., 2017). Several studies also report the induction of long-term plasticity during motor skill learning(Guo et al., 2015b; Li et al., 2017). These intrinsic and synaptic plasticities are thought to stabilize the patterns of activity in M1 which goes with motor learning (Peters et al., 2014; Li et al., 2017) and certainly contribute to the augmentation of movement-encoding L5 neurons in trained animals. It has also been

shown that new spines in the dendrites of L5 PC are generated when motor skills are learned, and their survivability is increased (Harms et al., 2008; Xu et al., 2009; Guo et al., 2015b). Using mice lacking paired immunoglobulin receptor B ($PirB^{-/-}$), Albarran and colleagues demonstrated that NMDA-dependent LTP, whose expression is under the control of PirB, promotes M1 PC stabilization of newly formed dendritic spines that are associated with enhanced acquisition and maintenance of motor skills (Albarran et al., 2021). The mechanistic target of the rapamycin (mTOR) pathway may also be involved here as it is crucial for spinogenesis (Li et al., 2010). Treadmill exercise in mice increases both spinogenesis and motor learning (at a rotarod test) *via* the mTor pathway (Chen et al., 2019b). These findings are consistent with previous studies showing that impairing intrinsic or/and synaptic plasticity in M1 is sufficient to impair motor skill learning (Hayashi-Takagi et al., 2015; Biane et al., 2019).

At the subcellular level, mRNA analysis showed that a wide number of genes were up-or down-regulated during the early learning stage of the SPRT in rats (Hertler et al., 2016). Interestingly, this analysis revealed that a sequential gene expression regulation occurs, with non-overlapping gene regulated 1h, 7h, or 24h after the training session, meaning that specific genes are regulated at specific times and a higher number of gene regulation after 24h. This 24h peak in gene regulation is consistent with the need to have the same amount of time between training sessions to improve its performances during skill learning (Lugassy et al., 2018).

2.3. Dopamine in M1

2.3.1. Dopamine innervation and receptors in M1

In primates, dopaminergic fibers are found in all M1 layers while in rodents they are mainly located in the deepest layers (Descarries et al., 1987; Berger et al., 1991; Hosp and Luft, 2013). By labeling the dopamine transporter, it has been shown in rodents that dopamine fibers seem to project on the forelimb area in M1, and preferably the deep layers (Vitrac et al., 2014; Hosp et al., 2015) (Figure 1.6). Retrograde labeling also demonstrated that the dopaminergic fibers are coming mainly from the VTA, and to a lesser extent from the SNc (Molina-Luna et al., 2009; Hosp et al., 2011). These VTA projections are functional as stimulation of the VTA triggers activity in M1 (Hosp et al., 2011) and this triggered activity can be blocked by D1 or D2 receptors antagonists. The mesocortical dopamine pathway seems preserved across species, indicating that it is certainly a functionally important pathway for M1 computation. In humans, it has also been shown that VTA dopaminergic neurons project to motor areas (Hosp et al., 2019). D1-like and D2-like dopamine receptors are expressed in the primary motor cortex of many species (Camps et al., 1990; Mansour et al., 1990; Huntley et al., 1992; Gaspar et al., 1995). Indeed, M1 PT neurons express D1, D2, and D5 dopamine receptors (Awenowicz and Porter, 2002a).

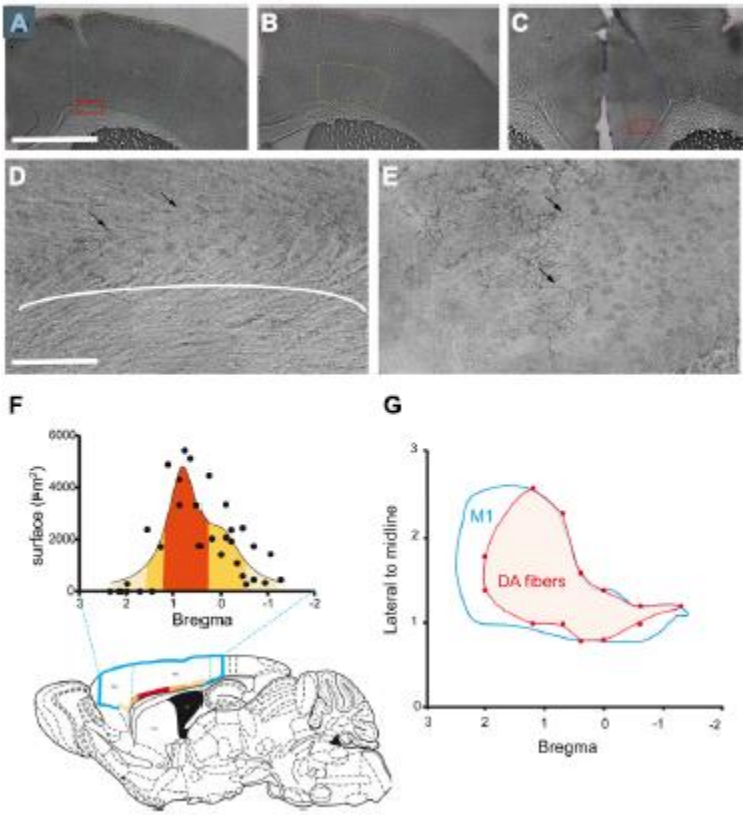

Figure 1.6: Distribution of dopaminergic terminals in M1 in mice. A-C, example images of DAT immunostaining in M1 (A), M1 deepest layer (B), and cingular cortex (C). **D-E**, zoomed view of the DAT immunostaining in M1 deep layer (D) and the cingular cortex (E). **F**, Rostrocaudal distribution of DAT immunostaining in the cortex (top) and sagittal view of the mouse brain (bottom) the brain. **G**, Distribution of DAT staining on a top view of the brain. M1 is circled with a blue line. Adapted from Vitrac et al., 2014.

2.3.2. The effect of dopamine on M1 neuronal populations

Intracellular cascades induced by dopaminergic receptor activation are complex and vary with the cell types and the brain region. In M1, little is known about the signaling pathways used by dopaminergic receptors to modulate neuronal excitability. Traditionally, activation of D1-like versus D2-like receptors has opposite physiological effects, stimulating or inhibiting respectively the protein kinase A (PKA) signaling cascade (Mishra et al., 2018). However, in M1, DA receptors have been shown to work differently. Indeed, phospholipid C (PLC) inhibitors and PKA inhibitors impair the long-term plasticity in M1 neurons (Rioult-Pedotti et al., 2015). In addition, D1 or D2 blockade in M1 induces impairment in motor skill learning and M1 long-term plasticity, but PLC agonist injection is sufficient to prevent those impairments. These data, therefore, suggest a similar effect of both types of receptors in M1, as it can be found in the prefrontal cortex (Trantham-Davidson, 2004). Several studies have looked at the modulations exerted by dopamine on M1 neuronal populations, mainly on PC (Huda et al., 1999, 2001; Awenowicz and Porter, 2002a; Vitrac et al., 2014; Chen et al., 2019a; Aeed et al., 2021; Li et al., 2021; Swanson et al., 2021). However, the net effect of dopamine on M1 neurons seems controversial. Indeed, some groups find that dopamine has an excitatory effect on L5 PC for example (Parr-Brownlie, 2005; Vitrac et al., 2014). However, other labs have also reported that D2 activation induces an inhibitory effect on PC excitability (Huda et al., 1999, 2001; Awenowicz and Porter, 2002a). Those differences may first be due to the experimental differences (*ex vivo versus in vivo*) or to the drugs and their delivery methods (locally or i.p., dopaminergic receptors agonists or antagonists, or dopamine depletion). The fact that different sub-classes of PC exist should also be considered. Overall, activation of D1 or D2 receptors seems to have an inhibitory effect on PC (Huda et al., 1999, 2001; Awenowicz and Porter, 2002a). This mono-

directional effect of both types of dopaminergic receptors is not surprising to be found in M1, as it is also found in the prefrontal cortex (Gee et al., 2012). Indeed, numerous pieces of evidence have shown the effect of dopamine on both glutamatergic and GABAergic transmission and neurons' properties in the prefrontal cortex (Trantham-Davidson, 2004). The downstream β-arrestin2 signaling pathway (Urs et al., 2016) or the release of neurotensin via activation of D2 autoreceptors of M1 dopaminergic neuron terminals could explain the D2 excitatory effect (Petrie et al., 2005), as is the case in the prefrontal cortex. Nonetheless, it has been shown that *in vivo* dopamine infusion in the forepaw representation of the motor cortex decreases the activity of PT neurons and their evoked response to callosal and thalamic inputs (Huda et al., 1999, 2001); those effects are rescued by the application of dopaminergic antagonists, for either D1 or D2 (Huda et al., 2001; Awenowicz and Porter, 2002b). This decrease in PT neurons activity could be due to the dopamine-mediated increased excitability of PV interneurons. Indeed, neurons from the VTA, the main source of dopamine for M1, project directly to M1 GABAergic neurons (Duan et al., 2020).

2.3.3. Role of dopamine in M1 plasticity

Dopamine is also crucial for M1 plasticity. The *in vivo* pharmacological blockage of both D1 or D2 dopamine receptors in M1 induces a decrease in the long-term potentiation in layer 2/3 (Molina-Luna et al., 2009). In addition, the selective blockade of D2 receptors in M1 induces a decrease of M1 neurons' activity (Parr-Brownlie, 2005). This leads to a slowness of the movement, *i.e.,* bradykinesia, during a skilled reaching task. Moreover, spine turnover in M1 L5 PC is under the control of dopamine: while the elimination of spines involves D1 receptors, spine formation

involves D2R (Guo et al., 2015b). However, the selective blockade of dopaminergic receptors does not affect skill performance once the skill is learned. These data emphasize the role of the meso-cortical pathway and hence cortical dopamine in the acquisition of motor skills, but not in their maintenance, by selecting and potentiating the newly formed spines necessary for the execution of the movement in the learning process while depressing the unnecessary ones. Study of the dopaminergic neurons projecting to M1 seems to confirm this idea. Dopaminergic neurons from the VTA projecting to M1 are specifically activated during successful motor skill learning in mice (Leemburg et al., 2018). Indeed, those neurons, especially the ones located in the caudal VTA, were specifically activated during SPRT training sessions. However, they were not activated by the food reward alone while dopaminergic neurons not projecting to M1 were, regardless of whether the mice were training or not. Once the mice have learned the task, the M1 projecting VTA dopaminergic neurons are not activated anymore during the SPRT, indicating that dopamine release may be increased in M1 specifically during early training sessions. Concomitant with this early dopamine activity in M1, the mRNA-levels analysis revealed that the expression of D1 and D2 dopamine receptors are up-regulated during the early stage of SPRT training (Hertler et al., 2016).

2.4. M1 in Parkinson's disease model

2.4.1. PD animal models

To have a better understanding of the role of dopamine in the pathophysiology of M1 in PD, different animal models have been developed. Neurotoxins such as the 6-hydroxydopamine (6-OHDA) or the 1-Methyl-4-phenyl-1,2,3,6 tetrahydropyridine (MPTP) are used to selectively destroy dopaminergic neurons from the midbrain. These methods try to mimic the loss observed in PD patients and their symptoms (Betarbet et al., 2002; Schober, 2004). Among the studies focusing on M1 in the context of PD, it is important to distinguish those performed with toxin injection in the midbrain (in the medial forebrain area or the SNc) which dramatically reduces the dopamine tone across the brain from those depleting the dopamine only in M1. In the first case, the differences observed on M1 will be due to the lack of M1 dopamine but also to alteration of the basal ganglia which project on M1. On the other hand, specific depletion of M1 dopamine allows the investigation of the specific role of M1 dopamine in its physiology.

2.4.2. Changes in M1 physiology in PD animal models

In 6-OHDA parkinsonian rats, the forelimb representation map is disrupted (Plowman et al., 2011; Viaro et al., 2011), emphasizing the need to investigate the importance of M1 dopamine in movement execution and learning. Motor skills and dexterity have been assessed on this model using the single pellet reaching tasks (SPRT). This motor task is a relevant task to study motor dexterity as the movement

realized is composed of different phases, which are strongly similar between rodents and humans (Klein et al., 2012). M1 activity is disturbed during the grasping phase of the movement after DA depletion (Hyland et al., 2019). Recent studies also reported a decreased activity of PC during reaching movements in dopamine depleted rodents (Aeed et al., 2021; Li et al., 2021). In addition, manipulation of M1 PC was able to partially restore motor behavior (Li et al., 2021). This may underlie that dexterity disturbance observed in PD patients could be due to M1 alteration following dopamine loss, highlighting the need for cortical treatment to target those fine motor troubles. Projection from M1 to subcortical structures is also disturbed in those models. Indeed, direct glutamatergic input from M1 to the STN, known as the hyper-direct pathway, is highly reduced in Parkinsonian rats (Wang et al., 2018). Physiologically, the activation of the hyperdirect pathway leads to an inhibition of movements, and together with the direct and indirect pathways, allows proper control of motor behaviors. This decrease in input from M1, together with a decreased amount of glutamate vesicular transporter 1 in the STN, could be responsible for the abnormal activity of this pathway observed in PD patients.

2.4.3. Alteration of GABAergic neurons in PD animal models

As discussed earlier, GABAergic neurons play a key role in M1 network activity. It is not surprising to find out that inhibition is disturbed in PD patients (Chu et al., 2009). Disturbances in GABAergic cells are also found in rodent PD models. Indeed, MPTP infusion in the rat cortex leads to a destabilization of dendritic spines as well as impairments in motor learning (Chen et al., 2019a). This MPTP infusion also leads to a suppression of SST neurons activity and increased calcium activity in pyramids apical dendrites. However, re-establishing an activity in SST neurons, with a chemogenetics approach, rescues dendritic spines loss and motor deficits. Furthermore, parvalbumin levels are increased in Parkinsonian rats (Capper-Loup et al., 2005). PV neurons' electrical properties are strongly linked to their parvalbumin levels (Donato et al., 2013), indicating a putative dysfunction of PV neurons in this model. In addition, M1 proteomic analysis showed modification in proteins involved in autophagy, mRNA processing, ATP binding, or maintaining the balance of neurotransmitters (Li et al., 2017). PET imaging in this model also revealed that M1 also undergoes glucose hypometabolism, which is also observed in PD patients (Jang et al., 2012). Altogether, those data emphasize the importance and the relevance of this model in PD studies, to look for new therapeutic targets and methods.

DBS of the STN is a PD symptomatic treatment but only a minority of PD patients are eligible for it (Valverde et al., 2020). It is then primordial to find out how DBS can suppress PD symptoms in order to make it accessible to a larger amount. DBS in the STN counters the hyperactivity of M1 pyramidal cells observed in hemi-parkinsonian rats. *In vivo* patch-clamp recordings showed a reduced excitability of PC following STN stimulation. However, DBS of the STN has opposite effects on

cortical GABAergic neurons by decreasing the firing rate of PV neurons while increasing the one of SST neurons. In addition, by specifically increasing SST neurons activity *via* an optogenetic approach, Valverde et al. did alleviate motor symptoms in Parkinsonian rats. The optogenetic activation of M1 neurons leads to motor improvement to a lesser extent. Those data suggest that the disturbance of M1 circuitry may come from the inputs that PC receives and not in their own properties. Indeed, SST neurons are projecting to the apical dendrites of PC, thus controlling the excitatory inputs they receive. Opto-activation of SST neurons in parkinsonian rats can then lead to improved processing of the information in M1. PV neurons are known to control the spiking activity of PC, their opto-activation may only shut down PC activity, not helping the processing of disturbed excitatory inputs to M1. It may explain the lesser impact on motor symptoms when PV neurons are stimulated rather than SST neurons. Altogether, it is nonetheless suggesting that cortico-motor GABAergic neurons could be a putative target for a more precise alternative than STN DBS.

2.4.4. Motor learning in DA loss models

As said earlier, in addition to motor deficits, PD patients exhibit alteration in skill learning. Acquisition of dexterous skills is studied in rodents thanks to a food prehension task; the single pellet reaching task. Selective depletion of dopaminergic fibers projecting to the M1 corresponding to the trained limb alters the acquisition of this skill in rats and mice (Molina-Luna et al., 2009). The selective blockade of either D1 or D2 dopamine receptors in M1 is also sufficient to alter skill learning. However, neither the M1 dopamine depletion nor the selective blockade of

dopaminergic receptors affected skill performances. Those data emphasize the role of M1 dopaminergic fibers in motor skill acquisition but not in their maintenance. Guo and colleagues also showed the impact of dopamine loss on M1 dendritic spines in the context of skill learning (Guo et al., 2015b). Throughout the training to a new motor skill, the survivability of those spines increases and is still increased 30 days after the last training sessions. This increased spine survivability is only present during the first training session in M1 dopamine depleted mice and is no longer present 30 days after the last training. This destabilization of spines' survival, in both formation and elimination, may contribute to learning deficiency observed in those dopamine depleted mice. MPTP intoxication in non-human primates has different effects regarding the different cortico-motor neuronal populations (Pasquereau and Turner, 2011). M1 activity related to movement is decreased, mainly in PT neurons, not in IT-CStr (Pasquereau et al., 2016). In addition, M1 timing activation is also disturbed in this model. Indeed, PT neurons' movement-related activity is impaired, with earlier onset activation and a longer activation.

IV. Parvalbumin neurons

PV neurons are one of the main GABAergic neurons in M1. The parvalbumin is an excellent marker for these neurons and allows post hoc immunolabeling to identify PV neurons (Celio, 1986; Eggermann and Jonas, 2012). The PV is an acidic, cytosolic Ca2+ binding protein with a low molecular weight and serve as a calcium and magnesium buffer (Arif, 2009). In addition, the PV has also antioxidative properties, and the decrease of PV in a cell could lead to oxidative damages observed in schizophrenia (Permyakov et al., 2014). It also has been shown that PV could impact synaptic release through its Ca2+ buffer property (Eggermann and Jonas, 2012). The high selectivity of the PV gene promoter is useful to produce transgenic animal lines and/or viral approaches to genetically target PV neurons.

4.1. Embryonic origin

Neocortical PV neurons' embryonic origin, as the other GABAergic cells, is different from pyramidal cells. Indeed, they originate from the same embryonic region as the neurons from the basal ganglia, i.e. the embryonic subpallium (Anderson, 1997). The subpallium is part of the striatum primordium and PV neurons are coming from the medial ganglionic eminence (MGE) (Figure 1.7). Progenitor cells underwent a long tangential migration from the MGE toward the marginal zone of the embryonic neocortex to finally go through a radial migration into their final neocortical layer. The determination of the final fate of cortical GABAergic neurons is still unclear. However, the establishment of their ending

position seems to depend on both intrinsic and extrinsic factors (Peyre et al., 2015). Indeed, at a given time point in development, the terminal destination of cortical GABAergic neurons depends on their cellular age (Lopez-Bendito et al., 2008).

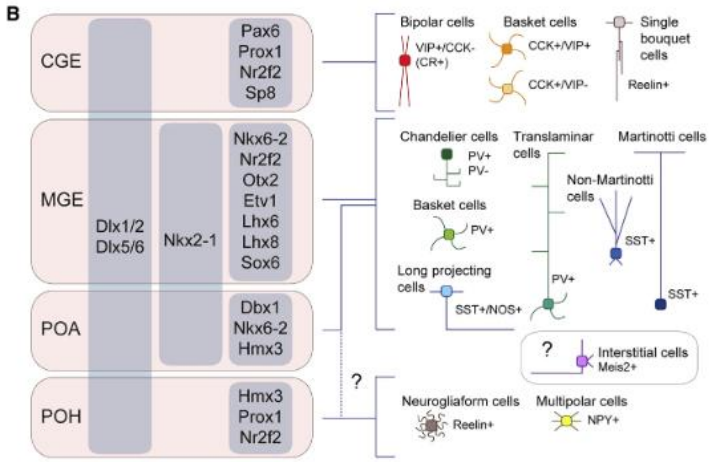

Figure 1.7: Developmental origin of cortical GABAergic neurons. Regional origin of cortical GABAergic populations. CGE: caudal ganglionic eminence, MGE: medial ganglionic eminence, POA: Preoptic area, POH: preoptic-hypothalamic. Figure from Lim et al., 2018.

4.2. PV electrical and morphological properties

PV neurons present salient electrical properties. They are called fast-spiking neurons due to their ability to generate short action potentials at a very high rate (Hu et al., 2014). This electrical phenotype makes them easily identifiable in experimental conditions. If we look at the morphological properties of PV neurons, 3 major subclasses stand out: the chandelier cells, the basket cells, and the translaminar cells. The most abundant type of PV neurons in the neocortex is the basket cells. This name derives from the fact that their axon takes a basket-like shape around pyramidal cells' somata and proximal dendrites and other GABAergic neurons (Hu et al., 2014). They are distributed across layers 2 to 6 in the neocortex. Chandelier cells, also called axo-axonic, exhibit the most recognizable morphology as the very characteristic shape of their axonal arborization looks like a chandelier light. Chandelier cells are making axo-axonic synapses onto pyramidal cells' axonal initial segment (Somogyi et al., 1982). They are particularly abundant in layer 1, 2, and 6 (Taniguchi et al., 2013) and their regional distribution are very heterogeneous (Inda et al., 2009). Translaminar PV neurons are the less common PV neurons and their somata can be found in layers 5 and 6 (Buchanan et al., 2012; Bortone et al., 2014). They are targeting pyramidal cells across all layers (Bortone et al., 2014). PV neurons are densely covered by synapses, mainly excitatory, and receive information from different layers. It allows them to process the information from pyramidal cells over a large area through the feedforward and feedback inhibition pathways.

Contrary to other GABAergic neurons in the neocortex, PV neurons exhibit a long and extensively arborized axon (Karube, 2004). By targeting the perisomatic areas of a large number of PC (somata and proximal dendrites or the axon initial segment for basket cells or chandelier cells, respectively), PV neurons exert a strong

inhibition over their synaptic targets. Indeed, their post-synaptic innervation patterns trigger inhibition close to the action potential initiation site, giving them control over principal cells output.

4.3. Role in the local network

Even if they are low in number in comparison to pyramidal cells, their role is nonetheless crucial. By massively projecting onto somata and proximal dendrites of PC, PV neurons are powerful regulators of cortical activity (Ferguson and Gao, 2018; Serrano-Reyes et al., 2020), and are well-placed to select the inputs coming to the motor cortex to refine its outputs. PV neurons are involved in two kinds of inhibition mechanisms. Firstly, they are involved in feedforward inhibition (Figure 1.8.A). In this context, the same excitatory input stimulates a PV neuron plus a PC itself receiving input from the PV (Isaacson and Scanziani, 2011). This type of inhibition can have different purposes. One of them is to narrow the windows for temporal summation of excitatory inputs to the inhibited PC (Pouille and Scanziani, 2001). It also allows the expansion of the dynamic recruitment of principal cells (Pouille et al., 2009). This feedforward inhibition may be an important feature for motor learning as movement noise and variability may be crucial for learning (Dhawale et al., 2017). The second inhibition type in which PV neurons are involved is the feedback inhibition. In this case, there is a reciprocal connection between a PV neuron and a PC (Isaacson and Scanziani, 2011, Figure 1.8.B). Feedback inhibition comes into two forms: recurrent and lateral. This inhibition form allows a 'winner-takes-all' mechanism in the local microcircuitry (de Almeida et al., 2009a, 2009b). The leading PC, with the strongest excitatory input, shuts down the activity of competing

neighboring PC through PV inhibition. To sum up, PV neurons have a strong impact on the cortical microcircuitry by shaping its output activity.

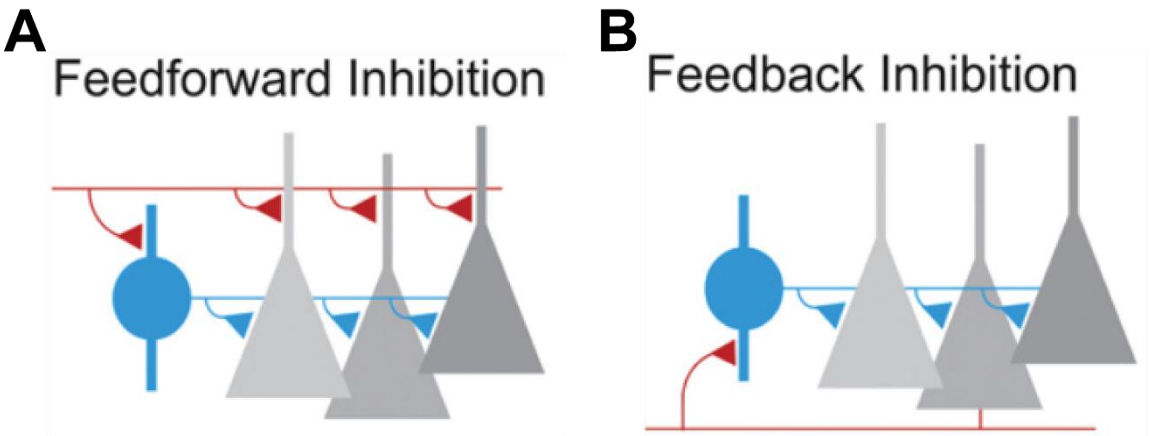

Figure 1.8: Schematics representing the feedback and feedforward inhibitions. **A**, Feedback inhibition is generated when a PC (grey) make excitatory synaptic connections on local inhibitory neurons (blue) that will then form inhibitory connections on multiple PC. **B**, Feedforward inhibition is generated when long-range excitatory input (red) contacts PC (grey) and an inhibitory neuron (blue). Figure from Isaacson and Scanziani, 2011.

4.4. Connectomics

4.4.1. Inputs to PV

4.4.1.1. Local inputs:

Pyramidal cells are highly targeted by their neighboring PV neurons. The connectivity from pyramidal cells to PV neurons is up to 50% (Jouhanneau et al., 2018), which is much higher than PC to PC connectivity (6-7%) (Holmgren et al., 2003; Jouhanneau et al., 2018). This dual connectivity between PC and PV neurons leads to two main functionalities in the microcircuit dynamics described earlier: feedforward and feedback inhibitions (see part 4.3 of the introduction). VIP interneurons have also been shown to project onto PV neurons (Donato et al., 2013). PV neurons receives also input from other GABAergic neurons: other PV neurons are projecting to their dendrites while VIP neurons are targeting their soma (Hioki et al., 2013; Pfeffer et al., 2013). A small number of GABAergic inputs can also come from SST neurons (Pfeffer et al., 2013), mainly in layer 4, allowing disinhibition of PC through inhibition of PV neurons (Xu et al., 2013). however, the presence of the layer 4 is debated in M1 (Yamawaki et al., 2014).

4.4.1.2. Long-range inputs:

Recently, a whole-brain map of long-range inputs to the major GABAergic populations, including PV neurons, in the mouse Caudal forelimb Area has been made combining a monosynaptic rabies virus system and a PV-Cre mouse line (Duan et al., 2020). The caudal forelimb area is composed of both motor and sensory primary cortices representing the forelimbs, and in which an electric stimulation elicits a forelimb movement. This study shows that the major long-range inputs are coming from other cortical regions, and another important number of inputs are coming from the pallidum and the thalamus.

4.4.1.3. Autapses:

A synapse made by a neuron on itself is called an autapse. PV neurons in the motor cortex are frequently making autapses. Indeed, morphological analysis of PV neurons filled with biocytin revealed axon collaterals juxtaposed to their somata (Thomson et al., 1996; Cobb et al., 1997; Tamás et al., 1997). It has also been shown that this GABAergic feedback autaptic transmission is activated each time the cell fires in the sensorimotor cortex (Bacci et al., 2003). In the somatosensory cortex, the synapses made by PV neurons on themselves have a more powerful strength than synapses they made to other PV neurons or PC (Deleuze et al., 2019), exposing the putative importance of autapses in PV neurons operation. Indeed, while PV neurons are known to have a fast and precise spike-timing activity, the blockade of autaptic transmission in the somatomotor cortex leads to alteration of this spike-timing precision (Bacci and Huguenard, 2006) and slow down their firing activity (Connelly and Lees, 2010).

4.4.2. PV's Outputs

4.4.2.1. Local outputs:

As said before, the main synaptic target of PV neurons is local pyramidal cells. Indeed, inhibition of PC in the cortex is mainly intralaminar (Kätzel et al., 2011). They are highly connected to PC close to their cell body (up to 70% connectivity under 200 microns), and this connectivity slowly decreases with the distance (Holmgren et al., 2003; Kapfer et al., 2007; Jouhanneau et al., 2018). Apart from PC, PV neurons are mainly projecting to other PV neurons (Hioki et al., 2013; Pfeffer et al., 2013) and can

be connected through electrical coupling (Meyer et al., 2002). They can also project in a lesser extent on VIP neurons(Pfeffer et al., 2013).

4.4.2.2. Long-range projections:

PV neurons are often called interneurons. However, in cortical structure, especially in M1, PV neurons can be long-range GABAergic cells. It has been shown that they project to the striatum (Jinno and Kosaka, 2004; Melzer et al., 2017). By projecting preferentially on spiny projection neurons from the direct pathway (dSPN) in the striatum, their activation leads to reduced locomotion in mice. This shows that corticostriatal PV neurons can directly modulate motor output. Cortical PV neurons also project to the contralateral hemisphere. Indeed, it has been reported that PV neurons from the motor, visual and auditory cortices are projecting to their contralateral homotypic area (Rock et al., 2016; Zurita et al., 2018). Quantitative analysis in the auditory cortex even revealed that 40% of the PV neurons are callosal cells. While quantitative analysis for M1 has not been done, it seems that they are present in all layers and are going through the corpus callosum (Rock et al., 2018), Figure 1.9).

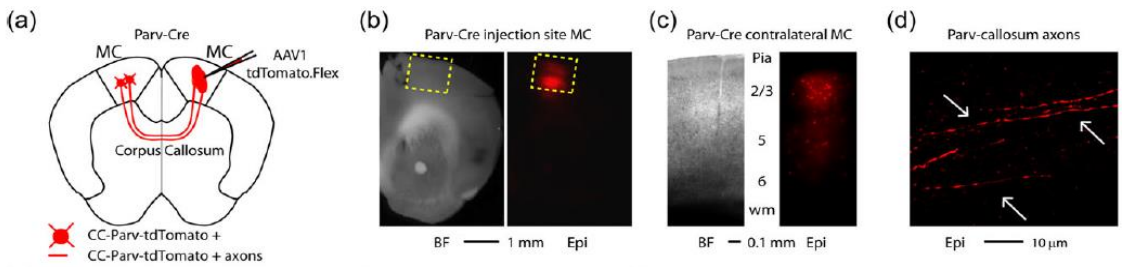

Figure 1.9: Long-range callosal PV neurons in M1. A, experimental protocol: a retrograde virus (AAV1-tdTomato-flex) is injected in M1 of PVCre mice. **B**, viral injection site in M1. **C**, transfected PV neurons in M1 contralateral to the injection site. **D**, Axons of transfected PV neurons in the corpus callosum. Adapted from Rock et al., 2018.

4.5. Dopamine modulation of PV neurons

M1 receives dopaminergic input from the midbrain, and PV neurons are a putative target for it. Indeed, it has been shown that PV neurons receive direct input from the ventral tegmental area (Duan et al., 2020), the main dopamine source for M1 (Descarries et al., 1987; Hosp et al., 2015). Little is known about dopaminergic modulation of PV neurons in M1, however, the depletion of dopamine in rats induces an increase in parvalbumin levels (Capper-Loup et al., 2005). As parvalbumin levels are linked to PV neurons' excitability (Donato et al., 2013), we can thus suppose that the electrical properties of those neurons may be altered in absence of dopamine.

Dopamine could be crucial for PV neurons from their developmental stage (Ohira, 2019, 2020). Indeed, *in vitro* studies on organotypic slices of frontoparietal cortex showed that dopamine accelerates the level of parvalbumin expression, first in layer 5 after 7 days, then in all layers at 14 days (Porter et al., 1999), mainly through D2R. Furthermore, co-culture with mesencephalic slices, that are reinnervating with dopaminergic fibers the cortical slices accelerated parvalbumin expression. As parvalbumin level increases during cortex development, dopamine could accelerate the maturation of cortical networks, and possibly play a role in parvalbumin expression changes in adulthood.

IV. Perineuronal nets (PNN)

4.1. PNN overview

Another feature to consider when studying PV neurons is perineuronal nets (PNN). They were first described by Camillo Golgi in the XIX century (Spreafico et al., 1999), but, if we take a look at the number of publications about PNN on Pubmed, we can see that the interest around them is flourishing since 2015 (Figure 1.10). Those articles include topics from plasticity, learning, memory, to pathologies such as schizophrenia and Alzheimer's disease.

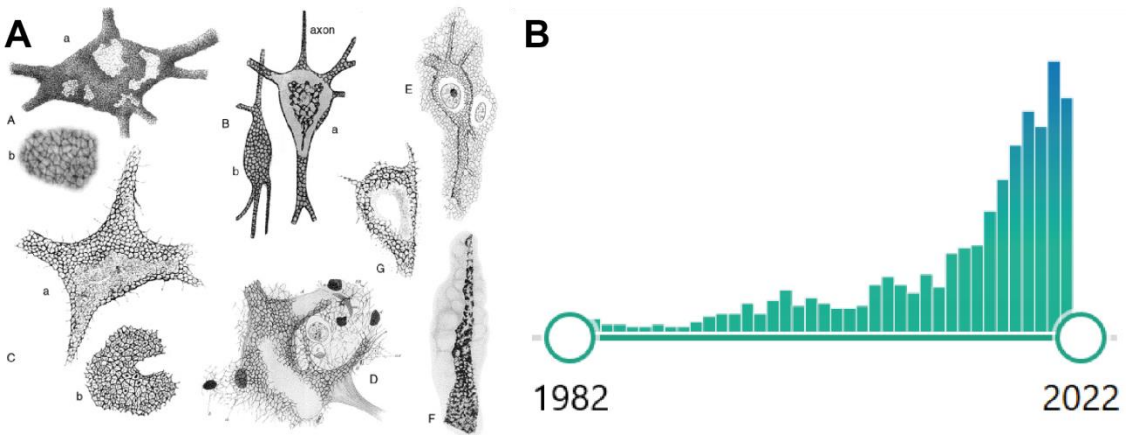

Figure 1.10: Perineuronal nets history. A, Perineuronal nets drawings from the last century. Images from Celio et al., 1998. **B,** Number of results by searching for "perineuronal nets" on PubMed, range by year of publication.

4.2. PNN composition

PNN are part of the extracellular matrix and form a dense structure surrounding certain mature neurons in the central nervous system. Five groups of extracellular matrix molecules formed them: Hyaluronan (HA) and its transmembrane synthesizing enzymes hyaluronan synthases (HAS), chondroitin sulfate proteoglycans (CSPGs), Tenascins (Tn), and hyaluronan/proteoglycans link proteins (HAPLNs) (Figure 1.11). HA, synthesized by the HAS at the cell surface, is the most abundant and key component of PNN. It forms the backbone of the PNN and dictates its mesh-like structure, allowing the binding of the other important component. CSPGs, the second may component of PNN, are lectins that can be aggrecan, versican, neurocan, or brevican (Galtrey and Fawcett, 2007; Kwok et al., 2011). HAPLNs serve as PNN stabilizers by linking HA and CSPGs (Koppe, 1997; Carulli et al., 2007, 2010; Kwok et al., 2010). Different composition creates PNN variations, giving them different chemical properties (Matthews et al., 2002; Dauth et al., 2016). The depletion of either the CSPGs, the hyaluronan, or the link proteins induces a complete loss of PNN, emphasizing the importance of every component in PNN formation and structural maintenance.

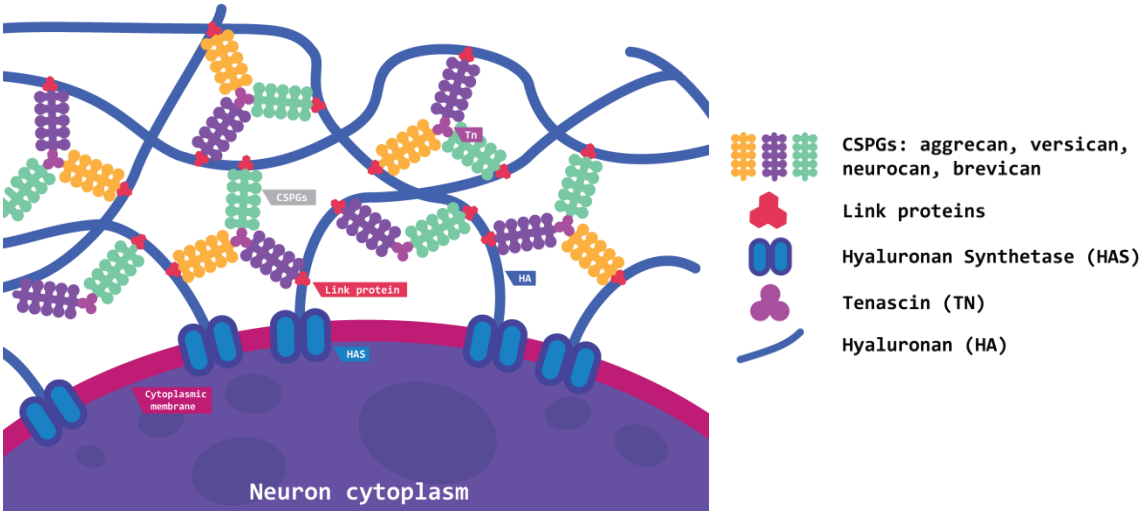

Figure 1.11: Perineuronal nets composition. Schematic representation of PNN composition, wrapping a neuron. PNN are composed of Hyaluronan (HA), hyaluronan synthase (HAS), chondroitin sulfate proteoglycans (CSPGs), Tenascin (Tn), and link proteins.

4.3. PNN synthesis, formation, and regulation

The PNN components are synthesized by both neurons and glial cells (Deepa et al., 2006; Frischknecht et al., 2009; Lensjø et al., 2017; Irvine and Kwok, 2018; Ueno et al., 2018; Bosiacki et al., 2019) across development and in adulthood. The CSPGs are produced by neurons and glial cells (Carulli et al., 2006) but the HAS is only produced by neurons (Galtrey et al., 2008), explaining why only neurons are surrounded by PNN. The synthesis of these components reaches its peak during development and is decreased in adulthood (Carulli et al., 2010). Neuronal activity during development has been shown to impact PNN formation. For instance, chronic neuronal depolarization *via* extracellular potassium ions application on organotypic slices increases PNN formation (Grosche and Bruckner, 2001). Conversely, the blockade of action potential with tetrodotoxin (TTX) decreases the formation of PNN

ex vivo in cultures (Dityatev et al., 2007; Reimers et al., 2007). PNN formation and turnover happen quite rapidly in the adult brain. There is a cyclic change in the amount of PNN in the brain on a daily basis (Pantazopoulos et al., 2020; Harkness et al., 2021). Indeed, in rodents, all over the brain, PNN intensity and number are at their minimum during the light phase (during sleeping time) and reach their peak during the night (awake phase). Interestingly, they also showed that the PV intensity fluctuates in the same manner as PNN does. These data may indicate once again that a decrease of PNN might cause higher plasticity during the sleeping phase. But PNN can also change rapidly following learning. Indeed, PNN expression is specifically increased in the auditory cortex by a fear conditioning test and is back to its normal expression the day after (Banerjee et al., 2017). PNN have to be viewed as something dynamic, but the mechanisms of rapid regulation are unknown and need to be explored. One hypothesis is the implication of microglia as regulators. Indeed, it has been shown that the depletion of microglia in mice leads to an increase in PNN number and intensity, which can be countered by microglia repopulation (Liu et al., 2021).

4.4. PNN in the neocortex

PNN distribution through the central nervous system is unequal (Seeger et al., 1994), but they are abundant in cortical structures, including M1. The PNN developmental window is crucial. Their establishment occurs at different rates and time points depending on the cortical region. Once fully established, they are marking the end of the developmental critical period (Pizzorusso et al., 2002; Nowicka et al., 2009). In the neocortex, PNN are enriched in layers 2 to 5 of motor and sensory areas (Brückner et al., 1999). The majority of neurons surrounded by

PNN in the neocortex are GABAergic, and mainly PV neurons (Härtig et al., 1992a; Dityatev et al., 2007). However, some glutamatergic neurons can be wrapped by PNN, which can also be PV positive (Hausen et al., 1996; Horii-Hayashi et al., 2015).

The presence of PNN can directly have an impact on the intrinsic properties of neurons they are wrapping. One of the main tools used to study the role of PNN is the chondroitinase ABC (ChABC). This enzyme digests the CSPGs leading to the degradation of the PNN. Using ChABC, it has been shown that PNN digestion in different cortices leads to a decreased excitability and to a modification of the action potential shape of PV neurons (Balmer, 2016; Hayani et al., 2018). PNN depletion could also alter other PV neurons properties across different regions in different ways (Wingert and Sorg, 2021). PNN removal can induce a decrease in PV excitability (Balmer, 2016; Favuzzi et al., 2017; Lensjø et al., 2017; Tewari et al., 2018; Christensen et al., 2021) are have no effect (Dityatev et al., 2007; Faini et al., 2018; Hayani et al., 2018). PNN is also able to regulate PV expression levels (Donato et al., 2013). However, it is important to note that the PNN removal methods and duration are not the same throughout the literature (*in vivo* vs *ex vivo*, depletion duration, animal age, etc…), and may explain the differences observed.

4.5. PNN as plasticity limiters and their role in memory

A widely accepted concept is that PNN are limiting plasticity in adulthood in different ways. Their digestion by the ChABC allows the reinstatement of a juvenile-like plasticity state. In other words, PNN may play a crucial role in learning and memory phenomena. For example, PNN degradation after a brain injury has been shown to increase axonal sprouting in the motor cortex (Harris et al., 2013).

Furthermore, this degradation leads to an increased number of neurons activated for a forelimb movement, indicating that PNN have an impact on the network activity. PNN limit plasticity in three different ways: by (1) forming a physical barrier, (2) fixing inhibitory molecules, and (3) limiting the mobility of receptors.

4.5.1. Physical barrier

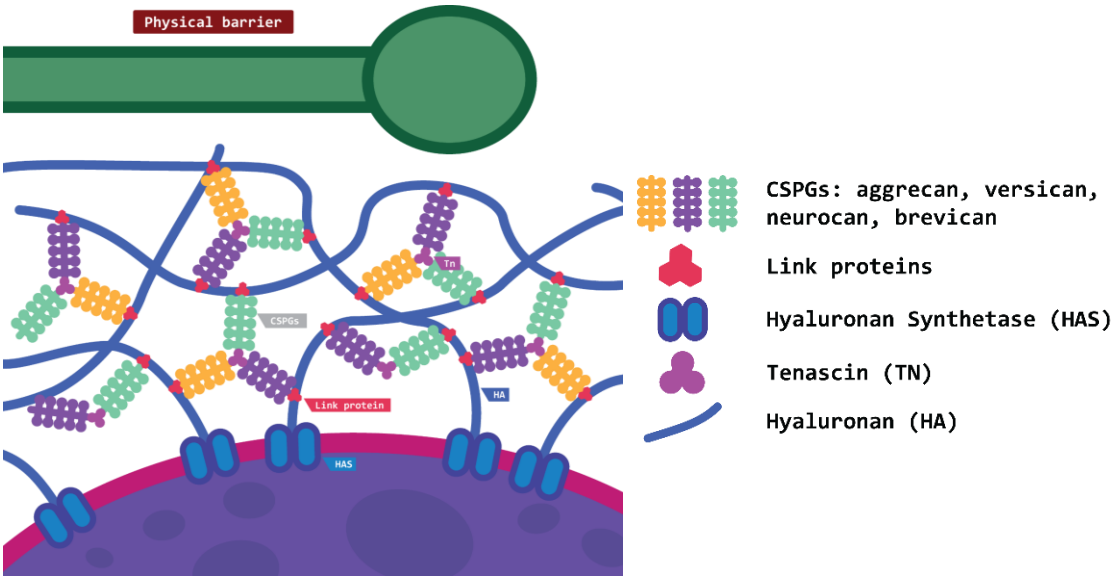

Figure 1.12: Perineuronal nets as a physical barrier. The presence of the PNN at the cell surface prevents the formation of new synapses (green). Perineuronal nets (PNN) are composed of Hyaluronan (HA), hyaluronan synthase (HAS), chondroitin sulfate proteoglycans (CSPGs), Tenascin (Tn), and link proteins.

PNN represent a physical barrier around PV neurons (Figure 1.12). They act as a local buffering compartment and protect them from oxidative stress (Cabungcal et al., 2013; Suttkus et al., 2014; Morawski et al., 2015). This barrier also has a protective effect against toxic molecules. Indeed, PNN seems to protect neurons from the toxicity effect of amyloid-beta (Miyata et al., 2007; Morawski et al., 2012). The fast-spiking activity of PV neurons makes them in need of cations for the proper operation of their synapses. HA and CSPGs are highly negatively charged, allowing the buffering of cations close to the synapse (Härtig et al., 1999), sustaining PV fast activity. PNN can also prevent neurites growth and synapse formation (Härtig et al., 1992b; Shinozaki et al., 2016).

4.5.2. PNN Bind to specific proteins:

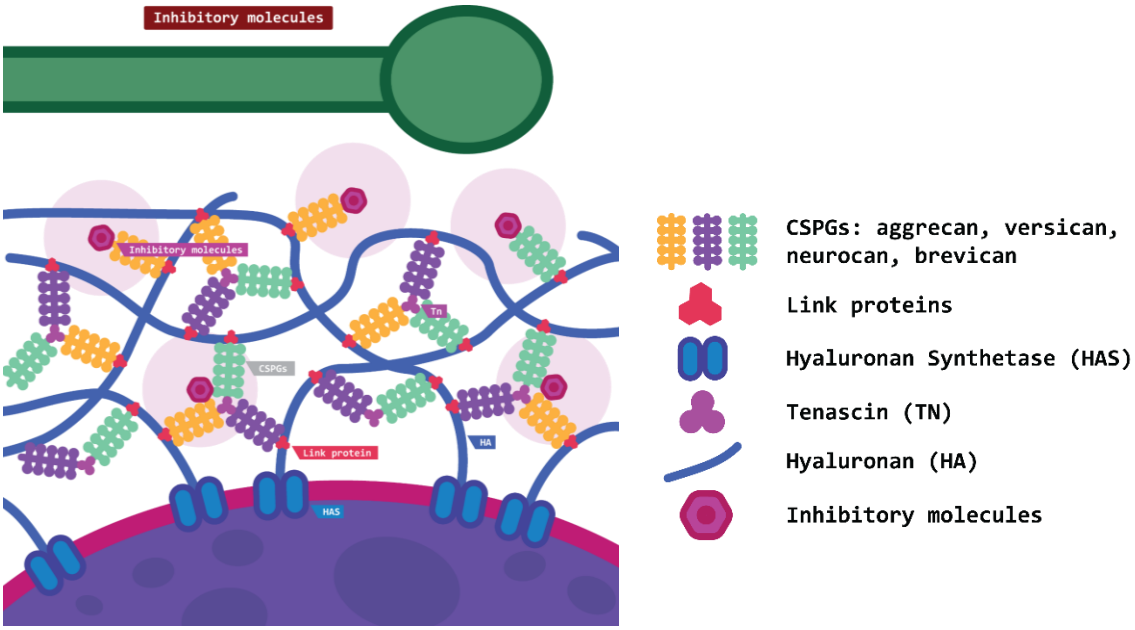

Figure 1.13: Perineuronal nets are binding inhibitory molecules. PNN can fix molecules that inhibit synaptogenesis. Perineuronal nets (PNN) are composed of Hyaluronan (HA), hyaluronan synthase (HAS), chondroitin sulfate proteoglycans (CSPGs), Tenascin (Tn), and link proteins.

The second property allowing PNN to limit plasticity is their ability to bind specific proteins (Figure 1.13). The Semaphorin3a, a chemorepulsive molecule, can bind to CSPGs and prevent the approach of other neuronal axons, preventing the formation of new synapses (de Winter et al., 2016). Some PNN components are also able to bind to membrane receptors and channels: Tn are also able to bind GABA receptors (Bukalo et al., 2007), brevican can modulate potassium channels and AMPA receptors (Favuzzi et al., 2017), and hyaluronan can modulate post-synaptic

L-type calcium channels in the hippocampus (Kochlamazashvili et al., 2010). PNN are also crucial for the capture and internalization of the transcription factor orthodenticle homeobox 2, which is necessary for PV neurons maturation and regulate plasticity (Beurdeley et al., 2012).

4.5.3. PNN limit receptors mobility:

The mobility of protein at the neuronal surface is limited by PNN (Figure 1.14). Indeed, it has been shown that ChABC application increases the lateral diffusion of AMPA receptors (Frischknecht et al., 2009). The fast diffusion of desensitized AMPA receptors is needed when the synapse undergoes a high stimulation. By limiting this diffusion, PNN act as an inhibitor of short-term plasticity.

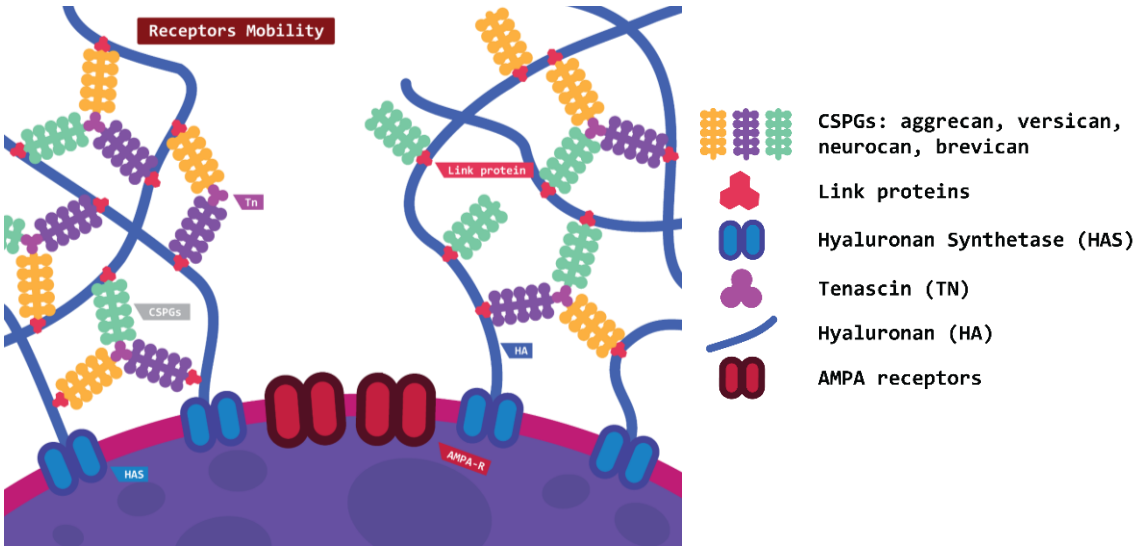

Figure 1.14: Perineuronal nets are limiting receptors' mobility at the cellular surface. PNN can prevent the mobility and internalization of AMPA receptors.

4.5.4. ChABC induced plasticity in the motor cortex

M1 PNN depletion through ChABC injection *in vivo* has been a tool to try to re-establish plasticity in the adult cortex. After a brain traumatic injury, a short and confined opening of a plasticity window occurs in rodents (Harris et al., 2013). Inhibition of axonal growth is hampered, within part the decrease of CSPGs and associated growth-inhibitory proteins (Harris et al., 2009; Yi et al., 2012). The use of ChABC after such injuries increases the windows' spatial and temporal size, allowing enhancing axonal sprouting in the cortex and improving rehabilitation (Harris et al., 2013). A spinal cord injury is also sufficient to decrease the amount of PNN in layer 5 of the motor cortex (Orlando and Raineteau, 2015). However, intracortical ChABC injection impairs the axonal sprouting in the injured spinal cord, revealing that the spatial and temporal windows of PNN removal have to be tightly controlled.

4.5.5. PNN role in memory

As PNN are inhibiting neuronal plasticity, it makes sense to investigate their importance in memory phenomena. Fear conditioning was the first to be investigated (Gogolla et al., 2009). PNN removal in the secondary visual cortex, the auditory cortex, the anterior cingulate cortex, or the amygdala was sufficient to prevent both acquisition and recall of fear memory (Gogolla et al., 2009; Banerjee et al., 2017; Thompson et al., 2018; Shi et al., 2019).

Regulation of the PNN is also observed in the cerebellum during associative learning (Carulli et al., 2020). During the conditioning phase of an eyeblink conditioning task, the PNN are reduced in the cerebellum. However, once the memory is fully established, the amount of PNN is restored. Carulli and colleagues also showed that this diminution of PNN was beneficial for learning as their digestion in the cerebellum is sufficient to improve learning.

Regulation of PNN linked with memory is also observed in birds. Seasonal songbirds have to learn their vocalization every year. Concomitant with this seasonal sensorimotor learning, PNN expression in the song control nuclei is decreased at this period, including in the HVC which is a cortex-like structure in birds (Cornez et al., 2021).

Altogether, these data tend to show that PNN are a key component in learning and memory formation, and, by mainly wrapping PV neurons, bring out the putative importance of this neuronal population in learning and memory phenomena in M1. Indeed, a decrease in PNN could play an important role in motor learning, creating a window of plasticity allowing microcircuitry modification to acquire the new stereotyped movement.

HYPOTHESIS AND OBJECTIVES

Motor skill learning plays an important part in our everyday life. It provides the ability to learn and maintain new motor skills such as how to ride a bike, write with a pen, or use a keyboard. Much more complex skills can be acquired, such as learning how to draw, to play a musical instrument, or the precise movements surgeons learn to practice its surgery. Losing this ability of learning and retention can be very disabling, which can be the case for patients affected by Parkinson's disease (PD) (Marinelli et al., 2017). The primary motor cortex activity is disturbed in PD patients and is a key brain structure for acquiring and maintaining new skills is the primary motor cortex. Indeed, lesion approaches or blockade of protein synthesis in M1 has been shown to impair these abilities in rodents and monkeys (Kawai et al., 2015; Ohbayashi, 2020). In addition, several plastic changes are occurring in M1 with skill acquisition. Studies in rodents have shown that PC's intrinsic properties and connectivity are increased following learning of a reaching and grasping task, the single pellet reaching task (SPRT) (Biane et al., 2019). SPRT learning is also inducing an increase in spine survivability of M1 neurons (Xu et al., 2009; Guo et al., 2015b). M1 dopamine is playing a crucial role in these plastic changes. First, selective depletion of dopaminergic fibers projecting to M1, or the blockade of either D1 or D2 dopamine receptors, is sufficient to alter SPRT learning (Molina-Luna et al., 2009; Guo et al., 2015b) Second, plasticity normally present during learning, such as increased in spine survival, is impaired in M1 dopamine depleted mice (Guo et al., 2015b). Studies have already looked at the dopamine modulation of M1 PC (Huda et al., 1999, 2001; Parr-Brownlie, 2005; Vitrac et al., 2014; Aeed et al., 2021; Li et al., 2021; Swanson et al., 2021), however little is known

about the dopaminergic modulation of GABAergic neurons in M1. PV neurons are the main GABAergic population in the neocortex. They are powerful regulators of cortical activity by massively projecting onto PV and participating in the feedback and feedforward inhibitions (Isaacson and Scanziani, 2011). *In vivo* recordings showed that they are recruited during reaching movement execution, even before PC. In addition, PV neurons are surrounded by the PNN. These mesh-like structures are known to be plasticity inhibitors, and a decrease in their intensity can be observed during learning phenomena in different brain structures (Gogolla et al., 2009; Banerjee et al., 2017; Thompson et al., 2018; Shi et al., 2019; Carulli et al., 2020; Cornez et al., 2021). These data emphasize that PV can play a major role in M1 during skill acquisition, especially the one from M1 L5 as they are controlling the activity of PT neurons, the output neurons of the structure.

Here we hypothesize that dopamine would exert a control over M1 neuronal circuitry by modulating the electrical and synaptic properties of PV neurons.

To answer this question, we first investigated if PV neurons were expressing the dopamine receptor in M1. Using *ex vivo* electrophysiology and optogenetics we tested if the activation of these receptors was able to modulate PV neurons intrinsic and synaptic properties.

Next, we investigated the role of PV neurons and PNN in motor skill learning with 4 objectives:

Objective1: We aimed to find modifications of PV intrinsic properties with motor skill learning. To this end, mice were trained to a food prehension task, the single pellet reaching task, and we looked for modifications induced by learning on the intrinsic properties of PV neurons in M1 L5.

Objective 2: We investigated for changes in PV synaptic transmission, using optogenetic and the same paradigm as in the first objective. To find if the changes occurring during skill learning were dopamine-dependent, the same experiments (1 and 2) were performed in M1 dopamine depleted mice.

Objective 3: We investigated for the creation of a new plasticity window in M1 through the diminution of PNN which could be at the origin of the plasticity's occurring and allowing motor learning. Thus, we investigated the role of PNN in the SPRT learning.

Objective 4: Finally, we aimed to understand the impact of M1 dopamine depletion on M1 network activity during the acquisition of a new skill was. To this end, using *in vivo* calcium imaging, the activity of M1 PC was recorded during each training session in control and M1 dopamine depleted mice.

MATERIEL AND METHODS

I. Animals and ethical approval

All animal procedures were performed according to institutional guidelines and the European Communities Council Directive of November 24th, 1986 (86/609/EEC). All the procedures were approved by the local ethical committee and the Research French Ministry (APAFIS #14255 and #26770).

Mice were hosted with a 12h light/dark cycle with an *ad libitum* access to water and food. Before the behavioral experiments, the mice were food-restricted to initiate body weight loss, and reduced body weight (~ 90 % of the original weight) was maintained throughout training. Adult (male or female) mice (10-20 weeks old) were used.

Transgenic mouse lines: PVCre and PVCre::Ai9T

PV-ires-Cre mice (#008069, Jackson Lab) express the Cre recombinase in parvalbumin-expressing neurons (PV neurons). Combined with viral approaches, this mouse line allowed us to specifically target PV neurons in M1 using the Cre-lox system (Figure 2.1.A). The Cre-LoxP system is a widely used powerful technology for gene editing. It consists of an enzyme, the Cre recombinase, which was discovered as a 38-kDa DNA recombinase produced from cre (cyclization recombinase) gene of bacteriophage P1 and which thereby recognizes the specific DNA fragment sequences called loxP (locus of x-over, P1) site and mediates site-specific deletion of DNA sequences between two loxP sites (Sauer, 1998). As its name stands, the Cre recombinase can recognize two directly repeated loxP sites to recombine them. The

enzyme will then excise the DNA part within these loxP sites (floxed). In the example of the Figure 2.1.B, the cre recombinase allows excising the transcription blocker coming from the loxP mouse. That way, in the new mouse line, the cells expressing the cre will also express the green fluorescent protein (GFP). This method was used for the PVCre::Ai9T mouse line by crossing the PV-ires-Cre with the Ai9T line (#007909, Jackson Lab). The Ai9T mice are reporter mice, which express a CAG promoter-driven tdTomato (red fluorescent protein) under the control of a loxP-flanked STOP cassette preventing its transcription. By crossing these two lines, the Cre/Lox system allows a conditional expression of the tdTomato exclusively in PV neurons.

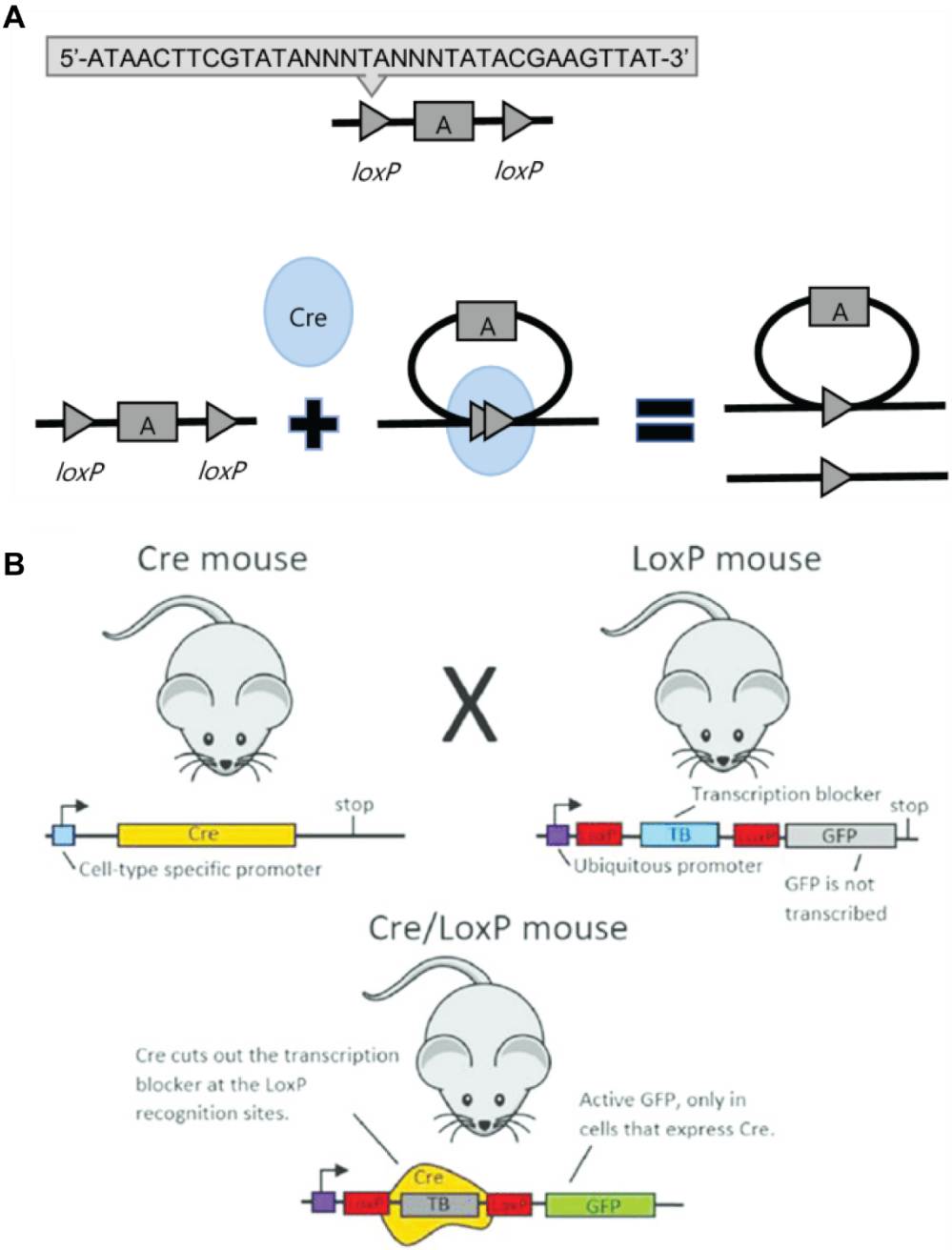

Figure2.1: The Cre-lox system. **A**, Overview of the Cre-lox system: the 38 kDA Cre recombinase recognizes loxP sites on DNA sequences to flox them. **B**, Example of the use of the Cre/lox system to create a reporter mouse model. Adapted from Son et al., 2021 (A), and from Cazemier et al., 2016 (B).

II. The Single Pellet Reaching Task

To uncover the dopamine-dependent changes which take place in M1 during motor skill learning, mice have been trained to perform a single pellet reaching task (SPRT), a task widely used to study motor learning. We have tested and adapted the protocol used by many labs (Chen et al., 2014; Guo et al., 2015b). The mouse learned to pass one paw through a narrow vertical slit to grab a food pellet. The experimental box was developed for us by Imetronic (Pessac, France, Figure 2.2). It consisted of a training chamber made with Plexiglas which allowed the mouse to see through the walls combined with an automatic pellet dispenser. A detection laser allowed to detect when the pellet was removed from the dispenser, allowing the system to withdraw the dispenser and present another pellet. This box was placed in a ventilated wooden cubicle to isolate the animal from the environment. A high-frequency video camera (Allied Vision Manta) was added to the system to decompose the pellet reaching movements of the animal. Kinematic tracking of the movement was performed using DeepLabCut (Mathis et al., 2018).

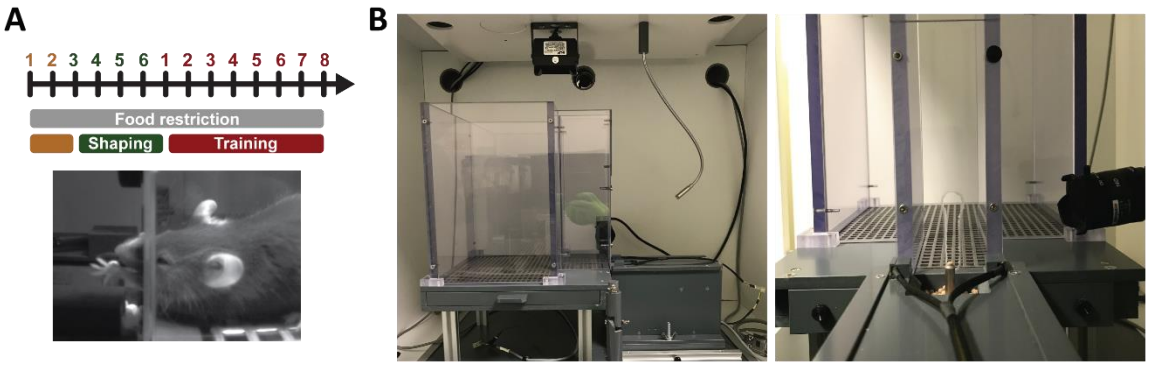

Figure 2.2: Automatized version of the single pellet reaching task. A, Timeline of the experimental protocol (top). Image of a mice trying to reach for the food reward (bottom). **B**, Side view (lef) and front view (right) of the automatized SPRT apparatus.

To start with, mice were food restrained to 90% of their basal weight to motivate them to do the task. A habituation phase was performed for 2 days. For that, each mouse was kept for 10 minutes per day inside the training chamber with chocolate-flavored food pellets (Dustless Precision Pellets, #F05301, Bio Serv) inside the tunnel in front of the vertical split. The habituation was followed by a shaping phase in which the mice had to understand the task they had to perform. This phase allowed us to determine their preferred limb for the task. During the shaping phase, mice were placed in the skill reaching box and had access to chocolate-flavored pellets displayed in a small petri dish outside the plexiglass chamber, just in front of the small vertical open window (0.6 cm wide), allowing mice to reach the pellet using only one of their forelimbs. Shaping was considered finished when 20 reach attempts were achieved within 20 minutes and 70 % limb preference was established. The shaping phase lasted for 1 to 4 days. Once the shaping phase was over, the training could begin the following day (or later when surgery was performed between the shaping and training phases).

Training consisted of a single training session per day, every day for 8 consecutive days. A training session consisted of one session of 50 trials with the preferred limb or 20 minutes (whichever occurred first). Pellets were presented one by one in front of the split and a light cue focused on the pellet was delivered at the activation of the pellet dispenser until the pellet was not detected anymore. To ensure that mice used their preferred paw, the vertical split was slightly shifted to the right or left, depending on the preferred paw of each individual (shifted on the right for right-handed, and left for left-handed). Reach attempts were displayed in 4 types: ‘miss”, 'no grasp', 'drop' and 'success’. A 'miss' corresponded to a reach in which the animal failed to touch the pellet. A ‘no grasp’ corresponded to a reach in which the mouse touched the pellet but did not catch it or knock it away. A 'drop' was

a reach in which the mouse retrieved the pellet but dropped it before putting it into its mouth. A 'success' was a reach in which the animal successfully retrieved the pellet with its preferred limb and put it into its mouth. Success rates were calculated as the percentage of 'successes' over the total reach attempts. As control, we used non-trained mice. They were removed from their home cages, placed in the training box where food pellets were dropped inside. All non-trained mice were littermates and underwent the same food restriction as trained mice. Animals have been divided into 7 groups: learners (L), non-learners (NL), non-trained (NT), dopamine-depleted non-trained (DD), dopamine depleted-trained (DDT), sham non-trained (Sham), and sham trained (ShamT).

III. Kinematics analysis on the reaching movement during SPRT

To better understand how training improved the movement of the paw, we performed a kinematic analysis of the reaching movement during SPRT trainings. A high-speed frequency camera in the SPRT apparatus was used to record all trials during the training sessions (150 frames per second). Then, the videos were analyzed using DeepLabCut (DLC, Mathis et al., 2018). DLC is a free and open-source tool used for markerless pose estimation using deep learning. First, we needed to train the DLC network: around 300 images were taken randomly from the behavioral videos of different mice performing the reaching/grasping movement. The position of the paw was manually labeled on each of these images. Then, the DLC neural network was trained to label the paw of the mice on different videos. Once done, we needed to evaluate the quality of the labeling. The mistakes made by DLC were corrected manually and the network was retrained. Once we were satisfied with the quality of the tracking, we then moved to video analysis. At that point, the network was able to automatically track the paw movements on the videos we wanted. The tracking of the paw was done from the beginning of the reach to the moment the paw comes back to the mouse mouth. For each mouse, the reference was the center of the food reward, on the food dispenser. Then, the trajectories of the 20 first trials of the first and last training sessions were plotted for comparison.

IV. *Ex vivo* electrophysiology

4.1. Slice preparation

Animals were first anesthetized with isoflurane (4%) then received an intraperitoneal injection of ketamine/xylazine (40mg/kg; 15 mg/kg). A thoracotomy was done to perform a 10 mL intracardiac perfusion of an oxygenated sucrose solution containing (in mM): KCl 2.5; $NaH_2PO_4.H_2O$ 1.25; $CaCl_2.2H_2O$ 0.5; $NaHCO_3$ 26; $MgSO_4.7H_20$ 10; Glucose 10; Sucrose 250. This step improves the quality of slices from mice older than 1 month. After decapitation, the brain was quickly extracted and transferred into an oxygenated sucrose solution close to 0°C. Then, 350 µm-thick slices were made using a vibratome (Leica VT 1200S). Slices were placed 1 h at 34°C in oxygenated artificial cerebrospinal fluid (aCSF) containing (in mM): NaCl 126 ; KCl 2.5 ; $NaH_2PO_4.H_2O$ 1.25 ; $CaCl_2.2H_2O$ 2 ; $NaHCO_3$ 2 ; $MgSO_4.7H_2O$ 2 and D-Glucose 10; and pyruvate (110 mg/L) and glutathion (1.5 mg/) in order to help cellular activity.

4.2. Patch-Clamp recordings

Brain slices were placed in a recording chamber of an optical microscope (NiE, Nikon Instruments). The M1 (more precisely the CFA) was located by referring to a stereotaxic atlas and the work from Tennant and colleagues (Tennant et al., 2011, Figure 2.3). Neuron cell bodies were observed with an infrared differential interference system using a 4x air lens and a 60x immersion lens. The image detection was done with a camera (Zyla, Andor technology). The chamber was perfused using a peristaltic pump with an oxygenated and heated artificial cerebrospinal fluid (aCSF) containing (in mM): NaCl 126 ;KCl 3 ; $NaH_2PO_4.H_20$ 1.25 ; $CaCl_2.2H_2O$ 2 ; $MgSO_4.7H_2O$ 2 and D-Glucose 10. 5 to 9 MΩ recording micropipettes

were made from borosilicate glass capillary (GC150F-10, Harvard Apparatus) with a micropipette puller (P97, Sutter instrument). For excitability experiments, micropipettes were filled with a solution mimicking the neuronal intracellular media containing (in mM): K-Gluconate 135, NaCl 3.8, $MgCl_2.6H_2O$ 1, HEPES 10, EGTA 0.1, Na_2GTP 0.4, and $Mg_{1.5}ATP$ 2. The osmolarity and pH of the intracellular solution were adjusted to 295 mOsm and 7.4. Current-clamp mode was used for recordings.

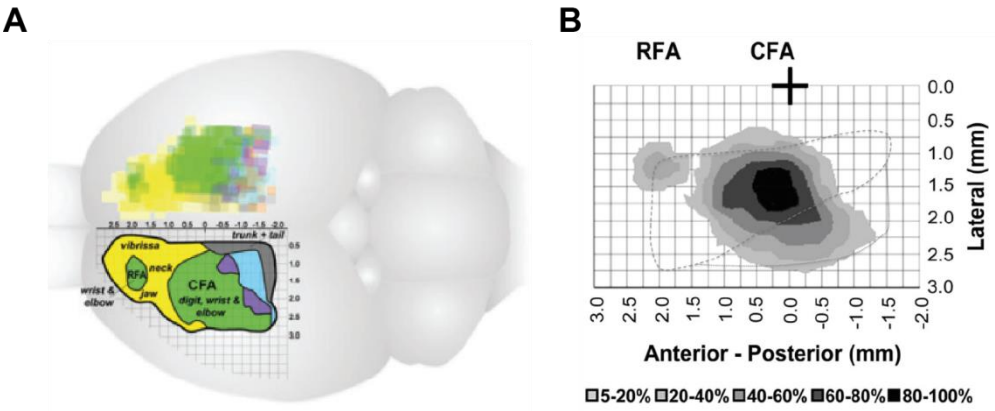

Figure 2.3: Organization of the mouse M1 and the caudal forelimb area. A, Representation of the dorsal mouse brain, highlighting the areas eliciting movement following electrical stimulation. **B**, Heat map of the frequency distribution of the CFA is mice. Positions are relative to the bregma. Adapted from Tennant et al., 2011.

Whole-cell patch-clamp recordings were performed on PV neurons or PC in the caudal forelimb area (CFA). For experiments following behavior, neurons were patched in the CFA corresponding to the preferred limb, which is contralateral to the preferred limb. In whole-cell configuration, positive pressure is put in the micropipette and a micromanipulator (Patchmaster, Scientifica) allows setting the

micropipette close to the membrane of the targeted neuron. When the electrode is close enough to the neuron's membrane, the pressure inside the pipette is released to stick the membrane to the tip of the pipette and to obtain a gigaseal. Then the membrane is broken by aspiration. The signals obtained were amplified using a multiclamp 700B amplifier (Molecular Devices) and digitized (Digidata 1440, Molecular Devices) at a 20 kHz acquisition frequency using the acquisition software PClamp10 (Molecular Devices). Once the recordings were finished, the slices were fixed overnight in PBS with 4% PFA for 24h and then stored in PBS with 0.03% sodium azide at 4°C.

For synaptic and autaptic transmission experiments, micropipettes were filled with a high [Cl^-] intracellular solution (in mM): K-gluconate (70), KCl (70), HEPES (10), EGTA (1), MgCl2 (2), MgATP (4), and NaGTP (0.3); pH 7.2 adjusted with KOH; 290 mOsm. For optogenetic experiments, QX 314 (2mM) was added to prevent action potentials. To ensure we were recording GABAergic currents, the glutamatergic transmission was blocked by adding 6,7-dinitroqui-noxaline-2,3-dione (DNQX, 20µM) and D-(-)2-amino-5-phosphonopentanoic acid (AP-5, 50µM) to the aCSF to selectively block AMPA and NMDA mediated currents. Biocytin was added to the intracellular solutions to identify post hoc the patched neurons during immunohistochemistry experiments. For double patch experiments, we based our protocol on the one from *Deleuze and colleagues* to observe autaptic current (Deleuze et al., 2019). PV-PC pairs were recorded in the L5 of the CFA. Both cells were held at -80 mV, a short step of 0.2ms to 0mV was done in PV neurons to observe both the autaptic current in the PV and the synaptic current in the PC.

V. Stereotaxic injections

5.1. 6-hydroxydopamine (6-OHDA) lesion of the M1 dopaminergic innervation

To study the effect of dopamine on M1 microcircuits, a variant of the 6-OHDA (6-hydroxydopamine) mouse model of dopamine depletion has been used (Molina-Luna et al., 2009; Guo et al., 2015b). In this model, the depletion of dopamine was only induced in M1, more precisely in the caudal forelimb area (CFA) which corresponds to the region of the forelimb in M1 (Tennant *et al.*, 2011). 6-OHDA (#2547, TOCRIS) was used at 4mg/mL and dissolved in 0.9 % w/v NaCl solution containing 0.02% w/v ascorbic acid. Mice were anesthetized with isoflurane (4%) and placed in a stereotaxic apparatus. Then 200 nL of 6-OHDA was injected bilaterally into M1 in both hemispheres at the intended stereotaxic coordinates: AP: - 0.2 mm; ML: +/-1.25 mm; DV: +1.4 mm. After the injection, the pipette was left in place for 2 min before being slowly retracted. Because 6-OHDA can also induce noradrenergic lesions, desipramine (a selective inhibitor of noradrenergic reuptake, 0.01ml/g, D3900-1G, Sigma) was injected intraperitoneally (i.p.) 30 minutes prior to the 6-OHDA injection to protect noradrenergic neighboring axons. Control Sham mice underwent the same surgical procedure, except that they received a saline injection. The cortical denervation of dopaminergic fibers was verified and determined by tyrosine hydroxylase (TH) staining at the end of the experiments (see VIII of the Materials and Methods). As it has been reported that M1 dopaminergic fibers are successfully destroyed one week after M1 6-OHDA injection (Guo et al.,

2015), and to allow the mice to recover before the food restriction, behavioral experiments were performed at least one week after the surgery.

5.2. Optogenetics stimulation of PV neurons

To specifically photoactivate PV neurons, stereotaxic injections were performed within M1, more precisely in the CFA contralateral to the preferred forelimb. The surgical procedure was the same as for 6-OHDA injections, except that the injection was performed only in the hemisphere contralateral to the preferred limb. 200 nL of the viral vector AAV2.5-EF1a-DIO-hChR2(H134R)-EYFP.WPRE.hGH (V2109TI; $6.72x10^{12}$ gc/mL; UNC Vector Core) was injected. To specifically target PV neurons, a double floxed inverse open reading frame (DIO) only allows the transcription of the fused protein in presence of the Cre recombinase. As PV neurons in PVCre::Ai9t express the Cre recombinase, when they are transfected by the virus, they express the fused protein (ChR2-eYFP). Mice were housed for 3 to 4 weeks before the behavioral experiments and/or the electrophysiological recordings. A LED-light source (473 nm, 100 mW; Prizmatix Ltd.) was connected to an optic fiber (Ø: 500 µm; numeric aperture: 0.63) placed close to the region of interest. Single or 10-Hz trains of light pulses of 1-ms duration were used to evoke synaptic transmission from PV neurons expressing ChR2 to PC on brain slices.

5.3. Chemogenetic manipulation of PV neurons excitability

To selectively manipulate PV neurons excitability *in vivo* we used a chemogenetic approach involving designer receptors exclusively activated by designer drugs (DREADDs). The inhibitory or excitatory DREADDs, hM4Di or hM3Dq (respectively), were specifically expressed into M1 PV neurons by stereotaxic injection of the viruses AAV5-hSyn-DIO-hM4Di-mCitrine ($3x10^{13}$ vg/mL, #50455, Addgene) or AAV5-hSyn-DIO-hM3Dq-mCitrine ($2.4x10^{13}$ vg/mL, #50454, AddGene) into the CFA of PVCre or PVCre::Ai9T mice. The surgical procedure was the same as the one previously described for the optogenetics experiments. The hM4Di/hM3Dq expression is under the control of the hSyn1 promoter, allowing its expression in neurons. For the cell-specificity, a double floxed inverse open reading frame (DIO) only allows the transcription of the fused protein in presence of the Cre recombinase. With this construct, hM4Di or hM3Dq were expressed only in cells expressing Cre, i.e, for PVCre::Ai9T and PVCre mice, in PV neurons. hM4Di and hM3Dq are modified forms of the human M muscarinic receptor and can be activated by the inert clozapine metabolite clozapine-N-oxide (CNO, #4936, TOCRIS). Those DREADDs are coupled to a G_i or Gq protein and once activated, it leads to an inhibitory or excitatory effect on the neurons expressing this receptor when it is activated by CNO.

For the SPRT experiments, CNO (1mg/kg) was injected i.p. 40 minutes before each training session. Control experiments consisted of the same experimental protocol except that the injected virus was an AAV5-EF1a-DIO-eYFP. It allowed us to verify that the observed effects were due to the activation of the DREADDs and not the viral transfection nor the CNO injections.

For the experiments where we needed to decrease the excitability of PV neurons (to see the effect on PNN), PVCre::Ai9t mice were injected in M1 with a pAAV8-hSyn-DIO-HA-hM4Di-IRES-mCitrine in one hemisphere, and a AAV2.5-DIO-eYFP in the other hemisphere. To decrease chronically the excitability of PV neurons, we used the protocol developed by Devienne et al. (Devienne et al., 2021). Four weeks after the viral injection, mice received 4 i.p. injections at 12h intervals of the DREADD agonist Clazopine-N-Oxide (CNO, 1mg/kg, #4936, TOCRIS). 24h following the last i.p. injection, mice were anesthetized with an i.p. injection of a ketamine/xylazine mix (40mg/kg and 15mg/kg respectively) and then transcardially perfused with aCSF (see part 4.1 of the methods). Brains were extracted and incubated for 24h at 4°C in PBS with 4% PFA. 50um slices were made using a vibratome (Leica VT1200S). After sectioning, they were incubated at 4°C in PBS-azide 0.03% until the immunohistochemistry was performed.

VI. PNN digestion

In order to study the importance of PNN in the physiology of PV neurons and the context of motor skill learning, we performed digestion of the PNN by using the Chondroitinase ABC enzyme (ChABC, C2905, Sigma).

6.1. *Ex vivo* PNN digestion

We first performed PNN digestion on brain slices. After slicing, 300µm slices were incubated for 1.5h at 37°C in an oxygenated aCSF containing 0.2U/mL of ChABC, or phosphate buffer saline (PBS, Na phosphate 10mM, NaCl 137 mM, KCl 2.7 mM, pH 7.4) for control slices. After incubation, the slices were moved to a new aCSF bath (without ChABC or PBS) at room temperature. After the recording, the slices were fixed in PBS with 4% PFA for 24h and then stored in PBS with 0.03% sodium azide at 4°C. The revelation of the PNN was performed using the WFA to confirm their digestion (see part VII of the methods).

6.2. *In vivo* PNN digestion

We also performed *in vivo* PNN digestion for the electrophysiological and behavioral experiments. ChABC diluted at 10U/mL in PBS was injected in one hemisphere of PVCre::Ai9t, and PBS was injected in the other hemisphere. Mice were sacrificed 5 to 7 days following the injection and slices were prepared as previously explained in the "*ex vivo* electrophysiology" part (part IV of the methods). After the

slices have been fixed, revelations of the PNN and the biocytin-filled neurons have been made to verify that the patched neurons were in the PNN digested area. Patched neurons outside the digested area were removed from the analysis.

For the behavioral experiments, PVCre::Ai9t mice were injected in the CFA corresponding to their preferred limb either with the ChABC diluted at 10U/mL diluted in PBS or with PBS alone. The injections were done either after the shaping was finished, or when the training phase was finished. In both cases, the training sessions were started again on the 3rd day after the surgery.

VII. Immunochemistry and tissue labeling:

2 types of slices were used for immunohistochemistry:

(1) The slices used for electrophysiology experiments were fixed overnight in 4% paraformaldehyde (PFA) and then immersed in 0.03% of sodium azide at 4°C until used. These slices were used to verify dopamine depletion (TH staining) and PNN digestion (WFA staining).

(2) The slices used for PNN analysis; brains were collected as explained in part III. Brains were then post-fixed in 4% paraformaldehyde (PFA) for 24h and then immersed in 0.03% of sodium azide at 4°C until used. Free-floating tissue sections (50 µm-thick coronal sections) were collected in series, washed in PBS using a vibratome (VT1000S, Leica Microsystems), and then immersed in 0.03% of sodium azide at 4°C until used.

Concerning the immunolabelling protocol, slices were first rinsed with PBS. Slices were blocked in 5% normal donkey serum in PBS containing 0.3% Triton X-100 for 1.5h. Thereafter, sections were incubated with primary antibodies overnight (Table 2.1). After rinsing, the sections were treated with the secondary antibody (Table 2.1) for 1 hour. Both immunoreagents were diluted in PBS 0.3% Triton X-100. Sections were rinsed, mounted on slides and the cover slipped in Fluoromount (F4680, Merk). The entire procedure was performed at room temperature under gentle agitation, except for the overnight primary incubation which has been done at 4°C. Images were collected using a sequential laser scanning confocal microscope with a 40x objective lens of the (SP5, Leica). For TH staining and verification of PNN

digestion, images were taken with an epifluorescent microscope (Olympus BX53, 20x).

Antigen	Host	Dilution	Supplier	catalog. #	experiment
PV	Guinea Pig	1/1000	Synaptic system	195004	PV labeling in PVCre mice
GFP	Rabbit	1/5000	Millipore	AB3080P	Revelation of the mCitrine expression
TH	Rabbit	1:1000	Abcam	GR199969-4	Dopamine depletion verification
WFA	Wisteria floribunda	1/500	Sigma	L1516	PNN revelation/quantification
Anti-Rabbit 488	Donkey	1/500	Life technologies	A21206	mCitrine/ eYFP revelation
Anti-Rabbit 647	Donkey	1/500	Jackson technologies	A21245	Dopamine depletion verification
Anti-Guinea Pig	Goat	1/500	Life technologies	1092009	PV labeling in PVCre mice
SA 488	none	1/500	Life technologies / invitrogene	S11223	Biocytine revelation
SA 647	none	1/500	Life technologies / invitrogene	S32357	PNN revelation/ quantification

Table 2.1: List of primary and secondary antibodies used in this project.

VIII. *In vivo* Ca^{2+} Imaging

8.1. Surgical procedure for miniature microscope implantation

Following the shaping phase, PVCre::Ai9t mice were first injected with 350µL of an AAV1-CaMIIa-GCaMP6f-WPRE-bGHpA ($3.35x10^{12}$ vg/mL, AAV61958, INSCOPIX) in the CFA corresponding to their preferred paw (same protocol as in part V of the methods).

1-2 weeks after the virus injection, mice underwent a second surgery to implant a GRIN lens and the baseplate of the miniature microscope (nVue, Inscopix, surgical procedure adapted from (Resendez et al., 2016; Gulati et al., 2017). Mice were anesthetized with isoflurane (4%) and placed in a stereotaxic apparatus with the head already shaved. To expose the skull, the skin and subcutaneous tissue where the baseplate will be fixed is removed. After leveling the skull, it was scratched to increase its adherence in order to have a better fixation surface for the dental cement used later to fix the baseplate. A craniotomy (a 1.2x1.2mm square) was performed at the future location of the prism (1x1mm square), which was glued to the GRIN lens (1mm in diameter) (Figure 2.4.A). The prism was always put to the left of the injection site because of the way it is built. Once the craniotomy was done, the dura was removed. Then, to insert the prism in the brain, an insertion was done with a small surgical blade, 200 µm to the left of the virus injection site (Figure 2.4.B). This incision was 1mm long in the anteroposterior axis and centered compared to the virus injection site. The prism probe can be slowly implanted where the incision has been done, up to 1.75 dorso-ventrally from bregma to center the face of the prism

with the virus injection site (Figure 2.4.C-D). Kwik-Sil™ was then applied around the calendric lens and on the top of the exposed brain to protect it. Dental cement was finally applied to fix the baseplate to the skull.

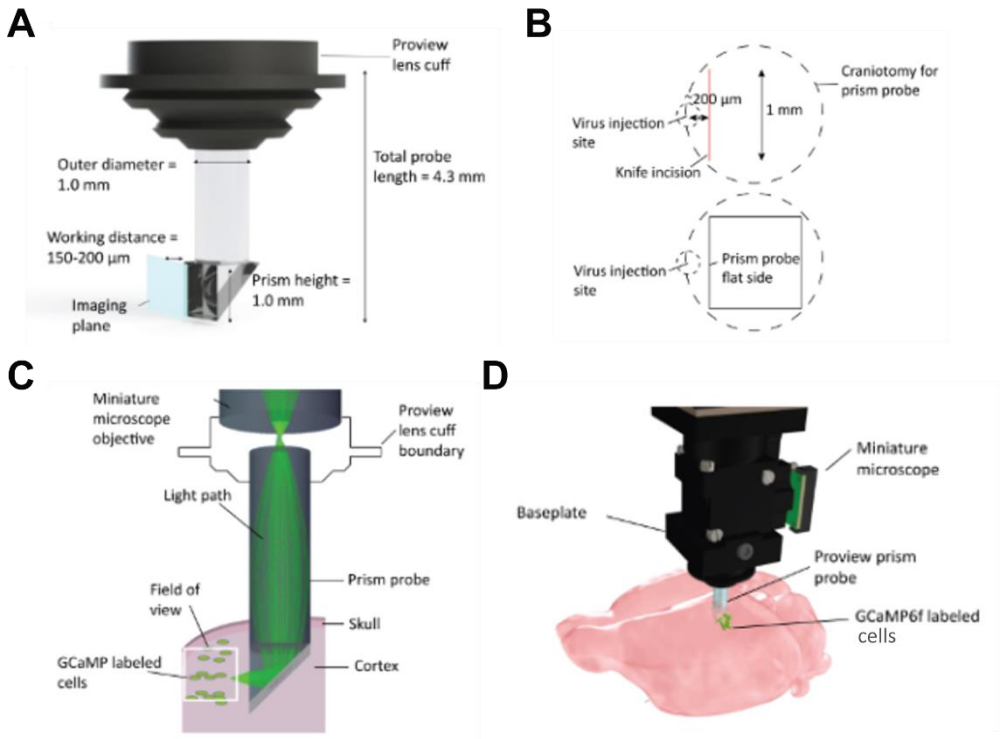

Figure 2.4: *In vivo* calcium imaging in freely moving mice. A, Schematic of the GRIN lens and prism probe used for this project. **B**, Schematics showing, from a top view of the brain, the probe placement compared to the viral injection site (top) and the final placement of the prism probe (bottom). **C**, Schematic of the *in vivo* calcium imaging setup showing the light path and the miniature microscope field of view. **D**, Schematics showing the placement of the miniature microscope once plugged on the baseplate. Adapted from Gulati et al., 2017.

8.2. Ca imaging acquisition

Ca imaging acquisition was performed during each SPRT training session. The miniature microscope was connected to a data acquisition box, itself connected to a computer. The mice were gently held to remove the baseplate cover and to plug the miniature microscope on the baseplate. The miniature microscope was held in place thanks to a set screw and magnets. The mice were placed inside the training chamber and the training session could start. Image acquisition was then started 3 seconds before the presentation of new pellets and stopped 3 seconds after the withdrawal of the pellet dispenser (at 20 fps with activation of a blue LED).

8.3. Ca^{2+} imaging analysis

The first step in the analysis workflow of Ca imaging videos was to treat them with the *Inscopix Analysis Software* to obtain DF/F fluctuation videos, identify the active cells and sort out their activity throughout the videos.

8.3.1. Preprocess

The first step, called ‘preprocess', is used to reduce the size of the video and remove fluorescent artifacts. To do so, raw fluorescent videos underwent spatial downsampling by a factor of 2, meaning that pixels from the videos were merged to divide the resolution by 2. Then the videos were cropped in the X and Y axis to only keep the area where neurons were active. The cropping values were kept for all the videos of the same mouse.

8.3.2. spatial filtering

Spatial filtering consists in filtering the low and high spatial frequency content from the videos. Low-frequency components are corresponding to out-of-focus cells and may thus be a problem for motion correction later on and cell identification.

8.3.3. Motion correction

The next step is to correct the motion between frames in a video. For each frame of the movie, motion correction first estimates a translation that minimizes the difference between the transformed frame and the reference frame, using an image registration method described in Thevenaz et al., 1998.

8.3.4. DF/F processing

The delta F/F algorithm of the *Inscopix Analysis System* normalized each pixel value in the movie to represent the modification of fluorescence compared to the baseline over time. First, the algorithm computed the baseline fluorescence which is the mean value of each pixel across the entire movie. Then, for each frame of the movie

8.3.5. cell identification and calcium event detection

Once the videos were processed, we needed to identify neurons in the recorded movies. The software used a PCA-ICA (Principal Component Analysis – Independent Components Analysis) algorithm to automatically identify them and trace a ROI around each of them. Once cells were detected, DF/F over time traces

are extracted from these ROIs. As calcium concentration in the cell is directly correlated with its activity, we could then detect transient calcic events (*via* fluorescence fluctuation) to extrapolate neuronal activity. Events are detected by their fast and monotonic increase in amplitude followed by a long exponential decay back to the baseline level.

IX. Data analysis

Statistical analysis has been done with *Prism 8* (GraphPad Software. USA). Data in the text are presented as mean value ± standard error of the mean (S.E.M.). For comparisons between two independent groups, a Student T-test was performed if the data followed normality. If not, a nonparametric Mann-Whitney test was used. For multiple group comparisons, a one-way ANOVA was used if the samples followed normality, followed by a Dunnett's multiple comparisons test. If not, we used the Friedman and Kruskal-Wallis ANOVA test followed by Dunn's multiple comparisons post-hoc tests for paired and unpaired comparisons. For comparison of groups or F-I response curves, statistical analysis was performed using two-way ANOVA, followed by Sidak's multiple comparison post hoc test. Data were considered significant for $p<0.05$.

9.1. Electrophysiological data analysis

Using Clampfit (pclamp), firing frequency was calculated from the total number of action potentials during current injection in whole-cell configuration. The mean firing frequency was calculated as the number of spikes per current stimulation duration. The rheobase was measured as the first current step able to elicit at least one action potential in the recorded neuron. The spike frequency adaptation (SFA) was measured as the mean of the intervals between the 2^{nd} and 5^{th} spikes divided by the mean of the intervals between the last (n) and last-5 (n-5) spikes of a given recording.

For optogenetics experiments, light-evoked IPSC amplitude was measured as the peak of the outward current relative to the baseline holding current preceding the light pulse. For 10Hz train stimulation, normalization was calculated by dividing the amplitude of each light-evoked IPSC with the first light-evoked IPSC of the train.

9.2. PNN intensity quantification

PNN labeling intensity was analyzed by quantifying the WFA fluorescence intensity. Images were analyzed using FIJI (NIH) and the macro plugin PIPSQUEAK ("Perineuronal net Intensity Program for the Standardization and Quantification of ECM Analysis") (Slaker et al., 2016). For each mouse used for PNN quantification, the analysis has been conducted on 3 slices containing the CFA. First, background subtraction is done by selecting 20 regions of interest (ROI) around the image perimeter. PNN detection was automatically done with the semi-autonomous mode PIPSQUEAK AI (post hoc verification allowed us to manually add or remove PNN ROI). The plugin then measures the intensity within the ROI of PNN identification. For PNN quantification in the DREADDs experiments, neurons transfected by the virus (mCitrine-positive or eYFP-positive) were also detected using PIPSQUEAK. The plugin then identified PNN colocalized with detected neurons. Thus, we were able to measure PNN intensity only around transfected neurons.

9.3. TH staining analysis

To verify that the dopamine depletion was well done in the CFA, TH staining was analyzed using FIJI on images acquired with an epifluorescent microscope (Olympus BX53, 20X). For each mouse, mean fluorescence has been measured in 2 ROIs. The first one has been placed over the CFA, and the second one in the primary somatosensory cortex (S1). This allowed us to normalize the fluorescence of the staining in the CFA over the S1 fluorescence for each brain slice.

RESULTS

Part I. Dopaminergic modulation of M1 L5 PV intrinsic and synaptic properties *via* activation of dopamine D2 receptors in M1

Numerous studies have reported that dopamine plays an important role in the physiology of M1, especially in motor skill learning (Molina-Luna et al., 2009; Guo et al., 2015b). However, little was known concerning the neuronal populations expressing dopaminergic receptors in M1, especially concerning GABAergic neurons. PV neurons are recruited for motor execution (Estebanez et al., 2017) and undergo plastic changes during motor skill learning. Thus, the first step in this project was to investigate if PV neurons in M1 express dopaminergic receptors and if the activation of these receptors can modulate PV neurons' electrical and synaptic properties.

The results for this part were published in the journal eNeuro in 2020 (Cousineau et al., 2020). In the following pages, you will find an overview of the results found in this research article, followed by the publication itself.

1.1. Distribution of D2R-expressing neurons in M1 in Drd2-Cre::Ribotag mice:

M1 layer 5 is the main output of the structure and *in situ* hybridization studies have shown that this layer of the cortex was enriched in D2R (Gaspar et al., 1995) and dopaminergic fibers are mainly projecting to deep cortical layers (Vitrac et al.,

2014). According to these data, we aimed to look for the GABAergic M1 population that is expressing dopamine D2-like receptors (D2R). To this end, we collaborated with Emmanuel Valjent from the *Institut de Génomique fonctionnelle* in Montpellier.

Taking advantage of the Drd2-Cre::Ribotag mice, a mice line in which neurons expressing D2R express a hemagglutinin tag (Puighermanal et al., 2015), Figure 1.A), it revealed that D2R-expressing cells were distributed across all cortical layers: around 47% in layer2/3 and around 38% in the deep layers 5/6 (Figure 1.B). In addition, immunostaining of the different classes of interneurons revealed that the main GABAergic population expressing D2R in M1 were PV neurons as they represented 26% of them while NPY neurons represented 14%, calbindin-D28k neurons represented 10%, and calretinin neurons only 3% (Figure 1.C and 1.D). In addition, the D2R-expressing PV neurons were found in both layers 2/3 and layers 5/6.

1.2. Electrophysiological characterization of D2R-expressing neurons in motor cortex M1 in Drd2-Cre::Ai9T mice.

We then wanted to determine the electrophysiological properties of M1 L5 neurons expressing the D2R. Whole-cell patch-clamp recordings were performed on tdTomato-positive neurons in M1 L5 from the DrD2-Cre::Ai9t mouse line (Figure 2.A). Three different neuronal populations were identified with their electrical properties: the fast-spiking neurons had short action potentials and fast-spiking responses, PC had a characteristic pyramidal soma, and regular spiking non-pyramidal that were not able to follow at high discharge frequency contrary to fast-spiking cells (Figure 2.C). Our data showed that on 21 patched neurons, 55% of them

were identified as fast-spiking neurons, while 30% were regular spiking non-pyramidal and 12% were PC (Figure 2.B). As fast-spiking neurons are mainly PV neurons (Hu et al., 2014), these data confirmed that PV neurons are the main GABAergic population expressing the D2R, but also showed that they were the more abundant neuronal population in M1 L5.

1.3. Quinpirole increases the excitability of M1 PV neurons

As PV neurons were the most abundant neurons expressing D2R in M1 L5, we investigated the effect of the activation of these receptors on PV neurons' electrical properties. To this end, PV neurons were patched in M1 L5 of PVCre::Ai9t mice and different electrophysiological properties were assessed (Figure 3.A). To activate D2R, a D2R-like agonist, quinpirole, was perfused in the perfusion bath. Steps of current of different amplitudes were injected in PV neurons to record their firing activity in response. This allowed us to measure their excitability in the control condition. After quinpirole was applied, the input/output curve was shifted to the left, meaning that PV neurons were more excitable (Figure 3.B). To confirm that this change was due to D2R activation, the same experiment was done in presence of a D2R antagonist, sulpuride. In presence of sulpuride, the quinpirole effect on PV excitability was blocked (Figure 3.C). We also showed that D2R activation through quinpirole application was increasing the resting potential and the input resistance while decreasing the rheobase of PV neurons (Figure 3.D-E). Altogether, these data showed that D2R activation can modulate PV neurons' intrinsic properties in M1 L5.

1.4. Effect of quinpirole on the electrical activity and sIPSCs (sIPSCs and mIPSCs) of PC

As D2R activation was able to modulate PV neurons' excitability, and we found that PC can also express the D2R in M1 L5, we investigated the effect of quinpirole application on PC intrinsic properties (Figure 4.A). We showed that D2R activation through quinpirole application did not affect PC intrinsic properties as it did not change the input/output curve of recorded neurons, nor the resting potential and input resistance (Figure 4.B).

Next, as PV neurons are massively projecting to PC soma, we investigated the effect of D2R activation on the spontaneous GABAergic transmission onto PC by recording spontaneous IPSCs (sIPSCs) and miniature IPSCs (mIPSCs). Our data showed that quinpirole application significantly increased the amplitude of sIPSCs but not their frequency (Figure4.C-E). In addition, D2R activation was increasing mIPSCs' mean amplitude but not their mean frequency (Figure4.F-H).

1.5. Quinpirole increases GABAergic synaptic transmission at the PV-PC synapse

After showing that spontaneous GABAergic transmission onto PC was modulated by D2R activation, we aimed to find if the transmission from PV neurons could be at the origin of such changes. To investigate if quinpirole could change synaptic transmission of PV neurons to PC, we used optogenetics. PVCre::Ai9t mice were injected with a virus allowing the selective expression of the channelrhodopsin 2 (ChR2) in M1 PV neurons (Figure 5.A). We could then photostimulated PV neurons

to drive their activity and record light-evoked IPSCs in M1 L5 PC (Figure5.B-D). We found that quinpirole application was significantly increasing the amplitude of these light-evoked IPSCs (figure 5.E). Furthermore, photostimulation with a 10Hz train revealed that D2R activation did not affect the short-term depression at this synapse (Figure 5.E-F).

To conclude, in this part we showed that M1 L5 PV neurons were among the main population expressing D2R. In addition, D2R activation on acute brain slice is able to increase the excitability of PV neurons and their synaptic transmission onto pyramidal cells (Figure 3.1).

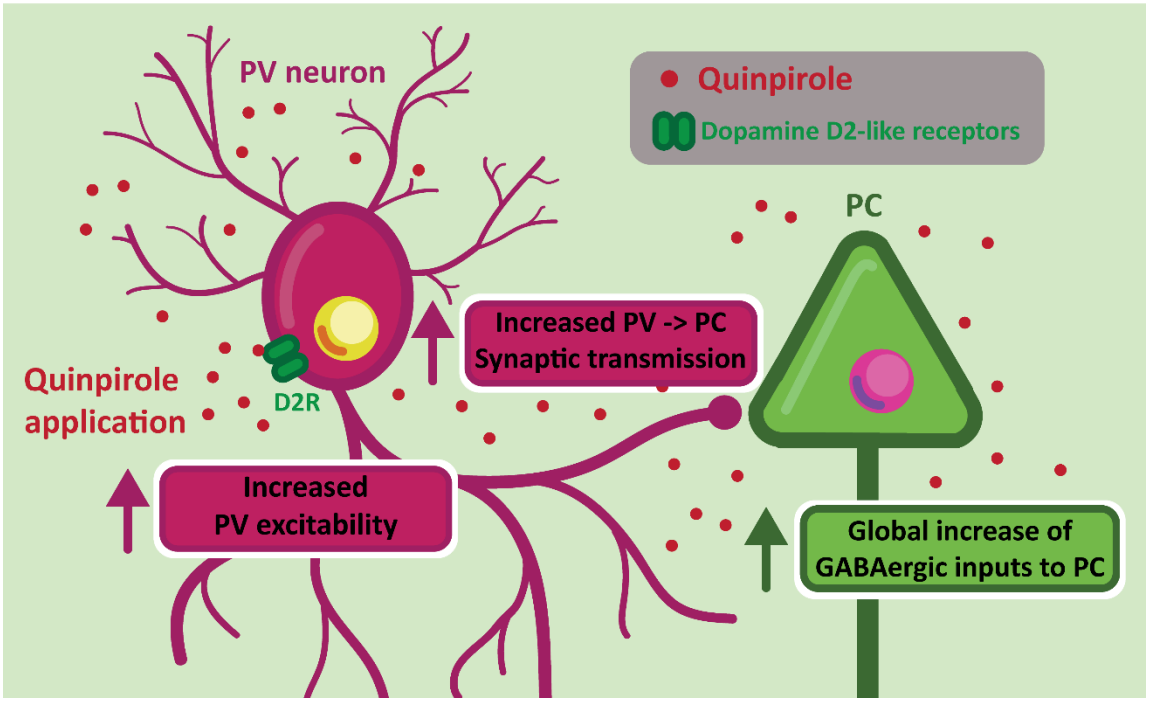

Figure 3.1: Effect of D2R activation of PV electrical and synaptic properties. Schematics summing up the effect of the bath application of D2R agonist on a PV neuron projecting onto a PC in M1 L5. Both the excitability and the synaptic transmission of PV neurons onto PC. GABA events on PC are also increased without altering their intrinsic properties.

Article: Dopamine D2-Like Receptors Modulate Intrinsic Properties and Synaptic Transmission of Parvalbumin Interneurons in the Mouse Primary Motor Cortex

Jérémy Cousineau[1,2], Léa Lescouzères[1,2,3], Anne Taupignon[1,2], Lorena Delgado-Zabalza[1,2,4], Emmanuel Valjent[5], Jérôme Baufreton[1,2], Morgane Le Bon-Jégo[6,2]

Affiliations

- [1] Université de Bordeaux, Institut des Maladies Neurodégénératives, Unité Mixte de Recherche 5293, Bordeaux F-33000, France.
- [2] Centre National de la Recherche Scientifique, Institut des Maladies Neurodégénératives, Unité Mixte de Recherche 5293, Bordeaux F-33000, France.
- [3] Institute for Neuroscience of Montpellier, Institut National de la Santé et de la Recherche Médicale, University of Montpellier, Montpellier 34091, France.
- [4] University of the Basque Country (Universidad del País Vasco/Euskal Herriko Unibertsitatea), Leioa 48940, Spain.
- [5] Institut de Génomique Fonctionnelle, Centre National de la Recherche Scientifique, Institut National de la Santé et de la Recherche Médicale, University of Montpellier, Montpellier 34094, France.
- [6] Université de Bordeaux, Institut des Maladies Neurodégénératives, Unité Mixte de Recherche 5293, Bordeaux F-33000, France morgane.jego@u-bordeaux.fr.

PMID: 32321772

PMCID: PMC7240291

DOI: 10.1523/ENEURO.0081-20.2020

Neuronal Excitability

Dopamine D2-Like Receptors Modulate Intrinsic Properties and Synaptic Transmission of Parvalbumin Interneurons in the Mouse Primary Motor Cortex

Jérémy Cousineau,[1,2*] Léa Lescouzères,[1,2,3*] Anne Taupignon,[1,2] Lorena Delgado-Zabalza,[1,2,4] Emmanuel Valjent,[5] Jérôme Baufreton,[1,2] and Morgane Le Bon-Jégo[1,2]

https://doi.org/10.1523/ENEURO.0081-20.2020

[1]Université de Bordeaux, Institut des Maladies Neurodégénératives, Unité Mixte de Recherche 5293, Bordeaux F-33000, France, [2]Centre National de la Recherche Scientifique, Institut des Maladies Neurodégénératives, Unité Mixte de Recherche 5293, Bordeaux F-33000, France, [3]Institute for Neuroscience of Montpellier, Institut National de la Santé et de la Recherche Médicale, University of Montpellier, Montpellier 34091, France, [4]University of the Basque Country (Universidad del País Vasco/Euskal Herriko Unibertsitatea), Leioa 48940, Spain, and [5]Institut de Génomique Fonctionnelle, Centre National de la Recherche Scientifique, Institut National de la Santé et de la Recherche Médicale, University of Montpellier, Montpellier 34094, France

Abstract

Dopamine (DA) plays a crucial role in the control of motor and higher cognitive functions such as learning, working memory, and decision making. The primary motor cortex (M1), which is essential for motor control and the acquisition of motor skills, receives dopaminergic inputs in its superficial and deep layers from the midbrain. However, the precise action of DA and DA receptor subtypes on the cortical microcircuits of M1 remains poorly understood. The aim of this work was to investigate in mice how DA, through the activation of D2-like receptors (D2Rs), modulates the cellular and synaptic activity of M1 parvalbumin-expressing interneurons (PVINs) which are crucial to regulate the spike output of pyramidal neurons (PNs). By combining immunofluorescence, *ex vivo* electrophysiology, pharmacology and optogenetics approaches, we show that D2R activation increases neuronal excitability of PVINs and GABAergic synaptic transmission between PVINs and PNs in Layer V of M1. Our data reveal how cortical DA modulates M1 microcircuitry, which could be important in the acquisition of motor skills.

Key words: D2 receptors; electrophysiology; neuromodulation; parvalbumin interneuron; primary motor cortex

Significance Statement

Primary motor cortex (M1), which is a region essential for motor control and the acquisition of motor skills, receives dopaminergic inputs from the midbrain. However, precise action of dopamine (DA) and its receptor subtypes on specific cell types in M1 remained poorly understood. Here, we demonstrate in M1 that DA D2-like receptors (D2Rs) are present in parvalbumin interneurons (PVINs) and their activation increases the excitability of the PVINs, which are crucial to regulate the spike output of pyramidal neurons (PNs). Moreover, the activation of the D2R facilitates the GABAergic synaptic transmission of those PVINs on Layer V PNs. These results highlight how cortical DA modulates the functioning of M1 microcircuit which activity is disturbed in hypodopaminergic and hyperdopaminergic states.

Received March 4, 2020; accepted March 10, 2020; First published April 13, 2020.
The authors declare no competing financial interests.

Author contributions: M.L.B.-J. designed research; J.C., L.L., A.T., L.D.-Z., E.V., J.B., and M.L.B.-J. performed research; J.C., L.L., A.I.T., E.V., J.B., and M.L.B.-J. analyzed data; A.I.T., E.V., J.B., and M.L.B.-J. wrote the paper.

Introduction

The neuromodulator dopamine (DA) plays a key role in the ability of neural circuits to adaptively control behavior (Schultz, 2007; Vitrac and Benoit-Marand, 2017; Berke, 2018). Indeed, the DA system plays a major role in motor and cognitive functions through its interactions with several brain regions, and its dysregulation leads to cognitive dysfunction (Duvarci et al., 2018) and pathologies like Parkinson's disease and schizophrenia (Nieoullon, 2002). Recently, it has been suggested that the primary motor cortex (M1) may also be influenced by DA (Hosp and Luft, 2013; Guo et al., 2015). The architecture of the dopaminergic inputs to M1 has been well characterized anatomically mainly in rodent and primate. Coming mainly from the ventral tegmental area (VTA) but also from the substantia nigra pars compacta (SNc), they richly innervate the superficial and deep layers of M1 (Descarries et al., 1987; Lewis et al., 1987; Vitrac et al., 2014; Hosp et al., 2015). However, their functional significance is poorly understood and reports of their effects remain conflicting, presumably because of the *in vivo* exploration and wide neuronal diversity in M1 (Hosp and Luft, 2013; Vitrac et al., 2014; Vitrac and Benoit-Marand, 2017).

DA acts via two main classes of receptors, the D1-like (D1R) and the D2-like (D2R) family, which differentially modulate adenylyl cyclase (Beaulieu and Gainetdinov, 2011). In M1, both families of DA receptors are present in the deep layers (Dawson et al., 1986; Lidow et al., 1989; Weiner et al., 1991; Gaspar et al., 1995). Based on *in situ* hybridization, it appears that Layer V of the cortex, the layer where pyramidal neurons (PNs) integrate inputs from many sources and distribute information to cortical and subcortical structures, mainly contains D2R mRNA (Gaspar et al., 1995).

Previous work in rats has described the effect of DA on neuronal activity M1 neurons *in vivo*, but most of these studies focused on PNs and draw different conclusions regarding an inhibitory or excitatory effect of DA on neuronal activity in M1 (Awenowicz and Porter, 2002; Vitrac et al., 2014). However, there is a large body of evidence supporting that inhibition is important in controlling the excitatory circuits. Among the various interneurons (INs; Ascoli et al., 2008; DeFelipe et al., 2013; Lodato et al., 2015; Markram et al., 2015), parvalbumin-expressing INs (PVINs) represent a minority cell type. However, they are crucial for normal brain function (Donato et al., 2013; Courtin et al., 2014): they powerfully regulate the spike output of PNs, mainly by targeting their somatic and perisomatic regions (Hu et al., 2014). In addition, they are also recruited for motor execution (Estebanez et al., 2017).

To better understand the cellular and network basis of DA action in M1, it is necessary to determine the cellular targets of DA innervation. We hypothesized that DA in M1 contributes to normal microcircuit processing by modulating the activity of PVINs in Layer V through D2R. To test this hypothesis, we performed qualitative mapping of the M1 neuronal population expressing D2R and electrophysiologically characterized these D2R-positive neurons. Then, we investigated the impact of D2R activation on the excitability of PVINs using patch-clamp electrophysiology and on GABAergic synaptic transmission between PVINs and PNs using optogenetics.

We found that D2Rs are broadly expressed in M1, in both superficial and deep layers. In Layer V, the majority of neurons expressing D2R are PVINs. Moreover, D2R agonists increase the excitability of PVINs and also enhance GABAergic synaptic transmission between PVINs and PNs. Our results clarify and highlight the role of DA in modulating the activity of cortical microcircuits in M1.

Animals

All experiments were performed in accordance with the guidelines of the French Agriculture and Forestry Ministry for handling animals (authorization number/license D34-172-13 and APAFIS #14 255). C57BL6J and three transgenic mouse lines were used for this study. Drd2-Cre:Ribotag mice were used for the morphologic study (Puighermanal et al., 2015). PV-Cre:Ai9T mice were generated by crossing PV-Cre mice (B6;129P2-*Pvalb*$^{tm1(cre)Arbr}$/J; JAX stock #008069; Kaiser et al., 2016) with Ai9T mice (B6.Cg-*Gt(ROSA)26Sor*$^{tm9(CAG-tdTomato)Hze}$/J; stock #007909) and the Drd2-Cre:Ai9T line was generated by crossing Drd2-Cre mice (Tg(Drd2-Cre)ER44Gsat; Gensat Project at Rockefeller University) with Ai9T mice (B6.Cg-*Gt(ROSA)26Sor*$^{tm9(CAG-tdTomato)Hze}$/J; stock #007909). These two lines express the red fluorescent protein double-tomato (tdTom) under endogenous regulatory elements of the parvalbumin gene locus and those of D2R, respectively. Males and females, 8–12 weeks old, were used for *ex vivo* experiments. All animals were maintained in a 12/12 h light/dark cycle, in stable conditions of temperature and humidity, with access to food and water *ad libitum*.

Tissue preparation and immunofluorescence

Mapping of the distribution of D2R

Male Drd2-Cre:Ribotag mice, 8–10 weeks old ($n = 6$), were used for the morphologic study. Mice were rapidly anesthetized with Euthasol (360 mg/kg, i.p.; Laboratoire TVM) and transcardially perfused with 4% (w/v) paraformaldehyde in 0.1 M sodium phosphate buffer (pH 7.5). Brains were postfixed overnight in the same solution and stored at 4°C. Sections of 30 μm were cut with a vibratome (Leica) and stored at −20°C in a solution containing 30% (v/v) ethylene glycol, 30% (v/v) glycerol, and 0.1 M

This work was supported by Centre National de la Recherche Scientifique, University of Bordeaux, Institut National de la Santé et de la Recherche Médicale, Fondation pour la Recherche Médicale (FRM), and the French National Research Agency Grant ANR-DOPAFEAR (to E.V.). J.C. received a Ph.D. fellowship from the FRM (ECO201806006853, Fondation Yolande Calvet).

This article was first published as a preprint and is available at: https://www.biorxiv.org/content/10.1101/802140v1.

*J.C. and L.L. contributed equally to this work.

Correspondence should be addressed to Morgane Le Bon-Jégo at morgane.jego@u-bordeaux.fr.

https://doi.org/10.1523/ENEURO.0081-20.2020

Table 1: List of primary antibodies for the mapping of the distribution of D2R

Antigen	Host	Dilution	Supplier	Catalog no.
HA	Mouse	1:1000	Covance	MMS101R
HA	Rabbit	1:1000	Rockland	600-401-384
CR	Rabbit	1:1000	Swant	CR7699/3H
Calbindin-D28k	Rabbit	1:1000	Swant	CB382
Parvalbumin	Rabbit	1:1000	Swant	PV25
NPY	Rabbit	1:500	Abcam	#ab10980
nNOS	Sheep	1:3000	Gift from Dr. V. Prevot (Herbison et al., 1996)	

sodium phosphate buffer until they were processed for immunofluorescence. M1 sections were identified using a mouse brain atlas; sections located between +1.60 and +0.98 mm from bregma were included in the analysis (Franklin and Paxinos, 2007). Sections were processed as follows: free-floating sections were rinsed 3 × 10 min in Tris-buffered saline (TBS; 50 mM Tris-HCl and 150 mM NaCl, pH 7.5). After 15-min incubation in 0.2% (v/v) Triton X-100 in TBS, sections were rinsed again in TBS and blocked for 1 h in a solution of 3% BSA in TBS. Finally, they were incubated 72 h at 4°C in 1% BSA, 0.15% Triton X-100 with the primary antibodies (Table 1). Sections were rinsed 3 × 10 min in TBS and incubated for 45 min with goat Cy2- and Cy3-coupled (1:500, Jackson ImmunoResearch) and/or goat Alexa Fluor 488 (1:500, Life Technologies). Sections were rinsed 2 × 10 min in TBS and twice in Tris-buffer (1 M, pH 7.5) before mounting in DPX (Sigma-Aldrich). Confocal microscopy and image analysis were conducted at the Montpellier RIO Imaging Facility. All images covering the M1 region were single confocal sections acquired using sequential laser scanning confocal microscopy (Leica SP8) and stitched together as a single image. Double-labeled images from each region of interest were also single confocal sections obtained using sequential laser scanning confocal microscopy (Leica SP8). Hemagglutinin (HA)-immunopositive cells were pseudo-colored cyan and other immunoreactive markers were pseudo-colored orange. Images used for quantification were all single confocal sections. HA-positive cells were manually counted using the cell counter plugin of the ImageJ software in M1, taking into account the cortical layers (Layer I, Layers II–III, and Layers V–VI). Adjacent serial sections were never counted for the same marker to avoid any double counting of hemisected neurons. Values in the histograms in Figure 1*B* represent the percentage of HA-expressing neurons in Layer I, Layers II–III, and Layers V–VI ($n = 5$–6 mice). Total numbers of HA- and marker-positive cells counted are indicated between parentheses.

Slice preparation

Coronal sections containing M1 were prepared from 8- to 12-week-old mice. Mice were first sedated by inhaling isoflurane (4%) for ~30 s and then deeply anesthetized with a mixture of ketamine and xylazine (100 and 20 mg/kg, i.p., respectively). After the disappearance of the reflexes, a thoracotomy was performed to allow transcardial perfusion of a saturated (95% O_2/5% CO_2) ice-cold solution containing 250 mM sucrose, 10 mM $MgSO_4 \cdot 7H_2O$, 2.5 mM KCl, 1.25 mM $NaH_2PO_4 \cdot H_2O$, 0.5 mM $CaCl_2 \cdot H_2O$, 1.3 mM $MgCl_2$, 26 mM $NaHCO_3$, and 10 mM D-glucose. After decapitation, each brain was quickly removed and cut into coronal slices (300–350 μm) using a vibratome (VT-

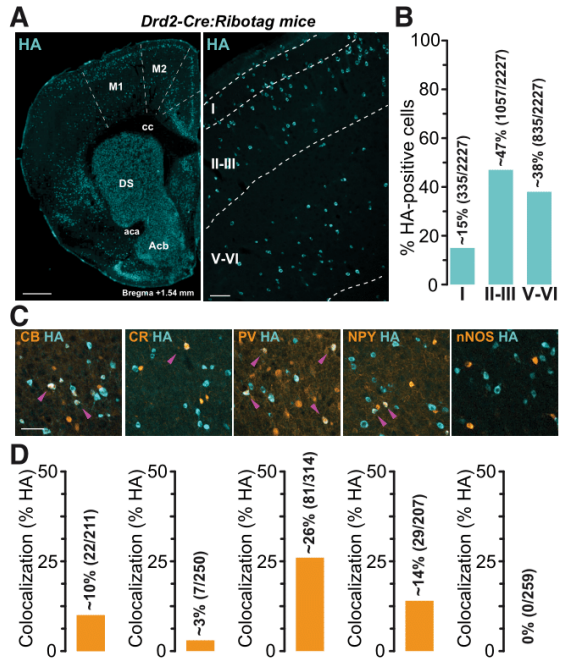

Figure 1. Distribution of D2R-expressing neurons in M1 in *Drd2-Cre:Ribotag* mice. ***A***, Coronal section from *Drd2-Cre:Ribotag* mice stained with hemagglutinin (HA) showing the distribution of D2R-expressing neurons in the different layers of M1. Scale bars: 500 μm (left) and 50 μm (right). ***B***, Histogram showing the distribution of HA-labeled neurons in Layer I, Layers II–III, and Layers V–VI of the M1 (17 hemispheres analyzed, 5 mice). The distribution is expressed as a percentage of HA-positive neurons in all layers. The number of HA-positive cells counted is indicated between parentheses. ***C***, HA (cyan) and calbindin-D28k (CB), Calretinin (CR), parvalbumin (PV), neuropeptide Y (NPY), and nNOS (orange) immunofluorescence in M1 Layers V–VI of *Drd2-Cre:Ribotag* mice. Magenta arrowheads indicate HA/markers-positive neurons. Scale bars: 40 μm. ***D***, Histograms showing the co-expression as a percentage of HA-positive cells in M1 Layers V–VI of *Drd2-Cre:Ribotag* mice (blue, left). The total numbers of HA- and marker-positive cells counted are indicated between parentheses. DS: dorsal striatum; cc: corpus callosum; Acb: nucleus accumbens; aca: anterior commissure.

1200S; Leica Microsystems). The slices were then incubated at 34°C for 1 h in a standard artificial CSF (ACSF) saturated by bubbling 95% O_2/5% CO_2 and containing 126 mM NaCl, 2.5 mM KCl, 1.25 mM $NaH_2PO_4{\cdot}H_2O$, 2 mM $CaCl_2{\cdot}H_2O$, 2 mM $MgSO_4{\cdot}7H_2O$, 26 mM $NaHCO_3$, and 10 mM D-glucose, supplemented with 5 μM glutathion and 1 mM sodium pyruvate. Slices were maintained at room temperature in the same solution until recording.

Electrophysiology

Whole-cell patch-clamp experiments were performed in a submersion recording chamber under an upright microscope (Ni-E workstation, Nikon). Slices were bathed in ACSF containing 126 mM NaCl, 3 mM KCl, 1.25 mM $NaH_2PO_4{\cdot}H_2O$, 1.6 mM $CaCl_2{\cdot}H_2O$, 2 mM $MgSO_4{\cdot}7H_2O$, 26 mM $NaHCO_3$, and 10 mM D-glucose. M1 Layer V neurons were visualized with infrared differential interference contrast and fluorescence microscopy (Spectra X light engine, Lumencor; Froux et al., 2018). PNs were identified on morphologic criteria (triangle-shaped soma) and D2R-positive cells and PV-positive INs (PVINs) were identified by the fluorescence of tdTom. Recording electrodes were pulled from borosilicate glass capillaries (G150–4; Warner Instruments) with a puller (Sutter Instrument, Model P-97) and had a resistance of 5–7 MΩ. They contained 135 mM K-gluconate, 3.8 mM NaCl, 1 mM $MgCl_2{\cdot}6H_2O$, 10 mM HEPES, 0.1 mM Na_4EGTA, 0.4 mM Na_2GTP, and 2 mM MgATP for the current-clamp experiments. For the recordings of spontaneous IPSCs (sIPSCs) and miniature IPSCs (mIPSCs) in voltage clamp experiments, K-gluconate was replaced by CsCl and 2 mM Qx-314 was added to prevent action potentials. In all cases, the osmolarity of the intrapipette solution was between 285 and 295 mOsm and pH was adjusted to 7.2. Experiments were conducted using a Multiclamp 700B amplifier and Digidata 1440 digitizer controlled by Clampex 10.3 (Molecular Devices) at 34°C. Data were acquired at 20 kHz and low-pass filtered at 4 kHz. Whole-cell patch clamp recordings with CsCl- or K-Glu- filled electrodes were corrected for a junction potential of 4 and 13 mV, respectively. In voltage clamp experiments, series resistance was continuously monitored by a step of −5 mV. Data were discarded when the series resistance increased by >20%. sIPSCs and mIPSCs were recorded at a holding potential of −64 mV.

To evaluate their intrinsic excitability, neurons were injected with increasing depolarizing current pulses (50-pA steps, ranging from 0 to +550 pA, 1000-ms duration). Action potential firing frequency was calculated for each current pulse. To measure the input resistance, a hyperpolarizing −100 pA pulse current of 1 s was applied and the voltage response was measured at steady state. Input-output curves (F-I curves, frequency of action potential firing as a function of injected current) were constructed.

Drugs

Unless otherwise stated, drugs were prepared in distilled water as concentrated stock solutions and stored at −20°C. Drugs were diluted daily at the experimental concentrations and perfused in the recording chamber. When indicated, ionotropic glutamatergic and GABAergic transmissions were blocked. NMDA receptors were inhibited by 50 μM D-(-)−2-amino-5-phosphonopentanoic acid (APV); AMPA/kainate receptors by 20 μM 6,7-dinitroquinoxaline-2,3-dione (DNQX); and $GABA_A$ receptors by 50 μM picrotoxin. To study sIPSCs or evoked IPSCs (eIPSCs), glutamate and $GABA_B$ receptors were blocked by APV, DNQX, and 1 μM (2S)−3-[[(1S)−1-(1,4-dichlorophenyl)ethyl]amino-2 hydroxypropyl](phenylmethyl) phosphinic acid [CGP55845; dissolved in dimethylsulfoxide (DMSO)]. The D2-like DA receptor agonist (4aR-trans)−4,4a,5,6,7,8,8a,9-octahydro-5-propyl-1H-pyrazolo[3,4-g] quino-line hydrochloride (quinpirole, 2 μM) and antagonist (sulpiride, 2 μM) were used. Sulpiride was dissolved in DMSO. Drug effects were measured at least 10 min after drug perfusion. Chemicals were purchased from Tocris Bioscience, Abcam, or Sigma-Aldrich.

Optogenetics

To specifically activate PVINs, the cation channelrhodopsin-2 (ChR2) was expressed in PVINs within M1. To this end, the viral vector AAV2.5-EF1a-DIO-hChR2(H134R)-EYFP.WPRE.hGH (V2109TI; $6.72e^{12}$ gc/ml; UNC Vector Core) was injected in M1 of PV-Cre:Ai9T mice. Ten mice received three unilateral injections of 0.5 μL viral vector solution in M1 at the following stereotaxic coordinates (from bregma): lateral, 1.125/1.125/1.375 mm, posterior, +1.4/+1.15/+1.4 mm and depth, −1.275/−1.275/−1.475 mm. The viral vector was pressure-injected using a picospritzer III (Intracel) connected to a glass pipette at a rate of 100 μl/min. After the injection, the pipette was left in place for 1 min before being slowly retracted. Animal were housed for two to three weeks before electrophysiological recordings. An LED-light source (473 nm, 100 mW; Prizmatix Ltd.) was connected to an optic fiber (Ø: 500 μm; numeric aperture: 0.63) placed close to the region of interest. Single or 10-Hz trains of light pulses of 1-ms duration were used to evoke synaptic transmission between PVIN-expressing ChR2 and PNs.

Experimental design and statistical analysis

Data analyses were performed with the Clampfit routine, Origin 7, and a custom-made software for the detection and measurement of sIPSCs and mIPSCs (Detection Mini 8.0; Chazalon et al., 2018). To build the cumulative probability distributions, the same number of events ($n = 300$) has been used for all neurons. Statistical analysis was performed with Prism 5 (GraphPad Software). Population data are presented as mean ± SEM. Paired data were compared using the Wilcoxon signed-rank (WSR) test. Comparisons of F-I relationships were performed with a two-way repeated-measures ANOVA test followed by a Bonferroni test for multiple comparisons (Bichler et al., 2017). The Kolmogorov–Smirnov (K-S) test was used to compare the cumulative distributions. Data were considered statistically significant at $p < 0.05$ ($*p < 0.05$, $**p < 0.01$, $***p < 0.001$; n.s., not significant).

Results

Distribution of D2R-expressing cells in the M1 of Drd2-Cre:Ribotag mice

We took advantage of the *Drd2-Cre:Ribotag* mice (Puighermanal et al., 2015), which express ribosomal

protein Rpl22 tagged with the HA epitope selectively in D2R-positive cells, to determine the expression pattern of D2R-positive cells in M1. The analysis of HA-immunoreactivity revealed that D2R-expressing cells are distributed in all cortical layers, with the highest density in Layers II–III (~47%), followed by the deep Layers (V–VI; ~38%) and Layer I (~15%; Fig. 1*A*,*B*). To determine the molecular identity of D2R-expressing cells located in Layers V–VI of M1, we performed double immunostaining and quantified the degree of co-localization of HA-immunoreactive neurons with markers of distinct classes of INs (Fig. 1*C*,*D*; Ascoli et al., 2008). As illustrated in Figure 1*C* and quantified in Figure 1*D*, HA-positive cells mainly correspond to PV-containing INs (~26%) and to a lesser extent, Calbindin-D28k (CB)- and Neuropeptide Y (NPY)-positive INs (~10% and 14%). In contrast, calretinin (CR)/HA co-labeled cells represent only ~3% of HA-positive cells, while neuronal NO synthase (nNOS)/HA neurons were not detected. Although D2R-positive neurons of Layers V–VI might constitute a subpopulation of cortical INs, our results revealed that they largely correspond to PVINs.

Electrophysiological characterization of M1 D2R-expressing cells

To determine the intrinsic properties of Layer V M1 D2R neurons, whole-cell patch-clamp recordings were performed using *ex vivo* slices from Drd2-Cre:Ai9T (Fig. 2). We patched neurons in acute brain slices and among the 19 neurons we recorded, three types of D2R-positive neurons were found differing in their electrophysiological properties and the shape of their soma (Fig. 2). 55% were fast spiking (FS) INs, 30% were regular spiking non-pyramidal (RSNP) and 15% were PNs. The FS neurons had a mean resting potential of -83.86 ± 2.02 mV ($n = 11$) and were able to fire fast action potentials at a high constant rate. Their action potentials had a short duration and a large afterhyperpolarization (AHP; Fig. 2*B*, inset) which are general characteristics of FS neurons. The discharge frequency increased as a function of the stimulation intensity and the maximal frequency, measured for high intensities of depolarizing currents ranging from 100 to 230 Hz (Fig. 2*D*). Their rheobase differed from one neuron to another and were on average 154.5 ± 17.13 pA. In addition, FS cells had a small input resistance (between 80 and 200 MΩ, except for a neuron). We performed immunohistochemistry to detect the expression of PV in seven neurons filled with biocytin during whole-cell recording. Six of seven were PV-immunoreactive (data not shown).

The second cell type did not maintain high-frequency repetitive discharges and was classified as RSNP because of the shape of the soma (Fig. 2*B*, central panel). Action potentials evoked by current injection in RSNP cells had a longer duration and a relatively smaller AHP than those recorded in FS cells. All RSNP cells displayed a resting potential close to -81.23 ± 0.93 mV ($n = 6$). They had a low maximal frequency of discharge associated with a low rheobase. At a low discharge frequency, RSNP cells emitted action potentials with moderate or no accommodation.

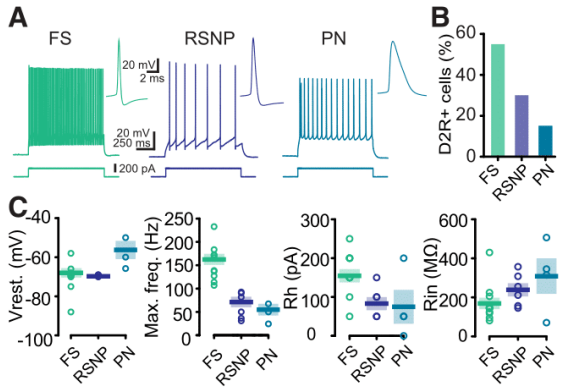

Figure 2. Electrophysiological characterization of D2R-expressing neurons in motor cortex M1 in *Drd2-Cre:Ai9T* mice. ***A***, Firing behavior of the three types of D2R-expressing neurons in Layer V of M1. A depolarizing current injection (200 pA, 1 s) evoked a high-frequency spike firing pattern in FS (left) and a lower frequency of discharge in RSNP (middle) and PNs (right). Next to each trace, an expanded view of single spikes and AHP is presented for the three groups of neurons. ***B***, Histogram showing the percentage of each type of D2R-expressing neurons in Layer V of M1 ($n = 21$). ***C***, Summary of resting membrane potential (Vrest.), maximal firing frequency (Max. freq.), rheobase (Rh), and input resistance (Rin) in the three cell types.

Finally, a few PNs were identified by the triangular shape of their soma. They exhibited a sustained action potential discharge in response to depolarizing current pulses with a low maximal frequency of discharge (Fig. 2*C*). PNs had a mean resting potential of -71.67 ± 6.45 mV, a mean input resistance of 309.5 ± 89.97 MΩ and a mean rheobase of 75.00 ± 43.30 pA ($n = 4$).

D2R activation increases the intrinsic excitability of PVINs

Since the majority of D2R cells recorded in Layer V of M1 were FS INs and expressed PV, we switched to the PV-Cre:Ai9T mouse line to focus our study on the PVINs, which are also mainly FS INs (Hu et al., 2014). In PV-Cre:Ai9T brains, PVINs can be easily targeted for recording as they express the fluorescent protein tdTom. We investigated the effect of a typical D2 agonist, quinpirole, on PVINs excitability in M1 Layer V (Fig. 3*A*). To prevent the influence of spontaneous excitatory and inhibitory inputs on action potential generation, fast glutamatergic and GABAergic transmissions were pharmacologically blocked using DNQX (10 μM)/D-AP5 (50 μM) and picrotoxin (50 μM), respectively. Bath application of quinpirole (2 μM) changed the intrinsic properties of the PVIN sample. A somatic injection of depolarizing current induced more action potentials in the presence of quinpirole for the same injected current, as exemplified in Figure 3*A*. This was true for all injected currents tested as shown by the frequency/current (F/I) input-output curve (Fig. 3*B*; $p < 0.0001$, $n = 10$; two-way repeated-measures ANOVA). Indeed, quinpirole changed the output-input curve of the 10 PVINs tested, shifting it to the left and thus inducing

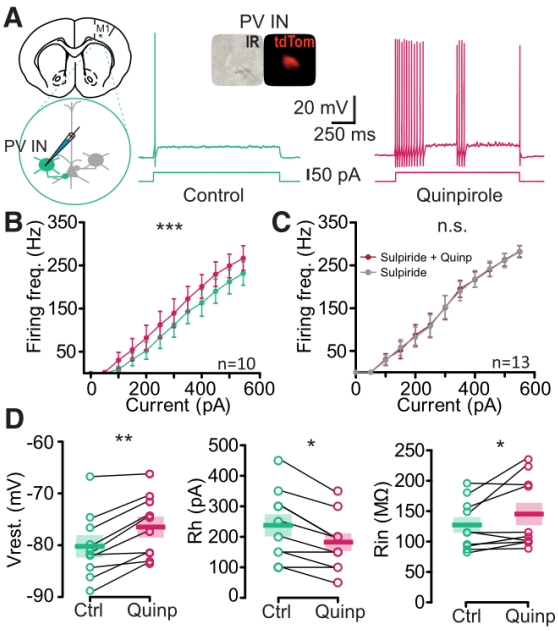

Figure 3. Quinpirole increases the excitability of M1 PVINs. ***A***, left, Schematic of the experiment. PVINs were identified as tdTomato (tdTom in inset) positive neurons in slices from *PV-Cre:Ai9T* mouse brain. Representative voltage responses to +50-pA current injection in a PVIN in control bath solution (green, middle) and after 10 min of perfusion of the D2R agonist quinpirole (Quinp, 2 μM, red, right). ***B***, Quinpirole enhanced the firing frequency (Firing freq.) of PVINs and significantly shifted the input-output curve to the left ($p < 0.0001$, $n = 10$, $F_{(1,96)} = 42.64$, two-way ANOVA). ***C***, Quinpirole does not increase the firing frequency of PVINs in presence of sulpiride ($p = 0.7645$, $n = 13$, $F_{(1,144)} = 0.09{,}011$, two-way ANOVA). Each symbol represents mean ± SEM. ***D***, Summary of the quinpirole effect on resting membrane potential (Vrest.), maximal firing frequency (Max. freq.), rheobase (Rh), and input resistance (Rin; WSR test). The thick bar and the color block represent the mean and the SEM, respectively. $GABA_A$, NMDA, and AMPA/kainate receptors were blocked throughout all of the recordings with PTX (50 μM), D-AP5 (50 μM), and DNQX (10 μM), respectively. $^*p < 0.05$, $^{**}p < 0.01$, $^{***}p < 0.001$; n.s., not significant.

increased excitability. Importantly, the application of the D2R antagonist sulpiride blocked the excitatory effect of quinpirole on PVINs excitability (Fig. 3*C*). Moreover, quinpirole significantly depolarized the PVINs resting potential from −80.19 ± 1.99 to −76.44 ± 1.87 mV ($p = 0.002$; $n = 10$; WSR test), increased their maximal firing frequency (221.1 ± 26.9 to 253.8 ± 28.7 Hz, $p = 0.002$; WSR test), decreased their rheobase from 235.0 ± 36.6 to 180.0 ± 29.1 pA ($p = 0.0115$; WSR test), and increased their mean input resistance from 127.3 ± 12.9 to 145.4 ± 18.3 MΩ ($p = 0.0020$; WSR test; Fig. 3*D*).

D2R activation increases afferent GABAergic synaptic transmission received by PNs

Since PVINs increased their excitability in the presence of quinpirole, we sought to determine whether in the presence of the D2R agonist, individual PNs in Layer V received more phasic $GABA_A$ receptor-mediated inhibition. We first assessed whether quinpirole per se changed the intrinsic properties of PNs. On average, a bath application of quinpirole had no effect, neither on the F/I curve nor on the resting potential or input resistance of the seven PNs recorded (Fig. 4*A*,*B*). To determine whether PNs received more GABAergic inhibition, we recorded the IPSCs in PNs, i.e., the sIPSCs and mIPSCs that reflect the action potential-dependent and action potential-independent activities of the inhibitory IN network, respectively. To specifically study the action of quinpirole on sIPSCs and mIPSCs, and to neutralize the potential confounding influence of excitatory and $GABA_B$ neurotransmissions, DNQX (10 μM), D-AP5 (50 μM), and CGP55845 (1 μM) were bath-applied before the perfusion of quinpirole. In these conditions (considered as a control condition), robust sIPSCs were observed in all the recorded PNs at a holding potential of −64 mV, confirming GABAergic inhibitory control of PNs by GABAergic INs (Fig. 4*C*,*F*).

The effects of 2 μM quinpirole on sIPSCs were studied on 10 neurons. Quinpirole increased the amplitude (Fig. 4*E*) without changing the frequency of the sIPSCs (Fig. 4*D*). Indeed, the cumulative probabilities of the frequency of sIPSCs in the control and the quinpirole groups were similar (Fig. 4*D*; $p > 0.05$, K-S test). However, the cumulative probability of the amplitude of the sIPSCs showed an increase in the quinpirole group (Fig. 4*E*; $p < 0.0001$, K-S test) compared with the control group. Moreover, quinpirole significantly increased the decay time from 7.68 ± 0.67 to 9.07 ± 0.75 ms ($p = 0.059$, $n = 10$; WSR test). Next, we examined the effect of quinpirole in PNs in the presence of 1 μm TTX, to isolate mIPSCs (Fig. 4*F*). As for sIPSCs, analysis of the cumulative probability (Fig. 4*G*,*H*) with the K-S test revealed that D2R activation increased mIPSC amplitude with no effect on their frequency. The decay time of IPSC was significantly increased from 7.66 ± 0.65 to 8.88 ± 0.70 ms ($p = 0.0273$, $n = 10$; WSR test). The frequency was unchanged on average, but it is important to note that quinpirole had a variable effect on individual neurons.

D2R activation enhances GABAergic transmission at PVIN-PN synapses

Our results on GABAergic IPSCs suggested that D2R activation by quinpirole induced more activity in the inhibitory network. However, the increase observed may be due to any type of inhibitory IN. To determine whether quinpirole changes synaptic transmission between PVINs and PNs, we used optogenetics to selectively study PVIN-PN synapse properties (Fig. 5). We expressed the channelrhodopsin ChR2 in PVINs via local viral transfection in M1 of PV-Cre:Ai9T mice using an AAV2.5-EF1a-DIO-hChR2(H134R)-EYFP vector (Fig. 5*A*). We used 473-nm light flashes to stimulate PVINs while recording from PNs. We first confirmed that 1 ms flashes of light were able to reliably trigger action potentials in PVINs. As illustrated by the raster plot in Figure 5*B*, each flash in the train evoked one or two action potentials in the transfected PVIN. In a second step, we recorded the optically-

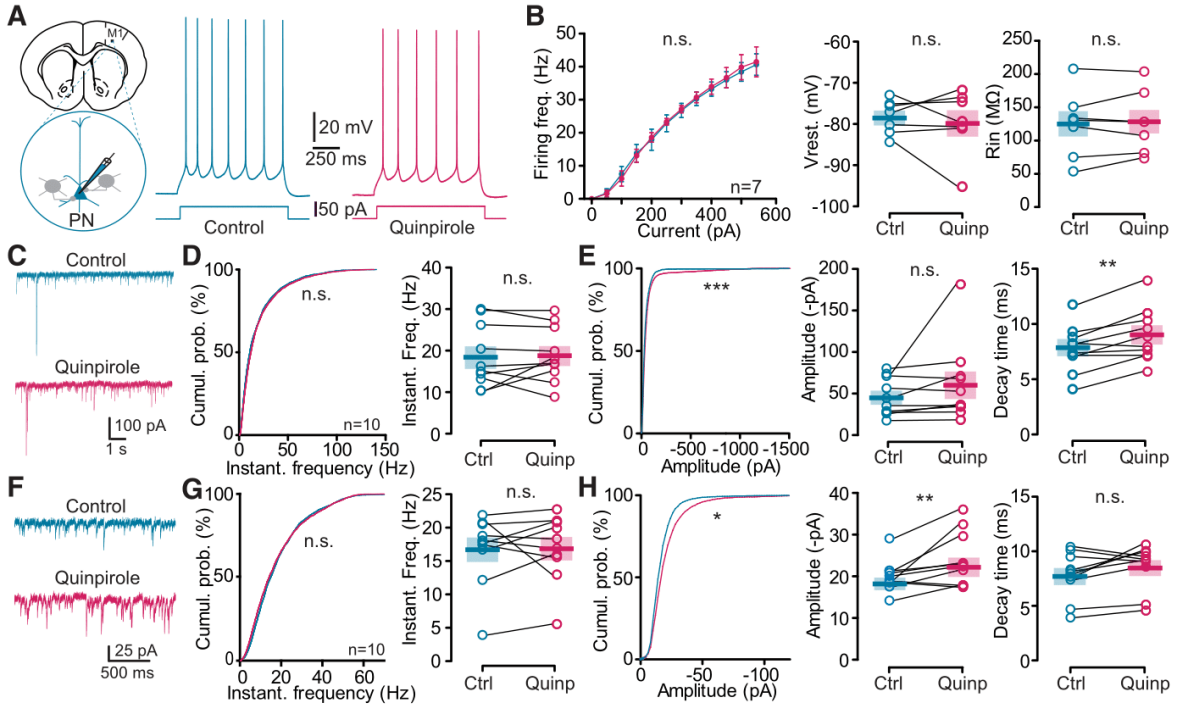

Figure 4. Effect of quinpirole on the electrical activity and sIPSCs (sIPSCs and mIPSCs) of PNs. ***A***, Schematic of the experiment. PNs were identified by their morphology, the absence of tdTomato in their soma as well as their intrinsic properties when possible. Example of voltage responses to +50-pA current injection recorded in a representative PN in control (left, blue) and in quinpirole (right, red). ***B***, Quinpirole did not change the firing frequency of PNs ($p = 0.6453$, $n = 7$, $F_{(1,72)} = 0.21$, two-way ANOVA), nor the resting potential or input resistance ($p = 1.000$ and $p = 0.8982$, respectively; $n = 7$, WSR test). ***C***, Representative traces of sIPSCs recorded from a M1 PN (left) in control conditions (top trace, blue) and in the presence of quinpirole (bottom trace, red). ***D***, Cumulative distribution (left) and mean (right) of sIPSC instantaneous frequency in the control (blue) and in the presence of quinpirole (red). No differences were observed ($p = 0.9987$, K-S test and $p > 0.9999$, WSR test). ***E***, Cumulative distribution (left) and mean (middle) of sIPSC amplitude and value of τ (right). Note that cumulative distribution of the amplitude and decay time differed significantly between control and quinpirole conditions ($p < 0.0001$, K-S, and $p = 0.0059$, WSR test, $n = 10$). ***F–H***, Same representations as in ***C–E*** for mIPSCs. Note that similarly to sIPSCs, only the cumulative distribution ($p < 0.05$, K-S test) and mean of mIPSC amplitude differed significantly between control and quinpirole conditions ($p = 0.0098$; $n = 10$, WSR test). $^*p < 0.05$, $^{**}p < 0.01$, $^{***}p < 0.001$; n.s., not significant.

evoked IPSCs from PNs (Fig. 5*C*). PNs were identified as described previously (Fig. 4) and displayed a PN-typical firing pattern on depolarizing current steps (Fig. 5*C*). Light flashes reliably elicited eIPSCs in PNs, which were potentiated by bath application of 2 μM quinpirole (Fig. 5*D*), increasing their mean amplitude from 280.3 ± 68.52 to 321.6 ± 75.67 pA ($p = 0.0371$, $n = 10$; WSR test). This result strongly suggested that GABAergic synaptic transmission between PVINs and PNs was enhanced by quinpirole. We further characterized the short-term plasticity of the PVINs-PNs synapses using 10 flashes of 1 ms at 10 Hz; Fig. 5*E*). The inhibitory inputs to PNs showed pronounced synaptic short-term depression, but bath-applied quinpirole did not change the profile of synaptic transmission, which remained depressed (Fig. 5*F*).

Discussion

In the present study, we first performed in mice a quantitative mapping of M1 neuronal populations expressing D2R. These neurons are largely present in Layers II/III and Layer V, and are mainly PVINs in Layer V, based on immunochemistry and electrophysiological characterization. Then, combining electrophysiology and optogenetics, we demonstrated *ex vivo* that the activation of D2R robustly increases the excitability of PVINs and enhances the synaptic transmission between PVINs and PNs.

D2R-expressing cells in Layer V of M1

Previous studies have shown that M1 cortical neurons express both D1 and D2 classes of DA receptors (Lidow et al., 1989; Seamans and Yang, 2004) and receive direct DA projections from VTA and SNc via meso-cortical pathways (Descarries et al., 1987). For many years, cortical D2R has been a focus of interest because of its involvement in many cognitive functions initiated or modulated by DA. However, the relatively low expression of cortical D2R makes its detection very difficult. Consequently, it is more difficult to identify the nature of the neurons expressing D2R, a difficulty further amplified by the massive heterogeneity of neurons. Most studies of cortical D2R

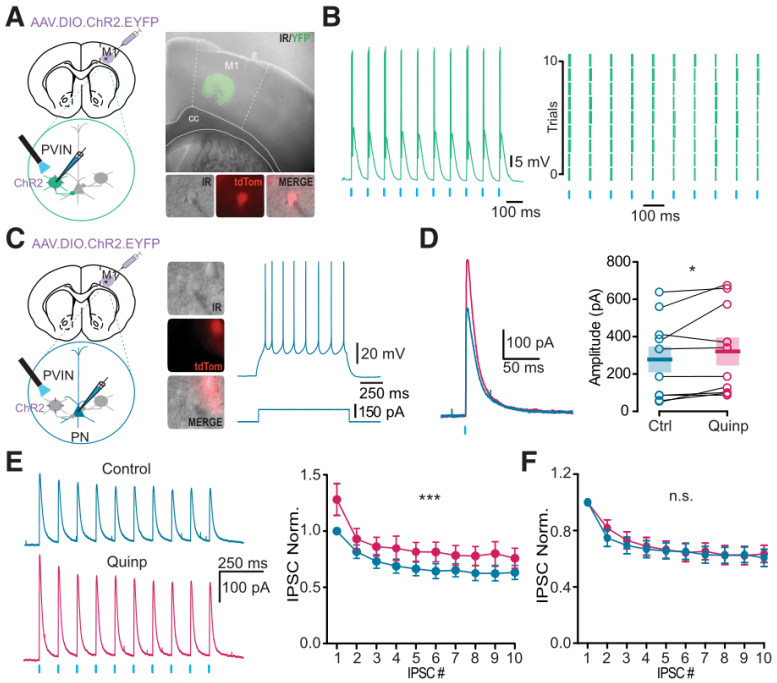

Figure 5. Quinpirole increases GABAergic synaptic transmission at the PVIN-PN synapse. ***A***, Schematic of the experiment. An AAV.DIO.ChR2.EYFP virus was injected in M1 two weeks before *ex vivo* recordings. Representative slice showing the expression of ChR2-EYFP in M1. PVINs (tdTom-positive) were patched to verify our ability to manipulate their activity. ***B***, Light reliably induced action potentials in a PVIN (left). Each flash of light (blue line) evoked one or two action potentials in PVINs as presented in an example (left) of an intracellularly recorded PVIN and in the raster plot of spiking in different trials (right). Each blue tick represents a flash of light (473 nm, 1 ms) and each green tick represents a spike. ***C***, Schematic of the recording configuration from a postsynaptic PN during photoactivation of PVINs (left). Soma of PNs had a triangular shape, were tdTom-negative and PV-negative (middle). Representative firing pattern of recorded PNs to a 150-pA, 500-ms current step (blue, right). ***D***, Sample traces and quantification of light-evoked IPSCs recorded in the same PN before (blue, control trace) and after 10 min of quinpirole perfusion (red). Mean of the amplitude of the evoked response ($p = 0.0371$, $n = 10$, WSR). Mean and SEM are represented. ***E***, Sample traces and quantification of responses to repetitive photostimulation (10 Hz) recorded before (blue) and after bath application of quinpirole (red). Photoactivation of PVINs produced large initial IPSCs that depress rapidly. In the graph, the IPSC amplitudes were normalized to that of the first IPSC in the control condition for each neuron recorded ($p < 0.0001$, $n = 10$, $F_{(1,180)} = 19.36$). ***F***, Short-term synaptic dynamics of the eIPSCs in PNs induced by the photoactivation of PVINs were not changed in presence of quinpirole. IPSC amplitudes were normalized to the first IPSC of the train in each condition ($p = 0.1563$, $n = 10$, $F_{(1,180)} = 0.4749$). $^{*}p < 0.05$, $^{***}p < 0.001$; n.s., not significant.

have focused on the prefrontal cortex and several studies have detected the presence of D2R mRNA in PFC by *in situ* hybridization, revealing its expression in PNs and minor subtypes of INs (Gaspar et al., 1995). Recently, technical limitations were overcome with a highly sensitive and multimodal approach to map cortical D2R-expressing neurons (Drd2-Cre:Ribotag mouse), which has allowed the identification of previously uncharacterized clusters of D2R-expressing neurons in limbic and sensory regions of the adult mouse brain (Khlghatyan et al., 2018). Unfortunately, the authors did not perform quantitative mapping of the M1 neuronal populations expressing D2R. In the present study, using both the Drd2-Cre:Ribotag and Drd2-Cre:Ai9T mouse lines, we show that D2R-expressing cells are distributed in all cortical layers of M1 and broadly expressed in Layer V. The molecular characterization of D2R-expressing cells in Layer V revealed a majority of PVINs and to a lesser extent, populations of CB- and NPY-positive cells. Electrophysiological characterization in the Drd2-Cre:Ai9T mouse line revealed three main classes of neurons expressing D2R in Layer V of M1: FS, RSNP and PN. The majority of the D2R-expressing cells are FS neurons, which are also mainly PV-positive neurons. Since PVINs account for a quarter of the D2R-positive neurons, they are likely to play a specific role, still unknown, as a target for the DA modulation of cortical microcircuits in M1.

D2R modulation of intrinsic excitability of PVINs in M1

Although dopaminergic fibers and DA receptors in M1 have been clearly demonstrated (Descarries et al., 1987; Hosp et al., 2011), their functional significance remains poorly understood. Conflicting evidence indicates excitatory and inhibitory effects on electrical activity *in vivo* (Vitrac and Benoit-Marand, 2017). It has been shown that

in pyramidal cells, D2R activation mediates inhibition occurring via postsynaptic inhibition of PKA and activation of PLC-IP3 and intracellular Ca^{2+}. Most studies have not tested specific cell types and there is no data available regarding DA modulation of specific subpopulations of INs in M1. In this study, we focused on PVINs of Layer V. It has been shown that PVINs in the motor cortex receives direct inputs from the VTA (Duan et al., 2020). We found that activating D2R caused the depolarization and an increase in the excitability of most of the PVINs recorded, even if an interindividual variability of the effect was observed. The excitatory effect of the D2R agonist quinpirole on INs has been already observed on INs in prefrontal cortex (PFC) slices from adult mice (Tseng and O'Donnell, 2006). As cell excitability was determined by assessing the response to intracellular injection alone and in the presence of fast synaptic blockers, this is likely to reflect the postsynaptic effects of the agonist and not a modulation of pre-synaptic afferents. However, further studies will be required to determine whether this excitatory effect reflects a direct D2R postsynaptic action on PVINs as observed in PFC (Tseng and O'Donnell, 2004). Such excitatory effect of D2R stimulation could be explained by the downstream β-arrestin 2 signaling (Urs et al., 2016), or activation of D2R autoreceptors and release of the co-transmitter neurotensin, which is present in a subpopulation of DA neurons from the VTA projecting to PFC (Petrie et al., 2005) that may also project to M1.

D2R modulation of GABAergic synaptic transmission in M1

Proper brain function depends on a correct balance between excitatory and inhibitory signaling (Markram et al., 2015) and PVINs are crucial for such network functionality. Indeed, they exert powerful actions on cortical network activity by contributing to feedback and feedforward inhibition of PNs (Hu et al., 2014). To determine whether the D2R agonist quinpirole modulates the afferent GABAergic synaptic transmission to PN in M1, we examined the IPSCs in PNs. Measurement of the changes in sIPSCs and mIPSCs are a sensitive means to estimate the locus of a drug effect. Typically, changes in IPSC amplitudes are associated with a postsynaptic site of modulator action, whereas changes in IPSC frequency are likely to be due to an interaction with a presynaptic site that changes the probability of transmitter release (Lupica, 1995). Since the excitability of PVINs was increased by quinpirole, we expected an increase in IPSC frequency, but this was not the case. Here, quinpirole increased the amplitude of both sIPSCs and mIPSCs recorded in PNs with no effect on their frequency. One possible explanation is that since the PVINs are not spontaneously firing at their resting potential, the 5 mV depolarization generated by quinpirole may not be large enough to raise the resting membrane potential to the spike threshold in the absence of excitatory transmission. Another possible explanation is the various origins of the GABAergic IPSCs. We studied all the GABAergic inhibitory currents received by PNs and cannot exclude an effect of quinpirole on other GABAergic INs that may mask the effect on frequency, or this may occur only in a subset of PVIN-PN synapses. Finally, the effect could be more complex and can combine a presynaptic and postsynaptic effects of DA.

D2R modulation of PVINs-PN synaptic transmission in M1

In order to be specific to PVIN-PNs synapses and to overcome the fact that these PVINs do not spontaneously fire in slices, we used optogenetics. Our results show that bath application of quinpirole potentiated the optically-evoked eIPSCs in PNs. Using a 10-Hz train of stimulations, we showed an adaptive depression of this synapse from the second optical stimulation that persisted with quinpirole. These observations suggest that quinpirole mainly acts on postsynaptic sites and show that the adaptive depression is maintained. It is also possible that quinpirole-induced depolarization of PVINs membrane potential allows the recruitment of a greater number of neurons during light activation, which can account for the increase in optically-evoked IPSC amplitude without changes in the depression profile. Finally, bath application of quinpirole clearly modulates the intrinsic properties of PVINs. However, as the timing of DA release is critical for plasticity induction (Yagishita et al., 2014), investigating how endogenous DA release controls PVIN-PN GABAergic synaptic transmission and plasticity using optogenetics is crucial.

Functional implications

M1 is particularly important in acquisition and maintenance of motor skills and is a central locus for motor learning. Indeed, pharmacological or optogenetic inactivation of M1 is highly effective in reducing motor aptitude (Peters et al., 2014; Guo et al., 2015; Otchy et al., 2015). The lesion of M1 before training abolishes the ability to learn stereotyped movements but does not impair the execution of an already learned motor skill (Guo et al., 2015; Kawai et al., 2015), demonstrating a role for M1 in "tutoring" subcortical circuits during skill learning. Moreover, recent studies have shown that DA plays a key role in motor learning and memory in M1 (Molina-Luna et al., 2009; Leemburg et al., 2018), particularly in spine regulation and synaptic plasticity (Xu et al., 2009; Guo et al., 2015). Interestingly, it has been recently shown that PVINs exhibit a gradual increase in axonal boutons during motor training (Chen et al., 2015). As we show that the activity of PVINs can be modulated by activation of D2R in M1, these data suggest that PVINs and D2R may be crucial for learning sophisticated motor sequences. Interestingly, it has been shown that striatal PVINs enhance behavioral performance in a reward-conditioning task, but their contribution declines as learning progresses (Lee et al., 2017), suggesting dynamic involvement during the learning of the task. Thus, we expect that following the loss of DA in M1 in conditions such as Parkinson's disease, plasticity of PVINs in M1 will be altered and can lead to the cognitive deficits observed in this pathology.

References

Ascoli GA, Alonso-Nanclares L, Anderson SA, Barrionuevo G, Benavides-Piccione R, Burkhalter A, Buzsáki G, Cauli B, Defelipe J, Fairén A, Feldmeyer D, Fishell G, Fregnac Y, Freund TF, Gardner D, Gardner EP, Goldberg JH, Helmstaedter M, Hestrin S, Karube F, et al. (2008) Petilla terminology: nomenclature of features of GABAergic interneurons of the cerebral cortex. Nat Rev Neurosci 9:557–568.

Awenowicz PW, Porter LL (2002) Local application of dopamine inhibits pyramidal tract neuron activity in the rodent motor cortex. J Neurophysiol 88:3439–3451.

Beaulieu JM, Gainetdinov RR (2011) The physiology, signaling, and pharmacology of dopamine receptors. Pharmacol Rev 63:182–217.

Berke JD (2018) What does dopamine mean? Nat Neurosci 21:787–793.

Bichler EK, Elder CC, García PS (2017) Clarithromycin increases neuronal excitability in CA3 pyramidal neurons through a reduction in GABAergic signaling. J Neurophysiol 117:93–103.

Chazalon M, Paredes-Rodriguez E, Morin S, Martinez A, Cristóvão-Ferreira S, Vaz S, Sebastiao A, Panatier A, Boué-Grabot E, Miguelez C, Baufreton J (2018) GAT-3 dysfunction generates tonic inhibition in external globus pallidus neurons in parkinsonian rodents. Cell Rep 23:1678–1690.

Chen SX, Kim AN, Peters AJ, Komiyama T (2015) Subtype-specific plasticity of inhibitory circuits in motor cortex during motor learning. Nat Neurosci 18:1109–1115.

Courtin J, Chaudun F, Rozeske RR, Karalis N, Gonzalez-Campo C, Wurtz H, Abdi A, Baufreton J, Bienvenu TCM, Herry C (2014) Prefrontal parvalbumin interneurons shape neuronal activity to drive fear expression. Nature 505:92–96.

Dawson TM, Gehlert DR, Wamsley JK (1986) Quantitative autoradiographic localization of central dopamine D-1 and D-2 receptors. Adv Exp Med Biol 204:93–118.

DeFelipe J, López-Cruz PL, Benavides-Piccione R, Bielza C, Larrañaga P, Anderson S, Burkhalter A, Cauli B, Fairén A, Feldmeyer D, Fishell G, Fitzpatrick D, Freund TF, González-Burgos G, Hestrin S, Hill S, Hof PR, Huang J, Jones EG, Kawaguchi Y, et al. (2013) New insights into the classification and nomenclature of cortical GABAergic interneurons. Nat Rev Neurosci 14:202–216.

Descarries L, Lemay B, Doucet G, Berger B (1987) Regional and laminar density of the dopamine innervation in adult rat cerebral cortex. Neuroscience 21:807–824.

Donato F, Rompani SB, Caroni P (2013) Parvalbumin-expressing basket-cell network plasticity induced by experience regulates adult learning. Nature 504:272–276.

Duan Z, Li A, Gong H, Li X (2020) A whole-brain map of long-range inputs to GABAergic interneurons in the mouse caudal forelimb area. Neurosci Bull. Advance online publication. Retrieved Jan 19, 2020. doi: 10.1007/s12264-019-00458-6.

Duvarci S, Simpson EH, Schneider G, Kandel ER, Roeper J, Sigurdsson T (2018) Impaired recruitment of dopamine neurons during working memory in mice with striatal D2 receptor overexpression. Nat Commun 9:2822.

Estebanez L, Hoffmann D, Voigt BC, Poulet JFA (2017) Parvalbumin-expressing GABAergic neurons in primary motor cortex signal reaching. Cell Rep 20:308–318.

Franklin K, Paxinos G (2007) The mouse brain in stereotaxic coordinates, Ed 3. San Diego: Elsevier Academic Press.

Froux L, Le Bon-Jego M, Miguelez C, Normand E, Morin S, Fioramonti S, Barresi M, Frick A, Baufreton J, Taupignon A (2018) D5 dopamine receptors control glutamatergic AMPA transmission between the motor cortex and subthalamic nucleus. Sci Rep 8:8858.

Gaspar P, Bloch B, Le Moine C (1995) D1 and D2 receptor gene expression in the rat frontal cortex: cellular localization in different classes of efferent neurons. Eur J Neurosci 7:1050–1063.

Guo L, Xiong H, Kim JI, Wu YW, Lalchandani RR, Cui Y, Shu Y, Xu T, Ding JB (2015) Dynamic rewiring of neural circuits in the motor cortex in mouse models of Parkinson's disease. Nat Neurosci 18:1299–1309.

Herbison AE, Simonian SX, Norris PJ, Emson PC (1996) Relationship of neuronal nitric oxide synthase immunoreactivity to GnRH neurons in the ovariectomized and intact female rat. J Neuroendocrinol 8:73–82.

Hosp JA, Luft AR (2013) Dopaminergic meso-cortical projections to M1: role in motor learning and motor cortex plasticity. Front Neurol 4:15.

Hosp JA, Nolan HE, Luft AR (2015) Topography and collateralization of dopaminergic projections to primary motor cortex in rats. Exp Brain Res 233:1365–1375.

Hosp JA, Pekanovic A, Rioult-Pedotti MS, Luft AR (2011) Dopaminergic projections from midbrain to primary motor cortex mediate motor skill learning. J Neurosci 31:2481–2487.

Hu H, Gan J, Jonas P (2014) Fast-spiking, parvalbumin+ GABAergic interneurons: from cellular design to microcircuit function. Science 345:1255263.

Kaiser T, Ting JT, Monteiro P, Feng G (2016) Transgenic labeling of parvalbumin-expressing neurons with tdTomato. Neuroscience 321:236–245.

Kawai R, Markman T, Poddar R, Ko R, Fantana AL, Dhawale AK, Kampff AR, Ölveczky BP (2015) Motor cortex is required for learning but not for executing a motor skill. Neuron 86:800–812.

Khlghatyan J, Quintana C, Parent M, Beaulieu JM (2018) High sensitivity mapping of cortical dopamine D2 receptor expressing neurons. Cereb Cortex 29:3813–3827.

Lee K, Holley SM, Shobe JL, Chong NC, Cepeda C, Levine MS, Masmanidis SC (2017) Parvalbumin interneurons modulate striatal output and enhance performance during associative learning. Neuron 93:1451–1463.

Leemburg S, Canonica T, Luft A (2018) Motor skill learning and reward consumption differentially affect VTA activation. Sci Rep 8:687.

Lewis DA, Campbell MJ, Foote SL, Goldstein M, Morrison JH (1987) The distribution of tyrosine hydroxylase-immunoreactive fibers in primate neocortex is widespread but regionally specific. J Neurosci 7:279–290.

Lidow MS, Goldman-Rakic PS, Rakic P, Innis RB (1989) Dopamine D2 receptors in the cerebral cortex: distribution and pharmacological characterization with [3H]raclopride. Proc Natl Acad Sci USA 86:6412–6416.

Lodato S, Shetty AS, Arlotta P (2015) Cerebral cortex assembly: generating and reprogramming projection neuron diversity. Trends Neurosci 38:117–125.

Lupica CR (1995) Delta and mu enkephalins inhibit spontaneous GABA-mediated IPSCs via a cyclic AMP-independent mechanism in the rat hippocampus. J Neurosci 15:737–749.

Markram H, Muller E, Ramaswamy S, Reimann MW, Abdellah M, Sanchez CA, Ailamaki A, Alonso-Nanclares L, Antille N, Arsever S, Kahou GAA, Berger TK, Bilgili A, Buncic N, Chalimourda A, Chindemi G, Courcol JD, Delalondre F, Delattre V, Druckmann S, et al. (2015) Reconstruction and simulation of neocortical microcircuitry. Cell 163:456–492.

Molina-Luna K, Pekanovic A, Röhrich S, Hertler B, Schubring-Giese M, Rioult-Pedotti M-S, Luft AR (2009) Dopamine in motor cortex is necessary for skill learning and synaptic plasticity. PLoS One 4: e7082.

Nieoullon A (2002) Dopamine and the regulation of cognition and attention. Prog Neurobiol 67:53–83.

Otchy TM, Wolff SBE, Rhee JY, Pehlevan C, Kawai R, Kempf A, Gobes SMH, Ölveczky BP (2015) Acute off-target effects of neural circuit manipulations. Nature 528:358–363.

Peters AJ, Chen SX, Komiyama T (2014) Emergence of reproducible spatiotemporal activity during motor learning. Nature 510:263–267.

Petrie KA, Schmidt D, Bubser M, Fadel J, Carraway RE, Deutch AY (2005) Neurotensin activates GABAergic interneurons in the prefrontal cortex. J Neurosci 25:1629–1636.

Puighermanal E, Biever A, Espallergues J, Gangarossa G, De Bundel D, Valjent E (2015) drd2-cre:ribotag mouse line unravels the possible diversity of dopamine d2 receptor-expressing cells of the dorsal mouse hippocampus. Hippocampus 25:858–875.

Schultz W (2007) Multiple dopamine functions at different time courses. Annu Rev Neurosci 30:259–288.

Seamans JK, Yang CR (2004) The principal features and mechanisms of dopamine modulation in the prefrontal cortex. Prog Neurobiol 74:1–58.

Tseng KY, O'Donnell P (2004) Dopamine-glutamate interactions controlling prefrontal cortical pyramidal cell excitability involve multiple signaling mechanisms. J Neurosci 24:5131–5139.

Tseng KY, O'Donnell P (2006) Dopamine modulation of prefrontal cortical interneurons changes during adolescence. Cereb Cortex 17:1235–1240.

Urs NM, Gee SM, Pack TF, McCorvy JD, Evron T, Snyder JC, Yang X, Rodriguiz RM, Borrelli E, Wetsel WC, Jin J, Roth BL, O'Donnell P, Caron MG (2016) Distinct cortical and striatal actions of a β-arrestin–biased dopamine D2 receptor ligand reveal unique antipsychotic-like properties. Proc Natl Acad Sci USA 113: E8178–E8186.

Vitrac C, Benoit-Marand M (2017) Monoaminergic modulation of motor cortex function. Front Neural Circuits 11:72.

Vitrac C, Péron S, Frappé I, Fernagut PO, Jaber M, Gaillard A, Benoit-Marand M (2014) Dopamine control of pyramidal neuron activity in the primary motor cortex via D2 receptors. Front Neural Circuits 8:13.

Weiner DM, Levey AI, Sunahara RK, Niznik HB, O'Dowd BF, Seeman P, Brann MR (1991) D1 and D2 dopamine receptor mRNA in rat brain. Proc Natl Acad Sci USA 88:1859–1863.

Xu T, Yu X, Perlik AJ, Tobin WF, Zweig JA, Tennant K, Jones T, Zuo Y (2009) Rapid formation and selective stabilization of synapses for enduring motor memories. Nature 462:915–919.

Yagishita S, Hayashi-Takagi A, Ellis-Davies GCR, Urakubo H, Ishii S, Kasai H (2014) A critical time window for dopamine actions on the structural plasticity of dendritic spines. Science 345:1616–1620.

Part II.1. Impact of motor skill training and learning on PV neurons properties

2.1.1. Automated single pellet reaching task as motor skill model in mice

After showing that PV neurons intrinsic properties can be modulated by dopamine, we wanted to know if dopamine was acting on them during motor skill learning to allow skill acquisition. In a first set of experiments, we investigated if modifications of M1 PV neurons' electrical properties are occurring with motor learning. To study M1 in this context, we choose a widely used behavioral protocol in mice: the Single Pellet Reaching Task (SPRT) (Xu et al., 2009; Chen et al., 2014; Guo et al., 2015b). The SPRT has been used in rodents to study the acquisition and execution of a dexterous forelimb movement. In this project, we used an automated version of this task. We first verified that our mice were able to realize the reaching and grasping movement and learn it over training days with this experimental equipment. PVCre::Ai9t mice were food-restricted to motivate them to do the task. After 2 days of habituation, mice entered the shaping phase in which they had to understand the task and choose a preferred paw (Figure 3.2.A). Once shaping was done, mice were trained for the SPRT for 8 consecutive days. Mice were able to reach for and grasp the food pellet and retrieve it to their mouth (Figure 3.2.B). To measure motor learning, their performances (the success rate) were assessed every day during this training phase (Figure 3.2.C). Mice were able to significantly increase their performances across training sessions, starting at 24 ± 4 % to ending up at 60 ± 2 % ($n = 16$ mice, One way ANOVA, $p < 0.05$, Figure 3.2.C). To confirm the task was

well learned, some mice were re-trained 5 days after the 8th training session (Figure 2.2.D). Our data showed that they were maintaining their performances after these 5 days. To assess the acquisition of a stereotyped movement following 8 days of training, the movement of the paw was tracked on each trial at the first and 8th training session, giving us a 2D representation of the paw movements (Figure 3.2.E). The superimposed 20 first trials of one mouse at the first (grey) and the eighth (red) training session are displayed in Figure 3.2.E. This qualitative analysis revealed that, at the first training session, the trajectories of the reaching movements are very variable and sparse in space. However, after 8 days of daily training, reaching movements variability was reduced, they are superposed, meaning that the same movement is realized at each trial.

Here we validated that our behavioral protocol was sufficient to have proper motor skill learning in mice: they were able to increase their success rate over training days at the SPRT and to acquire a stereotyped movement by the end of the training phase. In the next experiments, this protocol was used to investigate the role of PV and M1 dopamine in motor skill learning.

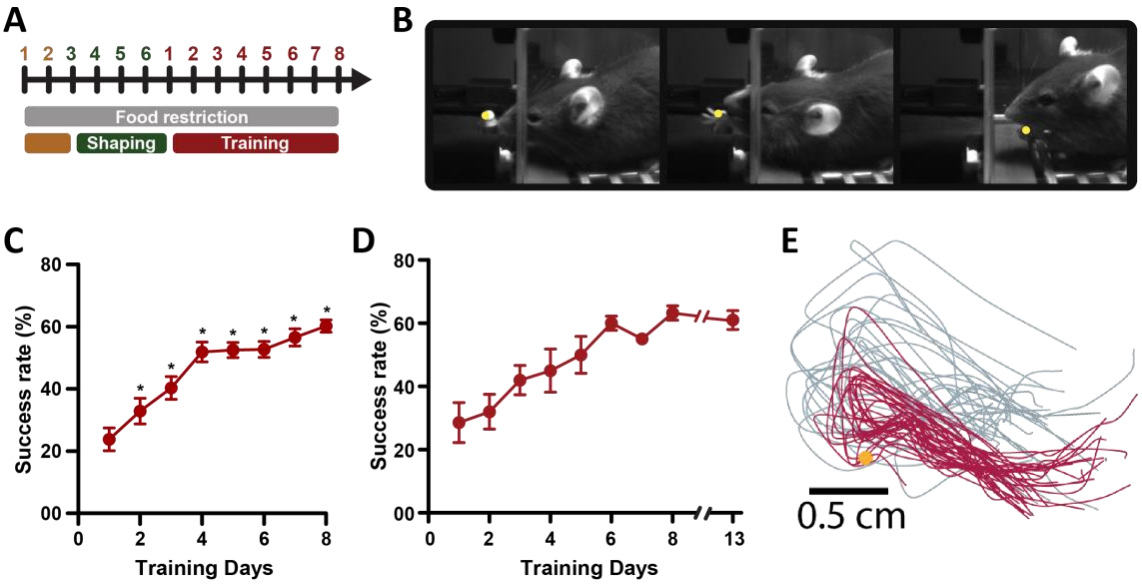

Figure 3.2: Automated Single Pellet Reaching Task (SPRT) in mice. A, Experimental protocol. **B**, Images of a mouse reaching and grasping a food pellet (the pellet is highlighted in yellow). **C**, Success rate over training days at the SPRT training for learners (* represent significant differences compared to the first days of training). **D**, Mice were able to maintain their performances 5 days after the last training session (n = 4 mice). **E**, Paw trajectories of the 20 first trials at the 1st (grey) and 8th (red) training session of a learner mouse.

2.1.2. M1 L5 PV neurons intrinsic plasticity during motor skill learning

2.1.2.1. Motor skill learning decreased the excitability of M1 L5 PV neurons

As mentioned in the introduction, it has been previously shown that M1 dopamine is necessary for skill acquisition (Molina-Luna et al., 2009; Guo et al., 2015b), and for the concomitant plastic changes in M1. In the paper we have recently published, we also demonstrated that PV neurons are the main GABAergic population expressing dopamine D2 receptors, and the activation of these D2R modulates PV neurons properties (Cousineau et al., 2020). In addition, *in vivo* recording showed that M1 L5 PC and PV neurons are recruited during forelimb movement execution (Isomura et al., 2009; Huber et al., 2012; Li et al., 2017; Levy et al., 2020). However, the role of PV neurons in motor learning has not been investigated. As PC neurons are undergoing plastic changes with SPRT learning (Biane et al., 2016, Biane et al., 2019), we hypothesized that PV neurons in M1 L5 may also undergo dopamine-dependent plastic changes during skill learning to allow skill acquisition. As dopamine through its action on D2R can modulate PV neurons' intrinsic properties, we first looked if motor skill learning would induce modification in these properties in M1 L5. To do this, PVCre::Ai9t mice trained for the SPRT and non-trained controls (NT) were sacrificed 1 to 3 days following the last training session to make 300 µm-thick coronal slices containing M1 (Figure 3.3.A). PV neurons were patched in whole-cell configuration in M1 corresponding to the preferred paw (i.e., M1 contralateral to the preferred paw). Different steps of currents were injected in the neurons to measure their driven firing activity, which

allowed us to assess if a modification in the firing rate of M1 PV neurons was induced by the motor skill learning (Figure 3.3.B). The firing frequency curve for learners was significantly shifting on the right compared to the one from NT, meaning that M1 L5 PV neurons excitability was decreased (2way ANOVA, $p = 0.0173$, $F_{(1,66)} = 5.963$, Figure 3.3.C). The resting potential was also significantly decreased from -67.04 ± 1.20 mV to -70.42 ± 0.61 mV following skill learning (Unpaired T-test, $p = 0.0071$, Figure 3.3.D) together with the maximal frequency which decreased from 293.4 ± 18.9 Hz to 236.9 ± 14.0 Hz (Unpaired T-test, $p = 0.0210$, Figure 2.3.E). However, the rheobase (248.1 ± 23.3 pA to 286.8 ±20.76 pA, Unpaired T-test, $p = 0.2240$, Figure 3.3.F), the input resistance (104.0 ± 8.8 MOhm to 102.7 ± 4.9 MOhm, Mann-Whitney test, $p = 0.8978$, Figure 3.3.G) and the spike frequency adaptation (1.33 ± 0.23 to 1.24 ± 0.29, Mann-Whitney test, $p = 0.1019$, Figure 3.3.H) were not changed after learning. To conclude on this figure, here we showed that learning the SPRT with 8 training sessions was able to decrease the excitability of PV neurons in the M1 L5 forelimb area.

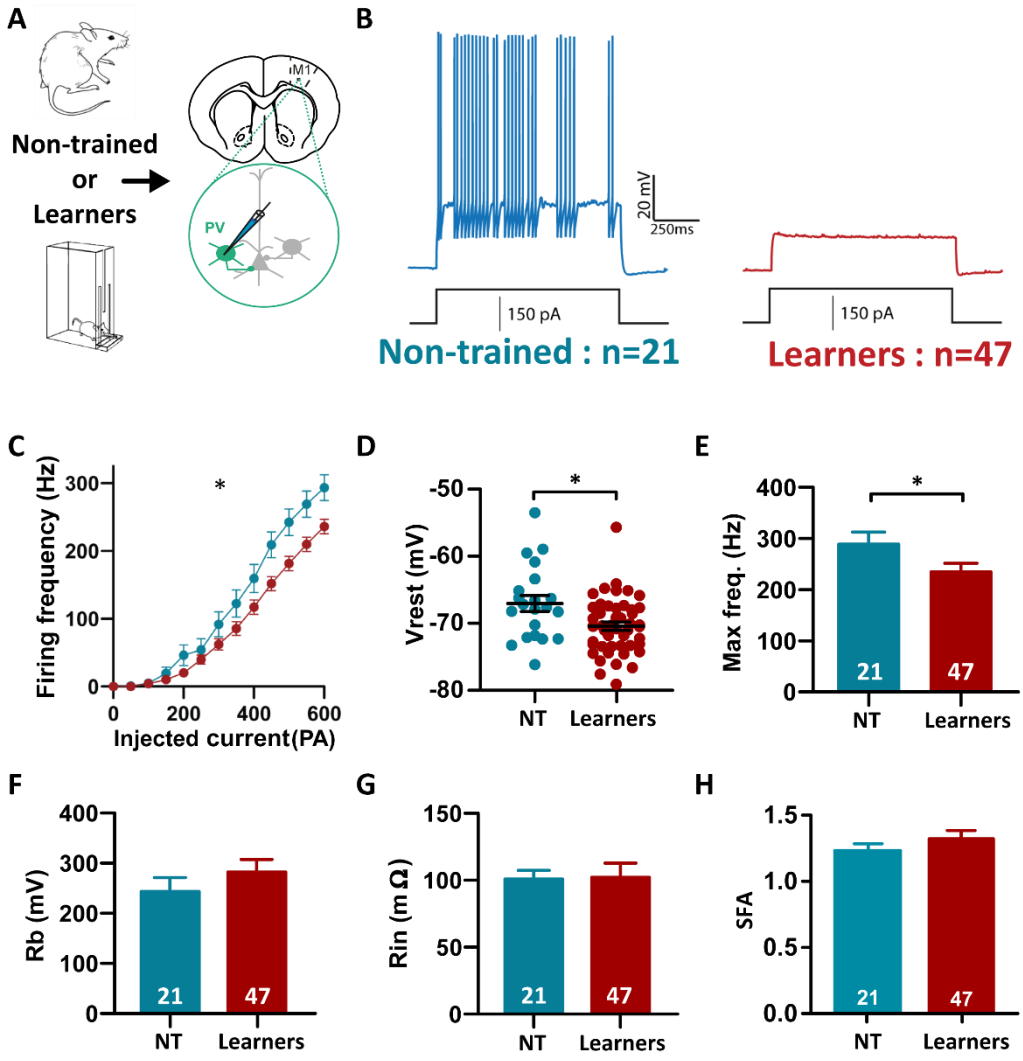

Figure 3.3: M1 PV neurons excitability is decreased with motor skill learning. **A**, Schematic of the experiment. PV neurons were identified as tdTomato positive neurons in M1 from brain slices of learners or non-trained (NT) PVCre::Ai9t mice. **B**, Representative voltage responses to a 150 pA current injection in PV neurons from a learner (red) or non-trained mice (NT, blue). **C**, the firing rate of PV neurons is increased with motor skill training. **D**, the resting potential is decreased with motor skill learning (Vm). **E**, motor skill learning significantly decreased the maximal frequency (Max freq.). **F,** Motor skill learning did not affect the rheobase (Rb). **G**, motor skill learning did not affect the input resistance (Rin), **H**, nor on the spike frequency adaptation (SFA).

2.1.2.2. M1 L5 PV neurons properties of non-learners mice were not modified after training.

In the publication using the SPRT, non-learner mice are usually removed for the experimental groups (Chen et al., 2014). We also found that a portion (around 50%) of the trained PVCre::Ai9t mice were not able to increase their success rate over training days: starting at 18.5 ± 3.2 % and ending up at 25.8 ± 4.6 % (Figure 3.4.A-B). However, the qualitative kinematic analysis of the paw movements seemed to reveal that non-learners (NL) mice may acquire a stereotyped movement after 8 days of training (Figure 3.4.C). This led us to investigate if we could also find changes in M1 L5 PV neurons properties following SPRT training in this group of mice. The same protocol as described in part 2.1.1 was performed. PV neurons were patched in M1 L5 corresponding to the preferred paw of NL. The excitability of M1 L5 PV was assessed by recording the firing responses to different steps of current injections. This firing activity was not affected after SPRT training in NL compared to NT as the input/output curves are almost identical (n_{NT} = 21, n_{NL} = 21, 2way ANOVA, p = 0.5303, $F_{(1,40)}$ = 0.4007, Figure 3.4.B). The resting potential (from -67.04 ± 1.20 mV to -67.04 ± 1.20 mV, Unpaired T-test, p > 0.9999, Figure 3.4.E), the rheobase (235.7 ± 26.7 Hz to 238.1 ±39.9 Hz, Mann-Whitney test, p = 0.7497, Figure 2.4.F), the input resistance (104.0 ± 8.8 MΩ to 92.5 ± 6.4 MΩ, Mann-Whitney test, p = 0.1864, Figure 3.4.G), as well as the maximal firing frequency (293.4 ±18.9 Hz to 239.2 ± 12.6 Hz, Unpaired T-test, p = 0.1983, Figure 3.4.H) were unchanged. Overall, M1 L5 PV neurons did not experience changes in their intrinsic properties in NL mice, contrary to learners.

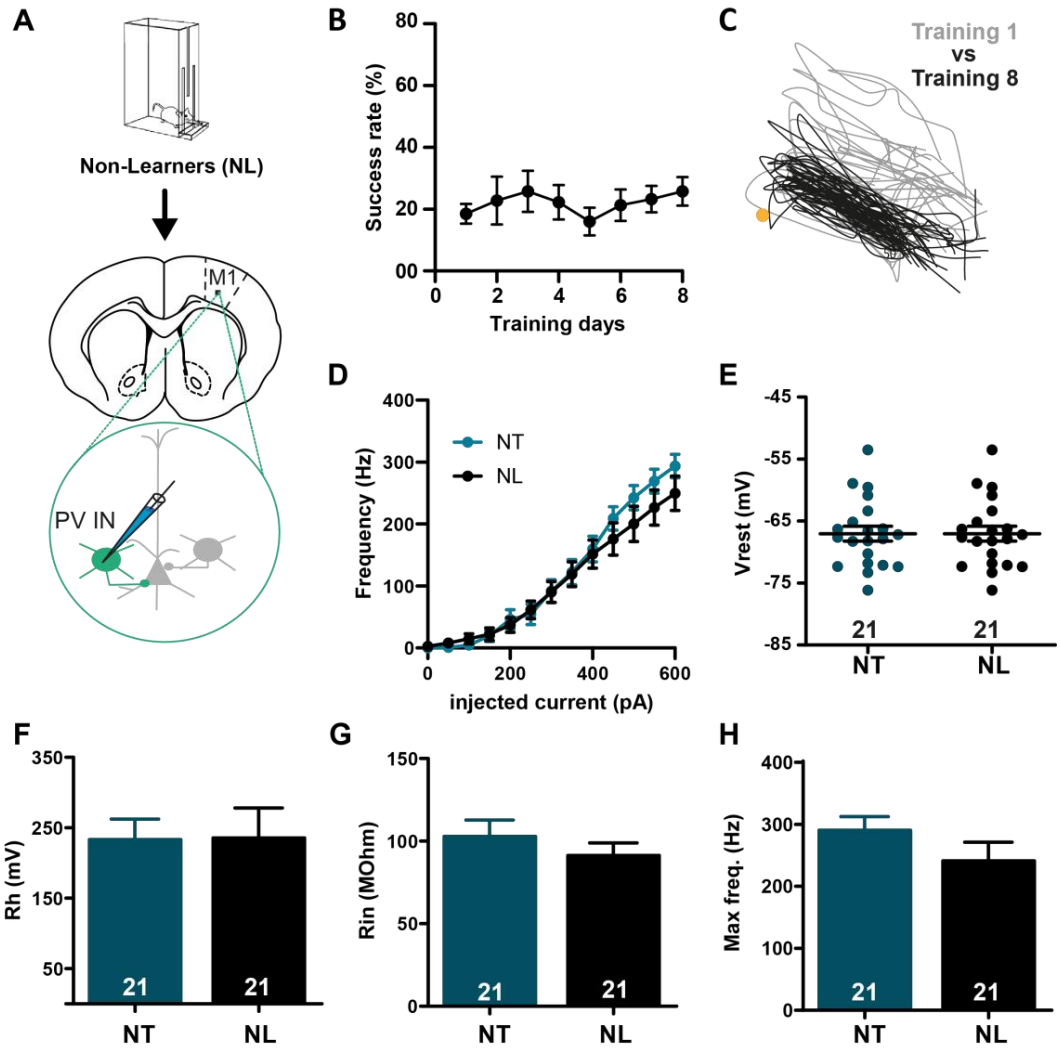

Figure 3.4: M1 L5 PV neurons intrinsic properties are not changed with motor skill training in non-learners mice. A, Experimental protocol: PVCre::Ai9t mice were trained to the SPRT for 8 days, and PV neurons were then patched in M1. **B**, Non-Learners mice were not able to increase their success rate over time (n = 10)**. C,** Tracking of the movement of the paw of a NL, the 20 first trials of the 1st training session (grey) are compared to the 20 first from the 8th session (black). **D**, Firing rate of PV neurons in response to different step of injected current (n_{NT} = 21, n_{NL} = 21). **E**, The resting potential (Vrest) of PV neurons is not changed in L compared to NL, **F**, nor the rheobase (Rh), **G**, nor the input resistance (Rin), F, nor the maximal firing frequency (Max freq.).

2.1.2.3. M1 L5 PV neurons intrinsic properties were dynamically modified during motor learning acquisition

In the previous section, we identified that M1 L5 PV neurons' excitability is decreased after motor skill learning. As plastic changes are dynamic processes, we wanted to determine the critical time-window when this modification in intrinsic properties occurs during skill training. It has already been reported that M1 neurons' intrinsic properties can be modulated after a single training session and be differently modulated across training (Kida et al., 2016). Indeed, *Kida et al.* showed that M1 PC excitability in layers 2/3 is decreased after a single session of rotarod training. However, after the second session of training, their excitability is modified in the other direction: their excitability is then increased compared to non-trained. In addition, we showed earlier that PV neurons' excitability was decreased after 8 days of training, while we showed that dopamine D2R activation increased their excitability. We then hypothesized that dopamine play a role earlier in the training, increasing PV neurons' excitability in early training stages. For these reasons, we investigated for differential regulation of PV properties across the learning at the SPRT.

To test his hypothesis, PVCre::Ai9t mice were trained at the SPRT and sacrificed after a different time points during training (1, 3, or 5 days of training: T1D, T3D, and T5D, respectively, Figure 3.5.A). It is important to note here that the different groups are composed of both 'learners' and 'non-learners' as it is not possible to differentiate these two groups at these time points (especially at T1D and T3D). M1 L5 PV neurons were then patched in M1 L5 as in part 2.12.1. Our data showed that the resting potential of PV neurons at T3D was significantly higher than the one of neurons recorded at T5D (-65.96 ± 0.92 mV versus -70.84 ± 1.00 mV, One-way ANOVA followed by a Tukey's multiple comparison test, p = 0.0026, Figure

3.5.B). The rheobase of PV neurons was significantly higher at T5D compared to those recorded at T1D and T3D (285.2 ± 18.7 pA (T5D) versus 193.0 ± 16.1 pA (T1D) and 184.7 ± 18.4 pA (T3D), Kruskal-Wallis test followed by a Dunn's multiple comparison test, p = 0.0067 versus T1D, p = 0.0006 versus T3D, Figure 3.5.C). However, the maximal frequency was decreased at T3D compared to NT and T1D (218.4 ± 13.0 Hz (T3D) versus 293.4 ± 18.9 Hz (NT) and 284.3 ± 17.7 Hz (T1D), Kruskal-Wallis test followed by a Dunn's multiple comparison test, p = 0.0103 versus NT, p = 0.0351 vesus T1D, Figure 3.5.D). Finally, PV neurons' input resistance at T3D was significantly higher than at NT and T5D (153.4 ± 14.37 MOhm (T3D) versus 104.0 ±8.8 MOhm (NT) and 103.2 ± 5.6 MOhm (T5D), Kruskal-Wallis test followed by a Dunn's multiple comparison test, p = 0.0102 versus NT, p = 0.0138 vesus T5D, Figure 3.5.E).

Overall, these data showed that PV neurons' excitability seemed to be regulated in a complex and bi-directional manner across SPRT training, with the most changes observed at T3D. However, since learners and non-learners are pulled in each group, it is not possible to conclude on the effect of learning versus the effect of training.

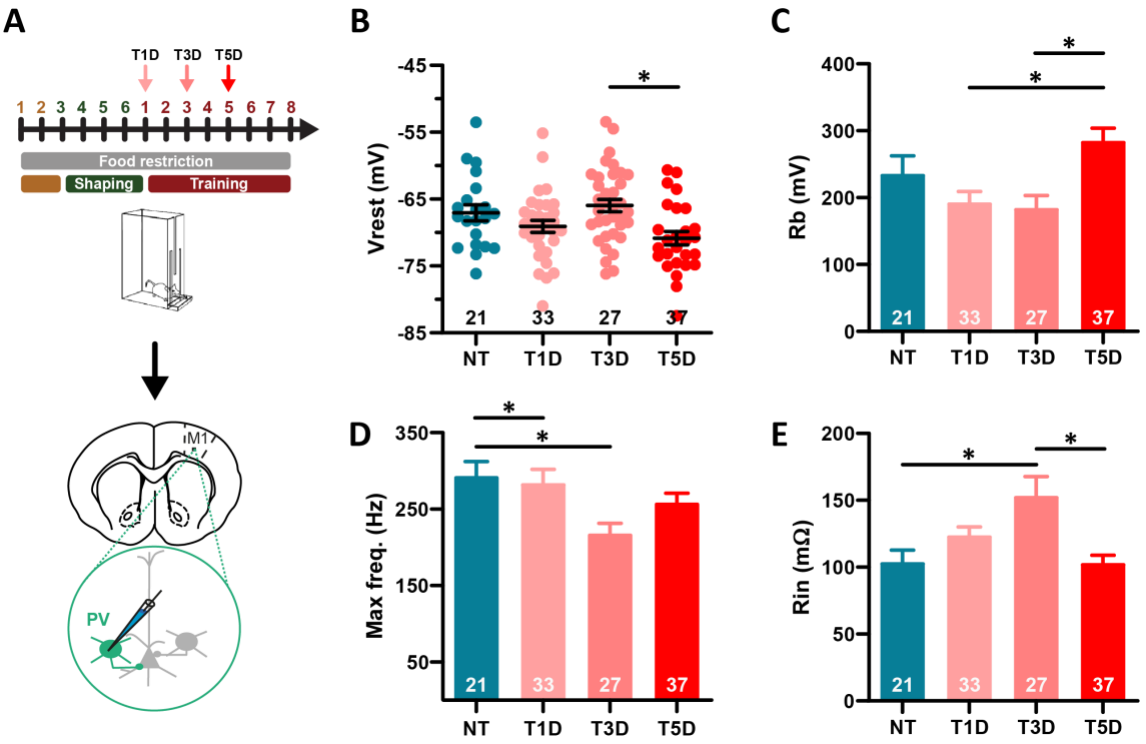

Figure 3.5: PV neurons' electrical properties across motor skill training. A, Experimental protocol. **B**, Resting potential (Vrest) of M1 L5 PV neurons from non-trained, trained for 1, 3, or 5 days (NT, T1D, T3D, and T5D respectively). **C**, Rheobase (Rb) of M1 L5 PV neurons across motor skill training in NT, T1D, T3D, and T5Ds. **D**, Maximal frequency (max freq.) of M1 L5 PV neurons across motor skill training in NT, T1D, T3D, and T5D. **E**, Input resistance (Rin) of M1 L5 PV neurons across motor skill training in NT, T1D, T3D, and T5D.

2.1.3 Motor skill learning decreases the synaptic transmission from PV neurons to PC

2.1.3.1. PV autaptic transmission was increased by motor skill learning

During motor skill learning, in humans, it has been shown that the amount of GABA in the motor cortex is reduced while glutamate concentration is not changed (Kolasinski et al., 2019). In addition, *Kolasinski et al.* showed that the concentration of GABA in M1 was correlated with the learning performances: the higher the GABA concentration, the lower the learning performances. We can then think that, as PV neurons' excitability is decreased with SPRT learning, PV neurons could be responsible for this decrease in M1 GABA concentration. With lower excitability, they may be less recruited and thus reduce their synaptic transmission in M1.

In order to investigate the impact of motor skill learning on PV neurons' synaptic transmission onto PC, we first plan to use a double patch-clamp recording approach. We choose to use the method developed by *Deleuze et al., 2019* which allows studying both the synaptic transmission between these 2 neurons and the autaptic transmission (from PV neurons to themselves). After this double patch protocol was set up, we tried to record transmission from PV neurons to PC from Learners and NT mice (Figure 3.6.A). Unfortunately, after more than 30 pairs of patched neurons in several adult mice (10-14 weeks, the age we usually train our mice), only 1 pair of neurons was found to be synaptically connected, with low fidelity. After a look at the bibliography, data published concerning double patched experiments usually use young mice (under 5 weeks old). To test if the age was the reason for the poor degree of connectivity we observed between PV and PC, we run

paired recordings in a 3 weeks old mouse to this if age was the problem. Indeed, we patched two PV/PC pairs in this mouse and were able to record the synaptic transmission from PV neurons to PC here.

However, the protocol used by *Deleuze et al.* allowed us to successfully record the PV autaptic transmission in some cells from Learners and NT (Figure 3.6.B) (Deleuze et al., 2021). Our data suggest that the autaptic transmission of M1 L5 PV neurons tended to increase following motor skill learning from 184.8pA ± 38.5 to 284.3pA ± 79.8 (Mann-Whitney test, p = 0.0556, Figure 3.6.B). However, the number of neurons here was small (n_{NT} = 5, $n_{Learners}$ = 5), and more recordings are needed to conclude on those results. No differences in the proportion of PV neurons exhibiting autaptic IPSCs were observed (5 neurons out of 6 exhibited autaptic IPSCs in NT, and 5 out of 7 in learner mice).

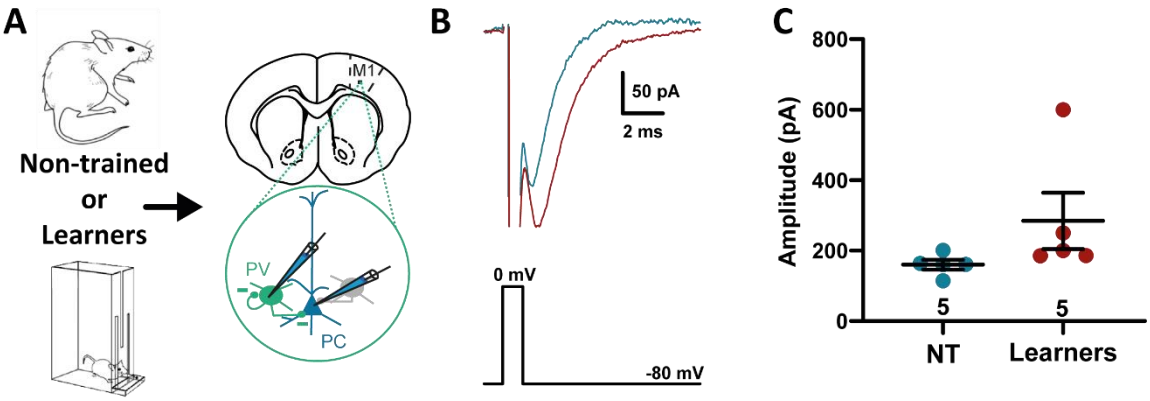

Figure 3.6: Recordings of PV autaptic IPSCs in NT and Learners. A, Experimental procedure: Pairs of PC-PV neurons were patched in M1 L5 of NT and learners. **B**, Representative traces of elicited autaptic IPSCs observed in a PV from a NT (blue) and a learner (red) in response to a 1ms voltage step to 0 mV from -80 mV. **C**, Analysis representing the mean and S.E.M. of the evoked autaptic IPSCs recorded in M1 L5 PV neurons from NT (blue) or Learners (red).

2.1.3.2. PV to PC synaptic transmission was reduced in M1 L5 following motor skill learning

To overcome the problem with the double patch experiments, we decided to use optogenetics. An AAV2.5-EF1a-DIO-hChR2(H134R)-eYFP was injected in the M1 corresponding to the preferred paw of PVcre::Ai9t mice after the shaping. With this strategy, transfected PV neurons were expressing the excitatory rhodopsin ChR2. We waited 4 weeks before sacrificing the mice to have sufficient ChR2 expression in PV neurons. Slices containing the CFA from Learners or NT mice were prepared to perform *ex vivo* optogenetic experiments, 1 to 3 days after the last training session (Figure 3.7.A). We first confirmed that 1ms photostimulation with a 473nm light flash was sufficient to trigger action potential with high reliability in PV neurons at a 10Hz photostimulation rate (Figure 3.7.B-C). Each flash of light (1ms, 473 nm) triggered an action potential in an intracellularly recorded PV neuron (Figure 3.7.D).

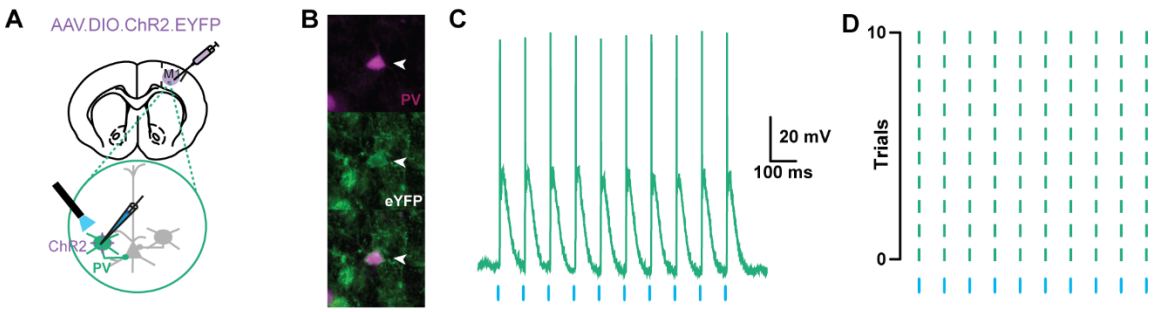

Figure 3.7: Driving PV neurons activity with photostimulation. **A**, Experimental protocol: PV neurons were patched in M1 from PVCre::Ai9t mice injected with an AAV allowing the expression of the ChR2 in a cre-dependent manner. **B**, Epifluorescent images of a PV neuron in M1 expressing the eYFP .**C**, Representative voltage traces of a PV neuron responding to a 473 nm light pulse at 10Hz (blue lines, 1ms). **D**, Reliability of light-evoked action potential in PV neurons. Each green line represents an action potential.

Whole-cell patch-clamp recording of M1 PC confirmed that the 473nm light flashes were able to reliably elicit light-evoked inhibitory postsynaptic currents (eIPSCs) (Figure 3.8.A-C). As we were using an internal solution with a high concentration of Cl^- (see method), both GABAergic and glutamatergic currents were inward current in voltage-clamp configuration. To make sure that recorded currents were not due to glutamatergic transmission, AMPA and NMDA receptors were pharmacologically blocked with DNQX and AP-5, respectively. PC were identified with their pyramidal shape, and as non-tdTomato (i.e. not expressing the PV) cells.

Following motor skill learning, the amplitude of the light-evoked IPSCs was significantly decreased in M1 L5 of the preferred paw, moving from 766.0 ± 100.9 pA (n=17 neurons, N=5 mice) to 473.3 ± 80.3 pA (n=18 neurons, N=3 mice) (unpaired T-test, p=0.0290, Figure 3.8.D). Those results suggest a decrease in GABAergic transmission from PV neurons to PC following motor skill training.

Short-term plasticity was also assessed with 10Hz photostimulations (473nm). These 10Hz photostimulation were able to reliably trigger light evoked IPSC in patched PC (Figure 3.8.E). The amplitude of the 10 light-evoked IPSCs was decreased following motor skill learning (2way ANOVA, p=0.0104, $F_{(1,28)}$ = 7.543, Figure 3.8.F) when a 10Hz photostimulation train was applied. The amplitude of the 10 light-evoked IPSCs were normalized to the first one to compare the short-term depression observed at this synapse between NT and learner mice (Figure 3.8.G). The similar time-course of the normalized eIPSCs between the two conditions indicates that motor skill learning did not affect the short-term depression at PV to PC synapses (2way ANOVA, p=0.8569, $F_{(1,28)}$ = 0.0331).

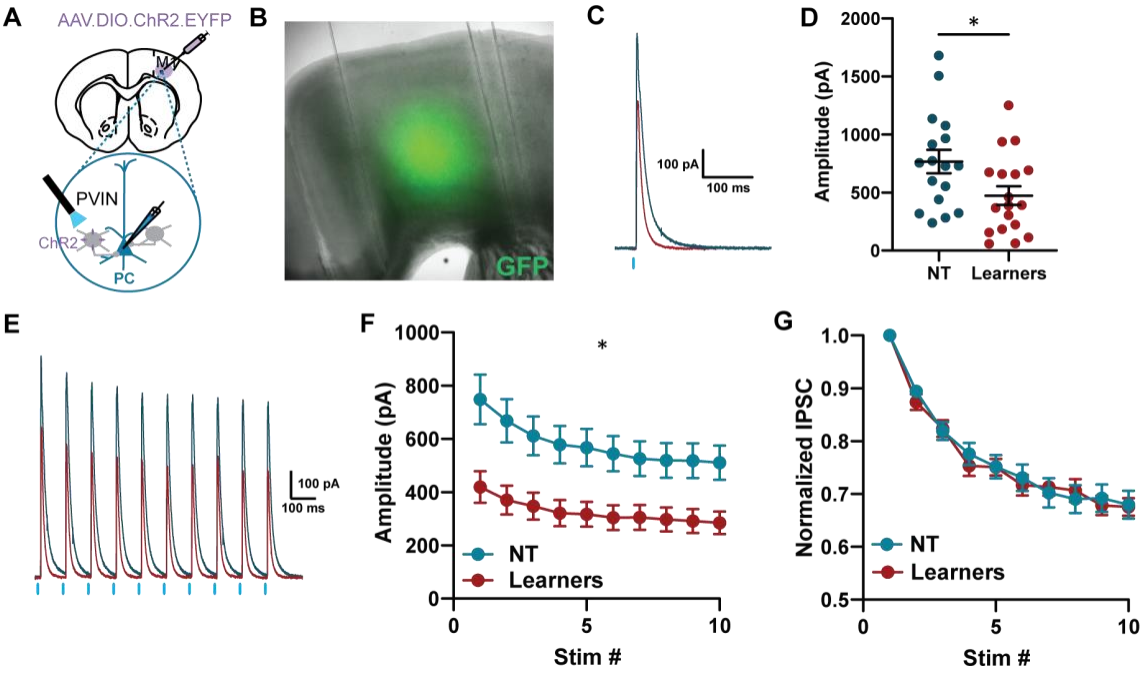

Figure 3.8: Motor skill learning decreased the synaptic transmission from PV to PC neurons in M1. A, Schematic of the recording configuration from a postsynaptic PC during photoactivation of PV neurons in non-trained (NT) or learner mice. **B**, Example of the virus (GFP in green) expression in M1. **C**, Sample traces light-evoked IPSCs recorded in PC from a non-trained (blue) and a learner (red). **D**, Mean and SEM of the recorded evoked IPSCs. **E**, Sample traces of responses to repetitive photostimulation (10 Hz) recorded in a non-trained (blue) or a learner (red). Photoactivation of PV neurons produces large initial IPSCs that depress rapidly. **F**, Mean of the amplitude of the repeatedly evoked IPSCs. **G**, Short-term synaptic dynamics of the evoked IPSCs. IPSC amplitudes were normalized to the first IPSC of their respective train stimulation.

2.1.4 Selective manipulation of PV neurons excitability slightly reduced motor learning

We demonstrated that PV neurons' excitability is decreased with motor skill learning, but it is not clear if this is instrumental for learning a new motor skill. To investigate this, we manipulated PV excitability throughout training using a chemogenetic approach. PVCre mice were injected in the CFA corresponding to the preferred paw with an AAV8-hsyn-DIO-HA-hM3Dq-IRES-mcitrine. The DREADDs receptor hM3Dq activation leads to increased excitability of the transfected neurons when activated by CNO (Pati et al., 2019; Townsley et al., 2021). By injecting CNO daily, 40 minutes prior to training sessions, our objective was to bypass the skill learning-induced decreased excitability of PV (Figure 3.9.A-B). Our data showed that even if decreasing the excitability of PV neurons during training sessions tended to decrease the performances, this was not significant (n_{hM3Dq} = 9, n_{eYFP} = 4, 2way ANOVA, p = 0.2325, $F_{(1,11)}$ = 1.596, Figure 3.9.C).

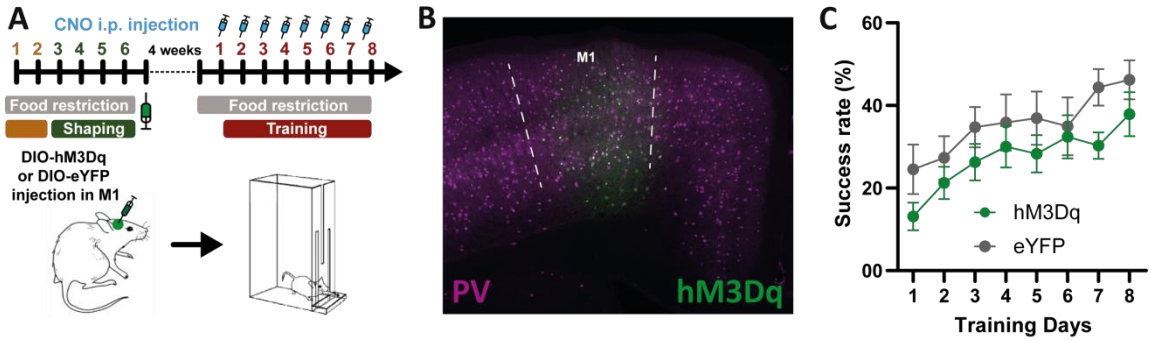

Figure 3.9 Chemogenetic manipulation of PV neurons during SPRT training slightly reduced the learning. A, experimental protocol: PVCre mice were injected with a virus allowing the expression of the excitatory DREADDs hM3Dq specifically in M1. **B**, a representative epifluorescent image of the viral transfection in M1 (hM3Dq in green, PV in red). **C**, learning curves representing the success rate over training days from mice injected with the hM3Dq or the controls injected with the eYFP.

Part II.2. Impact of M1 selective dopamine denervation on motor learning and PV neurons intrinsic and synaptic properties

2.2.1. The loss of M1 dopaminergic inputs prevents motor skill learning

Dopaminergic innervation of the motor cortex is crucial for the acquisition of new motor skills (Molina-Luna et al., 2009; Guo et al., 2015b). To study the role of dopaminergic inputs in motor learning, dopaminergic fibers were lesioned by bilateral injections of the neurotoxin 6-OHDA directly in the CFA (Figure 3.10.A). Noradrenergic fibers were protected by the administration of desipramine during the surgeries. Sham animals underwent the same experimental protocol, except there were injected with saline in place of the 6-OHDA. First, we verified that M1 dopamine depletion was able to alter the learning of the SPRT with our automated skill reaching box. Dopamine-depleted mice were then trained to the SPRT (DDT mice), and their motor performances measured. As observed in other studies (Molina-Luna et al., 2009; Guo et al., 2015b), specific M1 dopamine depletion impaired the learning of the SPRT. Indeed, the increase in the success rate over 8 training sessions was significantly lower in DDT compared to sham trained mice (ShamT): DDT started at 17 ± 4 % to end up at 20 ± 4 %of success rate while ShamT started at 12 ± 4 % to end up at 48 ± 5 % after 8 training sessions (2way ANOVA, $p = 0.0421$, $F_{(1,20)} = 4.665$, Figure 3.10.B). These data showed that dopaminergic fibers projecting to M1 are necessary for improving the motor skill required for the acquisition of this task. As a failure in properly increasing their success rate over time

could be due to a reduction in motivation, the number of trials mice were performing each session was measured. Interestingly, M1 dopamine depletion did not affect the number of attempts per session, as DDT were doing 46.97 ± 0.88 trials/session and shamT did 47.42 ± 2.03 trials/session (Mann-Whitney test, $p = 0.1454$, Figure 3.10.C). Moreover, to assess if M1 dopamine depletion altered the acquisition of the stereotyped movement, qualitative kinematic analysis of the paw trajectories was performed. It reveals that the paw movements were still spread in space and variable after 8 days of training in DDT mice (Figure 3.10.D). TH immunostaining in DD and sham mice was performed to verify that dopaminergic fibers were well depleted after 6-OHDA injection (Figure 3.10.E). TH staining in M1 was significantly reduced in DD mice compared to Sham (Unpaired T-test, $p > 0.0001$, Figure 3.10.F). Altogether, those data show that M1 dopaminergic fibers are necessary to learn the skill required to perform correctly the SPRT.

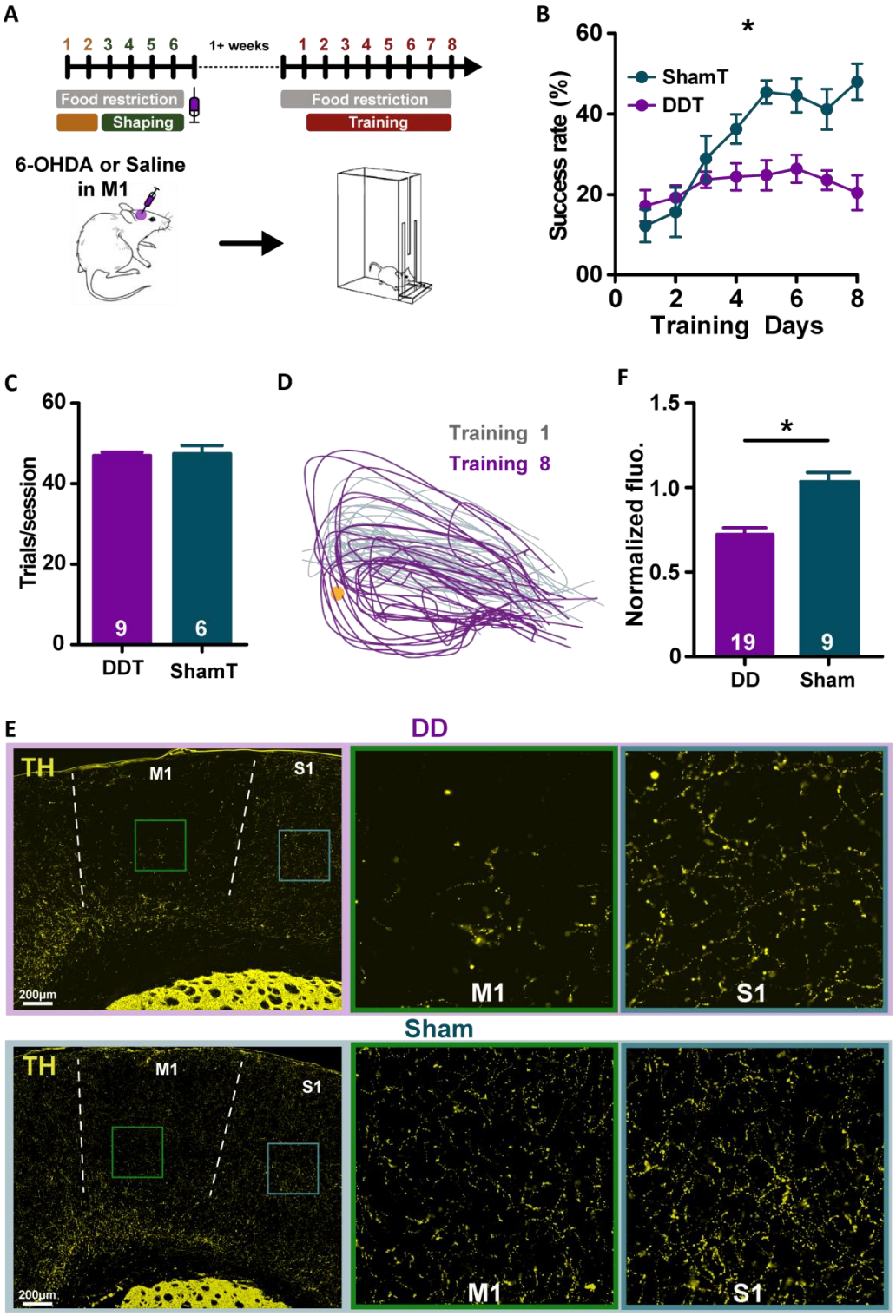
A
1 2 3 4 5 6
1+ weeks
1 2 3 4 5 6 7 8
Food restriction
Shaping
Food restriction
Training
6-OHDA or Saline
in M1
B
*
ShamT
DDT
Success rate (%)
60
40
20
00
0 2 4 6 8
Training Days
C
Trials/session
60
40
20
0
9
6
DDT
ShamT
D
Training 1
Training 8
F
*
Normalized fluo.
1.5
1.0
0.5
0
19
9
DD
Sham
E
DD
TH
M1
S1
200µm
M1
S1
Sham
TH
M1
S1
200µm
M1
S1

Figure 3.10: M1 dopamine depletion altered learning of the SPRT. A, PVCre::AI9t mice were injected in M1 with 6-OHDA or saline and then trained to the SPRT. **B**, M1 dopamine depletion decreased the increase in performances at the SPRT (n_{DDT} = 9, n_{ShamT} = 8). **C**, Dopamine depletion did not alter the number of trials performed per session. **D**, paw trajectories of the 20 first trials at the 1st (grey) and 8th (purple) training session of a DD mouse. **E**, confocal images of the tyrosine hydroxylase (TH) staining in M1 and S1 from a DD (left) or Sham mice (right). **F**, quantitative analysis of the TH staining: the TH fluorescence in M1 has been normalized with S1 fluorescence.

2.2.2. M1 L5 PV neurons excitability is altered in dopamine depleted trained mice

After the validation of our M1 dopamine-depleted model, we investigated the impact of this depletion on M1 L5 PV neurons in the context of skill learning. The objective of this set of data was to know if the decrease in PV excitability observed with motor learning was dependent on M1 dopamine. To assess this question, brain slices from DD or DDT mice were prepared to record M1 L5 PV neurons' intrinsic properties (Figure 3.11.A). As observed in Figure 2.11.B, motor skill training significantly increased the excitability of M1 L5 PV neurons in DDT compared to DD as the input/output curve is shifted to the left (n_{DD} = 17 neurons from 4 mice, n_{DDT} = 22 neurons from 4 mice, 2way ANOVA, $p < 0.0001$, $F(1.481) = 87.14$, Figure 3.11.C). However, contrary to what we observed with control mice in the part 2.1.2.1 of the results, motor skill learning did not affect the resting potential of M1 PV neurons in dopamine depleted mice (moved from -60.25mV ± 1.70 to -59.60mV ± 1.75, Mann-Whitney test, p = 0.6475, Figure 3.11.D). Motor skill training also increased significantly the maximal firing frequency from 283.8 ± 18.8 Hz to 379.1 ± 18.8 Hz (Unpaired T-test, p = 0.0006, Figure 3.11.E). The rheobase was significantly decreased from 201.1 ± 27.9 pA to 114.1 ± 29.6 pA following motor training (Unpaired T-test, p = 0.0379, Figure 2.11.F). The input resistance was not affected (moved from 110.6 ±6.4 MOhm to 110.8 ± 10.17 MOhm, Mann-Whitney test, p=0.6700, Figure 3.11.G). The spike frequency adaptation was also increased from 0.89 ± 0.05 to 1.19 ± 0.11 following skill training in those mice (Mann-Whitney test, p = 0.0007, Figure 3.11.H). Interestingly, the selective depletion of M1 dopamine fibers inverts the changes occurring on M1 L PV neurons' excitability with skill learning. Instead of the normal decrease in excitability, M1 PV neurons underwent an increase in excitability.

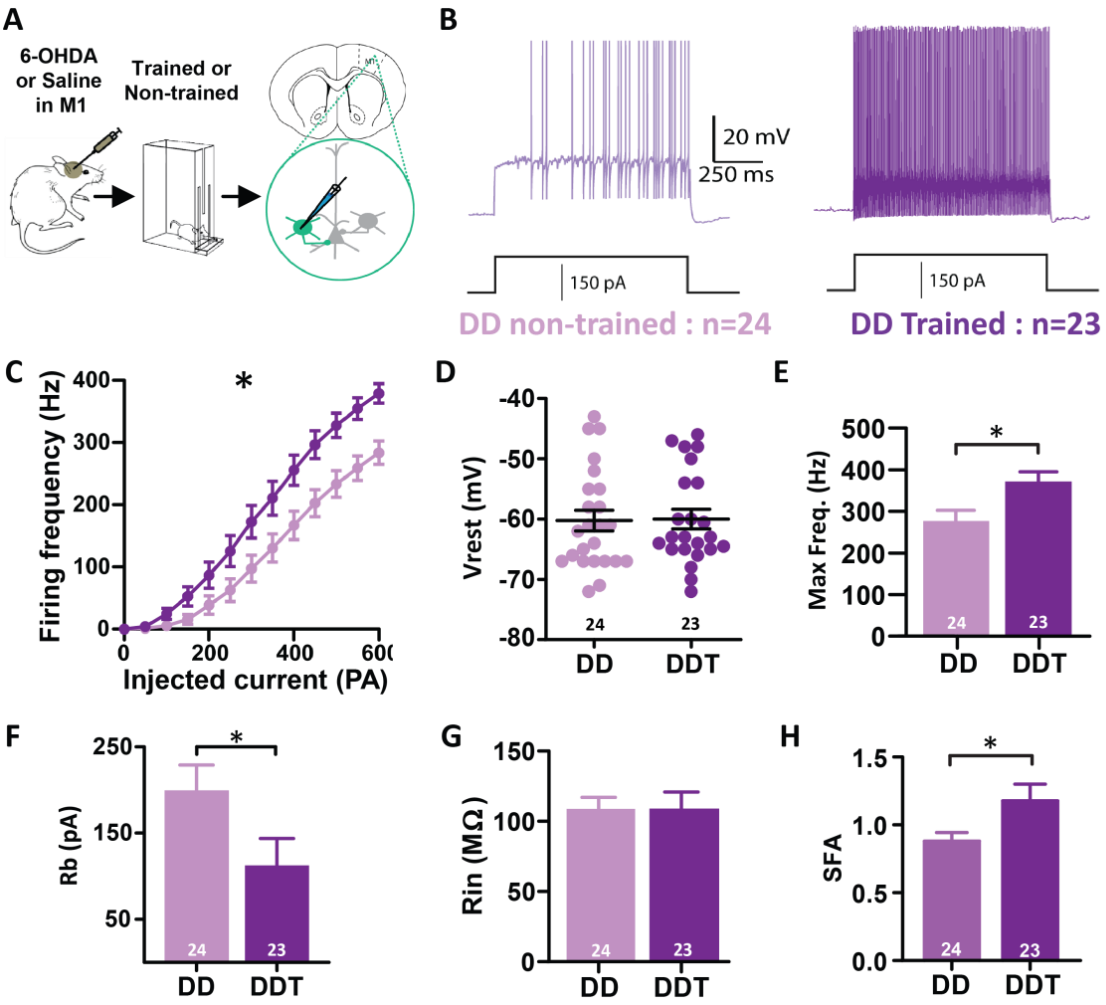

Figure 3.11: Altered PV neurons excitability following motor skill training in M1 dopamine depleted mice. **A**, Experimental protocol. PVCreAi9t mice received a stereotaxic injection of 6-OHDA in M1. These M1 dopamine depleted mice were then trained (DDT) or not (DD). **B**, Representative voltage responses to a 150 pA current injection in PV neurons from a DD (light purple) and a DDT (dark purple). **C**, Quantitative analysis of the firing rate of PV neurons in response to different steps of current injections. Their firing rate is increased with motor skill training (n_{DD} = 24 neurons from 4 mice, n_{DDT} = 23 neurons from 4 mice). **D**, motor skill training had no effect on the resting potential (Vrest) of DDT mice. **E**, motor skill training increased the maximal frequency (Max freq) of M1 L5 neurons. **F**, motor

skill training decreased the rheobase (Rb) of M1 L5 PV neurons. **G**, the input resistance was not changed (Rin). **H**, motor skill training increased spike frequency adaptation (SFA).

2.2.3. M1 L5 PV neurons synaptic transmission is disturbed in dopamine depleted mice

As the changes in PV neurons' excitability observed with motor skill learning seemed to be a dopamine-dependent phenomenon, we wondered if this was also the case for the synaptic transmission changes.

Using the same approach as in 2.3.2, the excitatory rhodopsin ChR2 was expressed in M1 PV neurons (in the hemisphere corresponding to the preferred paw). Three weeks later, mice received a bilateral stereotaxic injection of 6-OHDA (or saline for sham control mice) (Figure 3.12.A-B). Then, at least 1 week later, mice were trained to the SPRT. The synaptic transmission from PV neurons to PC was then assessed once the training was achieved. PV neurons were then photostimulated and the light-evoked IPSCs were recorded *ex vivo* in M1 L5 PC (Figure 3.12.C). Interestingly, motor skill training induced a decrease in the amplitude of the evoked-IPSC from PV neurons to PC in M1 following motor skill training, both in Sham and dopamine depleted mice. The eIPSC amplitude decreased from 1158.7pA ± 167.3 to 668.2pA ± 121.1 following motor skill training (Figure 3.12.D). For Sham mice, the amplitude decreased from 1303.4pA ± 206.9 to 834.2pA ± 160.4 (2way ANOVA, effect of training: $p = 0.0076$, $F_{(1,50)} = 7.749$; effect of dopamine depletion: $p = 0.3718$, $F_{(1,50)} = 0.8123$, Figure 3.12.D). To study the impact of M1 dopamine depletion on the short-term plasticity of PV to PC synapses, PV neurons were stimulated with 10Hz photostimulation trains (Figure 3.12.E-F). However, while the short-term plasticity remained the same between non-trained and trained Sham mice, the short-term

plasticity was disturbed in dopamine depleted non trained mice. Indeed, the short-term depression in DD was significantly decreased compared to DDT as the curve is shifted to the top (3way ANOVA, Figure 3.12.G)

Altogether, these data suggest that the decrease of the amplitude in the PV-PC synaptic transmission occurring with skill training does not depend on dopamine, while the plasticity of this synapse seemed to be altered in DDT mice.

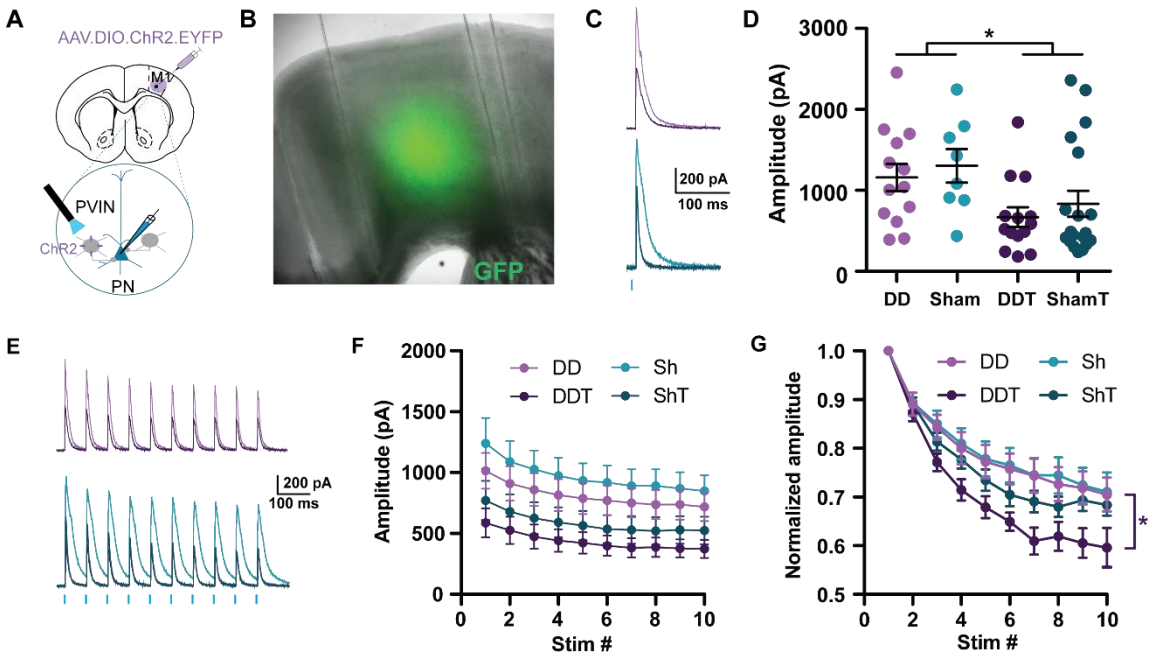

Figure 3.12: Impact of M1 dopamine depletion on PV synaptic transmission onto PC in the context of skill learning. **A**, Schematic of the recording configuration from a postsynaptic PC during photoactivation of PV neurons. **B**, Example of the viral transfection in M1. **C**, Representative traces of the recorded light-evoked IPSCs. **D**, Mean and SEM of the recorded evoked IPSCs (nDD = 13 neurons from 6 mice, nDDT = 14 neurons from 5 mice, nSham = 8 neurons from 4 mice, nShamT = 19 neurons from 5 mice). **E**, Sample traces of responses to repetitive photostimulation (10 Hz) recorded in DD, DDT, Sham, and ShamT mice. **F**, Mean of the repeatedly light-evoked IPSCs. **G**, Short-term synaptic dynamics of the light-evoked IPSCs. IPSC amplitudes were normalized to the first IPSC of their respective train stimulation (* : significant difference between the DD and DDT groups).

To sum up this part II, we showed that M1 L5 PV neurons underwent plastic changes with motor skill training: (1) their excitability was decreased and (2) their synaptic transmission onto PC was decreased after 8 training sessions (Figure 3.13). In addition, mice with selective dopamine depletion in M1, displayed an altered skill learning, and exhibited an increased in PV excitability. However, the SPRT training-induced decrease in their synaptic transmission was still observed.

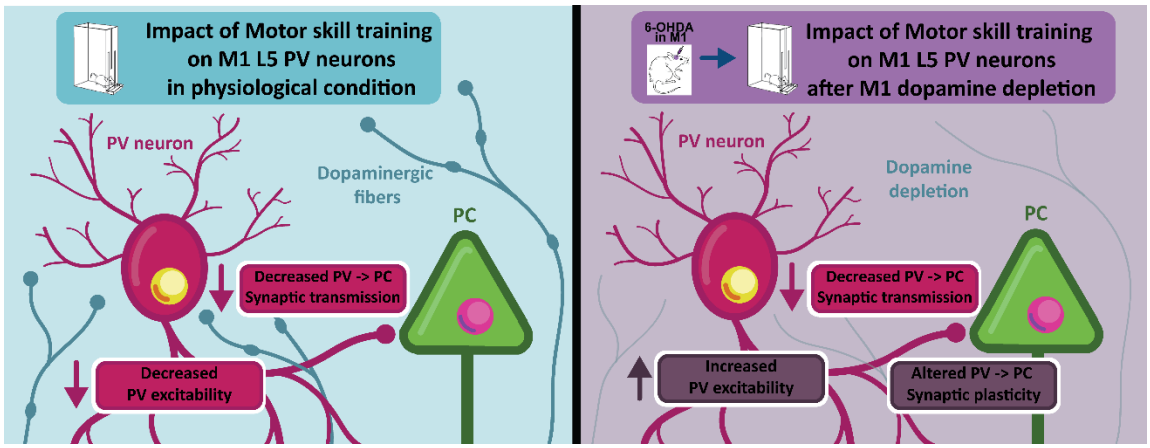

Figure 3.13: Summary of the modulation of PV neurons following motor skill training in control condition versus in M1 dopamine depleted mice. Schematics representing a PV neuron projecting on a PV in the control condition (left) and in M1 dopamine depleted mice (right). Motor skill learning induced a decrease of M1 L5 PV neurons excitability and synaptic transmission onto PC (left). In M1 dopamine depleted trained mice, in addition to impairment in skill learning, mice exhibited alterations in (1) the excitability of PV neurons and (2) the synaptic plasticity (right).

Part III. The role of PNN in M1 during motor skill learning

3.1. M1 PNN are decreased during SPRT training

PNN may play a role in the good operation of neural networks (Wingert and Sorg, 2021). It has been shown that following motor exercise, the amount and labeling intensity of PNN is decreased in a wide variety of brain regions (Smith et al., 2015). It has also been shown that PNN can limit plasticity (Härtig et al., 1992b; Bukalo et al., 2007; Frischknecht et al., 2009; Beurdeley et al., 2012; de Winter et al., 2016; Shinozaki et al., 2016; Favuzzi et al., 2017). Therefore, we hypothesized that during motor skill learning, PNN would decrease in M1 in order to open a new plasticity window which would allow network changes necessary for learning.

To investigate this idea, we decided to measure the intensity of PNN at different stages of the training. PVCre::Ai9t mice were trained at the SPRT and sacrificed at different time points of the training phase to access PNN intensity. Mice were sacrificed after 3, 5, or 8 days of training (T3D, T5D, and T8D respectively) and compared to control non-trained mice (NT) (Figure 3.14.A). We assessed the performances of the mice across training days and their success rate over training days curves showed no differences between the 3 groups of trained mice (Figure 3.14.B). Analysis of the intensity of the WFA labeling (Figure 3.14.C) was used to measure the intensity of PNN in the M1 corresponding to the preferred paw. It revealed that PNN intensity was significantly decreased after 5 days of training (Dunn's multiple comparisons test, $p = 0.0043$); furthermore, this decrease was

maintained after the 8th training day (compared to NT mice, Dunn's multiple comparisons test, p = 0.0184, Figure 3.14.D).

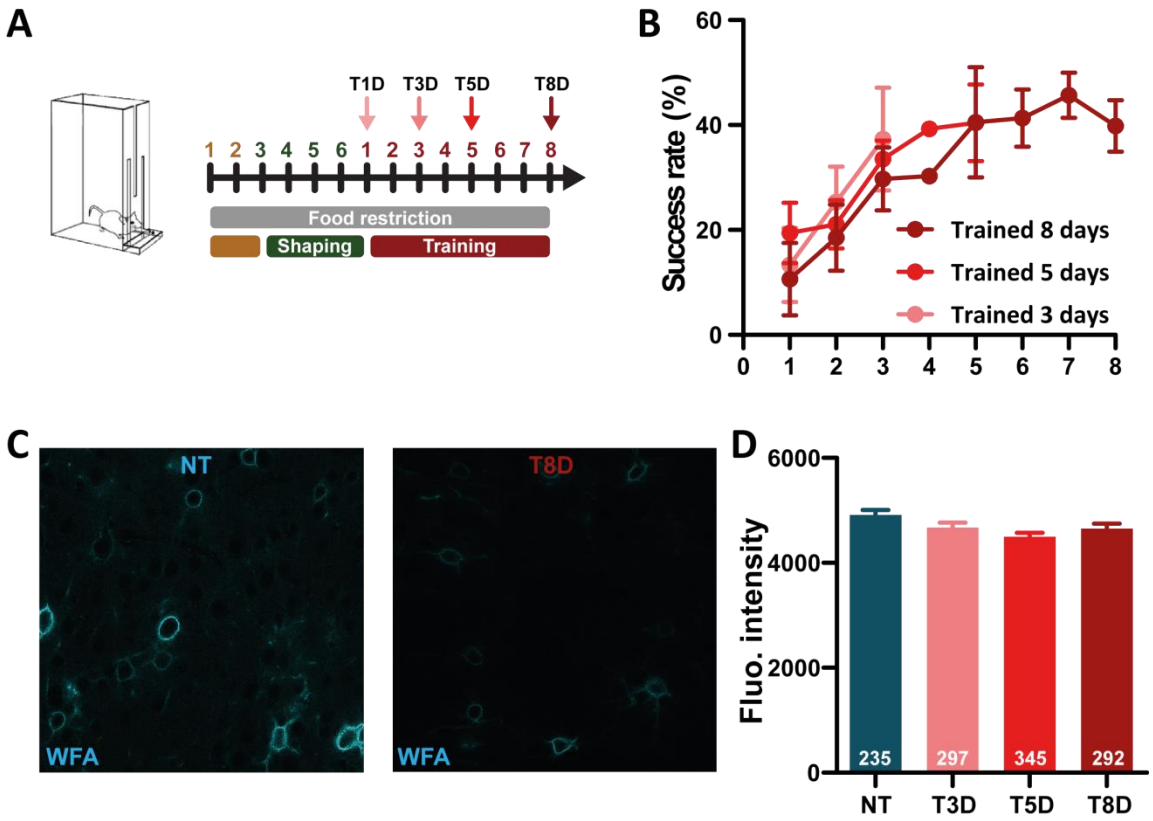

Figure 3.14: PNN intensity regulation across motor skill training. A, Experimental procedure, PVCre::AI9t mice were trained at the SPRT for 3, 5, or 8 days (T3D, T5D, and T8D, respectively, n = 3 mice per group). **B**, Success rate over SPRT training days for T3D, T5D, and T8D. **C**, Representative WFA staining in M1, used to label PNN, in an NT (left) and a T8D (right). **D**, quantitative analysis of WFA intensity in M1 from NT, T3D, T5D, and T8D. The WFA intensity is significantly decreased after 5 and 8 days. The numbers of analyzed PNN are written in white on the histograms (Kruskal-Wallis test, p = 0.0046).

3.2. PNN digestion during SPRT training did not alter mice performances

3.2.1. Digestion of the PNN before SPRT training did not affect mice performances

Knowing that PNN intensity is decreased in M1 with motor skill learning, together with the fact that PNN are limiting plasticity, we hypothesized that the decrease in PNN was necessary to allow plastic changes in M1 during learning. To investigate if decreasing the PNN in M1 early in the training, and more drastically, we choose to digest them *in vivo* before starting the SPRT training. Once the shaping phase was done, PNN was digested in PVCre::Ai9t mice *via* a stereotaxic injection of the enzyme ChABC in the M1 corresponding to their preferred paw before the training phase (Figure 3.15.A). Control mice received an injection of PBS instead of ChABC. Three days after the stereotaxic injection, mice were trained to the SPRT for 8 days. Our data showed that PNN digestion in M1 was not affecting the success rate over training days (n_{PBS} = 6, n_{ChABC} = 5, 2way ANOVA, p = 0.4148, $F_{(1,9)}$ = 0.7307, Figure 3.15..B). Thus, PNN digestion in M1 through before the first training session did not affect the learning of the SPRT.

3.2.2. PNN digestion after 8 days of SPRT training did not affect mice performances

As digested the PNN before the training had no impact on the learning, we wanted to know if PNN integrity was important to maintain the learned skill. Indeed, PNN may play a role in the consolidation of the network after le learning is done. PVCre::Ai9t mice received a stereotaxic injection of ChABC in the CFA of their preferred paw 2 days after their 8th training session of SPRT (Figure 3.15.C). Three days later, they were retrained for 5 consecutive days. Control mice received a PBS injection instead of ChABC. Our data show no difference in performances between the control and PNN depleted mice, suggesting that PNN integrity is not needed in the CFA once the task has been learned ($n_{PBS} = 3$, $n_{ChABC} = 4$, 2way ANOVA, $p = 0.4320$, $F_{(1,5)} = 0.7297$, Figure 3.15.D). However, a decrease in the performances was observed at the first re-training session compared to the 8th training session in both groups. Once the training was done, mice were rapidly sacrificed to verify the correct digestion of M1 PNN with a WFA staining (Figure 3.15.E).

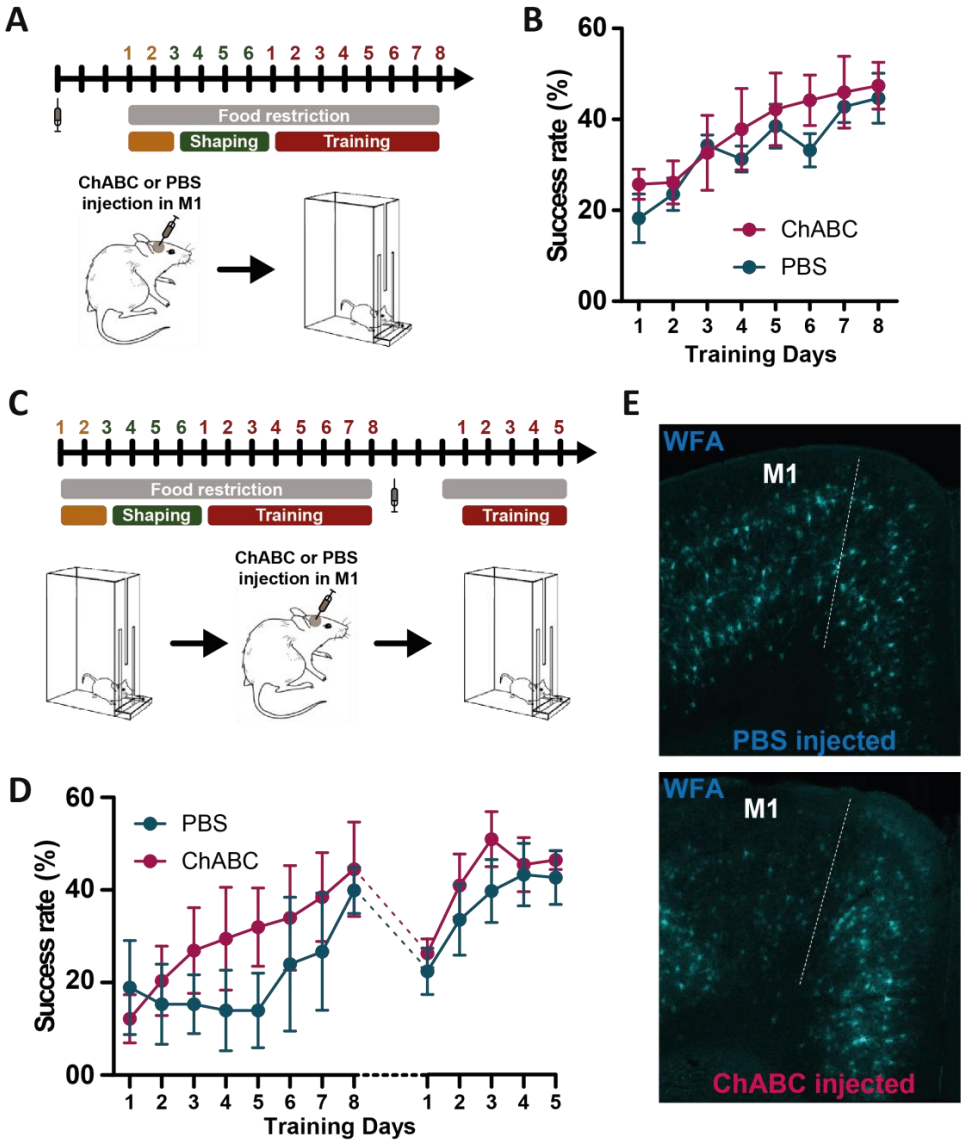

Figure 3.15: Impact of M1 PNN digestion on motor skill learning. A, Experimental protocol: PVCre::Ai9t mice received an injection of ChABC (10U/mL) or PBS in M1 before being trained to the SPRT. **B**, SPRT success rate over training days of PBS- and ChABC-injected mice. **C**, Experimental protocol: after 8 days of SPRT training, mice received an injection of PBS or ChABC in M1 and have been re-train for 5 days. **D,** SPRT success rate over training days of PBS- or ChABC-injected mice. **E**, Representative images of the immunolabelling of PNN (through WFA staining) to verify the PNN digestion in M1.

3.3. PNN degradation effect on PV neurons excitability in M1

3.3.1. PV electrical properties aftered *ex vivo* PNN digestion were not affected

We showed that PV excitability was decreased with motor skill learning. PV excitability and PNN expression are two highly linked parameters. Manipulation of one of them can have an impact on the other (Devienne et al., 2021; Wingert and Sorg, 2021). Our data showed that these two parameters were decreased in M1 with motor skill learning. Thus, we decided to check if these parameters were linked in M1. We first investigated if decreasing the PNN could have an impact on M1 PV neurons' intrinsic properties.

Brain slices from PVCre::Ai9t mice containing M1 were made (Figure 3.16.A) and incubated for 1.5h in an aCSF with ChABC prepared in PBS (0.2U/mL) or an aCSF with PBS alone for control. PV neurons were then patched in M1 L5 and filled with biocytin. The good digestion of the PNN was verified post hoc by the WFA immunolabelling (Figure 3.16.B). Surprisingly, our data showed that the *ex vivo* digestion of PNN did not affect neither the excitability, the resting potential, the rheobase, the membrane resistance, nor the spike frequency adaptation of these PV neurons (Figure 3.16.C-F).

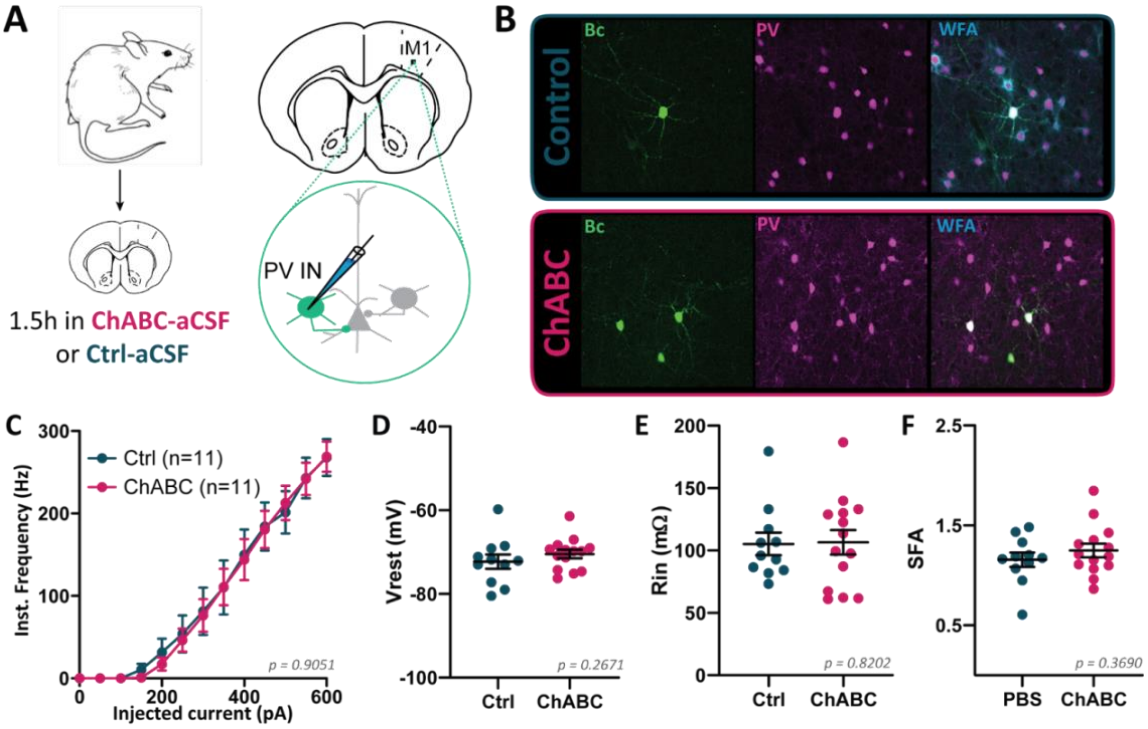

Figure 3.16: *Ex vivo* PNN digestion did not affect M1 L5 PV neurons' properties. **A**, Experimental protocol, slices containing M1 from PVCre::Ai9t mice were incubated for 1.5h in an aCSF with ChABC prepared in PBS (0.2U/mL) or an aCSF with PBS alone for control. PV neurons were then patched in M1 L5. **B**, Immunolabeling of PV neurons patched in M1 in slices treated with ChABC or control slices (Bc= biocytin, PV = Parvalbumin, WFA= Wisteria Floribunda Agglutinin). **C**, ChABC treatment did not affect the firing frequency of PV neurons (p=0.9051, n=11 for both groups, F(1.20)=0.1459, two-way ANOVA). **D**, The ChABC treatment did not affect the resting potential (Vrest, in mV, p=0.2671, Mann-Whitney test) nor, **E**, the membrane resistance (Rin, in MOhm, p=0.8202, Mann-Whitney test), nor **F**, the spike frequency adaptation (SFA, p=0.3690, Unpaired T-test).

3.3.2. PV electrical properties were not altered after *in vivo* PNN digestion

As *ex vivo* PNN digestion did not affect PV neurons' electrical properties, we hypothesized that modification of PV intrinsic properties may take some time to appear. Indeed, with this *ex vivo* application, only some minutes/hours separated the PNN digestion for our measurements. Modification in PV neurons due to the absence of PNN may take time and be delayed with the PNN degradation. To investigate if a longer period without PNN could alter PV intrinsic properties, we decided to digest *in vivo* the PNN. PVCre::Ai9t mice received a stereotaxic injection of ChABC *in vivo* in M1. PBS was injected in the other hemisphere as a control e. 5-7 days after the ChABC/PBS injection, mice were sacrificed for *ex vivo* electrophysiology experiments (Figure 3.17.A). Patched PV neurons were filled with biocytin in order to verify post-hoc that the recorded neurons were not surrounded by PNN in the ChABC-injected side (Figure 3.17.B). Increasing steps of currents were injected in PV neurons to record their firing activity (Figure 3.17.C). As observed with the *ex vivo* PNN digestion, the *in vivo* digestion of PNN leading to a longer period without PNN around the neurons did not alter their excitability (Figure 3.17.C), neither their membrane potential, their membrane resistance, nor their spike frequency adaptation (Figure 3.17.D-F).

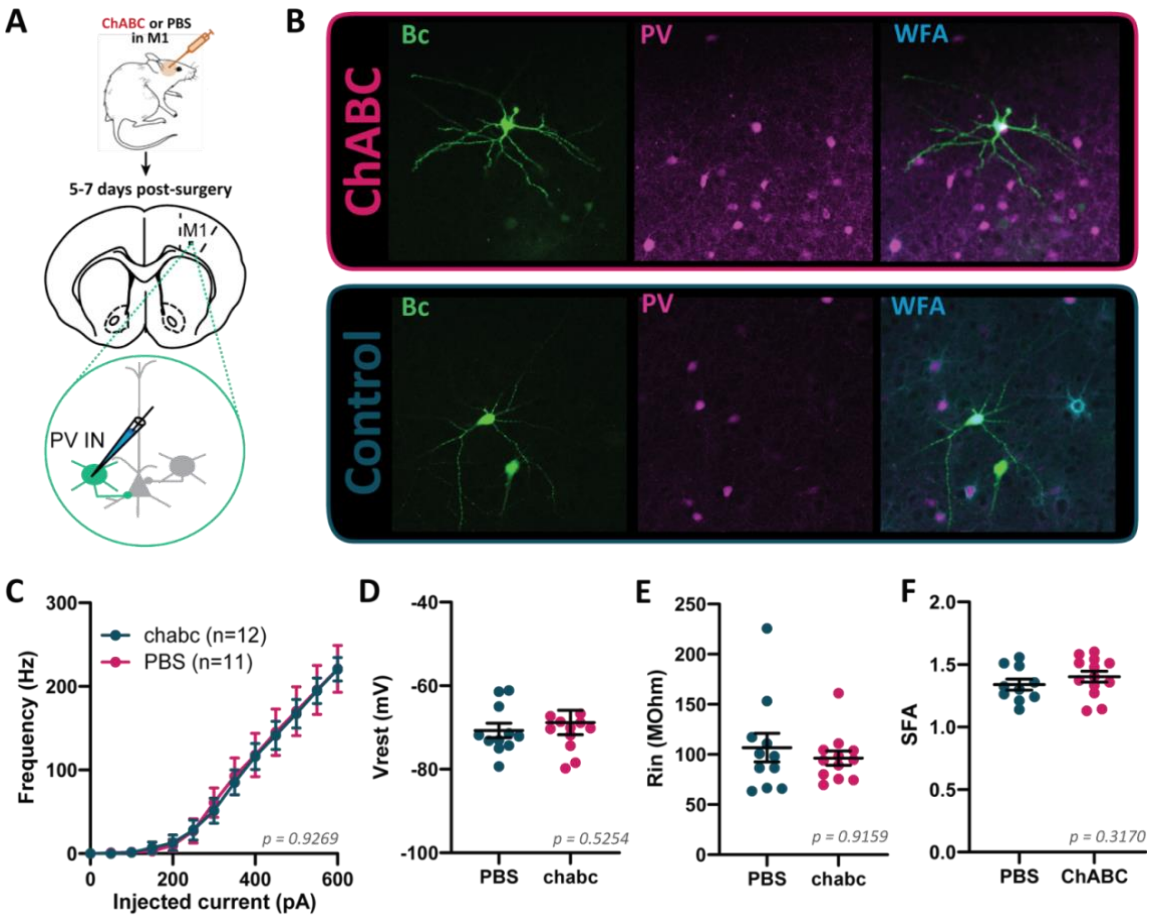

Figure 3.17: In vivo PNN digestion did not affect PV neurons' intrinsic properties in M1. A, Schematics of the experiments: PVCre::Ai9t mice received an injection of ChABC (10U/mL) or PBS in M1, PV neurons were then patched in M1 L5 5 to 7 days after receiving the surgery. **B,** Immunolabelling of PV neurons patched in M1 L5. **C**, The ChABC treatment did not affect the firing rate of PV neurons (p=09269, F(1,21)=0.008622, Two-way ANOVA). **D**, The ChABC treatment did not affect the resting potential of PV neurons (Vrest, p=0.5254, Mann-Whitney test). **E**, The ChABC treatment did not affect the membrane resistance of PV neurons (Rin, p=0.9159, Mann-Whitney test). **F**, The ChABC treatment did not affect the spike frequency adaptation (SFA, p=0.3170, Unpaired T-test).

3.3.3. PNN digestion on PV synaptic transmission tended to increase PV-PC synaptic transmission

Then we wanted to know if the digestion of PNN in M1 could lead to modification in their synaptic transmission onto neighboring pyramidal cells. PVCre::AI9t mice received a stereotaxic injection of an AAV2.5-EF1a-DIO-hChR2(H134R)-eYFP in M1 to selectively express the excitatory rhodopsin ChR2 in PV neurons. Then, as for 3.3.2, 3 weeks after the viral injection, mice received a stereotaxic injection of either PBS or ChABC in M1. PC were then patched in M1 L5 and PV neurons were photostimulated with a 1ms 473nm light flash to record light-evoked IPSCs (Figure 3.18.A). Our data showed that PNN digestion tended to increase the amplitude of the light-evoked IPSCs (Figure 3.18.B). 10 Hz photostimulations with 473 light flashes were also done to assess the short-term depression of this synapse following PNN digestion. Our data suggest that PNN digestion does not alter this short-term plasticity (Figure 3.18.C). However, for this set of experiments, it is important to note the small number for each group, which needs to be increased to be able to conclude on this part.

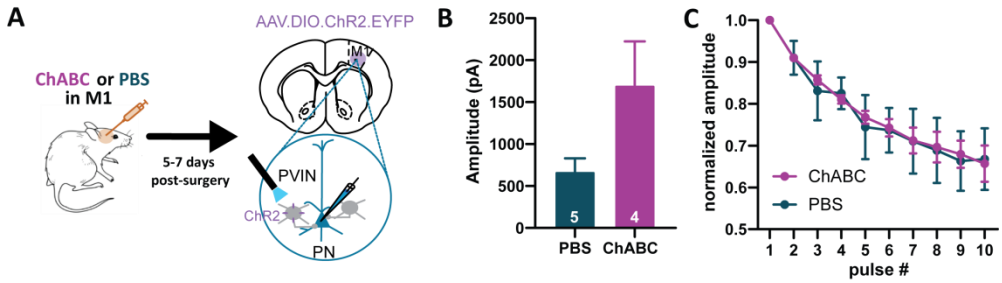

Figure 3.18: Impact of PNN digestion in M1 L5 on PV synaptic transmission onto PC. **A**, Experimental protocol, PVCre::Ai9t mice were injected in M1with both: a cre-dependent virus allowing the expression of the excitatory rhodopsin ChR2 selectively in PV neurons, and with ChABC (10U/mL) or PBS. **B**, Quantitative analysis of the light-evoked in PBS or ChABC injected mice. **C**, Quantitative analysis of the short-term depression observed at this synapse of light-evoked IPSCs elicited in M1 L5 pyramidal cells following 1ms 473nnm light flash at10Hz pulse (blue in PBS injected mice, purple in ChABC injected mice).

3.4. Chemogenetic decrease of M1 PV neurons excitability decreased PNN intensity

As said before, both PV neurons excitability and PNN intensity were decreased with motor skill learning, we tested if those two parameters influence each other in M1. After showing that PNN digestion had no impact on PV properties, we investigated if a decrease of PNN intensity could induce a decrease in the excitability of PV neurons in M1. We hypothesized that the manipulation of PV neurons' excitability *in vivo* could modulate PNN expression in M1. To test this hypothesis, we used a protocol developed by Devienne and colleagues in the visual cortex (Devienne et al., 2021). PVCre mice received a stereotaxic injection in M1 of an AAV8-hSyn-DIO-HA-hM4Di-mCitrine in one hemisphere and an AAV5-EF1a-DIO-eYFP in the other hemisphere for control. The inhibitory DREADD hM4Di allowed to specifically decrease the excitability of hM4Di-expressing neurons (PV neurons in PVCre mice) via i.p. injection of CNO, its specific agonist. Four weeks after the viral infections, mice received 4 i.p. injections of CNO, 12h apart, for 2 days (Figure 3.19.A). Mice were then sacrificed 24h after the last CNO injection. The intensity of the PNN (WFA labeling) around transfected neurons was measured (Figure 3.19.B). We observed that PNN intensity was significantly lower in neurons expressing the hM4Di compared to those expressing the eYFP (n_{eYFP} = 101 neurons in 4 mice, n_{hM4Di} = 101 neurons in 4 mice, Mann-Whitney test, $p < 0.0001$, Figure 3.19.C). Thus, we conclude that decreasing the excitability of PV neurons with this chemogenetic approach leads to a decrease in PNN.

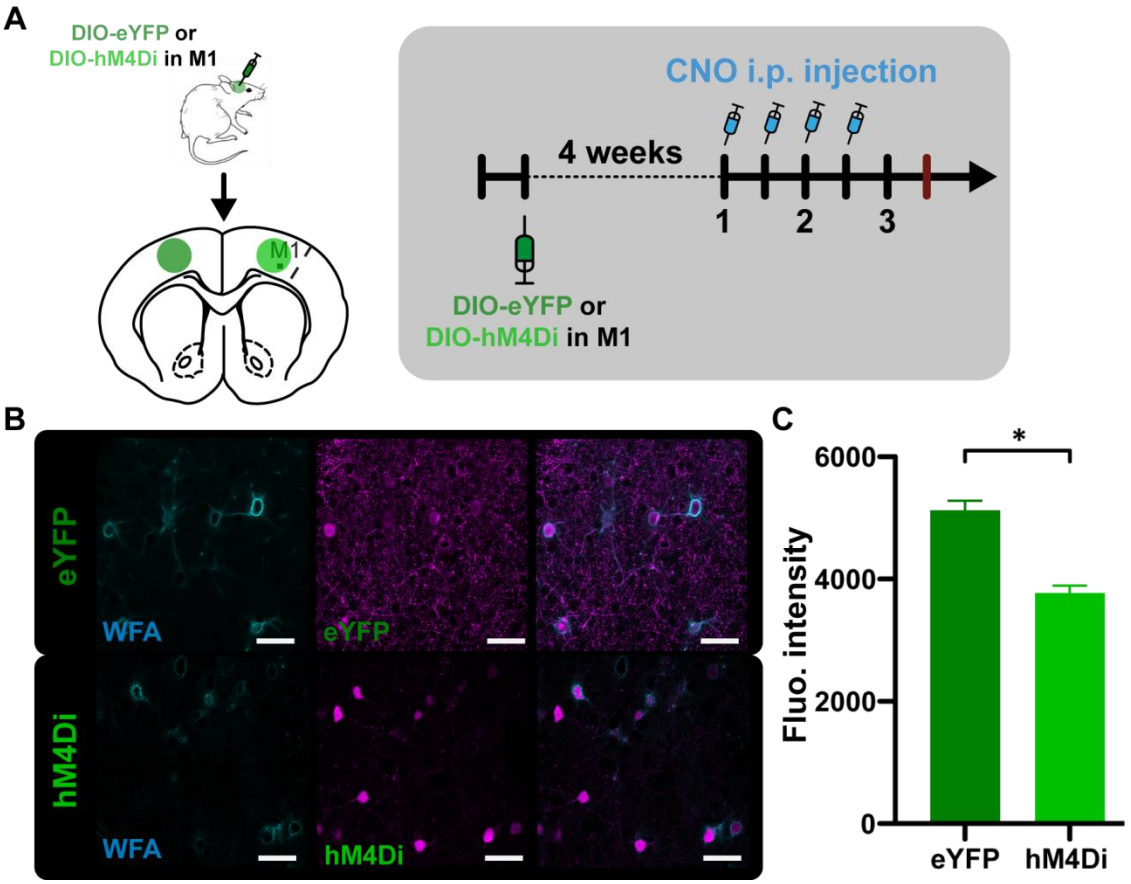

Figure 3.19: Chemogenetics decrease of PV neurons excitability decreased PNN intensity. A, experimental protocol, PVCre::Ai9t mice received a stereotaxic injection in M1 of a virus allowing the expression of the inhibitory DREADD hM4Di (or eYFP for controls) specifically in PV neurons. **B**, Representative images of the immunolabelling revealing the viral expression (mCitrine for hM4Di injected mice, or eYFP for controls) and WFA staining (to reveal PNN). **C**, the chemogenetic decreased excitability of PV neurons significantly decreased the labeling intensity of PNN in M1.

To conclude on our PNN study, we showed that PNN intensity is decreased in M1 during motor skill learning (Figure 3.20). In addition, we showed that in M1, a decrease in PNN is not affecting the excitability of PV neurons while a decrease of this excitability is able to decrease PNN intensity.

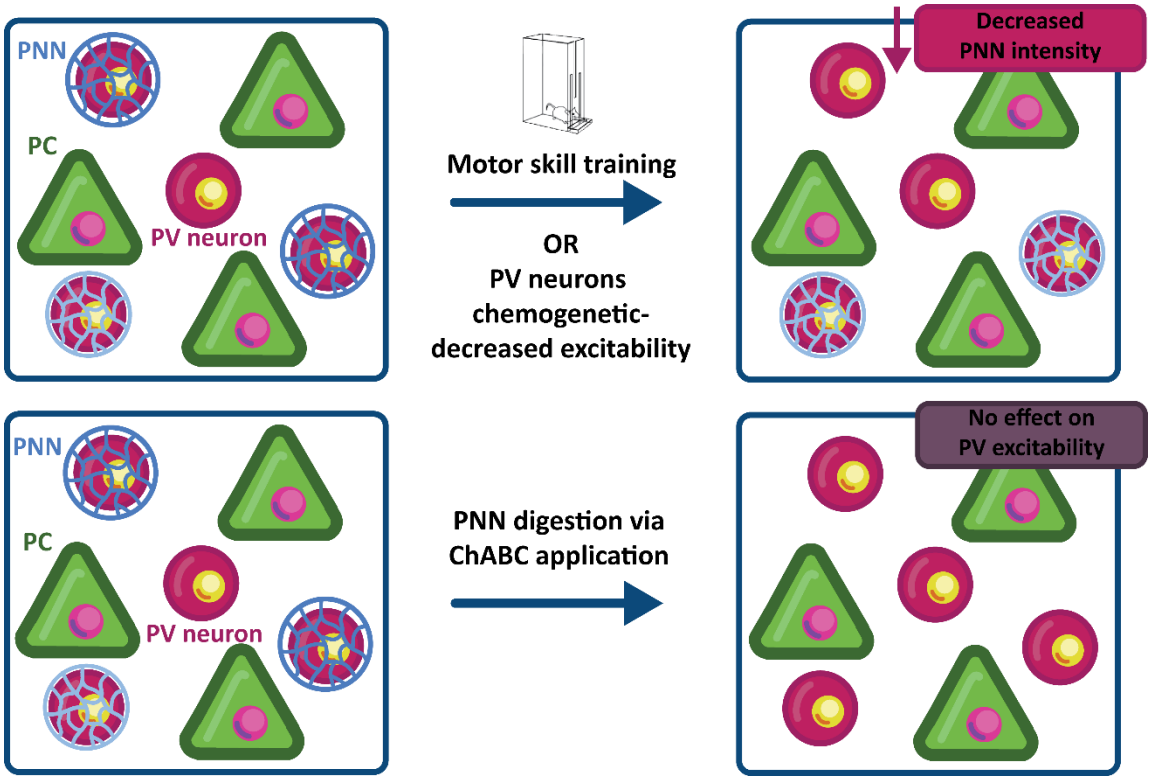

Figure 3.20. Summary of the PNN regulation during skill learning and the interaction between M1 PV neurons properties and PNN intensity. Schematics representing PC and PV neurons wrapped in PNN. We showed that motor skill learning induced a decrease in PNN intensity in M1. Decreasing the excitability of M1 PV neurons was also able to reduce PNN intensity. However, PNN digestion with ChABC did not affect PV neurons' intrinsic properties.

Part IV. Imaging M1 neuronal activity *in vivo* during motor skill training

4.1. Validation of *in vivo* calcium imaging during SPRT

So far, to investigate the changes occurring in M1 during motor skill acquisition we used several technics that each time required to sacrifice the mice to observe the adaptative changes. The first drawback here is that we were not able to follow the same parameter from the beginning of the training to the end of the learning. In order to observe the evolution of M1 circuitry across training sessions, we used *in vivo* calcium imaging coupled with a miniature microscope (miniscope). Following the shaping phase, PVCre::Ai9t mice were injected in the CFA corresponding to their preferred limb with a virus allowing the expression in PC of the calcium sensor, GCaMP6f, using a virus vector with a CaMKIIα promoter. A baseplate fixed to the GRIN lens was then implanted over the head of the mice to be able to plug the miniscope in order to image M1 transfected neurons activity. First, we checked if the mice were still able to do the task with the miniscope over their head. As presented in Figure 3.21.A, implanted mice were successfully able to do the reaching and grasping movement required to retrieve the food pellet. Since the SPRT training phase last 8 days, we wanted to know if we were able to record the activity of M1 neurons over consecutive days, in order to follow the activity of the same neurons across training sessions. As shown in Figure 3.21.B, we were able to record the fluorescence variation in M1 PC, and then extract calcium transients events that are indicative of neuronal activity. Furthermore, we were able to follow the activity

of the same cells across consecutive days, allowing to compare M1 microcircuit activity during motor skill learning.

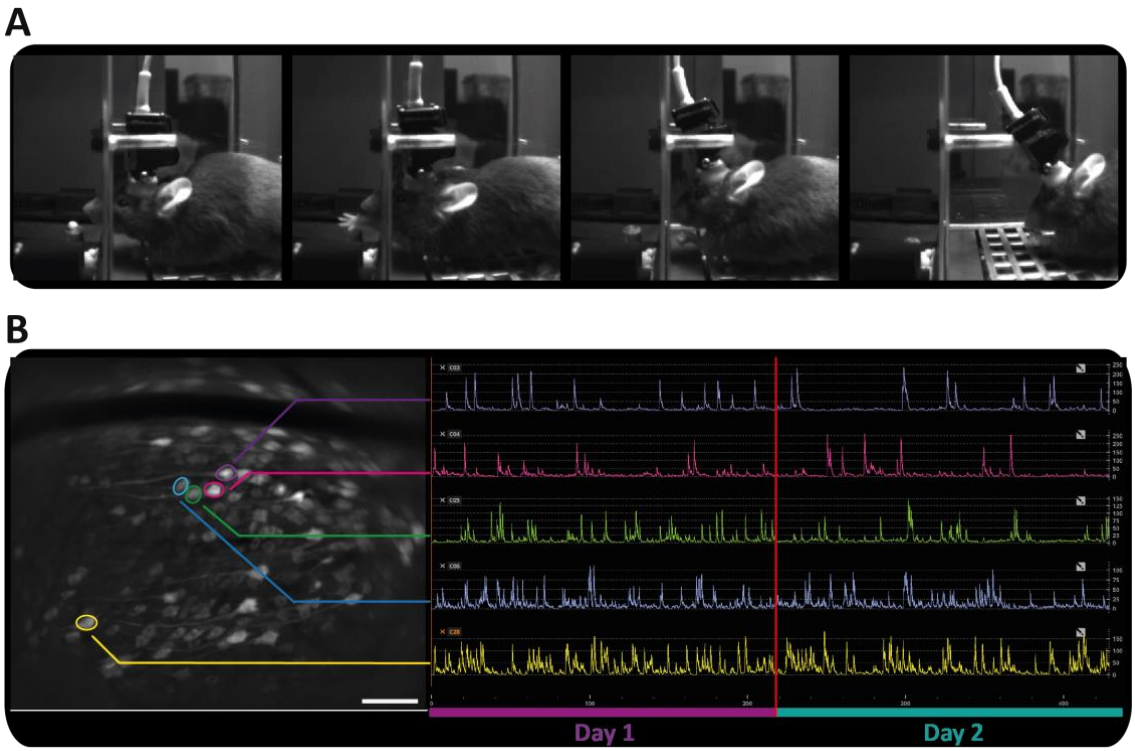

Figure 3.21: Validation of the *in vivo* calcium imaging technique to follow M1 PC activity during SPRT. **A**, Images of a PVCre::Ai9t mice reaching and grasping a food pellet with a miniature microscope plugged on the head. **B**, Maximal projection of a recorded video of GCaMP6f fluorescence with colored ROIs around selected PC (left). Measurement of GCaMP6f fluorescence fluctuations, expressed as DF/F over time, in the selected PC on two consecutive days (right).

4.2. The activity of M1 PC is increased with SPRT training

After validating that the implanted mice were able to do the task and that we could record the activity of the same cells across different days, mice were trained for the SPRT (Figure 3.22.A). They were able to increase their performances over training days, increasing their success rate from 16 ± 10% to 62 ± 10% (n = 3 mice, Figure 3.22.B). The activity of every detected M1 PC was assessed during SPRT at the first, second, and eighth training sessions (Figure 3.22.C). Our data showed that the activity of PC is increased at the 8th training session compared to the 2 first sessions, increasing from 0.117 ± 0.039 Hz (T1D, n = 143 neurons from 3 mice) and 0.124 ± 0.003 Hz (T2D, n = 129 neurons from 3 mice) up to 0.137 ± 0.003 Hz (T8D, n = 144 neurons from 3 mice) (Kruskal-Wallis test, $p < 0.0001$ versus T1D, $p = 0.0039$ versus T2D, Figure 3.22.D). Altogether, those data showed that motor skill learning increased the mean firing frequency of M1 PC.

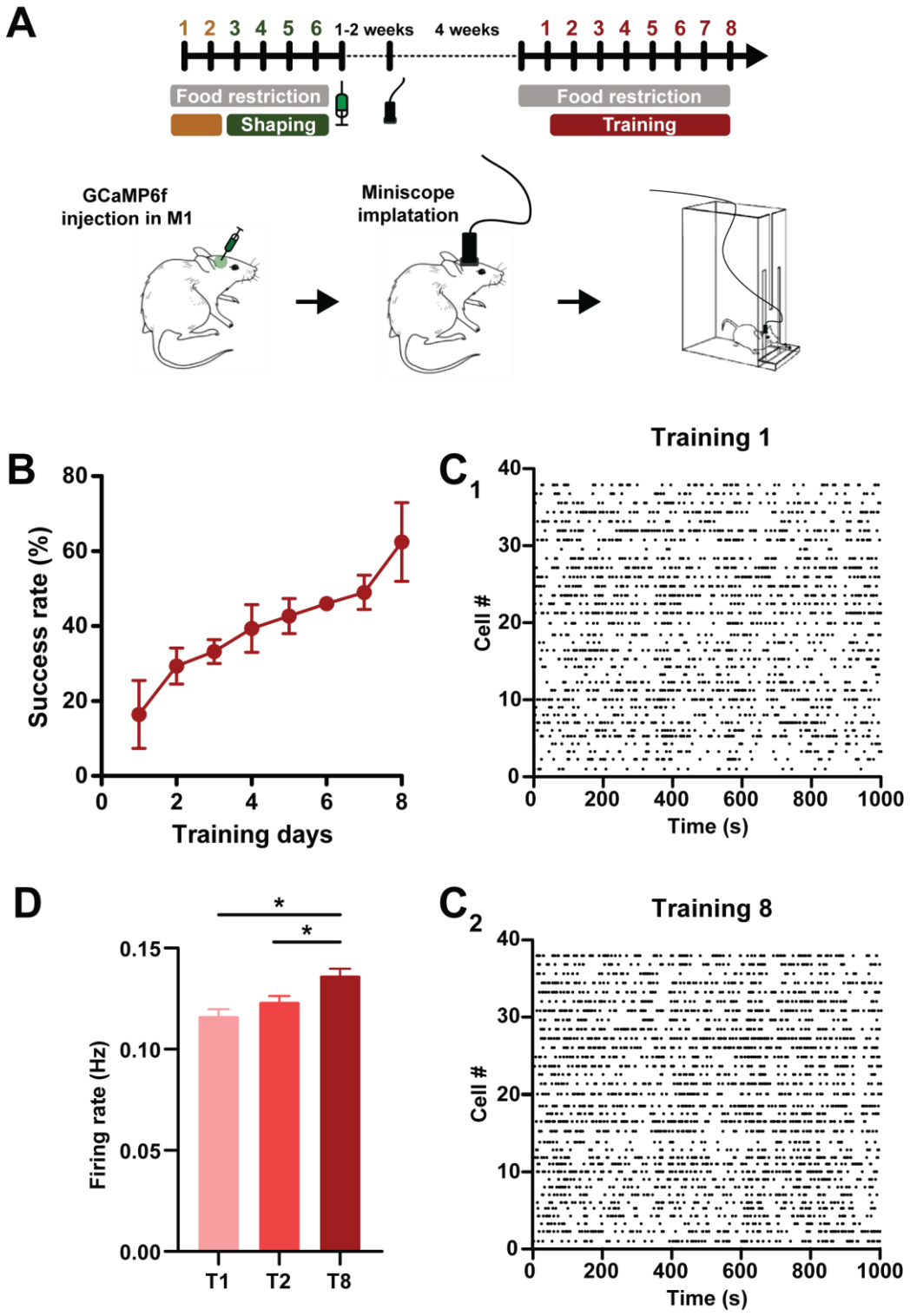
A
1 2 3 4 5 6
1-2 weeks
4 weeks
1 2 3 4 5 6 7 8
Food restriction
Shaping
Food restriction
Training
GCaMP6f injection in M1
Miniscope implatation
B
Success rate (%)
Training days
C1
Training 1
Cell #
Time (s)
C2
Training 8
Cell #
Time (s)
D
Firing rate (Hz)
T1
T2
T8
*
*

Figure 3.22: M1 PC *in vivo* activity across SPRT training. **A**, experimental protocol. **B**, Success rate over training days at the SPRT of implanted PVCre::Ai9t mice. **C**, Raster plot showing the activity of M1 PC in one mouse during the first ($\mathbf{C_1}$) and eighth ($\mathbf{C_2}$) training sessions. Each black dot represents a detected calcic event. **D**, Quantitative analysis of the mean firing frequency of M1 PC at the first, second, and eighth training sessions (T1, T2, and T8 respectively).

4.3. The activity of M1 PC is altered in DD mice during SPRT training

We showed that M1 dopamine depletion was sufficient to alter M1 L5 PV neurons' plastic changes occurring during SPRT training. In addition, it has been shown that LTP and motor skill learning-induced spine survival is impaired following M1 dopamine depletion (Molina-Luna et al., 2009; Guo et al., 2015b). We hypothesized that M1 activity should be disturbed following this depletion. Our next aim was to investigate this idea and record the activity of M1 principal cells across SPRT training in DDT and ShamT (Figure 3.23.A). Mice were injected and implanted as previously, except that they received an additional injection of either 6-OHDA or saline in M1. The success rate over training days curves of DDT was shifted to the right compared to ShamT, meaning that they seemed to have a learning impairment, as previously shown in *3.1*. (n_{DDT} = 2 mice, n_{ShamT} = 2 mice, no statistical analysis because of the small n, Figure 2.23.B). As in 5.2., the activity of M1 PC was assessed during SPRT training sessions (Figure 3.23.C). The mean firing frequency of every detected cell was calculated over the first, second, and third training sessions (Figure 3.23.D). Our data showed that M1 dopamine depletion impaired M1 PC activity during SPRT training (Kruskal-Wallis test, $p < 0.0001$). Concerning ShamT mice, M1

PC activity was significantly increased from 0.103 ± 0.003 Hz to 0.116 ± 0.003 Hz after 1 training session (post hoc Dunn's multiple comparison test, $p = 0.0178$), and was significantly increased to 0.138 ± 0.002 Hz again on the third day of training (post hoc Dunn's multiple comparison test, $p < 0.0001$ versus T1D, $p = 0.0068$ versus T2D). Concerning DDT mice, M1 PC activity was increased from 0.083 ± 0.002 Hz to 0.102 ± 0.003 Hz following one training session (post hoc Dunn's multiple comparison test, $p < 0.0001$) but was not further increased at the third day of training (0.112 ± 0.003 Hz, post hoc Dunn's multiple comparison test, $p < 0.0001$ versus T1D, $p = 0.0905$ versus T2D). Altogether, our data showed that M1 dopamine depletion decreased the global activity of M1 principal cells. In addition, the SPRT training-induced increase of the mean activity of M1 PC from the first to third training session was also impaired in DDT mice.

To conclude, these *in vivo* experiments showed that M1 PC activity is increased with SPRT training. In the early training phases, this increase was still observed in DD mice. However, M1 PC from DD mice displayed a decreased activity during these early training phases.

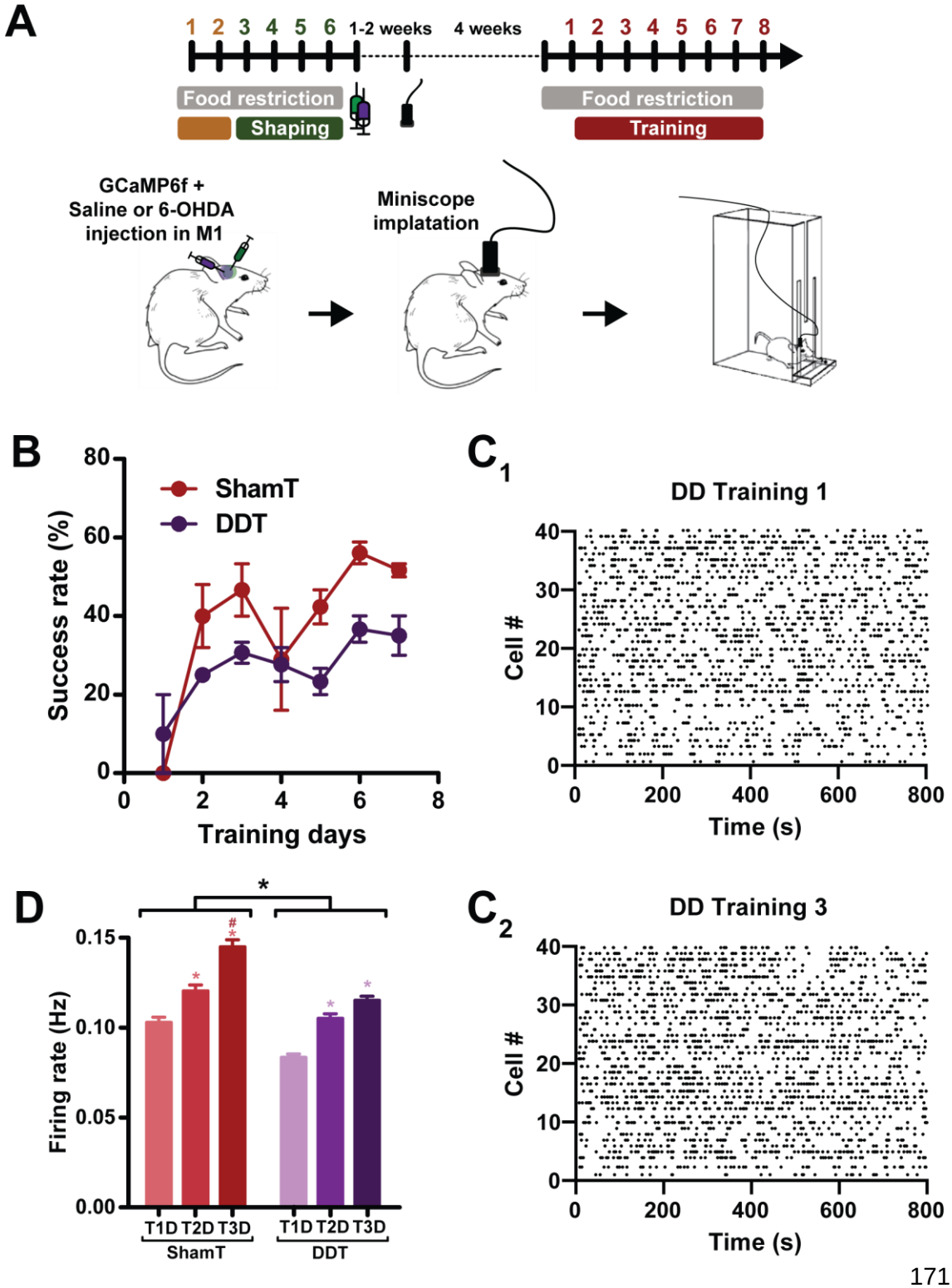
A
1 2 3 4 5 6
1-2 weeks
4 weeks
1 2 3 4 5 6 7 8
Food restriction
Shaping
Food restriction
Training
GCaMP6f +
Saline or 6-OHDA
injection in M1
Miniscope
implatation
B
Success rate (%)
ShamT
DDT
Training days
C1
DD Training 1
Cell #
Time (s)
D
Firing rate (Hz)
T1D T2D T3D
ShamT
DDT
C2
DD Training 3
Cell #
Time (s)

Figure 3.23: M1 PC *in vivo* activity across SPRT training in M1 dopamine depleted mice. **A**, experimental protocol. **B**, Success rate over training days at the SPRT of implanted M1 dopamine depleted (DDT) or Sham (ShamT) PVCre::Ai9t mice. **C**, Raster plot showing the activity of M1 PC in one DDT mouse during the first ($\mathbf{C_1}$) and third ($\mathbf{C_2}$) training sessions. Each black dot represents a detected calcic event. **D**, Quantitative analysis of the mean firing frequency of M1 PC at the first, second and third training sessions for ShamT and DDT (T1, T2, and T3 respectively) (number of neurons: ShamT: n_{T1D} = 131, n_{T2D} = 131, n_{T3D} = 132. DDT: n_{T1D} = 150, n_{T2D} = 150, n_{T3D} = 140, *: significant compared to respective T1D, #: significant compared to respective T2D).

DISCUSSION

This project aimed to better understand the role of M1 PV neurons and their modulation by dopamine during motor skill learning. Our results showed that PV neurons are one of the main neuronal populations in M1 expressing D2R, which once activated, modulate PV neurons' intrinsic and synaptic properties. Then, using the SPRT, we showed that PV neurons undergo plastic changes on their intrinsic and synaptic properties with motor skill acquisition. Their excitability and synaptic transmission are decreased with learning. M1 dopamine depletion has revealed that the changes in excitability are dopamine-dependent as DDT mice presented increased excitability of their PV neurons in M1. While the decrease of their synaptic transmission was not affected, we report that the synaptic plasticity of the PV-PC synapse is altered in DDT mice. We then showed that PNN are decreased in M1 during motor skill learning suggesting the involvement of this extracellular matrix in motor learning. In addition, PV neurons decreased excitability was able to decrease PNN intensity. Finally, using the activity of M1 L5 PC neurons activity as readout, we demonstrated that PC activity during SPRT is increased across learning while their activity is reduced in M1 dopamine depleted mice.

Part I. Modulation of M1 L5 PV intrinsic and synaptic properties *via* activation of dopamine D2 receptors

1.1 Dopamine D2-like receptors-expressing cells in M1

Although the expression of dopamine receptors has already been investigated in M1, it has never been done on M1 GABAergic populations (Camps et al., 1990; Mansour et al., 1990; Gaspar et al., 1995; Awenowicz and Porter, 2002a). PV neurons could be a putative target of M1 dopamine as they receive direct inputs from the VTA (Duan et al., 2020), the main source of dopamine for M1. Here, we reported that D2R is expressed across all cortical layers, with 47% of them in layers 2/3 and 38% of them in layers 5/6. In addition, PV neurons are the main GABAergic population of neurons expressing D2R in M1, representing 26% of D2R expressing cells. In addition, using *ex vivo* electrophysiology, we showed that neurons expressing the D2R in D2R-Cre::Ai9t in layer 5 of M1 were fast-spiking neurons (55%), The electrical properties of these neurons are characteristic from PV neurons in the cortex (Hu et al., 2014). Altogether, these two different approaches showed that PV neurons are accounting for a major part of D2R-expressing neurons in M1, which suggests that PV neurons play an important role in dopamine-dependent modulation of this brain structure.

1.2. Dopamine D2-like receptors activation modulate PV neurons intrinsic properties

Since PV neurons represent a major part of D2R expressing neurons, we investigated if the activation of these receptors was able to directly modulate PV neurons' intrinsic properties. Using *ex vivo* electrophysiology we showed that the application of a D2R agonist was able to increase the excitability of PV neurons in M1 L5. D2R receptors are usually expected to have an inhibitory effect on excitability; however, the D2R excitatory effect has already been reported in the prefrontal cortex (Tseng and O'Donnell, 2006). We assessed the intrinsic properties of PV neurons through the monitoring of their response to intracellular current injections in the presence of synaptic blockers. This approach allowed us to observe a post-synaptic effect of D2R activation and not modulation of presynaptic inputs to PV neurons. Further experiments are necessary to determine if this excitatory effect of D2R is similar to the one described in the prefrontal cortex (Trantham-Davidson, 2004). The downstream β-arrestin2 signaling pathway (Urs et al., 2016) or the release of neurotensin via activation of D2 autoreceptors of M1 dopaminergic neuron terminals could explain the D2 excitatory effect (Petrie et al., 2005).

1.3. Dopamine D2 receptor activation modulates GABAergic synaptic transmission in M1

The correct balance between excitatory and inhibitory signaling is the backbone of proper brain function (Markram et al., 2015). PV neurons are crucial for this balance, as they are exerting a strong regulation of cortical circuitry by participating in feedback and feedforward inhibitions (Hu et al., 2014). To investigate if D2R activation was able to modulate GABAergic synaptic transmission, we recorded sIPSCs and mIPSCs in M1 L5 PC. Changes in mIPSC amplitude are usually associated with postsynaptic modifications, while changes in their frequency are mainly due to presynaptic effects (Lupica, 1995). Here we showed that PV neurons' excitability was increased following quinpirole application, thus we hypothesized that we would see an effect on spontaneous IPSCs. However, such an effect was not observed, as D2R activation increased the amplitude but not the frequency of spontaneous IPSCs. This result may be explained by the fact that PV neurons are silent on acute brain slices, even after quinpirole application. They may be explained also by the fact that with this experimental approach, we are recording GABAergic events coming from every GABAergic neuron population projecting to PC. Finally, we cannot exclude that D2R activation could have both pre- and post-synaptic effects resulting in a more complex modulation.

1.4. Dopamine D2 receptor activation modulates PV neuron electrical and synaptic plasticity

We then wanted to be specific about the PV-PC synapse, and to overcome the fact that PV neurons are silent on acute slices we chose to manipulate their activity with optogenetics. Here we showed that quinpirole application was able to increase the amplitude of the light-evoked IPSCs, while did not affect the adaptative depression of this synapse. This increase in amplitude suggests that D2R activation has a postsynaptic effect. In addition, this increase in amplitude may be due to the increased excitability effect on quinpirole on PV neurons. For each light stimulation, we could recruit more PV neurons after D2R activation.

Part II.1. Impact of motor skill training and learning on PV neurons properties

2.1.1. Automatized single pellet reaching task

In this project, we used an automatized version of the widely used task: the SPRT. The automatization of this task had multiple advantages. First, it removes the variability that may come from the experimenter. Indeed, the pellet is always presented at the same position, and the interval of time between pellet presentations is always the same. In addition, it allows us to place the mice in a closed isolated box, thus preventing them from being disturbed by the experimenter or anything in the environment. The other big advantage was for *in vivo* calcium imaging experiments. We needed to synchronize the video acquisition from the behavioral video and the miniature microscope imaging system. That way we can properly and easily analyze and synchronize calcium imaging data with the behavioral data (movement initiation, grasping phase, etc…) and correlate the neuronal activity with the behavioral outcome precisely.

For future experiments, this automatized setup could also allow users to drive and synchronize optogenetic stimulation with the different behavioral stages. The setup has been developed so that mice can perform a more complex task. The aim of developing this new task would be for example to manipulate PV neurons *via* optogenetics at different stages of the movement. At the end of the tunnel, 2 grips can be placed and can serve as holders for mice. Those grips are detecting when the mouse is touching it. The goal would be to train mice to (1) place their paw on the 2

grips, which would allow the presentation of a new pellet, then (2) the mice would wait for an auditive cue to start their trial (if they would try before, it would trigger the withdraw of the pellet), and finally (3) they could grab the pellet and bring it back to their mouth. If the mice can learn this procedure, it would be possible to act during the 3 different steps, and for example shut down PV neurons activity using optogenetics during movement onset (just before 2), during the reaching (between 2 and 3), or during the grabbing (after 3). This method would be great to decipher more in detail the importance of PV neurons, or other neurons, during each step of the movement and across training.

2.1.2. PV neurons decrease excitability with skill learning

M1 is a key structure for the acquisition and maintenance of new motor skills (Kawai et al., 2015; Ohbayashi, 2020). It has already been reported that PC intrinsic properties are regulated throughout skill learning (Biane et al., 2019). As M1 dopamine is crucial for such learning and concomitant plastic changes (Molina-Luna et al., 2009; Guo et al., 2015b), we investigated if M1 L5 PV neurons were undergoing dopamine-dependent plasticity. Our data show that motor skill learning induces a decrease in PV neurons' excitability. These neurons are known to control PC output by projecting onto their somata and proximal dendrites (Hu et al., 2014). The global excitability of M1 has been shown to increase following motor skill learning in humans (Smyth et al., 2010). Thus, our data at the microcircuit level revealed a decrease in the excitability of PV neurons, which would be less recruited following skill learning, allowing easier recruitment of principal cells. In addition, our *in vivo* imaging data are in agreement with this increase in M1 activity during learning (see

part 4.1. of the discussion). However, concerning the PC, Biane and colleagues showed that only the excitability and connectivity of cortico-spinal PC, projecting to the area corresponding to the distal forelimb, were increased (Biane et al., 2019). This may underlie that PC recruited during the SPRT (the one projecting to the distal forelimb) are recruited more easily and may thus be the first to activate PV neurons, which then will inhibit the PC not related to the realized movement. At the late stages of the learning, only the neurons responsible for the learned stereotyped movement would be activated.

Having a decreased excitability does not mean that PV neurons are less activated during the SPRT training. To investigate the level of PV activity during training, we could take advantage of a neuronal activity-reporter mouse model, such as mice expressing the CaMPARI photoconvertible fluorescent protein (Moeyaert et al., 2018). The CaMPARI is a green fluorescent protein that can be irreversibly converted to a red fluorescent one in presence of high free calcium concentration (when the neurons are spiking) and the presence of an UV-light pulse. This strategy would allow to photoconvert neurons activated during specific movement executed to grasp the pellet. In addition, with this approach, we could photoconvert cells at the early stage of the learning and continue to train the mice, like this we would be able to differentiate between learners and non-learners and avoid the problem of discrimination between these two groups we had in the part 2.1.2.3. of the results.

In addition, impairing PV neurons activity has been shown to decrease both cortical network wide-synchrony and functional repertoire of neuronal assemblies (Agetsuma et al., 2018; Serrano-Reyes et al., 2020). These data may underlie that with motor skill learning, the specific increase in cortico-spinal PC excitability together with the decrease in excitability of PV neurons may lead to a reduction of wide synchrony in M1 circuitry. This reduction would allow the selection of a

neuronal ensemble responsible specifically for the learned stereotype movement and decrease the movement randomness. We can easily transfer this to M1 dopamine depleted mice, in which PV excitability is abnormally increased with skill training. In this case, PV over-excitability could lead to an over recruitment of them. Thus, it would prevent the decrease in synchrony and the selection of a specific neuronal ensemble and therefore the acquisition of the stereotyped movement. Further experiments must be conducted to explore this idea. PV excitability could be artificially decreased in DD mice, using a chemogenetic approach for example, to try to re-establish some learning capability in those DD mice.

2.1.3. Non-learner mice during SPRT training

If we look at the SPRT literature, the classical way of quantifying motor skill acquisition is to measure the success rate at the task over training sessions. Done that way, we end up with a subset of mice (around 50%) that are not improving their performances and are called 'non-learners'. However, it has already been reported that those mice are increasing their successes per time (Chen et al., 2014), meaning that they are gaining execution speed across training. In addition, in this project, we reported the non-learners, as for learners, seemed to acquire a stereotyped movement after 8 days of training. The definition of motor skill learning is the acquisition of a stereotyped movement, which is faster, smoother, and more accurate for a given task; we can then hypothesize that the so-called non-learners may in fact be learning a specific movement, sub-optimal for the SPRT. Indeed, this learned movement may not be perfect as they are not improving their success rate over time. One thing we noticed is that while learners acquired a movement with a large

opening of the hand, non-learners did not seem to improve their hand movement. In this project, we were tracking the paw of the mice and not the fingers. The idea here is that non-learners may learn a movement but lacking dexterity, i.e., they may learn a movement with their arm and wrist but not with their fingers, contrary to learners. Then, in addition to tracking the paw, we could track the fingers to verify this hypothesis. Our electrophysiological data may support this idea. Indeed, PV intrinsic properties remained the same in 'non-learners' compared to non-trained mice. We recorded PV properties in the CFA, which is mainly representing the M1 finger area in mice (Tennant et al., 2011). Following this idea, if non-learners are not acquiring fingers skills, it is not surprising that the intrinsic properties of CFA neurons were unchanged.

2.1.4. PV decreased synaptic transmission to PC with motor skill learning

We found that following motor skill learning, the amplitude of the synaptic current in M1 L5 PC, in response to a photostimulation of PV neurons, was decreased. This decrease may be explained by the fact that PV neurons are less excitable following motor learning. Thus, when photostimulating PV neurons, we might recruit a fewer number of them, explaining the decreased amplitude of the light-evoked IPSCs.

This decreased synaptic transmission is consistent with the literature as it has been shown that GABA is decreased in M1 with motor skill learning (Kolasinski et al., 2019). Our data suggest that PV neurons may be responsible, at least partly, for this decrease in GABA in M1. Indeed, we can hypothesize that PV neurons may be less

activated with learning (since they are less excitable), and, in addition to a decrease in their synaptic transmission, it would lead to a reduced GABA release from PV neurons. In addition, such reduction in GABAergic transmission has been shown to allow the opening of critical-period plasticity in the visual cortex (Harauzov et al., 2010; Kuhlman et al., 2013). In humans, cortical disinhibition can increase the induction of long-term plasticity in M1 (Cash et al., 2016). Thus, if PV neurons are responsible for the decrease in GABA observed in M1 with learning, it would place them as major actors of M1 plasticity during motor skill learning.

2.1.5. Chemogenetic manipulation of PV neurons excitability during SPRT

Since we showed that PV excitability was decreased with motor skill learning, we undertook to investigate if this change was crucial in the learning process. To this end, we decided to overwrite this effect by using a chemogenetic approach, to selectively increase their excitability during SPRT training sessions. Even if this manipulation tended to decrease mice performances at the SPRT, it was not significant. Due to the high variability of mice performances, we need to increase the numbers here to properly conclude. However, if after completing the dataset we found no differences in SPRT learning it could mean that this decrease in PV neurons' excitability is not needed, at least during training sessions, for correct skill acquisition. We cannot exclude that PV neurons decreased excitability may be needed not only during sessions but for a longer period. Indeed, motor learning is a process requiring time. It has been shown that 24h and a sleeping period need to separate two training sessions to increase performances between the 2 sessions

(Lugassy et al., 2018). Meanwhile, a vast regulation of different genes occurs at different times in this 24h window (Hertler et al., 2016). Then changes in PV neurons properties may be crucial not only during the training itself, but also during this 24h window, or during sleep. For example, a decrease of PV neurons excitability for a longer period may be responsible for a decrease in PNN, to open a new plasticity window in M1. *Ex vivo* electrophysiology experiments to measure PV neurons excitability in these mice after the learning may answer this question.

Part II.2. M1 dopamine depletion and Motor skill learning

2.2.1. M1 dopamine depletion impaired SPRT learning

Selective dopamine depletion in M1 has been shown to impair acquisition of the SPRT in mice (Molina-Luna et al., 2009; Guo et al., 2015b). Here we confirmed these data using our automatized SPRT. In addition, the qualitative analysis of the paw movement showed that M1 dopamine depleted mice seemed not to acquire a stereotyped movement after 8 days of training. A quantitative analysis of the paw and fingers movements should be performed in the future to confirm this. It would also allow exploring more in detail the movement impairments in these mice. Indeed, kinematic analysis of the movement may permit to determine if these M1 dopamine depleted mice have motor impairments on the first day of training, or if the depletion only affects the acquisition of the stereotyped movement. Since dopamine depletion in M1 does not affect the performances of an already learned movement (Molina-Luna et al., 2009), we could expect no effect on motor execution but only in the refining of the movement across time.

2.2.2. M1 PV neurons excitability is altered in M1dopamine depleted mice after motor skill training

We then investigated if the changes in PV neurons' intrinsic properties observed during skill acquisition are dopamine-dependent. To this end, we assessed the intrinsic properties of M1 L5 PV neurons in M1 dopamine-depleted trained and non-trained mice. Our data revealed that the excitability of PV neurons was increased following motor skill training, which is the opposite effect compared to control mice. These data suggest that the learning-induced decrease in PV excitability in M1 L5 is dopamine-dependent. Once again, neuronal excitability does not necessarily imply that PV neurons *in vivo* activity is increased. However, if such is the case, we could expect that they would shut down the activity of PC, resulting in a global decrease of activity in M1. This would be in accordance with the literature as the activity of M1 PC is decreased during movement execution following dopamine depletion (Aeed et al., 2021; Li et al., 2021).

To verify that the increased excitability of M1 PV neurons is leading to this deceased PC activity, future experiments could try to correct PV excitability. By transfecting PV neurons with inhibitory DREADDs, the hM4Di, we could correct and decrease the excitability of PV neurons. This correction may thus lead to an improvement in M1 activity and may re-establish motor skill learning.

2.2.3. M1 dopamine depletion altered M1 L5 PV synaptic plasticity in motor skill learning

As PV excitability was impaired following SPRT training in M1 dopamine depleted mice, we investigated if it was impairing the learning-induced decrease in synaptic transmission. Using optogenetics and *ex vivo* electrophysiology, she showed that the training-induced decrease in synaptic transmission of PV neurons onto PC in M1 L5 was not affected by the M1 dopamine depletion, indicating that this phenomenon is not dopamine-dependent. However, the short-term depression observed at this synapse was altered in M1 dopamine depleted mice. Previous work already reported that dopamine depletion did not affect synaptic transmission in M1 but is altering its plasticity (Molina-Luna et al., 2009).

Part III. PNN intensity throughout motor skill learning

3.1. PNN intensity is reduced with motor skill learning

PNN are known to limit plasticity in the neocortex (Härtig et al., 1992b; Bukalo et al., 2007; Frischknecht et al., 2009; Beurdeley et al., 2012; de Winter et al., 2016; Shinozaki et al., 2016; Favuzzi et al., 2017). Since we showed modifications on PV neurons are occurring with motor skill learning, and PNN are mainly wrapping PV neurons, we investigated if there was a regulation of them in M1 across SPRT training. Our data showed that PNN intensity was significantly reduced after 5 days of training and remains reduced after 8 days. These data may suggest that a plasticity window is created during the late phase of training and may allow skill acquisition. This result was not surprising as treadmill training has also been shown to reduce PNN intensity in a wide variety of brain regions (Smith et al., 2015) and that PNN diminution is often observed in memory phenomena (Gogolla et al., 2009; Banerjee et al., 2017; Thompson et al., 2018; Shi et al., 2019; Carulli et al., 2020; Cornez et al., 2021). However, further analysis should be conducted on these data. Indeed, we could also measure the number of neurons wrapped with PNN across SPRT training, which may go in the same direction as the intensity results. One other interesting experiment would be to determine if the PV neurons recruited during the task are the ones with a reduction in PNN.

In addition, it has been shown that a decrease in PNN in the hippocampus is able to increase the activity of VTA dopaminergic neurons (Shah and Lodge, 2013). We can then hypothesize that the observed decrease in PNN during SPRT learning

could lead to an increased dopamine-signaling in M1, enhancing dopamine-dependent changes that occur during learning.

3.2. Impact of PNN digestion on PV neurons properties

PNN intensity and PV neurons have been shown to be tightly linked (Wingert and Sorg, 2021 for review, Devienne et al., 2021). Indeed, PNN removal through ChABC treatment has been used in several cortices (both in the hippocampus and neocortex) to investigate their role in PV neurons physiology. Overall, PNN removal is inducing a reduction in PV excitability in most cases. In the motor cortex, PNN digestion is reducing the excitability of M1 PV neurons and increases the one of M1 PC in a mouse model of epilepsy (Tewari et al., 2018). In addition, manipulation of PV excitability has been shown to be able to impact PNN intensity. Indeed, chemogenetic manipulation of PV neurons in the visual cortex showed that decreasing their excitability for 2 days was sufficient to drastically reduce PNN intensity while increasing PV excitability has no effect. Thus, since we found that both PNN intensity and PV neurons' excitability were reduced with SPRT training, we aimed first to know if a reduction in PNN in M1 could reduce PV neurons' excitability.

Surprisingly, our data showed that PNN digestion with ChABC did not affect PV neurons' intrinsic properties in M1 L5. The previous work done in the M1 of mice with brain tumors (Tewari et al., 2018) together with our data may let us think that PNN have a protective effect on PV electrical properties in pathological states. More importantly in our case, it means that the observed decrease in PNN intensity with SPRT training is not responsible for PV training-induced decreased excitability.

PNN digestion may also impact synaptic transmission on PV neurons. Indeed, PNN are known to inhibit synaptogenesis (Bukalo et al., 2007; Frischknecht et al., 2009; Beurdeley et al., 2012; Favuzzi et al., 2017). It could be interesting to investigate if there is a change in the EPSC and IPSC received by PV neurons with PNN digestion in M1, as it has been observed in other structures (Liu et al., 2013; Carstens et al., 2016; Hirono et al., 2018; Bosiacki et al., 2019; Guadagno et al., 2020).

3.3. PNN digestion during SPRT training

Our data revealed that PNN integrity was not needed to properly increase SPRT performances during the 8 days of training. It may first suggest that M1 PNN integrity does not play a role in learning the motor task. In addition, we can also hypothesize that the decrease in PNN we observed during training is already sufficient to promote M1 plasticity and allow skill acquisition. Thus, digesting PNN with ChABC at this stage may not have an additional effect. To confirm this, it would be useful to develop a tool allowing an increase in PNN, or at least here, to prevent PNN digesting during training. Sadly, to our knowledge, such a tool is not currently available. It has been shown that BDNF application may have this effect (Donato et al., 2013), however, BDNF could also have many other 'side effects' due to its different mechanisms of action, which make this method not appropriate to be specific to PNN.

PNN are also thought to help stabilize newly formed synapses, and may then be important for long-term memory, as it is the case for fear memory (Gogolla et al., 2009; Banerjee et al., 2017; Thompson et al., 2018). Spine survival is increased during motor skill training (Guo et al., 2015b), and the maintenance of these new

synapses across longer periods may be crucial for maintaining the learning. One interesting experiment could be to digest the PNN during the training of the SPRT and retrain the mouse a month later, to see if they have well learned and retained the skill. It would not be surprising as digesting PNN in the secondary visual cortex during fear conditioning has been shown to impair fear memory a month later while recent memory was not affected (Thompson et al., 2018).

We also performed PNN digestion once the training was finished and retrained the mice for 5 days. Surprisingly, the performances of the mice, even the PBS injected mice, were decreased at the first retraining session compared to the last before the injections. This difference may be explained by multiple reasons. Firstly, mice were food-restricted only the day before the first retraining session and may not be as motivated as during the training or the later re-training sessions, explaining lower performances. Secondly, mice were re-trained only 3 days following the stereotaxic surgery. Mice still recovering from the surgery could also be a reason for this decrease in performances in both groups. As PNN rapidly reform after ChABC digestion (Orlando and Raineteau, 2015), re-trained must happen soon after the ChABC injection. To overcome this possibility, we could implant a cannula over the head of the mice before the behavioral experiments, allowing us to easily inject ChABC before re-training without having to wait for the mice to recover from surgery then. Using a viral approach with a virus allowing the expression of the ChABC in M1 would be another strategy to prevent the formation of PNN. In addition, with the viral approach, the PNN would not be able to be reformed with time, another advantage if we want to study the long-lasting effect of PNN digestion.

Finally, as we showed, decreasing PV neurons' excitability led to a decrease in PNN in M1. However, in dopamine depleted trained mice, we showed an increase in their excitability. It has already been shown in the visual cortex, increasing PV excitability does not affect PNN intensity (Devienne et al., 2021). We can then

hypothesize that, in these mice, there is no PNN degradation during SPRT training, thus no plasticity window is created, preventing the plastic changes occurring in M1 which allow skill acquisition. To verify this idea, we could quantify the intensity of PNN through motor skill learning in DDT mice: we would hypothesize that PNN intensity is not reduced in M1 of DDT mice. If PNN decrease during skill learning is needed for opening a new plasticity window, it may then explain why DDT mice have an impairment in SPRT learning. One experiment that should be conducted to answer this question is to inject ChABC in M1 from DD mice, to digest the PNN and allow the creation of a new plasticity window. Thus, we would expect to re-establish learning of the skill.

Part IV. Imaging M1 neuronal activity *in vivo* during motor skill training

4.1. M1 PC activity is increased with SPRT learning

As discussed earlier, with our previous *ex vivo* experiments it is difficult to discriminate between learners and non-learners in the early training stages. In addition, our experiments so far did not allow us to follow the same parameter across training days in the same mouse. In recent years, the use of miniature microscopes coupled with calcium imaging has been a powerful tool to study neuronal networks in the mammalian brain (Gulati et al., 2017; Kondo et al., 2018; Aharoni and Hoogland, 2019; de Groot et al., 2020; Rynes et al., 2021). Thus, we decided to use this method to record the activity of the M1 PC throughout the SPRT training. Our results showed that M1 PC activity is increased during training sessions throughout the learning. This is in accordance with works done in humans, that showed M1 neuronal excitability is increased with motor skill learning (Smyth et al., 2010). In addition, the decreased excitability and synaptic transmission of PV neurons we showed, together with the increase in PC excitability (Biane2019) may explain this increased PC activity *in vivo*. However, the amount of data collected with these experiments was massive, and a lot of analysis are still needed and are in process to get the most of it. Indeed, the objective would be to correlate the activity of individual neurons with the different stages of the movement (movement onset, reaching, grasping, etc..) and observe the modification of encoding activity across learning.

4.2. M1 PC activity is decreased during SPRT training in M1 dopamine depleted mice

We investigated the impact of M1 dopamine depletion on its neuronal activity during SPRT training sessions. The activity of M1 PC was decreased with dopamine depletion during the 3 first days of SPRT training. It has been shown that M1 activity is disturbed during the grasping phase of a forelimb movement (Hyland et al., 2019). In addition, a decreased activity of PC during reaching movements in dopamine depleted rodents has already been observed (Aeed et al., 2021; Li et al., 2021). However, our data also showed that PC activity was still increased with skill training in M1 dopamine deplete mice, to a lesser extent compared to control mice. This smaller increase may be responsible for the small increase in performances observed in these mice. As for the previous set of data, this dataset needs to be analyzed deeper. Depicting the activity of M1 PC neurons here with the behavioral outcome may highlight abnormalities in PC activity during training, explaining the impaired learning.

Perspectives and conclusion

To conclude, this project allowed us to better understand the role of dopamine modulation of M1 circuitry, especially on PV neurons (Figure 4.1). Our data highlighted PV as a target for cortical dopamine and thus a potential source of dysfunction in M1 pathology. To further understand the role of M1 dopamine, future experiments could focus on dopaminergic neurons projecting to M1. For example, monitoring the activity of dopaminergic neurons during SPRT training would give an insight into when dopamine is released during learning. Using the miniature microscopes, calcium imaging of dopaminergic fibers in M1 may unravel the precise period when dopaminergic signaling is crucial for skill acquisition. Understanding how dopamine works in M1 is crucial, as understanding its fundamental mechanism of action may be of great interest to find new insights in treatment for pathologies such as Parkinson's disease.

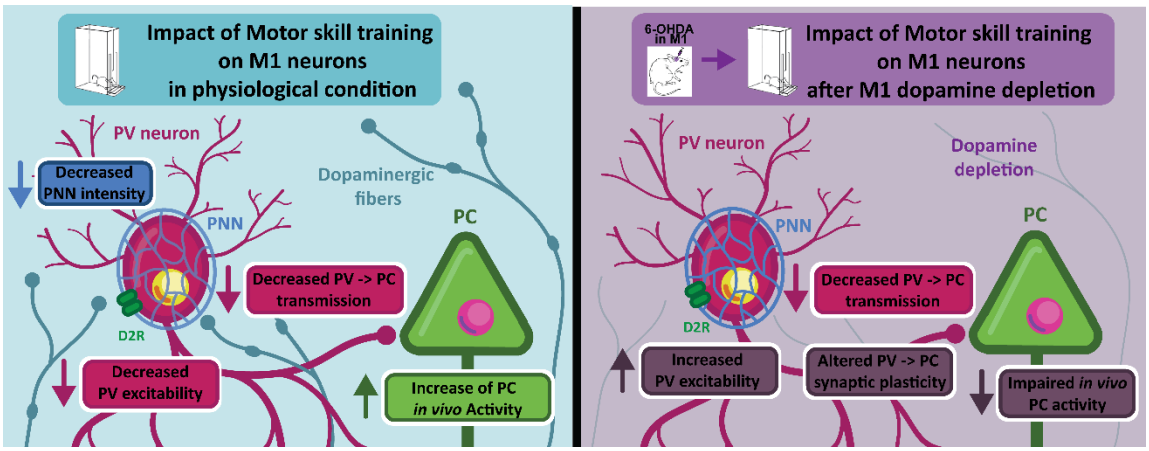

Figure 4.1: Schematics representing the main results found in this project.

List of publications, Posters, and oral communications

Publications :

- Cousineau, J., Lescouzères, L., Taupignon, A., Delgado-Zabalza, L., Valjent, E., Baufreton, J., Le Bon-Jégo M. (2020). Dopamine D2-Like Receptors Modulate Intrinsic Properties and Synaptic Transmission of Parvalbumin Interneurons in the Mouse Primary Motor Cortex. *eNeuro* 7, ENEURO.0081-20.2020. doi:10.1523/ENEURO.0081-20.2020.

- Cousineau, J., Plateau V., Baufreton, J., Le Bon-Jégo M. (under review). Dopaminergic modulation of primary motor cortex: from cellular and synaptic mechanisms underlying motor learning to cognitive symptoms in Parkinson's disease. Special issue in Neurobiology of Disease.

Posters :

- Cousineau, J., Baufreton, J., Le Bon-Jégo M. "Dopamine modulation of layer 5 Parvalbumin neurons in the primary motor cortex during motor skill learning". NeuralNet, December 2019, Bordeaux.

- Cousineau, J., Baufreton, J., Le Bon-Jégo M. "Dopaminergic control of primary motor cortex microcircuits during motor skill learning" NeuroFrance 2021, May 2021, Online event.

- Cousineau, J., Baufreton, J., Le Bon-Jégo M. "Dopaminergic control of primary motor cortex microcircuits during motor skill learning" NeuroCampusDay 2021, Bordeaux.

Oral communications :

- Cousineau, J., Baufreton, J., Le Bon-Jégo M. “Dopaminergic control of primary motor cortex microcircuits during motor skill learning”. Health and Biology Doctoral school day, 2021, Bordeaux. **Awarded**: Best oral presentation.

- Cousineau, J., Baufreton, J., Le Bon-Jégo M. “Dopaminergic control of primary motor cortex microcircuits during motor skill learning”. Bordeaux Neurocampus PhD day, 2021, Bordeaux. **Awarded**: Laureate of the Bordeaux Neurocampus Doctoral Research Award.

REFERENCES

Adams, J. A. (1971). A Closed-Loop Theory of Motor Learning. *Journal of Motor Behavior* 3, 111–150. doi:10.1080/00222895.1971.10734898.

Aeed, F., Cermak, N., Schiller, J., and Schiller, Y. (2021). Intrinsic Disruption of the M1 Cortical Network in a Mouse Model of Parkinson's Disease. *Mov Disord* 36, 1565–1577. doi:10.1002/mds.28538.

Agetsuma, M., Hamm, J. P., Tao, K., Fujisawa, S., and Yuste, R. (2018). Parvalbumin-Positive Interneurons Regulate Neuronal Ensembles in Visual Cortex. *Cerebral Cortex* 28, 1831–1845. doi:10.1093/cercor/bhx169.

Aharoni, D., and Hoogland, T. M. (2019). Circuit Investigations With Open-Source Miniaturized Microscopes: Past, Present and Future. *Front. Cell. Neurosci.* 13, 141. doi:10.3389/fncel.2019.00141.

Albarran, E., Raissi, A., Jáidar, O., Shatz, C. J., and Ding, J. B. (2021). Enhancing Motor Learning by Increasing Stability of Newly Formed Dendritic Spines in Motor Cortex. *SSRN Electronic Journal*. doi:10.2139/ssrn.3775181.

Albin, R. L., Young, A. B., and Penney, J. B. (1989). The functional anatomy of basal ganglia disorders. *Trends in Neurosciences* 12, 366–375. doi:10.1016/0166-2236(89)90074-X.

Amick, M. M., Schendan, H. E., Ganis, G., and Cronin-Golomb, A. (2006). Frontostriatal circuits are necessary for visuomotor transformation: Mental rotation in Parkinson's disease. *Neuropsychologia* 44, 339–349. doi:10.1016/j.neuropsychologia.2005.06.002.

Anderson, J. R. (1982). Acquisition of cognitive skill. *Psychological Review* 89, 369–406. doi:10.1037/0033-295X.89.4.369.

Anderson, S. A. (1997). Interneuron Migration from Basal Forebrain to Neocortex: Dependence on Dlx Genes. *Science* 278, 474–476. doi:10.1126/science.278.5337.474.

Aquino, C. C., and Fox, S. H. (2015). Clinical spectrum of levodopa-induced complications: L - DOPA-INDUCED COMPLICATIONS. *Mov Disord.* 30, 80–89. doi:10.1002/mds.26125.

Arif, S. H. (2009). A Ca^{2+} -binding protein with numerous roles and uses: parvalbumin in molecular biology and physiology. *BioEssays* 31, 410–421. doi:10.1002/bies.200800170.

Awenowicz, P. W., and Porter, L. L. (2002a). Local Application of Dopamine Inhibits Pyramidal Tract Neuron Activity in the Rodent Motor Cortex. *Journal of Neurophysiology* 88, 3439–3451. doi:10.1152/jn.00078.2002.

Awenowicz, P. W., and Porter, L. L. (2002b). Local application of dopamine inhibits pyramidal tract neuron activity in the rodent motor cortex. *Journal of Neurophysiology* 88, 3439–3451. doi:10.1152/jn.00078.2002.

Bacci, A., and Huguenard, J. R. (2006). Enhancement of Spike-Timing Precision by Autaptic Transmission in Neocortical Inhibitory Interneurons. *Neuron* 49, 119–130. doi:10.1016/j.neuron.2005.12.014.

Bacci, A., Huguenard, J. R., and Prince, D. A. (2003). Functional Autaptic Neurotransmission in Fast-Spiking Interneurons: A Novel Form of Feedback Inhibition in the Neocortex. *J. Neurosci.* 23, 859–866. doi:10.1523/JNEUROSCI.23-03-00859.2003.

Bachtiar, V., Johnstone, A., Berrington, A., Lemke, C., Johansen-Berg, H., Emir, U., et al. (2018). Modulating Regional Motor Cortical Excitability with Noninvasive Brain Stimulation Results in Neurochemical Changes in Bilateral Motor Cortices. *J. Neurosci.* 38, 7327–7336. doi:10.1523/JNEUROSCI.2853-17.2018.

Baldereschi, M., Di Carlo, A., Rocca, W. A., Vanni, P., Maggi, S., Perissinotto, E., et al. (2000). Parkinson's disease and parkinsonism in a longitudinal study: Two-fold higher incidence in men. *Neurology* 55, 1358–1363. doi:10.1212/WNL.55.9.1358.

Balmer, T. S. (2016). Perineuronal Nets Enhance the Excitability of Fast-Spiking Neurons. *eneuro* 3, ENEURO.0112-16.2016. doi:10.1523/ENEURO.0112-16.2016.

Banerjee, S. B., Gutzeit, V. A., Baman, J., Aoued, H. S., Doshi, N. K., Liu, R. C., et al. (2017). Perineuronal Nets in the Adult Sensory Cortex Are Necessary for Fear Learning. *Neuron* 95, 169-179.e3. doi:10.1016/j.neuron.2017.06.007.

Bédard, P., and Sanes, J. N. (2011). Basal ganglia-dependent processes in recalling learned visual-motor adaptations. *Exp Brain Res* 209, 385–393. doi:10.1007/s00221-011-2561-y.

Berding, G., Odin, P., Brooks, D. J., Nikkhah, G., Matthies, C., Peschel, T., et al. (2001). Resting regional cerebral glucose metabolism in advanced Parkinson's disease studied in theoff andon conditions with [18F]FDG-PET. *Mov Disord.* 16, 1014–1022. doi:10.1002/mds.1212.

Berger, B., Gaspar, P., and Verney, C. (1991). Dopaminergic innervation of the cerebral cortex: unexpected differences between rodents and primates. *Trends in Neurosciences* 14, 21–27. doi:10.1016/0166-2236(91)90179-X.

Betarbet, R., Sherer, T. B., and Timothy Greenamyre, J. (2002). Animal models of Parkinson's disease. *BioEssays* 24, 308–318. doi:10.1002/bies.10067.

Beurdeley, M., Spatazza, J., Lee, H. H. C., Sugiyama, S., Bernard, C., Di Nardo, A. A., et al. (2012). Otx2 Binding to Perineuronal Nets Persistently Regulates Plasticity in the Mature Visual Cortex. *Journal of Neuroscience* 32, 9429–9437. doi:10.1523/JNEUROSCI.0394-12.2012.

Biane, J. S., Takashima, Y., Scanziani, M., Conner, J. M., and Tuszynski, M. H. (2016). Thalamocortical Projections onto Behaviorally Relevant Neurons Exhibit Plasticity during Adult Motor Learning. *Neuron* 89, 1173–1179. doi:10.1016/j.neuron.2016.02.001.

Biane, J. S., Takashima, Y., Scanziani, M., Conner, J. M., and Tuszynski, M. H. (2019). Reorganization of Recurrent Layer 5 Corticospinal Networks Following Adult Motor Training. *The Journal of Neuroscience* 39, 4684–4693. doi:10.1523/JNEUROSCI.3442-17.2019.

Bogerts, B., Häntsch, J., and Herzer, M. (1983). A morphometric study of the dopamine-containing cell groups in the mesencephalon of normals, Parkinson patients, and schizophrenics. *Biol Psychiatry* 18, 951–969.

Bohannon, A. S., and Hablitz, J. J. (2018). Optogenetic dissection of roles of specific cortical interneuron subtypes in GABAergic network synchronization: Role of interneuron subtypes in cortical synchrony. *J Physiol* 596, 901–919. doi:10.1113/JP275317.

Bondi, M. W., and Kaszniak, A. W. (1991). Implicit and explicit memory in Alzheimer's disease and Parkinson's disease. *Journal of Clinical and Experimental Neuropsychology* 13, 339–358. doi:10.1080/01688639108401048.

Bortone, D. S., Olsen, S. R., and Scanziani, M. (2014). Translaminar Inhibitory Cells Recruited by Layer 6 Corticothalamic Neurons Suppress Visual Cortex. *Neuron* 82, 474–485. doi:10.1016/j.neuron.2014.02.021.

Bosiacki, M., Gąssowska-Dobrowolska, M., Kojder, K., Fabiańska, M., Jeżewski, D., Gutowska, I., et al. (2019). Perineuronal Nets and Their Role in Synaptic Homeostasis. *IJMS* 20, 4108. doi:10.3390/ijms20174108.

Bova, A., Kernodle, K., Mulligan, K., and Leventhal, D. (2019). Automated Rat Single-Pellet Reaching with 3-Dimensional Reconstruction of Paw and Digit Trajectories. *JoVE*, 59979. doi:10.3791/59979.

Braak, H., Tredici, K. D., Rüb, U., de Vos, R. A. I., Jansen Steur, E. N. H., and Braak, E. (2003). Staging of brain pathology related to sporadic Parkinson's disease. *Neurobiology of Aging* 24, 197–211. doi:10.1016/S0197-4580(02)00065-9.

Brown, A. R., and Teskey, G. C. (2014). Motor Cortex Is Functionally Organized as a Set of Spatially Distinct Representations for Complex Movements. *J. Neurosci.* 34, 13574–13585. doi:10.1523/JNEUROSCI.2500-14.2014.

Brückner, G., Hausen, D., Härtig, W., Drlicek, M., Arendt, T., and Brauer, K. (1999). Cortical areas abundant in extracellular matrix chondroitin sulphate proteoglycans are less affected by cytoskeletal changes in Alzheimer's disease. *Neuroscience* 92, 791–805. doi:10.1016/S0306-4522(99)00071-8.

Buchanan, K. A., Blackman, A. V., Moreau, A. W., Elgar, D., Costa, R. P., Lalanne, T., et al. (2012). Target-Specific Expression of Presynaptic NMDA Receptors in Neocortical Microcircuits. *Neuron* 75, 451–466. doi:10.1016/j.neuron.2012.06.017.

Bukalo, O., Schachner, M., and Dityatev, A. (2007). Hippocampal Metaplasticity Induced by Deficiency in the Extracellular Matrix Glycoprotein Tenascin-R. *Journal of Neuroscience* 27, 6019–6028. doi:10.1523/JNEUROSCI.1022-07.2007.

Burciu, R. G., and Vaillancourt, D. E. (2018). Imaging of Motor Cortex Physiology in Parkinson's Disease: BURCIU AND VAILLANCOURT. *Mov Disord.* 33, 1688–1699. doi:10.1002/mds.102.

Cabungcal, J.-H., Steullet, P., Morishita, H., Kraftsik, R., Cuenod, M., Hensch, T. K., et al. (2013). Perineuronal nets protect fast-spiking interneurons against oxidative stress. *Proceedings of the National Academy of Sciences* 110, 9130–9135. doi:10.1073/pnas.1300454110.

Camps, M., Kelly, P. H., and Palacios, J. M. (1990). Autoradiographic localization of dopamine D1 and D2 receptors in the brain of several mammalian species. *J. Neural Transmission* 80, 105–127. doi:10.1007/BF01257077.

Canavan, A. G. M., Passingham, R. E., Marsden, C. D., Quinn, N., Wyke, M., and Polkey, C. E. (1990). Prism adaptation and other tasks involving spatial abilities in patients with Parkinson's disease, patients with frontal lobe lesions and patients with unilateral temporal lobectomies. *Neuropsychologia* 28, 969–984. doi:10.1016/0028-3932(90)90112-2.

Cao, C., Li, D., Zhan, S., Zhang, C., Sun, B., and Litvak, V. (2020). L-dopa treatment increases oscillatory power in the motor cortex of Parkinson's disease patients. *NeuroImage: Clinical* 26, 102255. doi:10.1016/j.nicl.2020.102255.

Capper-Loup, C., Burgunder, J.-M., and Kaelin-Lang, A. (2005). Modulation of parvalbumin expression in the motor cortex of parkinsonian rats. *Experimental Neurology* 193, 234–237. doi:10.1016/j.expneurol.2004.12.007.

Carstens, K. E., Phillips, M. L., Pozzo-Miller, L., Weinberg, R. J., and Dudek, S. M. (2016). Perineuronal Nets Suppress Plasticity of Excitatory Synapses on CA2 Pyramidal Neurons. *J. Neurosci.* 36, 6312–6320. doi:10.1523/JNEUROSCI.0245-16.2016.

Carulli, D., Broersen, R., de Winter, F., Muir, E. M., Mešković, M., de Waal, M., et al. (2020). Cerebellar plasticity and associative memories are controlled by perineuronal nets. *Proc Natl Acad Sci USA* 117, 6855–6865. doi:10.1073/pnas.1916163117.

Carulli, D., Pizzorusso, T., Kwok, J. C. F., Putignano, E., Poli, A., Forostyak, S., et al. (2010). Animals lacking link protein have attenuated perineuronal nets and persistent plasticity. *Brain* 133, 2331–2347. doi:10.1093/brain/awq145.

Carulli, D., Rhodes, K. E., Brown, D. J., Bonnert, T. P., Pollack, S. J., Oliver, K., et al. (2006). Composition of perineuronal nets in the adult rat cerebellum and the cellular origin of their components. *J. Comp. Neurol.* 494, 559–577. doi:10.1002/cne.20822.

Carulli, D., Rhodes, K. E., and Fawcett, J. W. (2007). Upregulation of aggrecan, link protein 1, and hyaluronan synthases during formation of perineuronal nets in the rat cerebellum. *J. Comp. Neurol.* 501, 83–94. doi:10.1002/cne.21231.

Cash, R. F. H., Murakami, T., Chen, R., Thickbroom, G. W., and Ziemann, U. (2016). Augmenting Plasticity Induction in Human Motor Cortex by Disinhibition Stimulation. *Cereb. Cortex* 26, 58–69. doi:10.1093/cercor/bhu176.

Caviness, J. N., Lue, L.-F., Beach, T. G., Hentz, J. G., Adler, C. H., Sue, L., et al. (2011). Parkinson's disease, cortical dysfunction, and alpha-synuclein: Cortical Dysfunction in Parkinson's Disease. *Mov. Disord.* 26, 1436–1442. doi:10.1002/mds.23697.

Cazemier, J. L., Clascá, F., and Tiesinga, P. H. E. (2016). Connectomic Analysis of Brain Networks: Novel Techniques and Future Directions. *Front. Neuroanat.* 10. doi:10.3389/fnana.2016.00110.

Celio, M. R. (1986). Parvalbumin in Most γ-Aminobutyric Acid-Containing Neurons of the Rat Cerebral Cortex. *Science* 231, 995–997. doi:10.1126/science.3945815.

Celio, M. R., Spreafico, R., De Biasi, S., and Vitellaro-Zuccarello, L. (1998). Perineuronal nets: past and present. *Trends in Neurosciences* 21, 510–515. doi:10.1016/S0166-2236(98)01298-3.

Chen, C.-C., Gilmore, A., and Zuo, Y. (2014). Study Motor Skill Learning by Single-pellet Reaching Tasks in Mice. *JoVE*, 51238. doi:10.3791/51238.

Chen, K., Yang, G., So, K.-F., and Zhang, L. (2019a). Activation of Cortical Somatostatin Interneurons Rescues Synapse Loss and Motor Deficits after Acute MPTP Infusion. *iScience* 17, 230–241. doi:10.1016/j.isci.2019.06.040.

Chen, K., Zheng, Y., Wei, J., Ouyang, H., Huang, X., Zhang, F., et al. (2019b). Exercise training improves motor skill learning via selective activation of mTOR. *Sci. Adv.* 5, eaaw1888. doi:10.1126/sciadv.aaw1888.

Christensen, A. C., Lensjø, K. K., Lepperød, M. E., Dragly, S.-A., Sutterud, H., Blackstad, J. S., et al. (2021). Perineuronal nets stabilize the grid cell network. *Nat Commun* 12, 253. doi:10.1038/s41467-020-20241-w.

Chu, J., Wagle-Shukla, A., Gunraj, C., Lang, A. E., and Chen, R. (2009). Impaired presynaptic inhibition in the motor cortex in Parkinson disease. *Neurology* 72, 842–849. doi:10.1212/01.wnl.0000343881.27524.e8.

Cobb, S. R., Halasy, K., Vida, I., Nyiri, G., Tamás, G., Buhl, E. H., et al. (1997). Synaptic effects of identified interneurons innervating both interneurons and pyramidal cells in the rat hippocampus. *Neuroscience* 79, 629–648. doi:10.1016/s0306-4522(97)00055-9.

Collomb-Clerc, A., and Welter, M.-L. (2015). Effects of deep brain stimulation on balance and gait in patients with Parkinson's disease: A systematic neurophysiological review.

Neurophysiologie Clinique/Clinical Neurophysiology 45, 371–388. doi:10.1016/j.neucli.2015.07.001.

Connelly, W. M., and Lees, G. (2010). Modulation and function of the autaptic connections of layer V fast spiking interneurons in the rat neocortex. *The Journal of Physiology* 588, 2047–2063. doi:10.1113/jphysiol.2009.185199.

Contreras-Vidal, J. L., and Buch, E. R. (2003). Effects of Parkinson's disease on visuomotor adaptation. *Exp Brain Res* 150, 25–32. doi:10.1007/s00221-003-1403-y.

Cornez, G., Valle, S., Santos, E. B. dos, Chiver, I., Müller, W., Ball, G. F., et al. (2021). Perineuronal nets in HVC and plasticity in male canary song. 2021.05.19.444779. Available at: https://www.biorxiv.org/content/10.1101/2021.05.19.444779v1 [Accessed October 8, 2021].

Cotzias, G. C., Papavasiliou, P. S., and Gellene, R. (1969). Modification of Parkinsonism — Chronic Treatment with L-Dopa. *N Engl J Med* 280, 337–345. doi:10.1056/NEJM196902132800701.

Cousineau, J., Lescouzères, L., Taupignon, A., Delgado-Zabalza, L., Valjent, E., Baufreton, J., et al. (2020). Dopamine D2-Like Receptors Modulate Intrinsic Properties and Synaptic Transmission of Parvalbumin Interneurons in the Mouse Primary Motor Cortex. *eNeuro* 7, ENEURO.0081-20.2020. doi:10.1523/ENEURO.0081-20.2020.

Cunic, D., Roshan, L., Khan, F. I., Lozano, A. M., Lang, A. E., and Chen, R. (2002). Effects of subthalamic nucleus stimulation on motor cortex excitability in Parkinson's disease. *Neurology* 58, 1665–1672. doi:10.1212/WNL.58.11.1665.

Darling, W. G., Pizzimenti, M. A., and Morecraft, R. J. (2011). FUNCTIONAL RECOVERY FOLLOWING MOTOR CORTEX LESIONS IN NON-HUMAN PRIMATES: EXPERIMENTAL IMPLICATIONS FOR HUMAN STROKE PATIENTS. *J. Integr. Neurosci.* 10, 353–384. doi:10.1142/S0219635211002737.

Dauth, S., Grevesse, T., Pantazopoulos, H., Campbell, P. H., Maoz, B. M., Berretta, S., et al. (2016). Extracellular matrix protein expression is brain region dependent: Brain Extracellular Matrix Distribution Analysis. *J. Comp. Neurol.* 524, 1309–1336. doi:10.1002/cne.23965.

de Almeida, L., Idiart, M., and Lisman, J. E. (2009a). A Second Function of Gamma Frequency Oscillations: An E%-Max Winner-Take-All Mechanism Selects Which Cells Fire. *Journal of Neuroscience* 29, 7497–7503. doi:10.1523/JNEUROSCI.6044-08.2009.

de Almeida, L., Idiart, M., and Lisman, J. E. (2009b). The Input-Output Transformation of the Hippocampal Granule Cells: From Grid Cells to Place Fields. *Journal of Neuroscience* 29, 7504–7512. doi:10.1523/JNEUROSCI.6048-08.2009.

de Groot, A., van den Boom, B. J., van Genderen, R. M., Coppens, J., van Veldhuijzen, J., Bos, J., et al. (2020). NINscope, a versatile miniscope for multi-region circuit investigations. *eLife* 9, e49987. doi:10.7554/eLife.49987.

de Lau, L. M., and Breteler, M. M. (2006). Epidemiology of Parkinson's disease. *The Lancet Neurology* 5, 525–535. doi:10.1016/S1474-4422(06)70471-9.

de Winter, F., Kwok, J. C. F., Fawcett, J. W., Vo, T. T., Carulli, D., and Verhaagen, J. (2016). The Chemorepulsive Protein Semaphorin 3A and Perineuronal Net-Mediated Plasticity. *Neural Plast* 2016, 3679545. doi:10.1155/2016/3679545.

Deacon, R. M. J. (2013). Measuring Motor Coordination in Mice. *JoVE*, 2609. doi:10.3791/2609.

Deepa, S. S., Carulli, D., Galtrey, C., Rhodes, K., Fukuda, J., Mikami, T., et al. (2006). Composition of Perineuronal Net Extracellular Matrix in Rat Brain. *Journal of Biological Chemistry* 281, 17789–17800. doi:10.1074/jbc.M600544200.

Deleuze, C., Bhumbra, G. S., Pazienti, A., Lourenço, J., Mailhes, C., Aguirre, A., et al. (2019). Strong preference for autaptic self-connectivity of neocortical PV interneurons facilitates their tuning to γ-oscillations. *PLoS Biol* 17, e3000419. doi:10.1371/journal.pbio.3000419.

Descarries, L., Lemay, B., Doucet, G., and Berger, B. (1987). Regional and laminar density of the dopamine innervation in adult rat cerebral cortex. *Neuroscience* 21, 807–824. doi:10.1016/0306-4522(87)90038-8.

Devienne, G., Picaud, S., Cohen, I., Piquet, J., Tricoire, L., Testa, D., et al. (2021). Regulation of Perineuronal Nets in the Adult Cortex by the Activity of the Cortical Network. *J. Neurosci.* 41, 5779–5790. doi:10.1523/JNEUROSCI.0434-21.2021.

Devos, D. (2004). Subthalamic nucleus stimulation modulates motor cortex oscillatory activity in Parkinson's disease. *Brain* 127, 408–419. doi:10.1093/brain/awh053.

Dhawale, A. K., Smith, M. A., and Ölveczky, B. P. (2017). The Role of Variability in Motor Learning. *Annu. Rev. Neurosci.* 40, 479–498. doi:10.1146/annurev-neuro-072116-031548.

Dityatev, A., Brückner, G., Dityateva, G., Grosche, J., Kleene, R., and Schachner, M. (2007). Activity-dependent formation and functions of chondroitin sulfate-rich extracellular matrix of perineuronal nets. *Dev Neurobiol* 67, 570–588. doi:10.1002/dneu.20361.

Donato, F., Rompani, S. B., and Caroni, P. (2013). Parvalbumin-expressing basket-cell network plasticity induced by experience regulates adult learning. *Nature* 504, 272–276. doi:10.1038/nature12866.

Doshi, P. K. (2011). Long-Term Surgical and Hardware-Related Complications of Deep Brain Stimulation. *Stereotact Funct Neurosurg* 89, 89–95. doi:10.1159/000323372.

Duan, Z., Li, A., Gong, H., and Li, X. (2020). A Whole-brain Map of Long-range Inputs to GABAergic Interneurons in the Mouse Caudal Forelimb Area. *Neuroscience Bulletin* 36, 493–505. doi:10.1007/s12264-019-00458-6.

Dupont-Hadwen, J., Bestmann, S., and Stagg, C. J. (2019). Motor training modulates intracortical inhibitory dynamics in motor cortex during movement preparation. *Brain Stimulation* 12, 300–308. doi:10.1016/j.brs.2018.11.002.

Eggermann, E., and Jonas, P. (2012). How the “slow” Ca2+ buffer parvalbumin affects transmitter release in nanodomain-coupling regimes. *Nat Neurosci* 15, 20–22. doi:10.1038/nn.3002.

Eggers, C., Fink, G. R., and Nowak, D. A. (2010). Theta burst stimulation over the primary motor cortex does not induce cortical plasticity in Parkinson’s disease. *J Neurol* 257, 1669–1674. doi:10.1007/s00415-010-5597-1.

Estebanez, L., Hoffmann, D., Voigt, B. C., and Poulet, J. F. A. (2017). Parvalbumin-Expressing GABAergic Neurons in Primary Motor Cortex Signal Reaching. *Cell Reports* 20, 308–318. doi:10.1016/j.celrep.2017.06.044.

Eusebio, A., and Brown, P. (2009). Synchronisation in the beta frequency-band — The bad boy of parkinsonism or an innocent bystander? *Experimental Neurology* 217, 1–3. doi:10.1016/j.expneurol.2009.02.003.

Fahn, S. (2008). The history of dopamine and levodopa in the treatment of Parkinson’s disease: Dopamine and Levodopa in the Treatment of PD. *Mov. Disord.* 23, S497–S508. doi:10.1002/mds.22028.

Faini, G., Aguirre, A., Landi, S., Pizzorusso, T., Ratto, G. M., Deleuze, C., et al. (2018). Perineuronal nets set the strength of thalamic recruitment of interneurons in the adult visual cortex. 374587. Available at: https://www.biorxiv.org/content/10.1101/374587v1 [Accessed October 8, 2021].

Falowski, S. M., Ooi, Y. C., and Bakay, R. A. E. (2015). Long-Term Evaluation of Changes in Operative Technique and Hardware-Related Complications With Deep Brain Stimulation: Hardware-Related Complications with Deep Brain Stimulation. *Neuromodulation: Technology at the Neural Interface* 18, 670–677. doi:10.1111/ner.12335.

Favuzzi, E., Marques-Smith, A., Deogracias, R., Winterflood, C. M., Sánchez-Aguilera, A., Mantoan, L., et al. (2017). Activity-Dependent Gating of Parvalbumin Interneuron Function by the Perineuronal Net Protein Brevican. *Neuron* 95, 639-655.e10. doi:10.1016/j.neuron.2017.06.028.

Fenrich, K. K., May, Z., Hurd, C., Boychuk, C. E., Kowalczewski, J., Bennett, D. J., et al. (2015). Improved single pellet grasping using automated ad libitum full-time training robot. *Behavioural Brain Research* 281, 137–148. doi:10.1016/j.bbr.2014.11.048.

Ferguson, B. R., and Gao, W.-J. (2018). PV Interneurons: Critical Regulators of E/I Balance for Prefrontal Cortex-Dependent Behavior and Psychiatric Disorders. *Frontiers in Neural Circuits* 12, 1–13. doi:10.3389/fncir.2018.00037.

Filippi, M. M., Oliveri, M., Pasqualetti, P., Cicinelli, P., Traversa, R., Vernieri, F., et al. (2001). Effects of motor imagery on motor cortical output topography in Parkinson's disease. *Neurology* 57, 55–61. doi:10.1212/WNL.57.1.55.

Fitts, P. M. (1964). "Perceptual-Motor Skill Learning11This chapter is based in part on research supported by the U. S. Air Force, Office of Scientific Research, under Contract No. AF 49 (638)-449.," in *Categories of Human Learning* (Elsevier), 243–285. doi:10.1016/B978-1-4832-3145-7.50016-9.

Frischknecht, R., Heine, M., Perrais, D., Seidenbecher, C. I., Choquet, D., and Gundelfinger, E. D. (2009). Brain extracellular matrix affects AMPA receptor lateral mobility and short-term synaptic plasticity. *Nat Neurosci* 12, 897–904. doi:10.1038/nn.2338.

Frith, C. D., Bloxham, C. A., and Carpenter, K. N. (1986). Impairments in the learning and performance of a new manual skill in patients with Parkinson's disease. *Journal of Neurology, Neurosurgery & Psychiatry* 49, 661–668. doi:10.1136/jnnp.49.6.661.

Frost, S. B., Milliken, G. W., Plautz, E. J., Masterton, R. B., and Nudo, R. J. (2000). Somatosensory and motor representations in cerebral cortex of a primitive mammal (Monodelphis domestica): A window into the early evolution of sensorimotor cortex. *Journal of Comparative Neurology* 421, 29–51. doi:https://doi.org/10.1002/(SICI)1096-9861(20000522)421:1<29::AID-CNE3>3.0.CO;2-9.

Fukuda, M., Barnes, A., Simon, E. S., Holmes, A., Dhawan, V., Giladi, N., et al. (2004). Thalamic stimulation for parkinsonian tremor: correlation between regional cerebral blood flow and physiological tremor characteristics. *NeuroImage* 21, 608–615. doi:10.1016/j.neuroimage.2003.09.068.

Galiñanes, G. L., Bonardi, C., and Huber, D. (2018). Directional Reaching for Water as a Cortex-Dependent Behavioral Framework for Mice. *Cell Reports* 22, 2767–2783. doi:10.1016/j.celrep.2018.02.042.

Galtrey, C. M., and Fawcett, J. W. (2007). The role of chondroitin sulfate proteoglycans in regeneration and plasticity in the central nervous system. *Brain Research Reviews* 54, 1–18. doi:10.1016/j.brainresrev.2006.09.006.

Galtrey, C. M., Kwok, J. C. F., Carulli, D., Rhodes, K. E., and Fawcett, J. W. (2008). Distribution and synthesis of extracellular matrix proteoglycans, hyaluronan, link proteins and tenascin-R in the rat spinal cord. *Eur J Neurosci* 27, 1373–1390. doi:10.1111/j.1460-9568.2008.06108.x.

Galvan, A., and Wichmann, T. (2008). Pathophysiology of Parkinsonism. *Clinical Neurophysiology* 119, 1459–1474. doi:10.1016/j.clinph.2008.03.017.

Gaspar, P., Bloch, B., and Moine, C. (1995). D1 and D2 Receptor Gene Expression in the Rat Frontal Cortex: Cellular Localization in Different Classes of Efferent Neurons. *European Journal of Neuroscience* 7, 1050–1063. doi:10.1111/j.1460-9568.1995.tb01092.x.

Gaspar, P., Duyckaerts, C., Alvarez, C., Javoy-Agid, F., and Berger, B. (1991). Alterations of dopaminergic and noradrenergic innervations in motor cortex in Parkinson's disease. *Ann. Neurol.* 30, 365–374. doi:10.1002/ana.410300308.

Gee, S., Ellwood, I., Patel, T., Luongo, F., Deisseroth, K., and Sohal, V. S. (2012). Synaptic Activity Unmasks Dopamine D2 Receptor Modulation of a Specific Class of Layer V Pyramidal Neurons in Prefrontal Cortex. *Journal of Neuroscience* 32, 4959–4971. doi:10.1523/JNEUROSCI.5835-11.2012.

George, J. S., Strunk, J., Mak-McCully, R., Houser, M., Poizner, H., and Aron, A. R. (2013). Dopaminergic therapy in Parkinson's disease decreases cortical beta band coherence in the resting state and increases cortical beta band power during executive control. *NeuroImage: Clinical* 3, 261–270. doi:10.1016/j.nicl.2013.07.013.

Gogolla, N., Caroni, P., Lüthi, A., and Herry, C. (2009). Perineuronal Nets Protect Fear Memories from Erasure. *Science* 325, 1258–1261. doi:10.1126/science.1174146.

Golbe, L. I. (1991). Young-onset Parkinson's disease: A clinical review. *Neurology* 41, 168–168. doi:10.1212/WNL.41.2_Part_1.168.

Graziano, M. S. A., and Aflalo, T. N. (2007). Mapping Behavioral Repertoire onto the Cortex. *Neuron* 56, 239–251. doi:10.1016/j.neuron.2007.09.013.

Graziano, M. S. A., Aflalo, T. N. S., and Cooke, D. F. (2005). Arm Movements Evoked by Electrical Stimulation in the Motor Cortex of Monkeys. *Journal of Neurophysiology* 94, 4209–4223. doi:10.1152/jn.01303.2004.

Graziano, M. S. A., Taylor, C. S. R., and Moore, T. (2002). Complex Movements Evoked by Microstimulation of Precentral Cortex. *Neuron* 34, 841–851. doi:10.1016/S0896-6273(02)00698-0.

Grosche, J., and Brckner, G. (2001). Perineuronal nets show intrinsic patterns of extracellular matrix differentiation in organotypic slice cultures. *Experimental Brain Research* 137, 83–93. doi:10.1007/s002210000617.

Gross, C. G. (2007). The Discovery of Motor Cortex and its Background. *Journal of the History of the Neurosciences* 16, 320–331. doi:10.1080/09647040600630160.

Guadagno, A., Verlezza, S., Long, H., Wong, T. P., and Walker, C.-D. (2020). It Is All in the Right Amygdala: Increased Synaptic Plasticity and Perineuronal Nets in Male, But Not Female, Juvenile Rat Pups after Exposure to Early-Life Stress. *J. Neurosci.* 40, 8276–8291. doi:10.1523/JNEUROSCI.1029-20.2020.

Guerra, A., Asci, F., D'Onofrio, V., Sveva, V., Bologna, M., Fabbrini, G., et al. (2020). Enhancing Gamma Oscillations Restores Primary Motor Cortex Plasticity in Parkinson's Disease. *J. Neurosci.* 40, 4788–4796. doi:10.1523/JNEUROSCI.0357-20.2020.

Gulati, S., Cao, V. Y., and Otte, S. (2017). Multi-layer Cortical Ca^{2+} Imaging in Freely Moving Mice with Prism Probes and Miniaturized Fluorescence Microscopy. *JoVE*, 55579. doi:10.3791/55579.

Guo, J.-Z., Graves, A. R., Guo, W. W., Zheng, J., Lee, A., Rodríguez-González, J., et al. (2015a). Cortex commands the performance of skilled movement. *eLife* 4, e10774. doi:10.7554/eLife.10774.

Guo, J.-Z., Sauerbrei, B. A., Cohen, J. D., Mischiati, M., Graves, A. R., Pisanello, F., et al. (2021). Disrupting cortico-cerebellar communication impairs dexterity. *eLife* 10, e65906. doi:10.7554/eLife.65906.

Guo, L., Xiong, H., Kim, J.-I., Wu, Y.-W., Lalchandani, R. R., Cui, Y., et al. (2015b). Dynamic rewiring of neural circuits in the motor cortex in mouse models of Parkinson's disease. *Nature Neuroscience* 18, 1299–1309. doi:10.1038/nn.4082.

Hall, R. D., and Lindholm, E. P. (1974). Organization of motor and somatosensory neocortex in the albino rat. *Brain Research* 66, 23–38. doi:10.1016/0006-8993(74)90076-6.

Hall, S. D., Prokic, E. J., McAllister, C. J., Ronnqvist, K. C., Williams, A. C., Yamawaki, N., et al. (2014). GABA-mediated changes in inter-hemispheric beta frequency activity in early-stage Parkinson's disease. *Neuroscience* 281, 68–76. doi:10.1016/j.neuroscience.2014.09.037.

Harauzov, A., Spolidoro, M., DiCristo, G., De Pasquale, R., Cancedda, L., Pizzorusso, T., et al. (2010). Reducing Intracortical Inhibition in the Adult Visual Cortex Promotes Ocular Dominance Plasticity. *Journal of Neuroscience* 30, 361–371. doi:10.1523/JNEUROSCI.2233-09.2010.

Harkness, J. H., Gonzalez, A. E., Bushana, P. N., Jorgensen, E. T., Hegarty, D. M., Di Nardo, A. A., et al. (2021). Diurnal changes in perineuronal nets and parvalbumin neurons in the rat medial prefrontal cortex. *Brain Struct Funct* 226, 1135–1153. doi:10.1007/s00429-021-02229-4.

Harms, K. J., Rioult-Pedotti, M. S., Carter, D. R., and Dunaevsky, A. (2008). Transient Spine Expansion and Learning-Induced Plasticity in Layer 1 Primary Motor Cortex. *Journal of Neuroscience* 28, 5686–5690. doi:10.1523/JNEUROSCI.0584-08.2008.

Harris, N. G., Carmichael, S. T., Hovda, D. A., and Sutton, R. L. (2009). Traumatic brain injury results in disparate regions of chondroitin sulfate proteoglycan expression that are temporally limited. *Journal of Neuroscience Research* 87, 2937–2950. doi:10.1002/jnr.22115.

Harris, N. G., Nogueira, M. S. M., Verley, D. R., and Sutton, R. L. (2013). Chondroitinase Enhances Cortical Map Plasticity and Increases Functionally Active Sprouting Axons after Brain Injury. *Journal of Neurotrauma* 30, 1257–1269. doi:10.1089/neu.2012.2737.

Härtig, W., Brauer, K., and Brückner, G. (1992a). Wisteria floribunda agglutinin-labelled nets surround parvalbumin-containing neurons: *NeuroReport* 3, 869–872. doi:10.1097/00001756-199210000-00012.

Härtig, W., Brauer, K., and Brückner, G. (1992b). Wisteria floribunda agglutinin-labelled nets surround parvalbumin-containing neurons: *NeuroReport* 3, 869–872. doi:10.1097/00001756-199210000-00012.

Härtig, W., Derouiche, A., Welt, K., Brauer, K., Grosche, J., Mäder, M., et al. (1999). Cortical neurons immunoreactive for the potassium channel Kv3.1b subunit are predominantly surrounded by perineuronal nets presumed as a buffering system for cations. *Brain Research* 842, 15–29. doi:10.1016/S0006-8993(99)01784-9.

Hausen, D., Brückner, G., Drlicek, M., Härtig, W., Brauer, K., and Bigl, V. (1996). Pyramidal cells ensheathed by perineuronal nets in human motor and somatosensory cortex: *NeuroReport* 7, 1725–1729. doi:10.1097/00001756-199607290-00006.

Hayani, H., Song, I., and Dityatev, A. (2018). Increased Excitability and Reduced Excitatory Synaptic Input Into Fast-Spiking CA2 Interneurons After Enzymatic Attenuation of Extracellular Matrix. *Front. Cell. Neurosci.* 12, 149. doi:10.3389/fncel.2018.00149.

Hayashi-Takagi, A., Yagishita, S., Nakamura, M., Shirai, F., Wu, Y. I., Loshbaugh, A. L., et al. (2015). Labelling and optical erasure of synaptic memory traces in the motor cortex. *Nature* 525, 333–338. doi:10.1038/nature15257.

Hemptinne, C., Wang, D. D., Miocinovic, S., Chen, W., Ostrem, J. L., and Starr, P. A. (2019). Pallidal thermolesion unleashes gamma oscillations in the motor cortex in Parkinson's disease. *Mov Disord* 34, 903–911. doi:10.1002/mds.27658.

Hertler, B., Buitrago, M. M., Luft, A. R., and Hosp, J. A. (2016). Temporal course of gene expression during motor memory formation in primary motor cortex of rats. *Neurobiology of Learning and Memory* 136, 105–115. doi:10.1016/j.nlm.2016.09.018.

Hilker, R., Voges, J., Weisenbach, S., Kalbe, E., Burghaus, L., Ghaemi, M., et al. (2004). Subthalamic Nucleus Stimulation Restores Glucose Metabolism in Associative and Limbic Cortices and in Cerebellum: Evidence from a FDG-PET Study in Advanced Parkinson's Disease. *J Cereb Blood Flow Metab* 24, 7–16. doi:10.1097/01.WCB.0000092831.44769.09.

Hioki, H., Okamoto, S., Konno, M., Kameda, H., Sohn, J., Kuramoto, E., et al. (2013). Cell Type-Specific Inhibitory Inputs to Dendritic and Somatic Compartments of Parvalbumin-Expressing Neocortical Interneuron. *Journal of Neuroscience* 33, 544–555. doi:10.1523/JNEUROSCI.2255-12.2013.

Hirono, M., Watanabe, S., Karube, F., Fujiyama, F., Kawahara, S., Nagao, S., et al. (2018). Perineuronal Nets in the Deep Cerebellar Nuclei Regulate GABAergic Transmission and Delay Eyeblink Conditioning. *J. Neurosci.* 38, 6130–6144. doi:10.1523/JNEUROSCI.3238-17.2018.

Holmgren, C., Harkany, T., Svennenfors, B., and Zilberter, Y. (2003). Pyramidal cell communication within local networks in layer 2/3 of rat neocortex. *The Journal of Physiology* 551, 139–153. doi:10.1113/jphysiol.2003.044784.

Horii-Hayashi, N., Sasagawa, T., Matsunaga, W., and Nishi, M. (2015). Development and Structural Variety of the Chondroitin Sulfate Proteoglycans-Contained Extracellular Matrix in the Mouse Brain. *Neural Plasticity* 2015, 1–12. doi:10.1155/2015/256389.

Hosp, J. A., Coenen, V. A., Rijntjes, M., Egger, K., Urbach, H., Weiller, C., et al. (2019). Ventral tegmental area connections to motor and sensory cortical fields in humans. *Brain Structure and Function* 224, 2839–2855. doi:10.1007/s00429-019-01939-0.

Hosp, J. A., and Luft, A. R. (2013). Dopaminergic Meso-Cortical Projections to M1: Role in Motor Learning and Motor Cortex Plasticity. *Front. Neurol.* 4. doi:10.3389/fneur.2013.00145.

Hosp, J. A., Nolan, H. E., and Luft, A. R. (2015). Topography and collateralization of dopaminergic projections to primary motor cortex in rats. *Exp Brain Res* 233, 1365–1375. doi:10.1007/s00221-015-4211-2.

Hosp, J. A., Pekanovic, A., Rioult-Pedotti, M. S., and Luft, A. R. (2011). Dopaminergic Projections from Midbrain to Primary Motor Cortex Mediate Motor Skill Learning. *Journal of Neuroscience* 31, 2481–2487. doi:10.1523/JNEUROSCI.5411-10.2011.

Hu, H., Gan, J., and Jonas, P. (2014). Fast-spiking, parvalbumin+ GABAergic interneurons: From cellular design to microcircuit function. *Science* 345, 1255263–1255263. doi:10.1126/science.1255263.

Huang, Y.-Z., Edwards, M. J., Rounis, E., Bhatia, K. P., and Rothwell, J. C. (2005). Theta Burst Stimulation of the Human Motor Cortex. *Neuron* 45, 201–206. doi:10.1016/j.neuron.2004.12.033.

Huber, D., Gutnisky, D. A., Peron, S., O'Connor, D. H., Wiegert, J. S., Tian, L., et al. (2012). Multiple dynamic representations in the motor cortex during sensorimotor learning. *Nature* 484, 473–478. doi:10.1038/nature11039.

Huda, K., Salunga, T. L., Chowdhury, S. A., Kawashima, T., and Matsunami, K. (1999). Dopaminergic modulation of transcallosal activity of cat motor cortical neurons. *Neuroscience Research* 33, 33–40. doi:10.1016/S0168-0102(98)00108-4.

Huda, K., Salunga, T. L., and Matsunami, K. (2001). Dopaminergic inhibition of excitatory inputs onto pyramidal tract neurons in cat motor cortex. *Neuroscience Letters* 307, 175–178. doi:10.1016/S0304-3940(01)01960-7.

Huntley, G. W., Morrison, J. H., Prikhozhan, A., and Sealfon, S. C. (1992). Localization of multiple dopamine receptor subtype mRNAs in human and monkey motor cortex and striatum. *Molecular Brain Research* 15, 181–188. doi:10.1016/0169-328X(92)90107-M.

Hyland, B. I., Seeger-Armbruster, S., Smither, R. A., and Parr-Brownlie, L. C. (2019). Altered Recruitment of Motor Cortex Neuronal Activity During the Grasping Phase of Skilled Reaching in a Chronic Rat Model of Unilateral Parkinsonism. *J. Neurosci.* 39, 9660–9672. doi:10.1523/JNEUROSCI.0720-19.2019.

Inda, M. C., DeFelipe, J., and Munoz, A. (2009). Morphology and Distribution of Chandelier Cell Axon Terminals in the Mouse Cerebral Cortex and Claustroamygdaloid Complex. *Cerebral Cortex* 19, 41–54. doi:10.1093/cercor/bhn057.

Irvine, S. F., and Kwok, J. C. F. (2018). Perineuronal Nets in Spinal Motoneurones: Chondroitin Sulphate Proteoglycan around Alpha Motoneurones. *Int J Mol Sci* 19, E1172. doi:10.3390/ijms19041172.

Isaacson, J. S., and Scanziani, M. (2011). How Inhibition Shapes Cortical Activity. *Neuron* 72, 231–243. doi:10.1016/j.neuron.2011.09.027.

Isomura, Y., Harukuni, R., Takekawa, T., Aizawa, H., and Fukai, T. (2009). Microcircuitry coordination of cortical motor information in self-initiation of voluntary movements. *Nature Neuroscience* 12, 1586–1593. doi:10.1038/nn.2431.

Jang, D. P., Min, H.-K., Lee, S.-Y., Kim, I. Y., Park, H. W., Im, Y. H., et al. (2012). Functional neuroimaging of the 6-OHDA lesion rat model of Parkinson's disease. *Neuroscience Letters* 513, 187–192. doi:10.1016/j.neulet.2012.02.034.

Jenkinson, N., and Brown, P. (2011). New insights into the relationship between dopamine, beta oscillations and motor function. *Trends in Neurosciences* 34, 611–618. doi:10.1016/j.tins.2011.09.003.

Jinno, S., and Kosaka, T. (2004). Parvalbumin is expressed in glutamatergic and GABAergic corticostriatal pathway in mice. *J. Comp. Neurol.* 477, 188–201. doi:10.1002/cne.20246.

Jouhanneau, J.-S., Kremkow, J., and Poulet, J. F. A. (2018). Single synaptic inputs drive high-precision action potentials in parvalbumin expressing GABA-ergic cortical neurons in vivo. *Nat Commun* 9, 1540. doi:10.1038/s41467-018-03995-2.

Kaas, J. H. (2004). Evolution of somatosensory and motor cortex in primates. *Anat. Rec.* 281A, 1148–1156. doi:10.1002/ar.a.20120.

Kapfer, C., Glickfeld, L. L., Atallah, B. V., and Scanziani, M. (2007). Supralinear increase of recurrent inhibition during sparse activity in the somatosensory cortex. *Nat Neurosci* 10, 743–753. doi:10.1038/nn1909.

Karube, F. (2004). Axon Branching and Synaptic Bouton Phenotypes in GABAergic Nonpyramidal Cell Subtypes. *Journal of Neuroscience* 24, 2853–2865. doi:10.1523/JNEUROSCI.4814-03.2004.

Kätzel, D., Zemelman, B. V., Buetfering, C., Wölfel, M., and Miesenböck, G. (2011). The columnar and laminar organization of inhibitory connections to neocortical excitatory cells. *Nat Neurosci* 14, 100–107. doi:10.1038/nn.2687.

Kawai, R., Markman, T., Poddar, R., Ko, R., Fantana, A. L., Dhawale, A. K., et al. (2015). Motor Cortex Is Required for Learning but Not for Executing a Motor Skill. *Neuron* 86, 800–812. doi:10.1016/j.neuron.2015.03.024.

Kida, H., Tsuda, Y., Ito, N., Yamamoto, Y., Owada, Y., Kamiya, Y., et al. (2016). Motor Training Promotes Both Synaptic and Intrinsic Plasticity of Layer II/III Pyramidal Neurons in the Primary Motor Cortex. *Cereb. Cortex* 26, 3494–3507. doi:10.1093/cercor/bhw134.

Kim, C., and Alcalay, R. (2017). Genetic Forms of Parkinson's Disease. *Semin Neurol* 37, 135–146. doi:10.1055/s-0037-1601567.

Klein, A., Sacrey, L.-A. R., Whishaw, I. Q., and Dunnett, S. B. (2012). The use of rodent skilled reaching as a translational model for investigating brain damage and disease. *Neuroscience & Biobehavioral Reviews* 36, 1030–1042. doi:10.1016/j.neubiorev.2011.12.010.

Kochlamazashvili, G., Henneberger, C., Bukalo, O., Dvoretskova, E., Senkov, O., Lievens, P. M.-J., et al. (2010). The Extracellular Matrix Molecule Hyaluronic Acid Regulates Hippocampal Synaptic Plasticity by Modulating Postsynaptic L-Type Ca2+ Channels. *Neuron* 67, 116–128. doi:10.1016/j.neuron.2010.05.030.

Kojovic, M., Bologna, M., Kassavetis, P., Murase, N., Palomar, F. J., Berardelli, A., et al. (2012). Functional reorganization of sensorimotor cortex in early Parkinson disease. *Neurology* 78, 1441–1448. doi:10.1212/WNL.0b013e318253d5dd.

Kolasinski, J., Hinson, E. L., Divanbeighi Zand, A. P., Rizov, A., Emir, U. E., and Stagg, C. J. (2019). The dynamics of cortical GABA in human motor learning. *J Physiol* 597, 271–282. doi:10.1113/JP276626.

Kondo, T., Saito, R., Otaka, M., Yoshino-Saito, K., Yamanaka, A., Yamamori, T., et al. (2018). Calcium Transient Dynamics of Neural Ensembles in the Primary Motor Cortex of Naturally Behaving Monkeys. *Cell Rep* 24, 2191-2195.e4. doi:10.1016/j.celrep.2018.07.057.

Koppe, G. (1997). [No title found]. *The Histochemical Journal* 29, 11–20. doi:10.1023/A:1026408716522.

Krack, P., Pollak, P., Limousin, P., Benazzouz, A., and Benabid, A. (1997). Stimulation of subthalamic nucleus alleviates tremor in Parkinson's disease. *The Lancet* 350, 1675. doi:10.1016/S0140-6736(97)24049-3.

Krause, M. (2001). Deep brain stimulation for the treatment of Parkinson's disease: subthalamic nucleus versus globus pallidus internus. *Journal of Neurology, Neurosurgery & Psychiatry* 70, 464–470. doi:10.1136/jnnp.70.4.464.

Kuhlman, S. J., Olivas, N. D., Tring, E., Ikrar, T., Xu, X., and Trachtenberg, J. T. (2013). A disinhibitory microcircuit initiates critical-period plasticity in the visual cortex. *Nature* 501, 543–546. doi:10.1038/nature12485.

Kuhn, A. A., Kempf, F., Brucke, C., Gaynor Doyle, L., Martinez-Torres, I., Pogosyan, A., et al. (2008). High-Frequency Stimulation of the Subthalamic Nucleus Suppresses Oscillatory Activity in Patients with Parkinson's Disease in Parallel with Improvement in Motor Performance. *Journal of Neuroscience* 28, 6165–6173. doi:10.1523/JNEUROSCI.0282-08.2008.

Kwakkel, G., Kollen, B. J., van der Grond, J., and Prevo, A. J. H. (2003). Probability of Regaining Dexterity in the Flaccid Upper Limb: Impact of Severity of Paresis and Time Since Onset in Acute Stroke. *Stroke* 34, 2181–2186. doi:10.1161/01.STR.0000087172.16305.CD.

Kwok, J. C. F., Carulli, D., and Fawcett, J. W. (2010). In vitro modeling of perineuronal nets: hyaluronan synthase and link protein are necessary for their formation and integrity: Hyaluronan synthase and link protein in PNNs. *Journal of Neurochemistry*, no-no. doi:10.1111/j.1471-4159.2010.06878.x.

Kwok, J. C. F., Dick, G., Wang, D., and Fawcett, J. W. (2011). Extracellular matrix and perineuronal nets in CNS repair. *Devel Neurobio* 71, 1073–1089. doi:10.1002/dneu.20974.

Lashley, K. S. (1924). STUDIES OF CEREBRAL FUNCTION IN LEARNING: V. THE RETENTION OF MOTOR HABITS AFTER DESTRUCTION OF THE SO-CALLED MOTOR AREAS IN PRIMATES. *Arch NeurPsych* 12, 249. doi:10.1001/archneurpsyc.1924.02200030002001.

Leemburg, S., Canonica, T., and Luft, A. (2018). Motor skill learning and reward consumption differentially affect VTA activation. *Sci Rep* 8, 687. doi:10.1038/s41598-017-18716-w.

Lensjø, K. K., Christensen, A. C., Tennøe, S., Fyhn, M., and Hafting, T. (2017). Differential Expression and Cell-Type Specificity of Perineuronal Nets in Hippocampus, Medial Entorhinal Cortex, and Visual Cortex Examined in the Rat and Mouse. *eNeuro* 4, ENEURO.0379-16.2017. doi:10.1523/ENEURO.0379-16.2017.

Leodori, G., Belvisi, D., De Bartolo, M. I., Fabbrini, A., Costanzo, M., Vial, F., et al. (2020). Re-emergent Tremor in Parkinson's Disease: The Role of the Motor Cortex. *Mov Disord* 35, 1002–1011. doi:10.1002/mds.28022.

Levy, S., Lavzin, M., Benisty, H., Ghanayim, A., Dubin, U., Achvat, S., et al. (2020). Cell-Type-Specific Outcome Representation in the Primary Motor Cortex. *Neuron* 107, 954-971.e9. doi:10.1016/j.neuron.2020.06.006.

Leyton, A. S. F., and Sherrington, C. S. (1917). OBSERVATIONS ON THE EXCITABLE CORTEX OF THE CHIMPANZEE, ORANG-UTAN, AND GORILLA. *Exp Physiol* 11, 135–222. doi:10.1113/expphysiol.1917.sp000240.

Li, M., Wang, X., Yao, X., Wang, X., Chen, F., Zhang, X., et al. (2021). Roles of Motor Cortex Neuron Classes in Reach-Related Modulation for Hemiparkinsonian Rats. *Front. Neurosci.* 15, 645849. doi:10.3389/fnins.2021.645849.

Li, N., Lee, B., Liu, R.-J., Banasr, M., Dwyer, J. M., Iwata, M., et al. (2010). mTOR-Dependent Synapse Formation Underlies the Rapid Antidepressant Effects of NMDA Antagonists. *Science* 329, 959–964. doi:10.1126/science.1190287.

Li, Q., Ko, H., Qian, Z.-M., Yan, L. Y. C., Chan, D. C. W., Arbuthnott, G., et al. (2017). Refinement of learned skilled movement representation in motor cortex deep output layer. *Nature Communications* 8, 15834. doi:10.1038/ncomms15834.

Lim, L., Mi, D., Llorca, A., and Marín, O. (2018). Development and Functional Diversification of Cortical Interneurons. *Neuron* 100, 294–313. doi:10.1016/j.neuron.2018.10.009.

Lindenbach, D., and Bishop, C. (2013). Critical involvement of the motor cortex in the pathophysiology and treatment of Parkinson's disease. *Neuroscience & Biobehavioral Reviews* 37, 2737–2750. doi:10.1016/j.neubiorev.2013.09.008.

Liu, H., Gao, P.-F., Xu, H.-W., Liu, M.-M., Yu, T., Yao, J.-P., et al. (2013). Perineuronal nets increase inhibitory GABAergic currents during the critical period in rats. *Int J Ophthalmol* 6, 120–125. doi:10.3980/j.issn.2222-3959.2013.02.02.

Liu, Y.-J., Spangenberg, E. E., Tang, B., Holmes, T. C., Green, K. N., and Xu, X. (2021). Microglia Elimination Increases Neural Circuit Connectivity and Activity in Adult Mouse Cortex. *J. Neurosci.* 41, 1274–1287. doi:10.1523/JNEUROSCI.2140-20.2020.

Logan, G. D. (1988). Toward an instance theory of automatization. *Psychological Review* 95, 492–527. doi:10.1037/0033-295X.95.4.492.

Lopez-Bendito, G., Sanchez-Alcaniz, J. A., Pla, R., Borrell, V., Pico, E., Valdeolmillos, M., et al. (2008). Chemokine Signaling Controls Intracortical Migration and Final Distribution of GABAergic Interneurons. *Journal of Neuroscience* 28, 1613–1624. doi:10.1523/JNEUROSCI.4651-07.2008.

Lugassy, D., Herszage, J., Pilo, R., Brosh, T., and Censor, N. (2018). Consolidation of complex motor skill learning: evidence for a delayed offline process. *Sleep* 41. doi:10.1093/sleep/zsy123.

Lupica, C. (1995). Delta and mu enkephalins inhibit spontaneous GABA-mediated IPSCs via a cyclic AMP-independent mechanism in the rat hippocampus. *J. Neurosci.* 15, 737–749. doi:10.1523/JNEUROSCI.15-01-00737.1995.

Luppino, G., Matelli, M., Camarda, R. M., Gallese, V., and Rizzolatti, G. (1991). Multiple representations of body movements in mesial area 6 and the adjacent cingulate cortex: An intracortical microstimulation study in the macaque monkey. *J. Comp. Neurol.* 311, 463–482. doi:10.1002/cne.903110403.

Lyoo, C. H., Ryu, Y. H., and Lee, M. S. (2011). Cerebral cortical areas in which thickness correlates with severity of motor deficits of Parkinson's disease. *J Neurol* 258, 1871–1876. doi:10.1007/s00415-011-6045-6.

Mansour, A., Meador-Woodruff, J., Bunzow, J., Civelli, O., Akil, H., and Watson, S. (1990). Localization of dopamine D2 receptor mRNA and D1 and D2 receptor binding in the rat brain and pituitary: an in situ hybridization- receptor autoradiographic analysis. *J. Neurosci.* 10, 2587–2600. doi:10.1523/JNEUROSCI.10-08-02587.1990.

Marinelli, L., Crupi, D., Di Rocco, A., Bove, M., Eidelberg, D., Abbruzzese, G., et al. (2009). Learning and consolidation of visuo-motor adaptation in Parkinson's disease. *Parkinsonism & Related Disorders* 15, 6–11. doi:10.1016/j.parkreldis.2008.02.012.

Marinelli, L., Quartarone, A., Hallett, M., Frazzitta, G., and Ghilardi, M. F. (2017). The many facets of motor learning and their relevance for Parkinson's disease. *Clinical Neurophysiology* 128, 1127–1141. doi:10.1016/j.clinph.2017.03.042.

Markram, H., Muller, E., Ramaswamy, S., Reimann, M. W., Abdellah, M., Sanchez, C. A., et al. (2015). Reconstruction and Simulation of Neocortical Microcircuitry. *Cell* 163, 456–492. doi:10.1016/j.cell.2015.09.029.

Mathis, A., Mamidanna, P., Cury, K. M., Abe, T., Murthy, V. N., Mathis, M. W., et al. (2018). DeepLabCut: markerless pose estimation of user-defined body parts with deep learning. *Nat Neurosci* 21, 1281–1289. doi:10.1038/s41593-018-0209-y.

Matthews, R. T., Kelly, G. M., Zerillo, C. A., Gray, G., Tiemeyer, M., and Hockfield, S. (2002). Aggrecan Glycoforms Contribute to the Molecular Heterogeneity of Perineuronal Nets. *J. Neurosci.* 22, 7536–7547. doi:10.1523/JNEUROSCI.22-17-07536.2002.

Melzer, S., Gil, M., Koser, D. E., Michael, M., Huang, K. W., and Monyer, H. (2017). Distinct Corticostriatal GABAergic Neurons Modulate Striatal Output Neurons and Motor Activity. *Cell Reports* 19, 1045–1055. doi:10.1016/j.celrep.2017.04.024.

Meyer, A. H., Katona, I., Blatow, M., Rozov, A., and Monyer, H. (2002). In vivo labeling of parvalbumin-positive interneurons and analysis of electrical coupling in identified neurons. *J. Neurosci.* 22, 7055–7064. doi:20026742.

Middleton, F. A., and Strick, P. L. (2000). Basal Ganglia Output and Cognition: Evidence from Anatomical, Behavioral, and Clinical Studies. *Brain and Cognition* 42, 183–200. doi:10.1006/brcg.1999.1099.

Mishra, A., Singh, S., and Shukla, S. (2018). Physiological and Functional Basis of Dopamine Receptors and Their Role in Neurogenesis: Possible Implication for Parkinson's disease. *J Exp Neurosci* 12, 1179069518779829. doi:10.1177/1179069518779829.

Miyata, S., Nishimura, Y., and Nakashima, T. (2007). Perineuronal nets protect against amyloid β-protein neurotoxicity in cultured cortical neurons. *Brain Research* 1150, 200–206. doi:10.1016/j.brainres.2007.02.066.

Moeyaert, B., Holt, G., Madangopal, R., Perez-Alvarez, A., Fearey, B. C., Trojanowski, N. F., et al. (2018). Improved methods for marking active neuron populations. *Nat Commun* 9, 4440. doi:10.1038/s41467-018-06935-2.

Moisello, C., Crupi, D., Tunik, E., Quartarone, A., Bove, M., Tononi, G., et al. (2009). The serial reaction time task revisited: a study on motor sequence learning with an arm-reaching task. *Exp Brain Res* 194, 143–155. doi:10.1007/s00221-008-1681-5.

Molina-Luna, K., Pekanovic, A., Röhrich, S., Hertler, B., Schubring-Giese, M., Rioult-Pedotti, M.-S., et al. (2009). Dopamine in Motor Cortex Is Necessary for Skill Learning and Synaptic Plasticity. *PLoS ONE* 4, e7082. doi:10.1371/journal.pone.0007082.

Monfils, M.-H., Plautz, E. J., and Kleim, J. A. (2005). In Search of the Motor Engram: Motor Map Plasticity as a Mechanism for Encoding Motor Experience. *Neuroscientist* 11, 471–483. doi:10.1177/1073858405278015.

Moore, R. Y., Whone, A. L., and Brooks, D. J. (2008). Extrastriatal monoamine neuron function in Parkinson's disease: An 18F-dopa PET study. *Neurobiology of Disease* 29, 381–390. doi:10.1016/j.nbd.2007.09.004.

Morawski, M., Brückner, G., Jäger, C., Seeger, G., Matthews, R. T., and Arendt, T. (2012). Involvement of Perineuronal and Perisynaptic Extracellular Matrix in Alzheimer's Disease Neuropathology: Perineuronal and Perisynaptic Matrix in AD. *Brain Pathology* 22, 547–561. doi:10.1111/j.1750-3639.2011.00557.x.

Morawski, M., Reinert, T., Meyer-Klaucke, W., Wagner, F. E., Tröger, W., Reinert, A., et al. (2015). Ion exchanger in the brain: Quantitative analysis of perineuronally fixed anionic binding sites suggests diffusion barriers with ion sorting properties. *Sci Rep* 5, 16471. doi:10.1038/srep16471.

Morgante, F., Espay, A. J., Gunraj, C., Lang, A. E., and Chen, R. (2006). Motor cortex plasticity in Parkinson's disease and levodopa-induced dyskinesias. *Brain* 129, 1059–1069. doi:10.1093/brain/awl031.

Nilsson, M. H., Törnqvist, A. L., and Rehncrona, S. (2005). Deep-brain stimulation in the subthalamic nuclei improves balance performance in patients with Parkinson's disease, when tested without anti-parkinsonian medication: **DBS and balance performance in PD**. *Acta Neurologica Scandinavica* 111, 301–308. doi:10.1111/j.1600-0404.2005.00394.x.

Nowicka, D., Soulsby, S., Skangiel-Kramska, J., and Glazewski, S. (2009). Parvalbumin-containing neurons, perineuronal nets and experience-dependent plasticity in murine barrel cortex. *European Journal of Neuroscience* 30, 2053–2063. doi:10.1111/j.1460-9568.2009.06996.x.

Ohbayashi, M. (2020). Inhibition of protein synthesis in M1 of monkeys disrupts performance of sequential movements guided by memory. *eLife* 9, e53038. doi:10.7554/eLife.53038.

Ohira, K. (2019). Dopamine stimulates differentiation and migration of cortical interneurons. *Biochemical and Biophysical Research Communications* 512, 577–583. doi:10.1016/j.bbrc.2019.03.105.

Ohira, K. (2020). Dopamine as a growth differentiation factor in the mammalian brain. *Neural Regen Res* 15, 390. doi:10.4103/1673-5374.266052.

Orlando, C., and Raineteau, O. (2015). Integrity of cortical perineuronal nets influences corticospinal tract plasticity after spinal cord injury. *Brain Struct Funct* 220, 1077–1091. doi:10.1007/s00429-013-0701-9.

Padmashri, R., and Dunaevsky, A. (2019). Modulation of excitatory but not inhibitory synaptic inputs in the mouse primary motor cortex in the late phase of motor learning. *Neuroscience Letters* 709, 134371. doi:10.1016/j.neulet.2019.134371.

Pantazopoulos, H., Gisabella, B., Rexrode, L., Benefield, D., Yildiz, E., Seltzer, P., et al. (2020). Circadian Rhythms of Perineuronal Net Composition. *eNeuro* 7, ENEURO.0034-19.2020. doi:10.1523/ENEURO.0034-19.2020.

Parr-Brownlie, L. C. (2005). Bradykinesia Induced by Dopamine D2 Receptor Blockade Is Associated with Reduced Motor Cortex Activity in the Rat. *Journal of Neuroscience* 25, 5700–5709. doi:10.1523/JNEUROSCI.0523-05.2005.

Pasquereau, B., DeLong, M. R., and Turner, R. S. (2016). Primary motor cortex of the parkinsonian monkey: altered encoding of active movement. *Brain* 139, 127–143. doi:10.1093/brain/awv312.

Pasquereau, B., and Turner, R. S. (2011). Primary Motor Cortex of the Parkinsonian Monkey: Differential Effects on the Spontaneous Activity of Pyramidal Tract-Type Neurons. *Cerebral Cortex* 21, 1362–1378. doi:10.1093/cercor/bhq217.

Pati, S., Salvi, S. S., Kallianpur, M., Vaidya, B., Banerjee, A., Maiti, S., et al. (2019). Chemogenetic Activation of Excitatory Neurons Alters Hippocampal Neurotransmission in a Dose-Dependent Manner. *eNeuro* 6. doi:10.1523/ENEURO.0124-19.2019.

Pavese, N., and Brooks, D. J. (2009). Imaging neurodegeneration in Parkinson's disease. *Biochimica et Biophysica Acta (BBA) - Molecular Basis of Disease* 1792, 722–729. doi:10.1016/j.bbadis.2008.10.003.

Penfield, W., and Boldrey, E. (1937). SOMATIC MOTOR AND SENSORY REPRESENTATION IN THE CEREBRAL CORTEX OF MAN AS STUDIED BY ELECTRICAL STIMULATION. *Brain* 60, 389–443. doi:10.1093/brain/60.4.389.

Permyakov, S. E., Kazakov, A. S., Avkhacheva, N. V., and Permyakov, E. A. (2014). Parvalbumin as a metal-dependent antioxidant. *Cell Calcium* 55, 261–268. doi:10.1016/j.ceca.2014.03.001.

Peters, A. J., Chen, S. X., and Komiyama, T. (2014). Emergence of reproducible spatiotemporal activity during motor learning. *Nature* 510, 263–267. doi:10.1038/nature13235.

Petrie, K. A., Schmidt, D., Bubser, M., Fadel, J., Carraway, R. E., and Deutch, A. Y. (2005). Neurotensin activates GABAergic interneurons in the prefrontal cortex. *The Journal of neuroscience : the official journal of the Society for Neuroscience* 25, 1629–36. doi:10.1523/JNEUROSCI.3579-04.2005.

Peyre, E., Silva, C. G., and Nguyen, L. (2015). Crosstalk between intracellular and extracellular signals regulating interneuron production, migration and integration into the cortex. *Front. Cell. Neurosci.* 9. doi:10.3389/fncel.2015.00129.

Pfeffer, C. K., Xue, M., He, M., Huang, Z. J., and Scanziani, M. (2013). Inhibition of inhibition in visual cortex: the logic of connections between molecularly distinct interneurons. *Nat Neurosci* 16, 1068–1076. doi:10.1038/nn.3446.

Pfurtscheller, G., and Lopes da Silva, F. H. (1999). Event-related EEG/MEG synchronization and desynchronization: basic principles. *Clinical Neurophysiology* 110, 1842–1857. doi:10.1016/S1388-2457(99)00141-8.

Pierantozzi, M., Palmieri, M., Marciani, M., Bernardi, G., Giacomini, P., and Stanzione, P. (2001). Effect of apomorphine on cortical inhibition in Parkinson's disease patients: a transcranial magnetic stimulation study. *Experimental Brain Research* 141, 52–62. doi:10.1007/s002210100839.

Pizzorusso, T., Medini, P., Berardi, N., Chierzi, S., Fawcett, J. W., and Maffei, L. (2002). Reactivation of Ocular Dominance Plasticity in the Adult Visual Cortex. *Science* 298, 1248–1251. doi:10.1126/science.1072699.

Plowman, E. K., Thomas, N. J., and Kleim, J. A. (2011). Striatal dopamine depletion induces forelimb motor impairments and disrupts forelimb movement representations within the motor cortex. *J Parkinsons Dis* 1, 93–100. doi:10.3233/JPD-2011-11017.

Poewe, W., Seppi, K., Tanner, C. M., Halliday, G. M., Brundin, P., Volkmann, J., et al. (2017). Parkinson disease. *Nat Rev Dis Primers* 3, 17013. doi:10.1038/nrdp.2017.13.

Porter, L. L., Rizzo, E., and Hornung, J. P. (1999). Dopamine affects parvalbumin expression during cortical development in vitro. *J. Neurosci.* 19, 8990–9003.

Pouille, F., Marin-Burgin, A., Adesnik, H., Atallah, B. V., and Scanziani, M. (2009). Input normalization by global feedforward inhibition expands cortical dynamic range. *Nat Neurosci* 12, 1577–1585. doi:10.1038/nn.2441.

Pouille, F., and Scanziani, M. (2001). Enforcement of Temporal Fidelity in Pyramidal Cells by Somatic Feed-Forward Inhibition. *Science* 293, 1159–1163. doi:10.1126/science.1060342.

Puighermanal, E., Biever, A., Espallergues, J., Gangarossa, G., De Bundel, D., and Valjent, E. (2015). *drd2-cre:ribotag* mouse line unravels the possible diversity of dopamine d2 receptor-expressing cells of the dorsal mouse hippocampus: D2R-Expressing Neurons In Dorsal Hippocampus. *Hippocampus* 25, 858–875. doi:10.1002/hipo.22408.

Reimers, S., Hartlage-Rübsamen, M., Brückner, G., and Roßner, S. (2007). Formation of perineuronal nets in organotypic mouse brain slice cultures is independent of neuronal glutamatergic activity. *European Journal of Neuroscience* 25, 2640–2648. doi:10.1111/j.1460-9568.2007.05514.x.

Remple, M. S., Reed, J. L., Stepniewska, I., and Kaas, J. H. (2006). Organization of frontoparietal cortex in the tree shrew (Tupaia belangeri). I. Architecture, microelectrode maps, and corticospinal connections. *J. Comp. Neurol.* 497, 133–154. doi:10.1002/cne.20975.

Resendez, S. L., Jennings, J. H., Ung, R. L., Namboodiri, V. M. K., Zhou, Z. C., Otis, J. M., et al. (2016). Visualization of cortical, subcortical and deep brain neural circuit dynamics during naturalistic mammalian behavior with head-mounted microscopes and chronically implanted lenses. *Nat Protoc* 11, 566–597. doi:10.1038/nprot.2016.021.

Ridding, M. C., Rothwell, J. C., and Inzelberg, R. (1995). Changes in excitability of motor cortical circuitry in patients with parkinson's disease. *Ann Neurol.* 37, 181–188. doi:10.1002/ana.410370208.

Rioult-Pedotti, M.-S., Pekanovic, A., Atiemo, C. O., Marshall, J., and Luft, A. R. (2015). Dopamine Promotes Motor Cortex Plasticity and Motor Skill Learning via PLC Activation. *PLoS ONE* 10, e0124986. doi:10.1371/journal.pone.0124986.

Rock, C., Zurita, H., Lebby, S., Wilson, C. J., and Apicella, A. junior (2018). Cortical Circuits of Callosal GABAergic Neurons. *Cerebral Cortex* 28, 1154–1167. doi:10.1093/cercor/bhx025.

Rock, C., Zurita, H., Wilson, C., and Apicella, A. J. (2016). An inhibitory corticostriatal pathway. *Elife* 5. doi:10.7554/eLife.15890.

Rudy, B., Fishell, G., Lee, S., and Hjerling-Leffler, J. (2011). Three groups of interneurons account for nearly 100% of neocortical GABAergic neurons. *Devel Neurobio* 71, 45–61. doi:10.1002/dneu.20853.

Rynes, M. L., Surinach, D. A., Linn, S., Laroque, M., Rajendran, V., Dominguez, J., et al. (2021). Miniaturized head-mounted microscope for whole-cortex mesoscale imaging in freely behaving mice. *Nat Methods* 18, 417–425. doi:10.1038/s41592-021-01104-8.

Salameh, G., Jeffers, M. S., Wu, J., Pitney, J., and Silasi, G. (2020). The Home-Cage Automated Skilled Reaching Apparatus (HASRA): Individualized Training of Group-Housed Mice in a Single Pellet Reaching Task. *eNeuro* 7, ENEURO.0242-20.2020. doi:10.1523/ENEURO.0242-20.2020.

Sauer, B. (1998). Inducible Gene Targeting in Mice Using the Cre/loxSystem. *Methods* 14, 381–392. doi:10.1006/meth.1998.0593.

Savidan, J., Kaeser, M., Belhaj-Saïf, A., Schmidlin, E., and Rouiller, E. M. (2017). Role of primary motor cortex in the control of manual dexterity assessed via sequential bilateral lesion in the adult macaque monkey: A case study. *Neuroscience* 357, 303–324. doi:10.1016/j.neuroscience.2017.06.018.

Schnitzler, A., and Gross, J. (2005). Normal and pathological oscillatory communication in the brain. *Nat Rev Neurosci* 6, 285–296. doi:10.1038/nrn1650.

Schober, A. (2004). Classic toxin-induced animal models of Parkinson's disease: 6-OHDA and MPTP. *Cell and Tissue Research* 318, 215–224. doi:10.1007/s00441-004-0938-y.

Seeger, G., Brauer, K., Ha¨rtig, W., and Bru¨ckner, G. (1994). Mapping of perineuronal nets in the rat brain stained by colloidal iron hydroxide histochemistry and lectin cytochemistry. *Neuroscience* 58, 371–388. doi:10.1016/0306-4522(94)90044-2.

Serrano-Reyes, M., García-Vilchis, B., Reyes-Chapero, R., Cáceres-Chávez, V. A., Tapia, D., Galarraga, E., et al. (2020). Spontaneous Activity of Neuronal Ensembles in Mouse Motor Cortex: Changes after GABAergic Blockade. *Neuroscience* 446, 304–322. doi:10.1016/j.neuroscience.2020.08.025.

Shah, A., and Lodge, D. J. (2013). A loss of hippocampal perineuronal nets produces deficits in dopamine system function: relevance to the positive symptoms of schizophrenia. *Transl Psychiatry* 3, e215–e215. doi:10.1038/tp.2012.145.

Shepherd, G. M. G. (2013). Corticostriatal connectivity and its role in disease. *Nat Rev Neurosci* 14, 278–291. doi:10.1038/nrn3469.

Shi, W., Wei, X., Wang, X., Du, S., Liu, W., Song, J., et al. (2019). Perineuronal nets protect long-term memory by limiting activity-dependent inhibition from parvalbumin interneurons. *Proc Natl Acad Sci USA* 116, 27063–27073. doi:10.1073/pnas.1902680116.

Shinozaki, M., Iwanami, A., Fujiyoshi, K., Tashiro, S., Kitamura, K., Shibata, S., et al. (2016). Combined treatment with chondroitinase ABC and treadmill rehabilitation for chronic severe spinal cord injury in adult rats. *Neuroscience Research* 113, 37–47. doi:10.1016/j.neures.2016.07.005.

Smith, C. C., Mauricio, R., Nobre, L., Marsh, B., Wüst, R. C. I., Rossiter, H. B., et al. (2015). Differential regulation of perineuronal nets in the brain and spinal cord with exercise training. *Brain Research Bulletin* 111, 20–26. doi:10.1016/j.brainresbull.2014.12.005.

Smyth, C., Summers, J. J., and Garry, M. I. (2010). Differences in motor learning success are associated with differences in M1 excitability. *Human Movement Science* 29, 618–630. doi:10.1016/j.humov.2010.02.006.

Sommerauer, M., Hansen, A. K., Parbo, P., Fedorova, T. D., Knudsen, K., Frederiksen, Y., et al. (2018). Decreased noradrenaline transporter density in the motor cortex of Parkinson's disease patients: Cortical Noradrenaline Transporter. *Mov Disord.* 33, 1006–1010. doi:10.1002/mds.27411.

Somogyi, P., Freund, T. F., and Cowey, A. (1982). The axo-axonic interneuron in the cerebral cortex of the rat, cat and monkey. *Neuroscience* 7, 2577–2607. doi:10.1016/0306-4522(82)90086-0.

Son, J. W., Shin, J. J., Kim, M.-G., Kim, J., and Son, S. W. (2021). Keratinocyte-specific knockout mice models via Cre–loxP recombination system. *Mol. Cell. Toxicol.* 17, 15–27. doi:10.1007/s13273-020-00115-4.

Spreafico, R., De Biasi, S., and Vitellaro-Zuccarello, L. (1999). The Perineuronal Net: A Weapon for a Challenge. *Journal of the History of the Neurosciences* 8, 179–185. doi:10.1076/jhin.8.2.179.1834.

Squire, L. R., and Zola-Morgan, S. (1991). The Medial Temporal Lobe Memory System. *Science* 253, 1380–1386. doi:10.1126/science.1896849.

Stefan, K. (2000). Induction of plasticity in the human motor cortex by paired associative stimulation. *Brain* 123, 572–584. doi:10.1093/brain/123.3.572.

Strafella, A. P., Valzania, F., Nassetti, S. A., Tropeani, A., Bisulli, A., Santangelo, M., et al. (2000). Effects of chronic levodopa and pergolide treatment on cortical excitability in patients with Parkinson's disease: a transcranial magnetic stimulation study. *Clinical Neurophysiology* 111, 1198–1202. doi:10.1016/S1388-2457(00)00316-3.

Sullivan, K. L., Ward, C. L., Hauser, R. A., and Zesiewicz, T. A. (2007). Prevalence and treatment of non-motor symptoms in Parkinson's disease. *Parkinsonism & Related Disorders* 13, 545. doi:10.1016/j.parkreldis.2006.10.008.

Suppa, A., Marsili, L., Belvisi, D., Conte, A., Iezzi, E., Modugno, N., et al. (2011). Lack of LTP-like plasticity in primary motor cortex in Parkinson's disease. *Experimental Neurology* 227, 296–301. doi:10.1016/j.expneurol.2010.11.020.

Suttkus, A., Rohn, S., Weigel, S., Glöckner, P., Arendt, T., and Morawski, M. (2014). Aggrecan, link protein and tenascin-R are essential components of the perineuronal net to protect neurons against iron-induced oxidative stress. *Cell Death Dis* 5, e1119–e1119. doi:10.1038/cddis.2014.25.

Swann, N. C., de Hemptinne, C., Miocinovic, S., Qasim, S., Wang, S. S., Ziman, N., et al. (2016). Gamma Oscillations in the Hyperkinetic State Detected with Chronic Human Brain Recordings in Parkinson's Disease. *J. Neurosci.* 36, 6445–6458. doi:10.1523/JNEUROSCI.1128-16.2016.

Swanson, O. K., Semaan, R., and Maffei, A. (2021). Reduced dopamine signaling impacts pyramidal neuron excitability in mouse motor cortex. *eNeuro*, ENEURO.0548-19.2021. doi:10.1523/ENEURO.0548-19.2021.

Tamás, G., Buhl, E. H., and Somogyi, P. (1997). Massive Autaptic Self-Innervation of GABAergic Neurons in Cat Visual Cortex. *J. Neurosci.* 17, 6352–6364. doi:10.1523/JNEUROSCI.17-16-06352.1997.

Taniguchi, H., Lu, J., and Huang, Z. J. (2013). The Spatial and Temporal Origin of Chandelier Cells in Mouse Neocortex. *Science* 339, 70–74. doi:10.1126/science.1227622.

Taylor, A. E., Saint-Cyr, J. A., and Lang, A. E. (1990). Memory and learning in early Parkinson's disease: Evidence for a "frontal lobe syndrome." *Brain and Cognition* 13, 211–232. doi:10.1016/0278-2626(90)90051-O.

Tennant, K. A., Adkins, D. L., Donlan, N. A., Asay, A. L., Thomas, N., Kleim, J. A., et al. (2011). The Organization of the Forelimb Representation of the C57BL/6 Mouse Motor Cortex as Defined by Intracortical Microstimulation and Cytoarchitecture. *Cerebral Cortex* 21, 865–876. doi:10.1093/cercor/bhq159.

Tewari, B. P., Chaunsali, L., Campbell, S. L., Patel, D. C., Goode, A. E., and Sontheimer, H. (2018). Perineuronal nets decrease membrane capacitance of peritumoral fast spiking interneurons in a model of epilepsy. *Nat Commun* 9, 4724. doi:10.1038/s41467-018-07113-0.

Thevenaz, P., Ruttimann, U. E., and Unser, M. (1998). A pyramid approach to subpixel registration based on intensity. *IEEE Trans. on Image Process.* 7, 27–41. doi:10.1109/83.650848.

Thickbroom, G. W., Byrnes, M. L., Walters, S., Stell, R., and Mastaglia, F. L. (2006). Motor cortex reorganisation in Parkinson's disease. *Journal of Clinical Neuroscience* 13, 639–642. doi:10.1016/j.jocn.2005.06.013.

Thobois, S., Dominey, P., Decety, J., Pollak, P., Gregoire, M. C., and Broussolle, E. (2000). Overactivation of primary motor cortex is asymmetrical in hemiparkinsonian patients: *NeuroReport* 11, 785–789. doi:10.1097/00001756-200003200-00026.

Thompson, E. H., Lensjø, K. K., Wigestrand, M. B., Malthe-Sørenssen, A., Hafting, T., and Fyhn, M. (2018). Removal of perineuronal nets disrupts recall of a remote fear memory. *PNAS* 115, 607–612. doi:10.1073/pnas.1713530115.

Thomson, A. M., West, D. C., Hahn, J., and Deuchars, J. (1996). Single axon IPSPs elicited in pyramidal cells by three classes of interneurones in slices of rat neocortex. *The Journal of Physiology* 496, 81–102. doi:10.1113/jphysiol.1996.sp021667.

Touvykine, B., Mansoori, B. K., Jean-Charles, L., Deffeyes, J., Quessy, S., and Dancause, N. (2016). The Effect of Lesion Size on the Organization of the Ipsilesional and Contralesional Motor Cortex. *Neurorehabil Neural Repair* 30, 280–292. doi:10.1177/1545968315585356.

Townsley, K. G., Borrego, M. B., and Ozburn, A. R. (2021). Effects of chemogenetic manipulation of the nucleus accumbens core in male C57BL/6J mice. *Alcohol* 91, 21–27. doi:10.1016/j.alcohol.2020.10.005.

Trantham-Davidson, H. (2004). Mechanisms Underlying Differential D1 versus D2 Dopamine Receptor Regulation of Inhibition in Prefrontal Cortex. *Journal of Neuroscience* 24, 10652–10659. doi:10.1523/JNEUROSCI.3179-04.2004.

Tseng, K.-Y., and O'Donnell, P. (2006). Dopamine Modulation of Prefrontal Cortical Interneurons Changes during Adolescence. *Cerebral Cortex* 17, 1235–1240. doi:10.1093/cercor/bhl034.

Tulving, E. (1985). How many memory systems are there? *American Psychologist* 40, 385–398. doi:10.1037/0003-066X.40.4.385.

Ueki, Y., Mima, T., Ali Kotb, M., Sawada, H., Saiki, H., Ikeda, A., et al. (2006). Altered plasticity of the human motor cortex in Parkinson's disease. *Ann Neurol.* 59, 60–71. doi:10.1002/ana.20692.

Ueno, H., Fujii, K., Suemitsu, S., Murakami, S., Kitamura, N., Wani, K., et al. (2018). Expression of aggrecan components in perineuronal nets in the mouse cerebral cortex. *IBRO Reports* 4, 22–37. doi:10.1016/j.ibror.2018.01.002.

Uhl, G. R., Hedreen, J. C., and Price, D. L. (1985). Parkinson's disease: Loss of ineurons from the ventral tegmental area contralateral to therapeutic surgical lesions. *Neurology* 35, 1215–1215. doi:10.1212/WNL.35.8.1215.

Urban-Ciecko, J., and Barth, A. L. (2016). Somatostatin-expressing neurons in cortical networks. *Nat Rev Neurosci* 17, 401–409. doi:10.1038/nrn.2016.53.

Urs, N. M., Gee, S. M., Pack, T. F., McCorvy, J. D., Evron, T., Snyder, J. C., et al. (2016). Distinct cortical and striatal actions of a β-arrestin–biased dopamine D2 receptor ligand reveal unique antipsychotic-like properties. *Proceedings of the National Academy of Sciences* 113, E8178–E8186. doi:10.1073/pnas.1614347113.

Valverde, S., Vandecasteele, M., Piette, C., Derousseaux, W., Gangarossa, G., Aristieta Arbelaiz, A., et al. (2020). Deep brain stimulation-guided optogenetic rescue of parkinsonian symptoms. *Nat Commun* 11, 2388. doi:10.1038/s41467-020-16046-6.

Viaro, R., Morari, M., and Franchi, G. (2011). Progressive Motor Cortex Functional Reorganization Following 6-Hydroxydopamine Lesioning in Rats. *Journal of Neuroscience* 31, 4544–4554. doi:10.1523/JNEUROSCI.5394-10.2011.

Vitrac, C., Péron, S., Frappé, I., Fernagut, P.-O., Jaber, M., Gaillard, A., et al. (2014). Dopamine control of pyramidal neuron activity in the primary motor cortex via D2 receptors. *Front. Neural Circuits* 8. doi:10.3389/fncir.2014.00013.

Wang, Y.-Y., Wang, Y., Jiang, H.-F., Liu, J.-H., Jia, J., Wang, K., et al. (2018). Impaired glutamatergic projection from the motor cortex to the subthalamic nucleus in 6-hydroxydopamine-lesioned hemi-parkinsonian rats. *Experimental Neurology* 300, 135–148. doi:10.1016/j.expneurol.2017.11.006.

Waters, C. M., Peck, R., Rossor, M., Reynolds, G. P., and Hunt, S. P. (1988). Immunocytochemical studies on the basal ganglia and substantia nigra in Parkinson's disease and Huntington's chorea. *Neuroscience* 25, 419–438. doi:10.1016/0306-4522(88)90249-7.

Whitmer, D., de Solages, C., Hill, B., Yu, H., Henderson, J. M., and Bronte-Stewart, H. (2012). High frequency deep brain stimulation attenuates subthalamic and cortical rhythms in Parkinson's disease. *Front. Hum. Neurosci.* 6. doi:10.3389/fnhum.2012.00155.

Wichmann, T., and Dostrovsky, J. O. (2011). Pathological basal ganglia activity in movement disorders. *Neuroscience* 198, 232–244. doi:10.1016/j.neuroscience.2011.06.048.

Wingert, J. C., and Sorg, B. A. (2021). Impact of Perineuronal Nets on Electrophysiology of Parvalbumin Interneurons, Principal Neurons, and Brain Oscillations: A Review. *Frontiers in Synaptic Neuroscience* 13, 22. doi:10.3389/fnsyn.2021.673210.

Woolsey, C. N., Settlage, P. H., Meyer, D. R., Sencer, W., Pinto Hamuy, T., and Travis, A. M. (1952). Patterns of localization in precentral and "supplementary" motor areas and their relation to the concept of a premotor area. *Res Publ Assoc Res Nerv Ment Dis* 30, 238–264.

Xu, H., Jeong, H.-Y., Tremblay, R., and Rudy, B. (2013). Neocortical Somatostatin-Expressing GABAergic Interneurons Disinhibit the Thalamorecipient Layer 4. *Neuron* 77, 155–167. doi:10.1016/j.neuron.2012.11.004.

Xu, T., Yu, X., Perlik, A. J., Tobin, W. F., Zweig, J. A., Tennant, K., et al. (2009). Rapid formation and selective stabilization of synapses for enduring motor memories. *Nature* 462, 915–919. doi:10.1038/nature08389.

Yamadori, A., Yoshida, T., Mori, E., and Yamashita, H. (1996). Neurological basis of skill learning. *Cognitive Brain Research* 5, 49–54. doi:10.1016/S0926-6410(96)00040-7.

Yamawaki, N., Borges, K., Suter, B. A., Harris, K. D., and Shepherd, G. M. G. (2014). A genuine layer 4 in motor cortex with prototypical synaptic circuit connectivity. *eLife* 3, e05422. doi:10.7554/eLife.05422.

Yamawaki, N., Stanford, I. M., Hall, S. D., and Woodhall, G. L. (2008). Pharmacologically induced and stimulus evoked rhythmic neuronal oscillatory activity in the primary motor cortex in vitro. *Neuroscience* 151, 386–395. doi:10.1016/j.neuroscience.2007.10.021.

Yi, J.-H., Katagiri, Y., Susarla, B., Figge, D., Symes, A. J., and Geller, H. M. (2012). Alterations in sulfated chondroitin glycosaminoglycans following controlled cortical impact injury in mice. *Journal of Comparative Neurology* 520, 3295–3313. doi:10.1002/cne.23156.

Zarow, C., Lyness, S. A., Mortimer, J. A., and Chui, H. C. (2003). Neuronal Loss Is Greater in the Locus Coeruleus Than Nucleus Basalis and Substantia Nigra in Alzheimer and Parkinson Diseases. *Arch Neurol* 60, 337. doi:10.1001/archneur.60.3.337.

Zurita, H., Feyen, P. L. C., and Apicella, A. J. (2018). Layer 5 Callosal Parvalbumin-Expressing Neurons: A Distinct Functional Group of GABAergic Neurons. *Front. Cell. Neurosci.* 12, 53. doi:10.3389/fncel.2018.00053.